Biologically Active Natural Products. Ochromycinone Analogues and Aurein Peptides.

A Thesis Presented for the Degree of

DOCTOR OF PHILOSOPHY

By

Tomas Rozek

Department of Chemistry

The University of Adelaide

Australia

October 2000

Statement

This thesis contains no material which I have presented for any other degree or diploma at any university and to my best knowledge the material presented here is original and has not been previously published, except where due reference is made in the text.

This thesis is less than one hundred thousand words in length.

Tomas Rozek

October 2000

NAME: Tomas Rozek **COURSE:** PhD

I give consent to this copy of my thesis, when deposited in the University Libraries, being available for photocopying and loan.

SIGNATURE: **DATE:** 1-11-2000

Table of Contents

Abstract

The boron triacetate assisted Diels-Alder reaction between racemic 5,5-dimethyl-3-vinyl-2-cyclohexanyl acetate and 5-hydroxy-1,4-naphthoquinone yields racemic 11-hydroxy-3,3-dimethyl-7,12-dioxo-1,2,3,4,6,6a,7,12,12a,12b-decahydrobenzo[*a*]anthracen-1-yl acetate as the sole stereoisomer by regio- and stereo-selective *anti endo* addition. Aromatization of the Diels-Alder adduct followed by hydrolysis of the acetate and oxidation of resultant 1-hydroxy group gives 11-hydroxy-3,3-dimethyl-1,2,3,4-tetrahydrobenzo[*a*]anthracene-1,7,12-trione, an analogue of the natural angucyclinone ochromycinone, in an overall yield of 37% from 5-hydroxy-1,4-naphthoquinone.

The reduction of racemic 8-hydroxy-6-methoxy-3,3-dimethyl-1,2,3,4,,5,6,6a,7,12,12a-decahydrobenzo[*a*]anthracene-1,7,12-trione, with either (i) sodium borohydride and cerium (iii) chloride in ethanol (the Luche reagent) or (ii) sodium borohydride in ethanol, was shown (by NMR and X-ray crystallographic data), 7,8-dihydroxy-6-methoxy-3,3-dimethyl-1,2,3,4-5,6,6a,7,12,12a-decahydrobenzo[*a*]anthracene-1,2-dione in which the 7-OH and 6-OMe groups are *cis* to each other. This reduction procedure may find use in the synthesis of the biologically active elmycin A group of angucyclines.

The Diels-Alder condensation between 3,3-dimethyl-5-vinyl-1,5-cyclohexadienyl acetate and 5-acetoxy-2-bromo-1,4-naphthoquinone yields racemic 1-acetoxy-12a-bromo-3,3-dimethyl,-7,12-dioxo -3,4,6,6a,7,12,12a,12b-octahydrobenzo[*a*]anthracen-8-yl acetate formed by regio- and stereo-selective *endo* addition. Epoxidation of both double bonds of the Diels-Alder adduct followed by acid catalysed epoxide opening, aromatisation of the B ring and hydrolysis of the acetate protecting groups gives the angucyclinone 2,8-dihydroxy-3,3-dimethyl-1,7,12,trioxo-1,2,3,4,7,12-hexahydrobenzo[*a*]-anthracene in an overall yield of 40 % (from 5-acetoxy-2-bromo-1,4-naphthoquinone). This product contains an α-hydroxy ketone functional group, a group that also occurs in biologically active angucyclinones of the PD 116779 type. This convenient synthesis may possibly be adopted to synthesise angucyclinones of this type.

Sixteen aurein peptides are present in the host defence secretion from the granular dorsal glands of the Green and Golden Bell Frog *Litoria aurea* and seventeen from those of the related Southern Bell Frog *Litoria raniformis.* All peptides have been sequenced using a combination of electrospray mass spectrometry and Lys-C digestion, with each sequence

confirmed by automated Edman sequencing. The peptides are named in five groups, viz aureins 1-5. Ten of these peptides are common to both species of frog. Thirteen of the aurein peptides show wide-spectrum antibiotic and anticancer activity. Amongst the more active peptides are aurein 1.2 (GLFDIIKKIAESF-NH_2), the smallest peptide from an anuran reported to have both antibiotic and anticancer activity; aurein 2.2 (GLLDIVKKVIGAFGSL-NH_2) and aurein 3.1 (GLFDIVKKIAGHIAGSI-NH_2). The aurein 4 and 5 peptides, e.g. aurein 4.1 (GLIQTIKEKLKELAGGLVTGIQS-OH) and aurein 5.1 (GLLDIVTGLLGNLIVDVLKPKTPAS-OH) show neither antibacterial nor anticancer activity.

Acknowledgements

I wish to express deepest gratitude to my PhD supervisor, Professor John H. Bowie for giving me the opportunity to work in a professional and experienced environment. His guidance and knowledge of quinones were appreciated, and I thank him for giving me the freedom to explore my own ideas; especially the synthetic project. I am grateful to Professor Bowie for creating the opportunity for me to work overseas. Additionally, I would like to thank Professor D.W. Cameron for thought provoking ideas. Thanks must also go to Dr S. Dua for his synthetic skills and wisdom, Dr S. Pyke for his help with the interpretation of the highly complex NMR experiments, Dr D.K. Taylor and both X-ray Crystallographers Professor A.H. White and Dr E.R.T. Tiekink.

To past and present members of the Bowie group: John Hevko, Steve Blanksby, Paul Wabnitz, Simon Steinborner, Brian Chia, Kate Wegener, Charm, Craig Brinkworth; all of whom stood by me with support, loyalty and friendship (I will never forget the fun filled group lunches!).

Thank you to the technical staff of the department for their invaluable assistance throughout my time at the University of Adelaide.

Thanks to my colleagues for the highly enjoyable and distracting Friday nights. You know who you are: Wayne, Peter, Martyn, Jason, Tom, Penny, Mark (there are too many to mention).

Finally, to my fondest friend Kristina, who put up with me for the last five years. And lastly, thank you Mum and Dad. If it had not been for you, I would not have reached this goal.

I would also like to acknowledge the Australian Research Council and the financial assistance of an Australian Postgraduate Research Award.

Abbreviations

BuLi	n-butyl lithium
b	broad
CAD	collisional activated dissociation
CAN	ceric ammonium nitrate
CA MS/MS	collisional activated mass spectrum
COSY	correlation spectroscopy
d	doublet
DMDO	dimethyldioxirane
DBU	diazobicycloundecane
eq	equivalents
ES	electrospray
ESMS	electrospray mass spectrometry
FAB	fast atom bombardment
GHMQC	gradient hetero nuclear quantum correlation
GHMBC	gradient hetero nuclear multiple bond correlation
HPLC	high performance liquid chromatography
hr	hour
IC_{50}	50% inhibition at the specified concentration
LDA	lithium diisopropylamide
LCQ	liquid chromatography quadropole
λ_{max}	ultraviolet absorption maxima (nm)
MeOH	methanol
MIC	minimum inhibitory concentration
m.p.	melting point
MS	mass spectrum
m/z	mass to charge ratio
$M^{+\cdot}$	molecular ion (mass spectrometry)
MW	molecular weight
m	multiplet
NBS	N-bromosuccinimide
NCI	National Cancer Institute
NMO	N-methylmorpholine N-oxide
NOE	nuclear Overhauser effect
NMR	nuclear magnetic resonance

p	pentet
ppm	parts per million
q	quartet
ROESY	rotating frame Overhauser effect spectroscopy
SES	surface electrical stimulation
s	singlet
TBAF	tetrabutylammonium fluoride
TBDMS	tertiarybutyldimethylsilyl
THF	tetrahydrofuran
pTSA	*para*-toluenesulfonic acid
TFAA	trifluoroacetic acid
t	triplet
ν_{max}	infrared absorption maxima (cm^{-1})
UV	ultraviolet

Chapter 1. Biologically Active Angular Quinones: An Introduction

1.1. Meaning, History and Biosynthesis

The discovery of new members of the angucycline class of quinones in recent years has stimulated great interest in these compounds due to their wide range of biological activities.[1,2]

The angucycline group of antibiotics now compromises more than one hundred secondary metabolites of microbial origin. All angucyclines are secondary metabolites of micro-organisms, mainly *Streptomycetes* species isolated from various soil samples.[3]

The terms angucycline/angucyclinone describe and include natural product consisting of angular tetracyclic (benz[*a*]anthracene) structural moieties bio-synthetically derived from decaketide chains formed *via* the polyketide biosynthetic pathway (Scheme 1).[1] The term 'angucycline' includes those with hydrolysable sugar moieties while 'angucyclinone' refers to a sugarless compound. The term 'aglycone' is defined as a chemical structure without hydrolysable sugars and traditionally has been used to refer to angucyclinones.

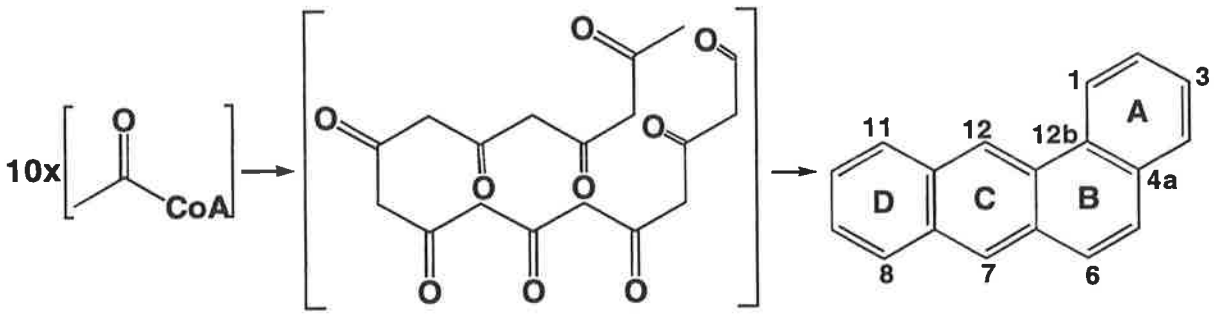

Scheme 1. Polyketide biosynthetic pathway towards the benz[*a*]anthracene framework.

The first naturally occurring angucyclines based on the angular tetracyclic framework were isolated in the 1960's and 1970's. Among these were the simple non sugar containing tetrangomycin **(1)**,[4] tetrangulol **(2)**[5] and ochromycinone **(3)**.[6] Angucyclinones **(1)**, **(2)** and **(3)** were isolated as secondary metabolites from the culture broths of *Streptomyces rimosus*. The more complex saccharide containing, and highly oxygenated aquayamycin **(4)** was first detected and described without structure in 1968 but the advent of more sophisticated structure determination techniques of the 1970's allowed the structure to be solved.[7] Aquayamycin **(4)** was shown to contain a C-glycosidic moiety, and a high degree of oxygenation in the A-ring especially at the C-4a,12b ring junction.[8] The non C-glycosidic sakyomycins eg. **(5)**, contains a α-hydroxy ketone moiety at position 2 in the A-ring together with the sugar containing *cis* dihydroxyl functional group at the A,B ring junction.[9]

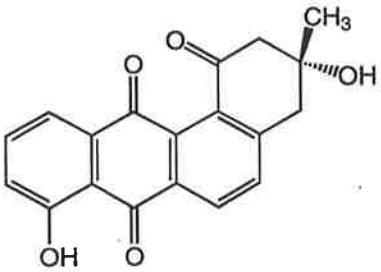

tetrangomycin **(1)**

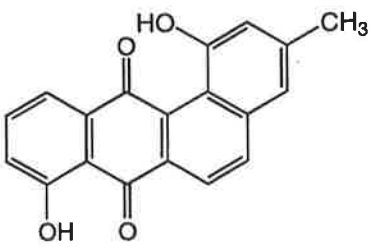

tetrangulol **(2)**

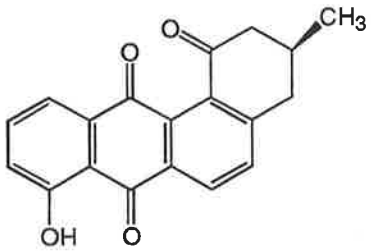

ochromycinone **(3)**

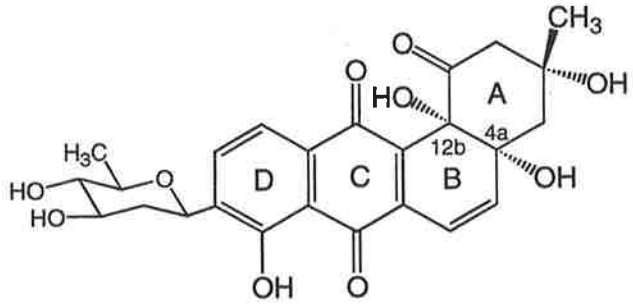

aquayamycin **(4)**

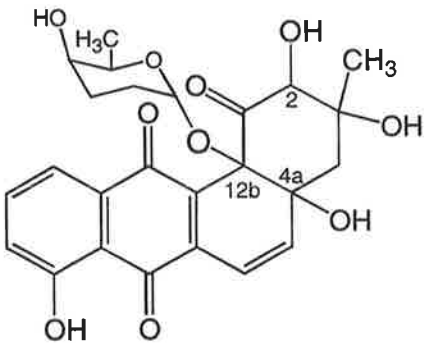

sakyomycin A **(5)**

Angucyclines such as the vineomycins have a linear structure resulting from enzymatic oxygenase-induced fragmentation of the C-1,12b bond, as determined by biosynthetic studies (Scheme 2).[10] This fragmentation can be reproduced in the laboratory using either acidic or basic conditions.

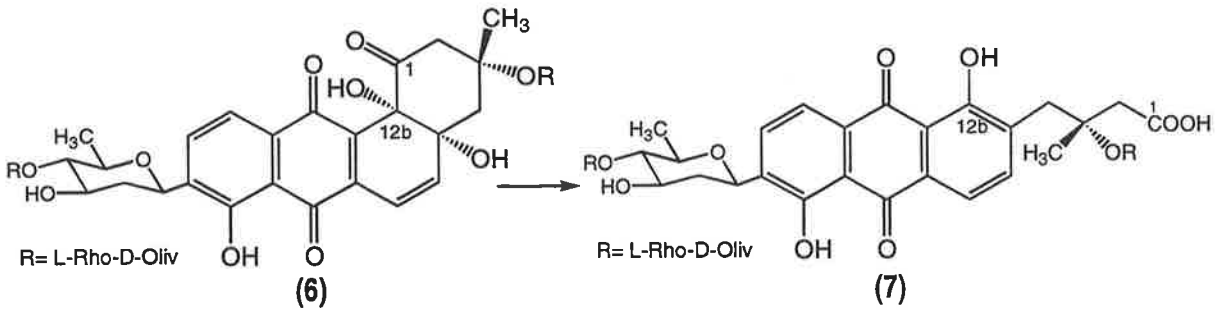

Scheme 2. Oxidative fragmentation of the C-1,12b bond of Vineomycin A_1 **(6)** to form the 'non-classical' angucycline Vineomycin B_2 **(7)** [Sugars: L-Rho = L-Rhodinose, D-Oliv = D-Olivose].

In early studies on the biosynthesis of angucyclines, the biogenetic origin of the oxygen atoms in the framework was determined by feeding the cultures with [1-$^{13}C^{18}O_2$] enriched acetate units and growing the cultures under an $^{18}O_2$ enriched atmosphere.[1,2] Taking aquayamycin as an example, all the oxygen atoms in the structure except one were derived from the [1-$^{13}C^{18}O_2$] enriched acetate units, only the position 12b hydroxyl arises from $^{18}O_2$ through incorporation by a mono-oxygenase enzyme. This result disproves the alternative hypothesis that the position 4a,12b *cis* diol functionality in the aquayamycins was incorporated (at a much later stage of biosynthesis on the fully B ring aromatic molecule) by fragmentation of a peroxide which was formed by a di-oxygenase enzyme.[1]

The late biosynthetic steps of urdamycin A **(10)**, (a complex, *cis*-dihyroxyl containing glycosylated angucycline) are outlined in Scheme 3. This sequence of steps was determined by studying blocked mutant products of *Streptomyces fradiae* Tu 2717.[2,11]

Starting from one acetyl CoA starter and nine malonyl CoA extender units, the first shown biosynthetic intermediate (Scheme 3) is condensed in head to tail fashion during the polyketide biosynthetic pathway. The C-glycosidic moiety is next incorporated by a glycosyl transfer step. After the glycosyl transfer step, the 6-ketone is reduced by the reductase, followed by oxygenation at 12b and 5, 6 dehydration to give the *cis* dihydroxylated aquayamycin **(4).** The glycosyl moiety attached *via* the 12b hydroxyl is then incorporated to give **(9)**, followed by two additional glycosyl transfers to generate urdamycin A. This biosynthetic sequence is supported by the isolation of rabelomycin **(11)**, 6-hydroxy-urdamycinone B **(12)** and urdamycinone B **(13)**; all formed as shown in Scheme 3.

The conclusions that can be drawn from the various biosynthetic studies indicate that the oxygenases cause more dramatic effects in addition to those arising from the obvious introduction of oxygen atoms. These include: (i) the C-C bond cleavages [*via* a biological Baeyer-Villinger oxidation] used to form the non-classical, linear vineomycin B_2 **(7)** angucyclines (Scheme 2), (ii) rearrangements and (iii) the introduction of, and in change of stereochemistry.[2]

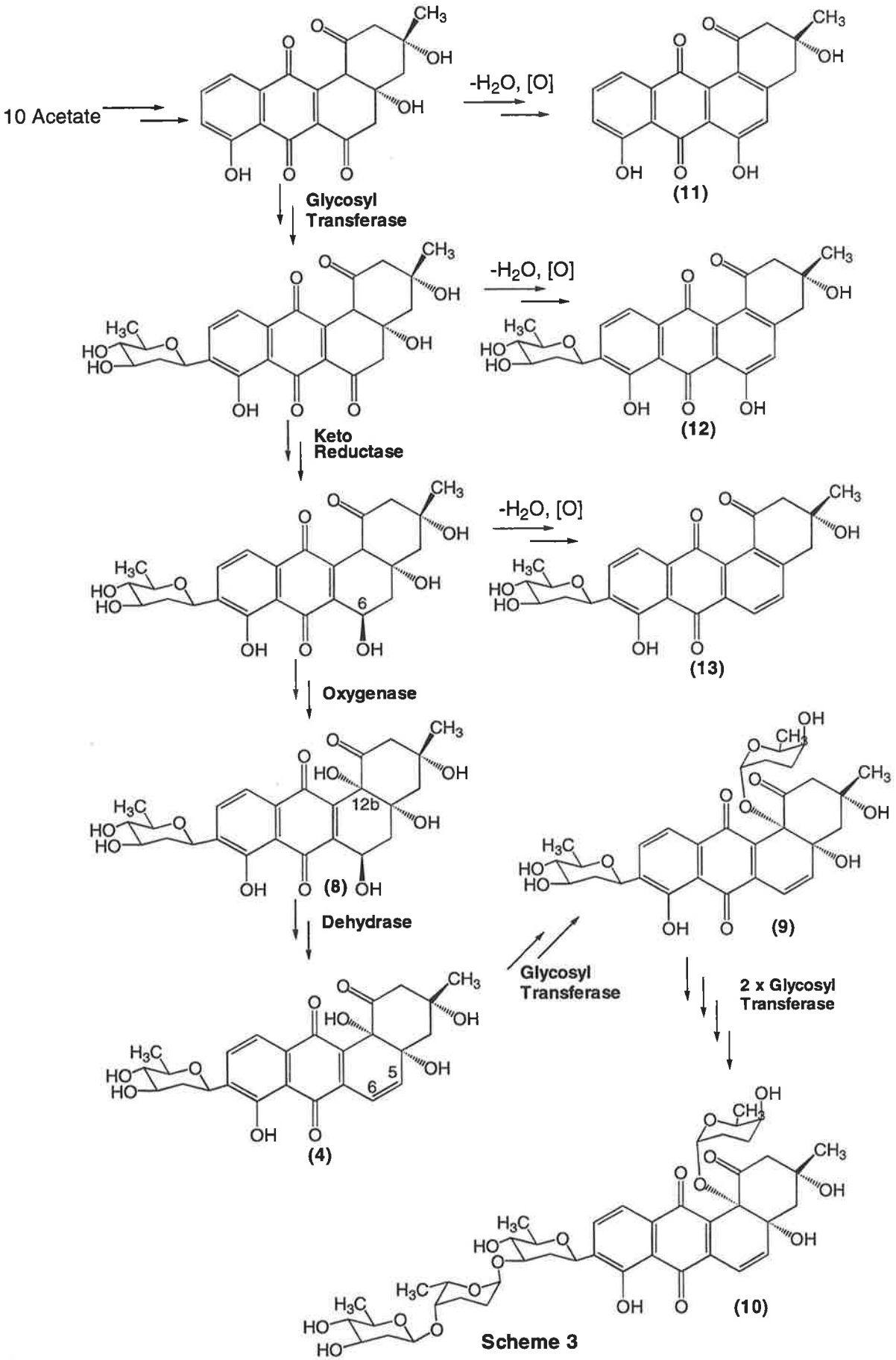
10 Acetate
-H2O, [O]
(11)
Glycosyl Transferase
-H2O, [O]
(12)
Keto Reductase
-H2O, [O]
(13)
Oxygenase
(8)
Dehydrase
(4)
Glycosyl Transferase
2 x Glycosyl Transferase
(9)
(10)

Scheme 3

1.2 Biological Properties and Modes of Action Against Cancer

Angucyclines show diverse biological activities. To date, the following types of biological activity have been reported *viz*; antitumour,[12,13,14] vincristine potentiating cytotoxicity,[15,16,17] antibacterial,[18,19] antiviral,[13] and antifungal activity.[20] Inhibition of enzyme activity,[21] and blood platelet aggregation,[22] have also been reported.

Some specific examples of the potency of these compounds are: (i) aquayamycin **(4)** inhibits the biosynthesis of noradrenaline and adrenaline respectively [50% inhibition (non-competitive) at a concentration of 37 ng/ml has been detected for tyrosine hydroxylase[21]]; (ii) rabelomycin **(11)**, shows pronounced antibacterial activity against Gram negative organisms; (iii) sakyomycin A **(5)**, inhibits HIV *in vitro*;[13] and (iv) saquayamycins A to D are perhaps the most useful angucyclines as potential pharmaceuticals because of their potent activities against doxorubicin-resistant and adriamycin-resistant cell lines,[13] as well as their activity against leukemia cells (50% inhibition at 4μg/ml).[14]

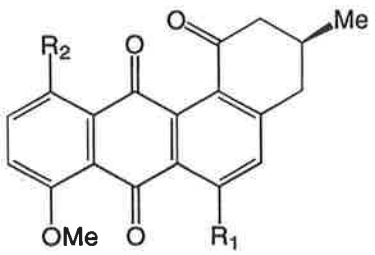

Hatomarubigin A **(14)** R_1 = OH R_2 = H
Hatomarubigin B **(15)** R_1 = H R_2 = OH
Rubiginone B_2 **(16)** R_1 = H R_2 = H

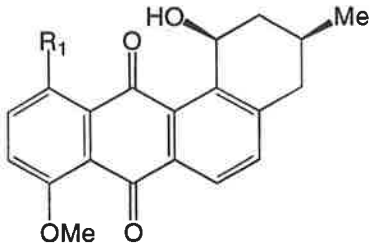

Hatomarubigin C **(17)** R_1 = OH
Rubiginone B_1 **(18)** R_1 = H

The rubigins **(14-18)** have been reported to complement/ assist the activity of other agents: for example (i) [**(14)-(17)**] increase the cytotoxicity of colchicine against colchicine-resistant cancer KB (CH^R) cell lines[15] [hatomarubigin A **(14)**, the most potent member of this group, is ten times more effective in this assay than [**(15)-(17)**] inhibiting 50% of the tumour growth on colchicine-resistant KB (CH^R) cell lines at IC_{50} of 8.5 μg/ml without colchicine and 0.9 μg/ml in the presence of 1.5 μg/ml of colchicine], (ii) the closely related rubiginone B_1 **(18)**, shows no cytotoxicity alone at up to 30 μg/ml but increases the cytotoxicity of vincristine **(19)** against vincristine-resistant human Moser cells 84-fold at 30 μg/ml, and 59-fold at 10 μg/ml concentration.[16,17] The mechanisms of such interactions are not understood.

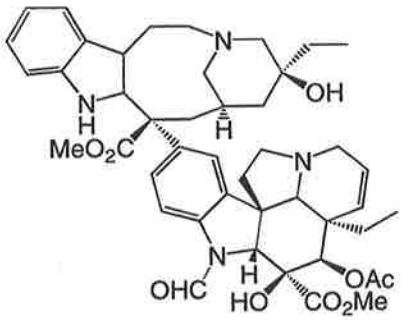

(19)

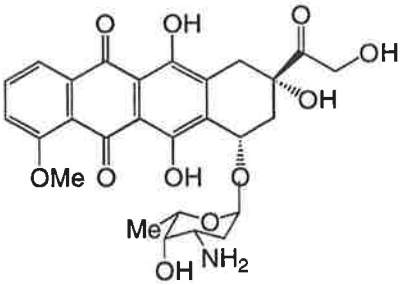

(20)

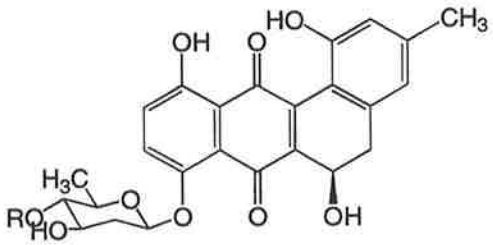

R= Rho-Oliv-Oliv-Rho-Oliv-

(21)

Figure 1. The chemotherapeutic drugs vincristine **(19)**, adriamycin **(20)**, landomycin A **(21)** [Sugars: Rho = Rhodinose, Oliv = Olivose].

Some cytotoxic quinones are known to bind to or react with DNA. As a consequence DNA replication is terminated, and cell division ceases. A good example is the anthracycline drug adriamycin **(20)**, shown in Figure 1, which is used in the clinical treatment of leukaemia, breast, lung, and prostate cancer.[23] The planar nature of adriamycin allows the molecule to interact with the double helix in such a way that the carbohydrate moiety sits in the minor groove of the DNA, with the amino functional group of the carbohydrate directly H-bonding to both deoxyribose and thymine residues. Two molecules of **(20)** insert themselves between adjacent cytosine/guanine base pairs causing a displacement between the base pairs effecting a small amount of double helix uncoiling thereby chemically altering the DNA structure.[24] It has been proven that the anti-cancer active angucycline landomycin A **(21)** also blocks replication of DNA (Figure 1).[25] The exact mechanisms of such interactions are not understood but DNA damage caused by the superoxide anion and the hydroxyl radical (formed from molecular oxygen by semiquinone radicals) has been implicated.[26]

1.3 Synthetic Methods in Angucyclinone Synthesis

Although there have been many complex angucycline/ angucyclinones isolated, synthetic attempts to date have been mainly of simple, non-saccharide containing angucyclinones. For example, tetrangomycin **(1)**,[27,28] tetrangulol **(2)**,[27,29] ochromycinone **(3)**,[30,31,32] X 14881 C **(26)**,[32] emycin A,[31,33,34,35] rabelomycin **(11)**,[28,36] 3-deoxy rabelomycin,[37] rubiginone B_1 **(18)** and B_2 **(16)**,[33,35] hatomarubigin B **(15)** and C **(17)**,[38] MM 47755 and X-14881 E.[39] Successful syntheses of the more complex 9 C-glycosyl containing angucyclines such as urdamycinone B **(13)** have been accomplished.[40,41] Attempted syntheses of the non aromatic, oxygenated angucyclinones include; PD 116740 **(32)** and TAN 1085 **(33)**,[42] analogs of SF 1315 A **(47)**,[43, 44, 46] and SS 2284 **(48)**.[43]

The most recent review by Krohn and Rohr has an extensive coverage of the methodologies available for angucycline syntheses.[2]

Friedel-Crafts Reactions

The first synthetic attempt of this class of natural products was by Brown and Thompson who synthesized tetrangulol **(2)** in a poor overall yield.[29] The synthesis failed in the final step yielding tetrangulol as the minor product. Snieckus and Katsura reported the first total synthesis of the angucyclinones X-14881 C **(26)** and ochromycinone **(3)**.[32]

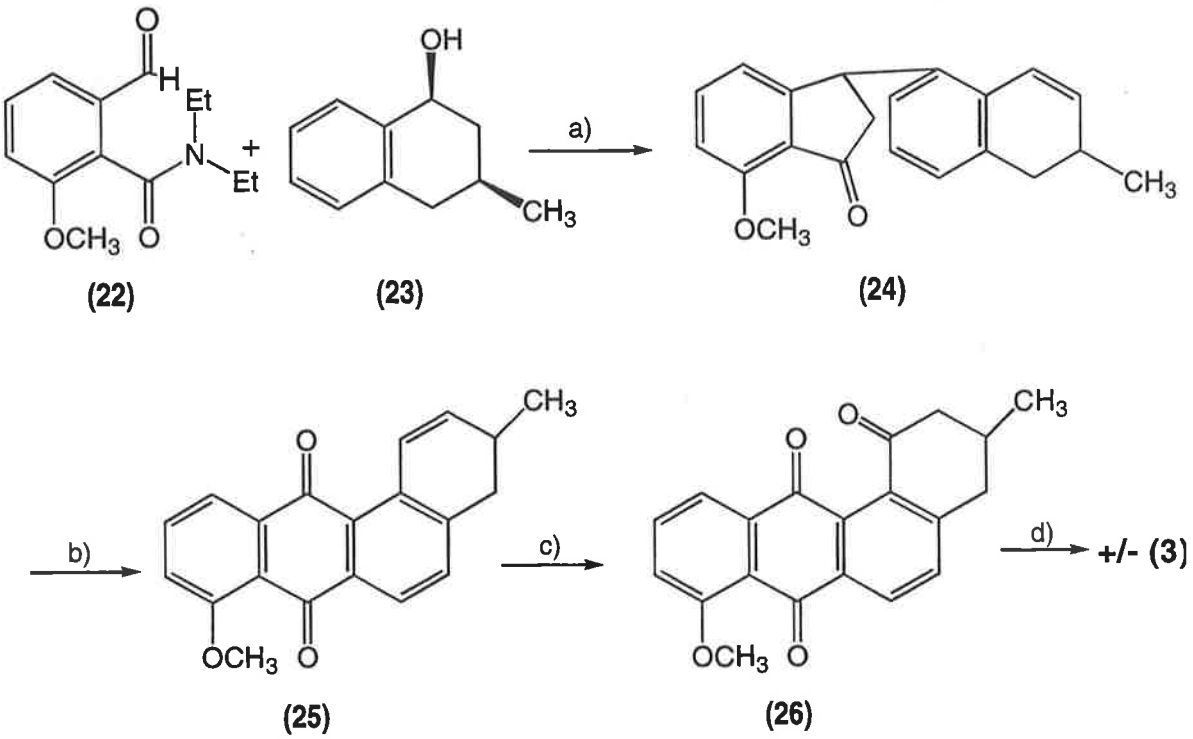

a) (i) BuLi/TMEDA, (ii) pTSA, (77%); b) (i) Zn/ NaOH (ii) TFAA (78%); c) (i) selenohydroxylation (ii) CrO_3 / pyridine 3) deselenation (54%); d) $AlCl_3$ (quantitative)

Scheme 4. Synthesis of ochromycinone **(3)** and X – 14881 C **(26).**

Their regiospecific convergent route utilized an aromatic *ortho*-directed metallation protocol (Scheme 4), to yield racemic ochromycinone **(3)** and its 8-O-methyl ether X – 14881 C **(26).** The key intermediate was phthalide **(24)** made by coupling the amide aldehyde **(22)** with dilithiated 3-methyl-1-tetralol **(23).** Zinc hydrogenolysis followed by an internal Friedel-Crafts cyclisation of the resultant benzoic acid derivative gave the dihydrobenz[a]anthraquinone **(25)** in a 77% yield. The carbonyl at C-1 was regenerated via selenohydroxylation and chromium (vi) oxidation followed by radical deselenation to form the O-methyl ether **(26)** which was cleaved using aluminum chloride to yield racemic ochromycinone **(3)** in an overall 17% yield. The identity of **(3)** was compared to that of the original sample supplied by Bowie.[6] Judging by the use of chiral starting material **(23),** the aim was to synthesize (+) ochromycinone but racemisation occurred during the formation of the phthalide.

Diels-Alder reactions

The Diels-Alder reaction is one of the most convenient and the most widely used way to construct the angular benz[*a*]anthracene framework. Guingant and Barreto published their pioneering paper describing the synthesis of racemic ochromycinone **(3)** in an overall yield of 25-40%.[30] This approach utilized a Diels-Alder cyclisation between 5-hydroxy-1,4-naphthoquinone and dienone **(29)** (Scheme 5). Starting from 5-methyl-3-ethoxycyclohex-2-ene-1-one **(27)**, the '*EE*'-dienone **(29)** was prepared by the addition of methanol to the acetylenic ketone **(28).** The boron triacetate facilitated Diels-Alder reaction of **(29)** with **(30)** produced a non isolated cycloadduct [probably the rearranged α,β-unsaturated carbonyl system **(30)**], which eliminated methanol and oxidized in air to yield racemic ochromycinone **(3).**[#]

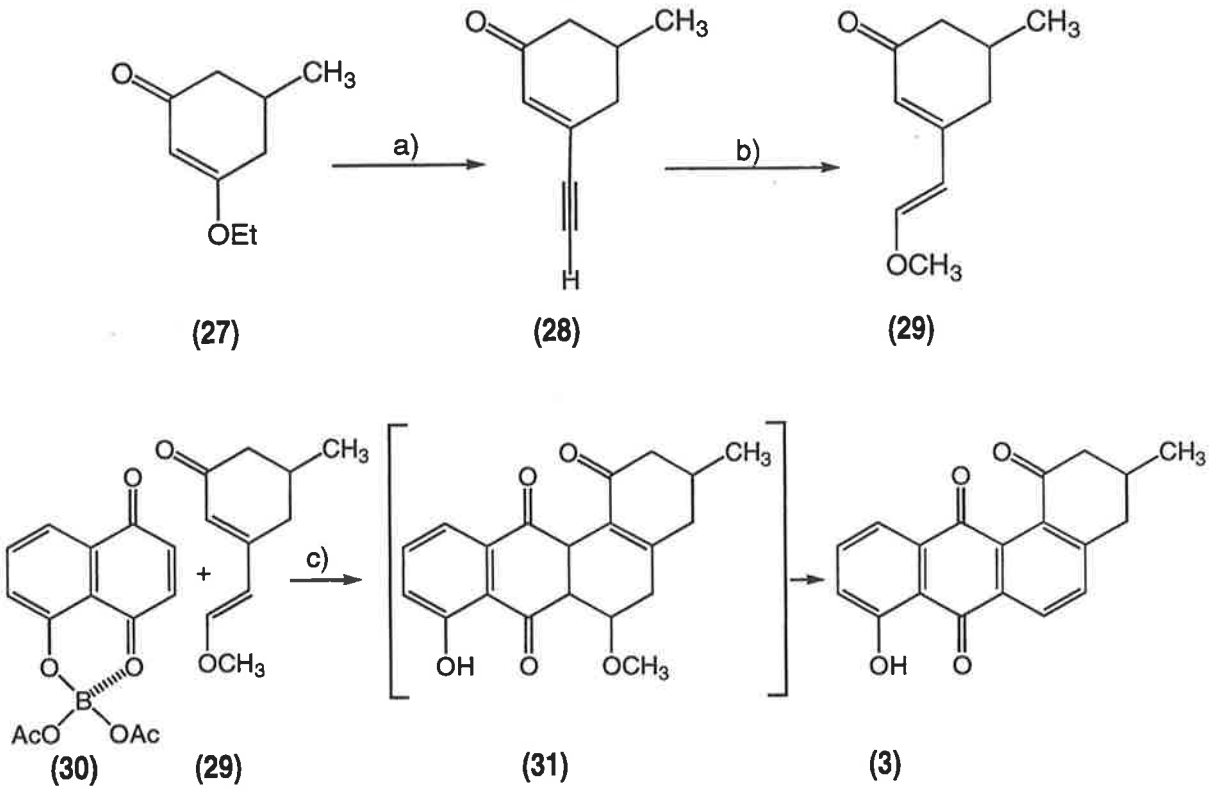

a) LiC ≡ CH, $H_2N(CH_2)_2NH_2$; b) MeOH, N-methylmorpholine 60% for the two steps; c) CH_2Cl_2 75%

Scheme 5. Synthesis of racemic **(3)** through a boron triacetate catalyzed Diels-Alder cyclisation.

[#] Boron triacetate was used to direct the facial regio-specificity and overcome the sluggish reactivity of the electron deficient dienone **(30)** through the electron withdrawing effect on the double bond of the dienophile **(31)**

Larsen and O'Shea have used the boron triacetate facilitated Diels-Alder procedure utilizing the condensation between a methoxy activated dienol and juglone to synthesize racemic rubiginone B_1 **(18)**,[33] B_2 **(16)**,[33] emycin A,[33,34] hatomarubigin B **(15)** and C **(17)**.[38] The authors also reported the first asymmetric synthesis of the natural angucyclinones (+) emycin A and (+) ochromycinone **(3)** *via* the kinetic resolution of a racemic diene in the Diels-Alder reaction promoted by a chiral Lewis acid.[31] The use of a methoxy-activated diene system allowed the formation of a stable, 4a,5 unsaturated, Diels-Alder adduct which was manipulated to effect concise entry to a model A ring aromatic and B ring hydroxylated angucyclinone related to TAN 1085 **(32)** and PD 116740 **(33)** (Scheme 6).[43]

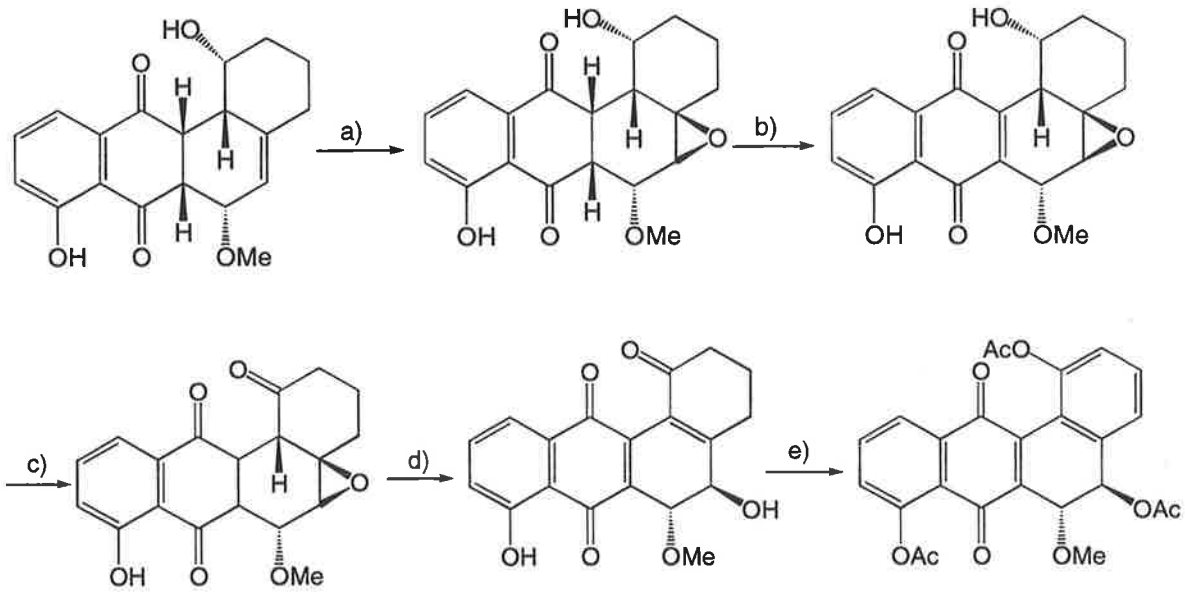

a) Dimethyldioxirane, 96%; b) MnO_2, 83%; c) Dess-Martin periodinate, 87%; d) silica gel, 89%; e) (i)Ac_2O, pyridine, (ii) ceric ammonium nitrate, 91%

Scheme 6. Entry to the ring systems of PD 116740 and TAN 1085.

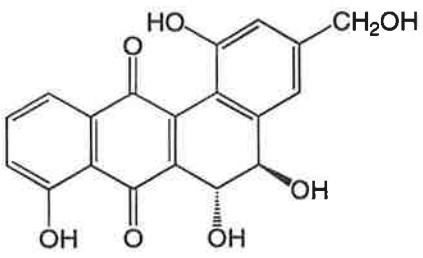

aglycone of TAN 1085 **(32)**

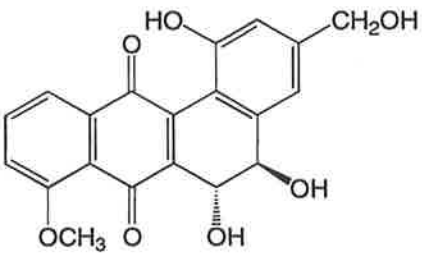

PD 116740 **(33)**

Synthetic approaches employing the chelating effect of the *peri*-hydroxy group of juglone[36] or 2-bromo or 2-chloro substituted naphthoquinone derivatives have also been used.[27, 39] This polarizes and activates dienophiles when reacted with polarized silyl ether containing dienes, in order to control the regioisomeric outcome of Diels-Alder condensations.

Krohn synthesized racemic rabelomycin **(11)**,[36] tetrangomycin **(1)**[27] and tetrangulol **(2)**[27] in good yields by condensing juglone **(34)** with either ketene acetal **(35)** or the siloxydiene **(36)** (Scheme 7), to give (non-isolated) Diels-Alder adducts which spontaneously aromatized and oxidized in air to form either a 1:1 mixture of the phenol **(37)** and ethyl ether **(38)** or the 6-deoxy benz[*a*]anthraquinone **(39)**. Treatment of the crude 1:1 phenol/ether mixture with tetrafluoroboric acid cleaved both the ether and the Ph-Si bond to give the dimethylfluorosilyl group. Rabelomycin **(11)** was generated by oxidative hydroxylation of the dimethylfluorosilyl group (KF, H_2O_2),[45] followed by photo-oxygenation of the resulting 1-deoxyrabelomycin. Racemic tetrangomycin **(1)** was made from **(39)** by applying the above chemistry to generate the 3-OH group followed by base catalyzed aromatisation of the A-ring to form **(2)**.

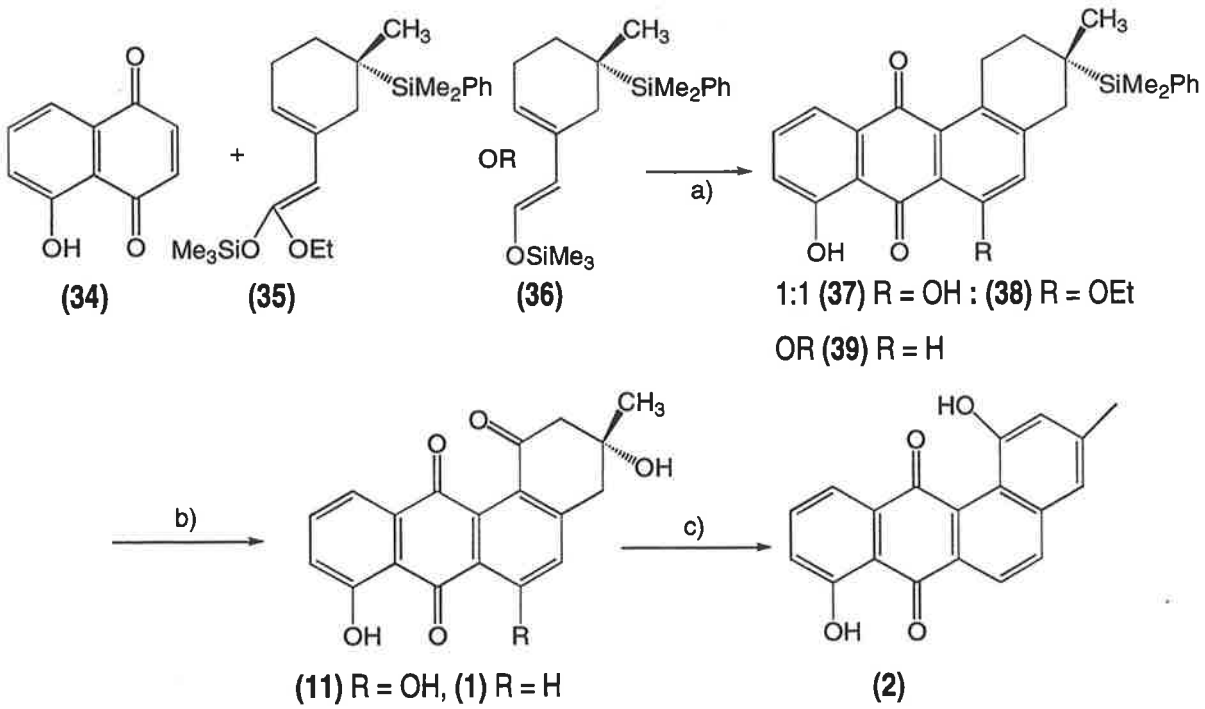

(34) **(35)** **(36)** 1:1 **(37)** R = OH : **(38)** R = OEt OR **(39)** R = H

(11) R = OH, **(1)** R = H **(2)**

a) CH_2Cl_2, 65% (35) (36) and 59% (37); b) (i) tetrafluoroboric acid (ii) KH, H_2O_2 (iii) sun light, O_2 56% (11) 33% (1); c) 1M NaOH 57%

Scheme 7. Synthesis of racemic rabelomycin **(11)**, tetrangomycin **(1)** and tetrangulol **(2)**.

Sulikowski has explored the synthesis of aquayamycin type angucyclines through a stereo and regio controlled cyclisation between a bromojuglone derivative **(40)** and the protected dienol **(41)** to generate the tetracyclic adduct **(42)** (Scheme 8).[47]

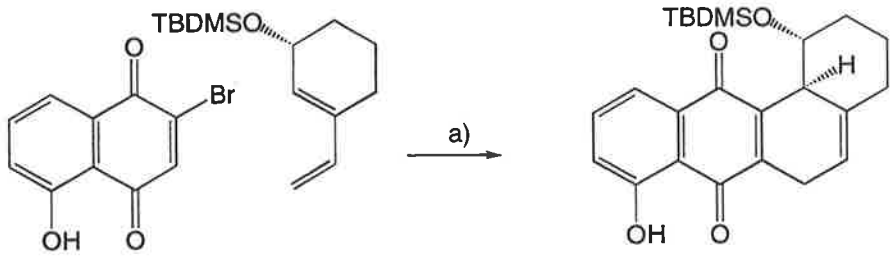

(40) **(41)** **(42)**

a) (i) Toluene, reflux, 74%; (ii) DBU, benzene, 90%

Scheme 8. Generation of tetracyclic Diels-Alder adduct **(42).**

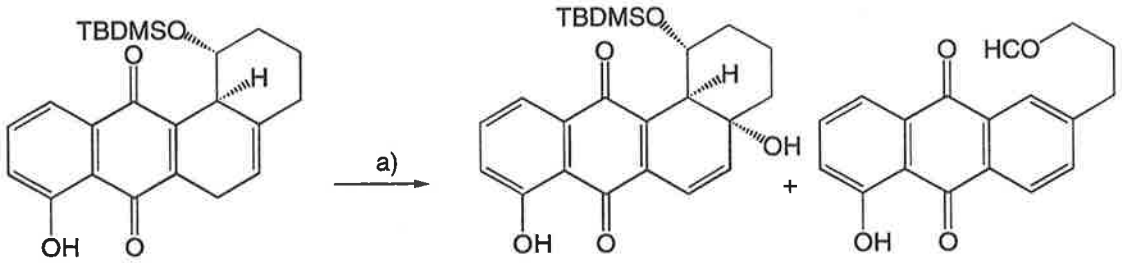

(42) **(43)** 24% **(44)** 27%

Scheme 9. Fragmentation of the A-ring during deprotection of the TBDMS group [a) $Bu_4N^+F^-$, THF].

Attempted deprotection of the protected 1-alcohol by treatment with anhydrous tetrabutylammonium fluoride generated two unexpected products, the carbinol **(43)** in 24% yield and the fragmentation product **(44)** in 27% yield (Scheme 9).

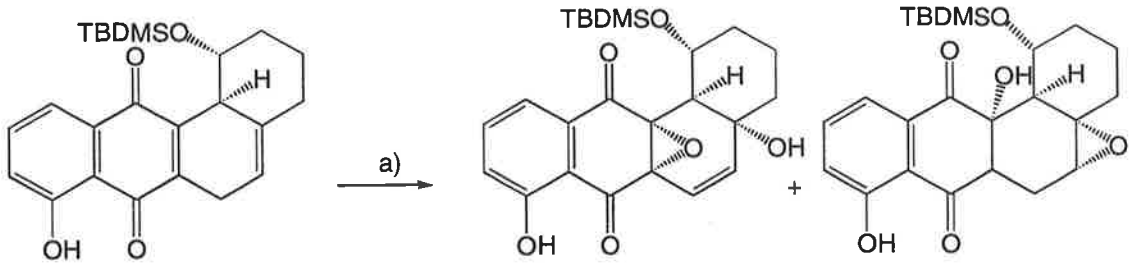

(42) **(45)** **(46)**

a) $Bu_4N^+F^-$, aq. THF,O_2

Scheme 10. Generation of epoxy alcohol **(45)**.

Treatment of adduct **(42)** with tetrabutylammonium fluoride in aqueous tetrahydrofuran under an atmosphere of oxygen gave the two new epoxy alcohol products **(45)** and **(46)** in 29% and 24% yields respectively (Scheme 10). The epoxy alcohol **(45)** possesses the correct bond connectivity and four of the five stereogenic centres present in the isotetracenone SF 2315B **(47)** a known bioactive compound.[1,2]

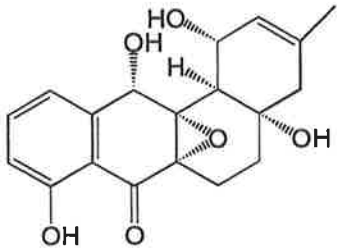

SF 2315 B **(47)**

The enantioselective synthesis of **(50)** is shown in Scheme 11.[44] The α-epoxide **(48)** undergoes an epoxide/allyl alcohol rearrangement using tetrabutylammonium fluoride to give allyl alcohol **(49)**. Several protection/deprotection steps followed by oxidation gave angucyclinone **(50)** which is closely related to SF 2315 A **(51)**.

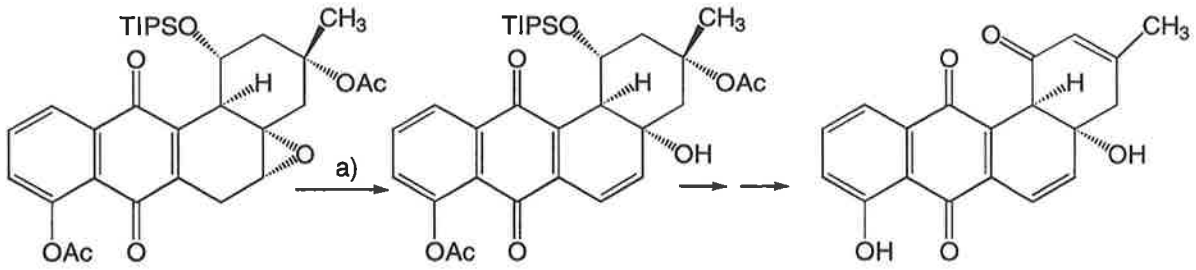

Scheme 11. Enantioselective synthesis of (+) angucyclinone **(50)** [a) (i) Ac_2O, (ii) TBAF 76%].

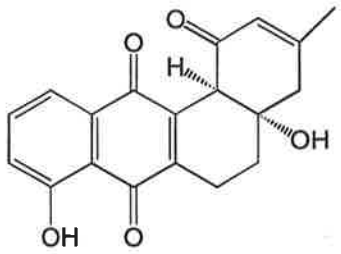

SF 2315 A **(51)**

Another interesting oxygenation of the B-ring of adduct angucyclinones, which has found widespread use in synthesis of tetrangomycin like compounds, was first reported by Boyd, Reibenspies and Sulikowski: *viz.* N-methylmorpholine N-oxide mediated oxidation of the 6 position of the B-ring.[48] Scheme 12 outlines this oxidation step in the total synthesis of landomycin A **(21)**.

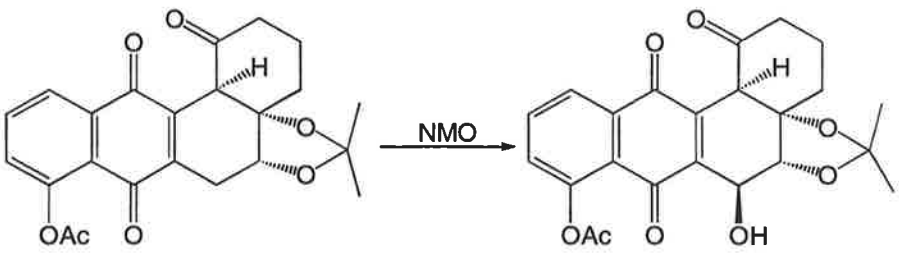

Scheme 12. N-methylmorpholine N-oxide mediated oxidation at the C-6 position.

Recent efficient enantioselective syntheses of (+) rubiginone B_2 **(58)** and (+) ochromycinone **(3)** were carried out by Carreno, Urbano and Di Vitta.[35] Their strategy involved reacting a racemic vinylcyclohexene **(55)** with enantiopure (S)-*p*-tolylsulfinyl naphthoquinone **(54)** in a Diels-Alder cyclisation (Scheme 13). The non-isolated cycloadduct **(56)** (attained from the favourable *anti-endo* transition in which the TBDMS and *p*-tolylsulfinyl groups are furthest away from each other as possible) spontaneously eliminates TolSOH at 0°C to form quinone **(57)**. Transformation of **(57)** to rubiginone **(58)** involves base catalyzed aerial aromatization of the B-ring, followed by HF facilitated removal of the TBDMS group and a Norrish type oxidation of the 1-alcohol.

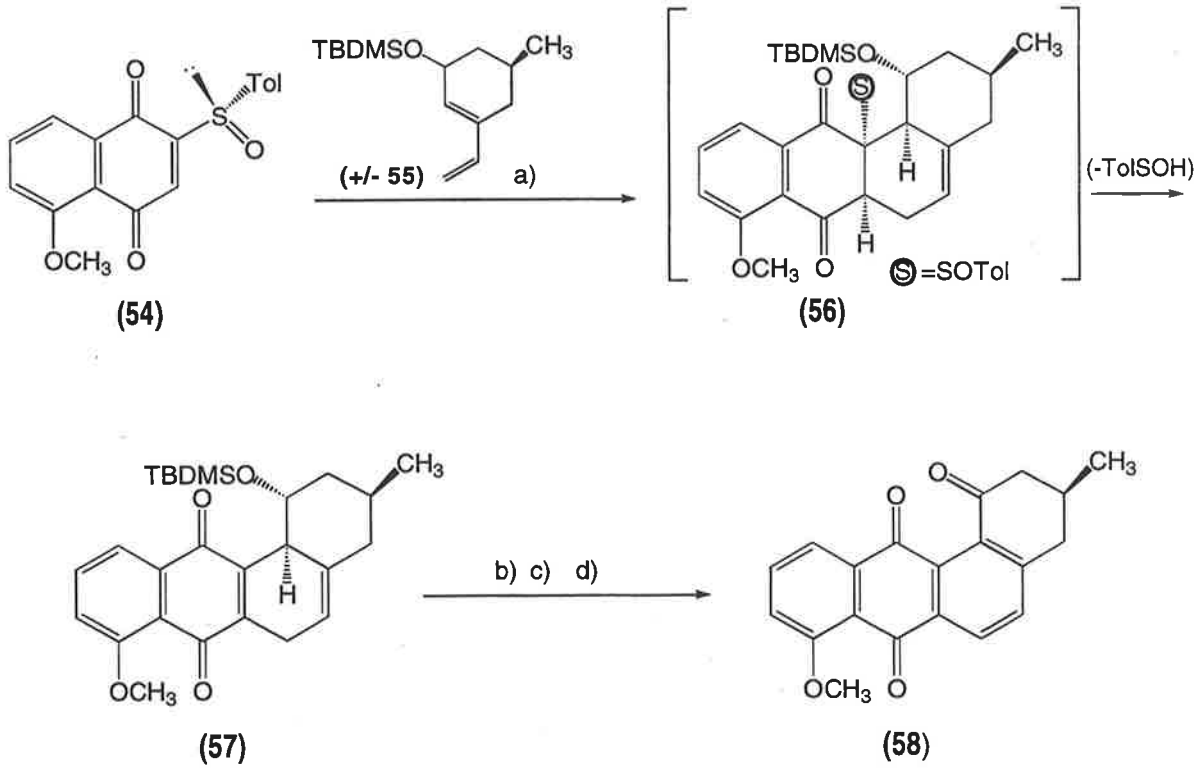

a) 2eq. **(55)**, CH_2Cl_2, 0°C, 48 hr, 75%; b) DBU, CH_2Cl_2, 0°C, 2 hr 81%; c) HF, CH_3CN, 20°C, 1 hr, 52%; d) hv, CH_2Cl_2, 20°C, 70%.

Scheme 13. Formation of (+)-rubiginone **(58)** by an asymmetric Diels-Alder cyclisation.

Transition Metal-Mediated Reactions

Gordon and Danishefsky attempted the synthesis of angucyclinone SF 2315 A **(51)** by employing a chromium (0) Fischer carbene complex benzannulation reaction.[49] This procedure is often used to generate the linearly condensed anthracyclinones, using a cycloalkyne to generate the BC ring system. Aldolisation of the quinone intermediate **(61)** then generates the required hydroxylated AB ring junction (Scheme 14). By appropriately functionalising the cycloalkyne **(60)** and the chromium-carbene complex **(59)**, a variety of angucyclines may be synthesized by this methodology.

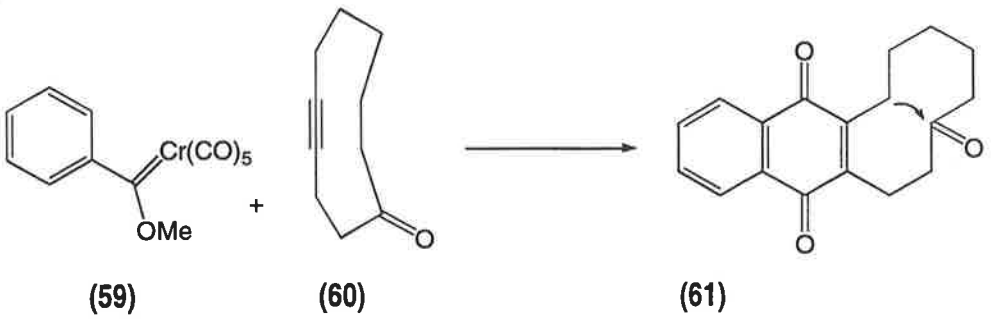

(59) **(60)** **(61)**

Scheme 14. Benzannulation reaction used in synthesis of quinone **(61).**

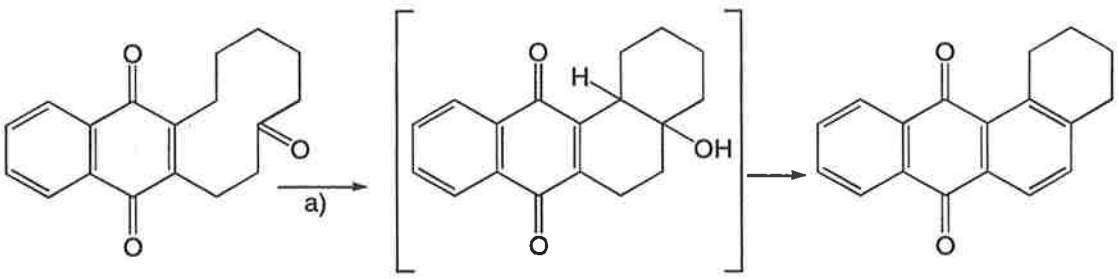

(61) **(62)** **(63)**

a) DBU, 20°C 65%

Scheme 15, Synthesis of model benzo[*a*]anthraquinone **(64).**

Treatment of the model ketone **(61)** (generated by benzannulation) with diazobicycloundecane at ambient temperature gave aldol intermediate **(62)** which eliminated water and aromatized to form the tetrahydrobenz[*a*]anthracene **(63)** in 65% yield (Scheme 15).[49]

Biomimetic-Type Syntheses

Yamaguchi *et al* were the first to exploit the biomimetic pathway to synthesize the 9 C-glycoside (L-olivose) containing (-) urdamycinone B **(13)**.[41] Recently, Krohn, Boker, Florke and Freud synthesized racemic rabelomycin **(11)** and tetrangomycin **(1)** by the biomimetic methodology shown in Scheme 16.[28]

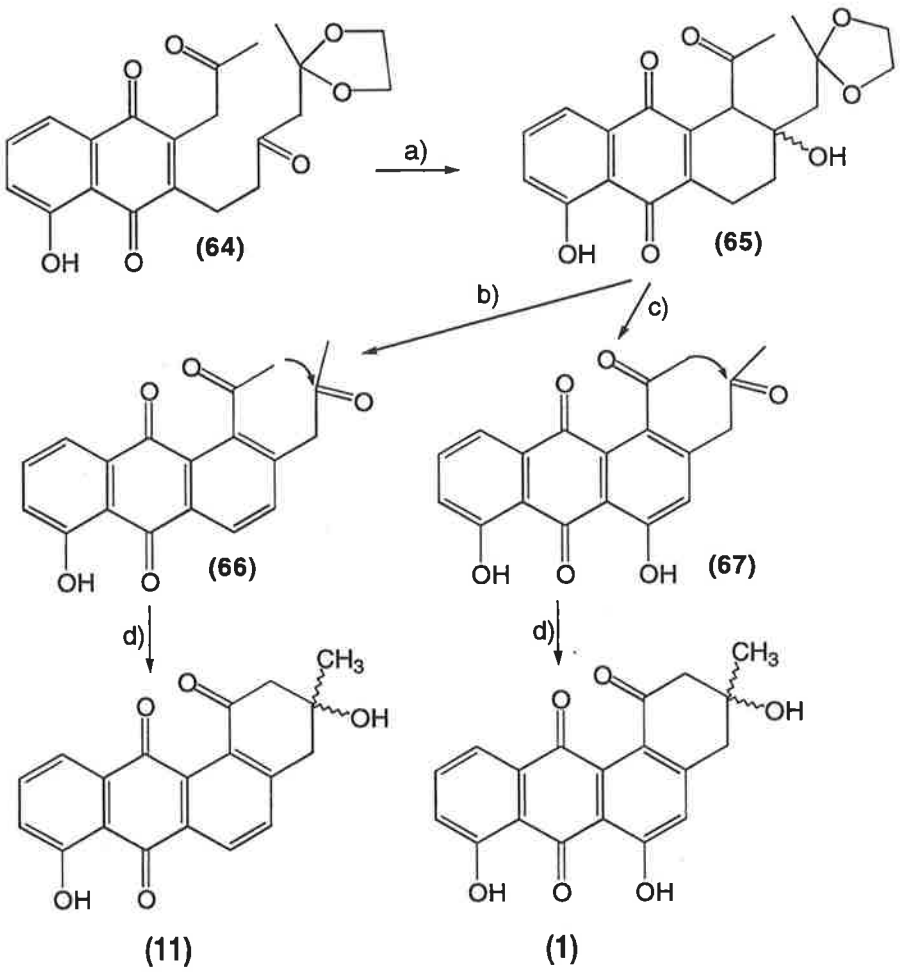

a) K_2CO_3/ isopropanol, 20°C, 66%; b) 1.2 eq. NMO, CH_2Cl_2, 40°C , 91%; c) 14 eq. NMO, CH_2Cl_2, 40°C, 54%; d) (i) SiO_2, H_2SO_4/CH_2Cl_2, 96%, (ii) 0.2N KOH, 90%.

Scheme 16. Synthesis of tetrangomycin **(1)** and rabelomycin **(11)** by the biomimetic pathway.

The key step used by Krohn *et al* to synthesise **(1)** and **(11)** was the base catalysed intramolecular aldol condensation of **(64)** to form the B-ring in **(65)**, followed by the introduction of a 6-hydroxy functionality into the B ring which enhanced aromatization through β-elimination of water (Scheme 16). The anthraquinone **(66)** was isolated in good yield when a moderate excess of N-methylmorpholine N-oxide (NMO) was used but the addition of a larger excess of NMO introduced an additional hydroxy group into the B-ring at position-6 to give **(67)** as the major product. Deprotection of **(66)** and **(67)** followed by a basic and kinetically controlled aldol condensation, gave racemic tetrangomycin **(1)** and rabelomycin **(11)** in good yields.

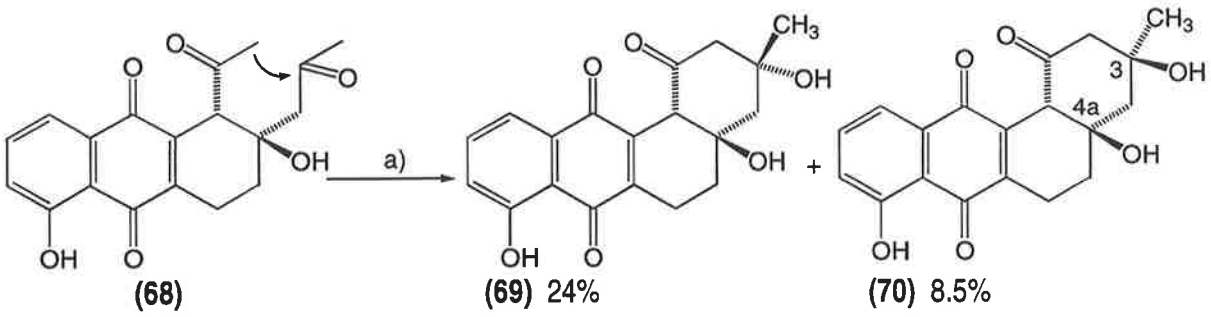

Scheme 17. Biomimetic-type syntheses of racemic angucyclinones **(69, 70)** of the SF 2315 type.

Mimicking nature may be advantageous in the synthesis of the *cis*-dihydroxylated aquayamycin **(4)** group of angucyclines, whose synthesis has so far remained elusive. In this context, treatment of racemic diketone **(69)**, with strong base gave trans diol **(69)** in a 24% isolated yield and the *cis* diol **(70)** in 8.5% yield (Scheme 17).[43] The *cis* diol product **(70)** has the same relative stereochemistry at positions 3 and 4a as aquayamycin **(4)** while the trans diol **(69)** has the stereochemistry of WP 3688-2 **(71)** type angucyclinones.[1]

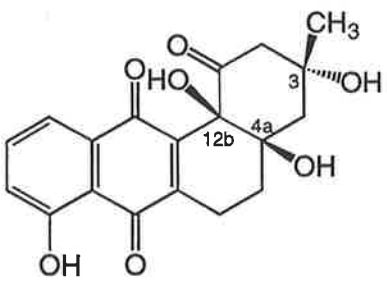

WP 3688-2 **(71)**

Annulation Type Reactions

A new method for the regiospecific synthesis of benz[*a*]anthraquinones and related angularly fused polycyclic compounds has been reported using squaric acid derived cyclobutenones.[50] This method relies on a dual annulation reaction: involving electrocyclic ring opening of appropriately substituted cyclobutenones to vinylketenes, and their subsequent reaction with ketenophiles. Scheme 18 shows the important aspects of this methodology for the synthesis of model benz[*a*]anthraquinone **(76)**. Cyclobutenone **(72)** undergoes a double ring closure (8π followed by 6π electrocyclization) upon mild thermolysis to give **(73)**. Treatment of **(73)** with phenyl cerium (III) chloride followed by acid hydrolysis gave cyclobutenone **(74)** which following thermalisation and oxidation gives the quinone **(75)**. Photofragmentation of **(75)** (as shown) yielded benz[*a*]anthraquinone **(76)**. This dual annulation sequence provides a regiospecific method for the syntheses of **(76)** and substituted derivatives.[50]

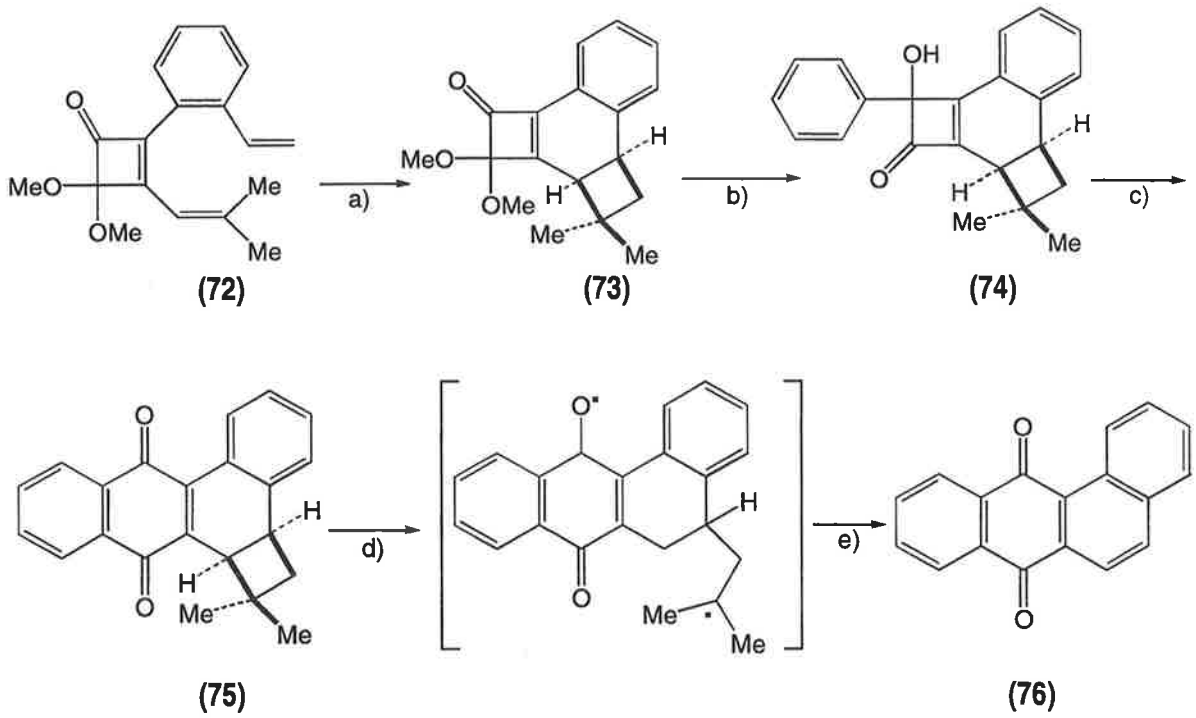

a) C_6H_6, 70°C, 90%; b) (i) PhLi, $CeCl_3$, THF, -78°C, (ii) HCl/THF; c) (i) C_6H_6, 70°C, (ii) Ag_2O, >90%; d) hv e) – C_4H_8, 87%

Scheme 18. Methodology leading to synthesis of model benz[*a*]anthraquinone **(76).**

Nucleophilic Reactions

3-Deoxyrabelomycin **(81)** has been prepared from the electron deficient naphthoquinone **(77)** in four steps in 17% overall yield.[37] Conjugate addition of 5-methylcyclohexane-1,3-dione to **(78)** followed by methylation gave **(79)** (Scheme 19), which on reaction with NaOH in methanol at elevated temperature gave the 8 methoxyanthraquinone **(80)** in a low yield. Deprotection of **(80)** using $AlCl_3$ gave 3-deoxyrabelomycin **(81)**.

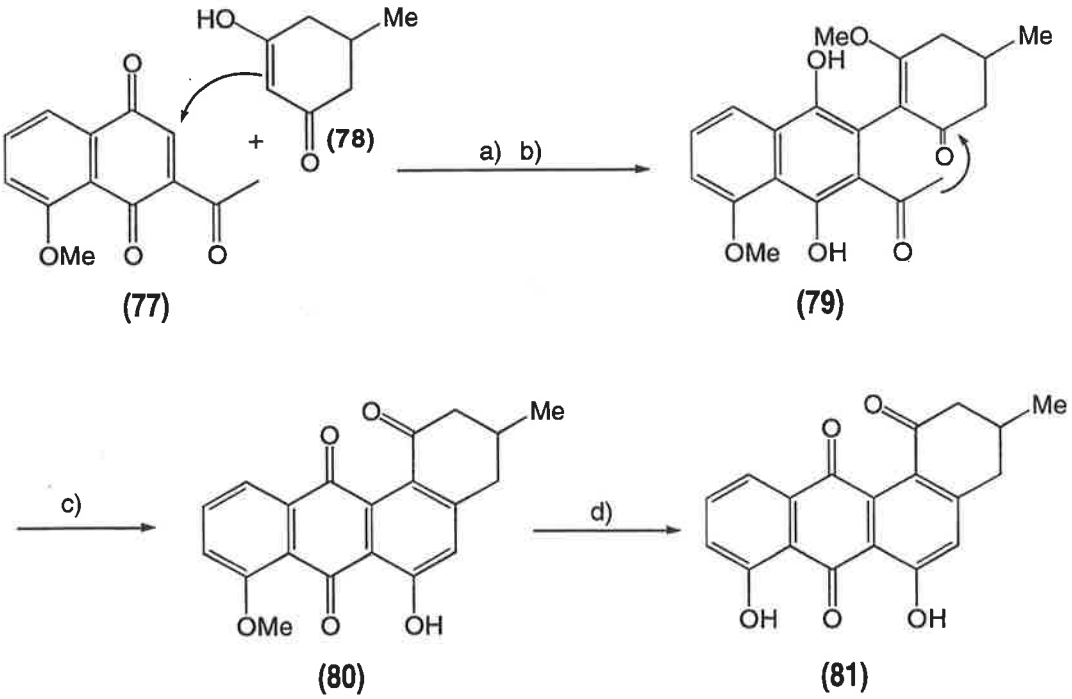

a) acetone, -20°C to 25°C; b) K_2CO_3, CH_3I, 64%; c) NaOH, CH_3OH, 140°C, 14 hr, 27%; d) $AlCl_3$, 25°C, 58%

Scheme 19. Synthesis of 3-deoxyrabelomycin.

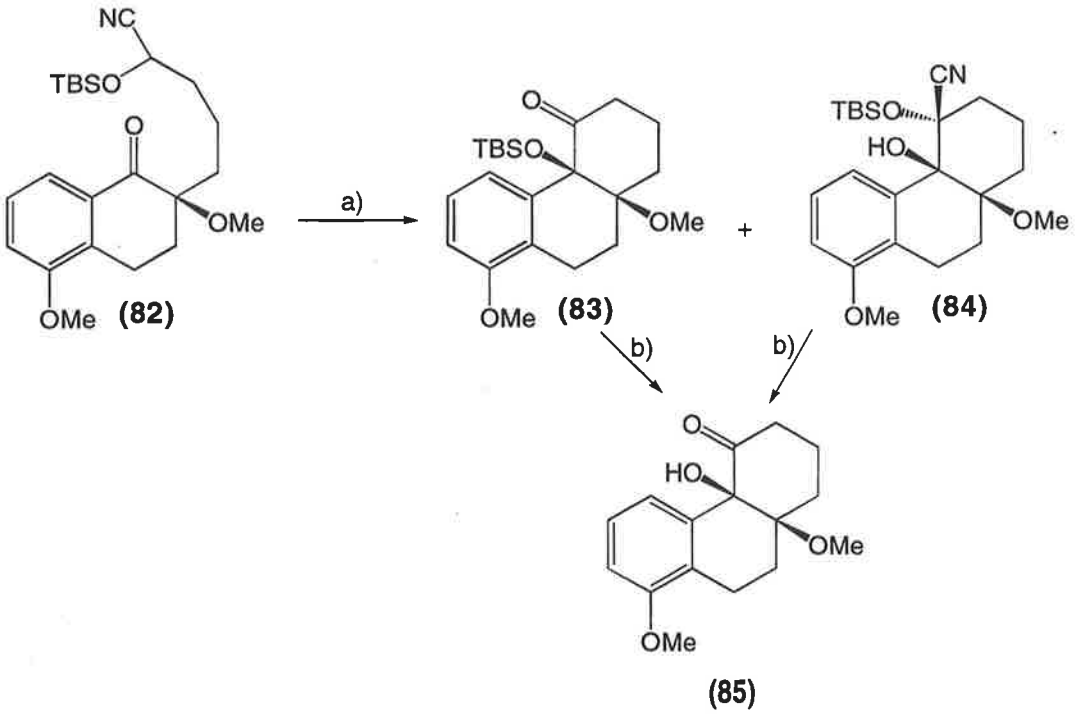

a) LDA, THF, -78°C, 3 hr; b) TBAF, 73%

Scheme 20. Synthesis of the A,B,C ring system of aquayamycin.

The synthesis of the A,B,C rings of aquayamycin **(4)** by a key intramolecular nucleophilic addition of the anion of a protected cyanohydrin to a ketone has been described.[51] Treatment of **(82)** with lithium diisopropyl amine afforded a mixture of the hydroxy ketone **(83)** and nitrile **(84)**. This mixture was treated with tetrabutylammonium fluoride to give α-hydroxy β-methoxy ketone **(85)**. The *cis* stereochemistry of the hydroxy and methoxy groups was confirmed by X-ray crystallography. This model chemistry may provide a possible approach to the A,B,C ring system of the cis dihydroxylated group of angucyclinones such as **(4)**.

Past Syntheses of Model Compounds Related to Ochromycinone by Our Research Group

Our research group has been involved in synthetic attempts towards angucyclinones based on the ochromycinone structure for a number of years. The overall aim of this project was to make a number of model angucyclinones, by an efficient route, so that such compounds could be tested for anticancer activity.

The model non-chiral system **(94)** was synthesised in poor overall yield as shown in Scheme 20.[52] The lack of chirality was accomplished through the insertion of an additional methyl substituent at position-3, creating a geminal dimethyl functionality.

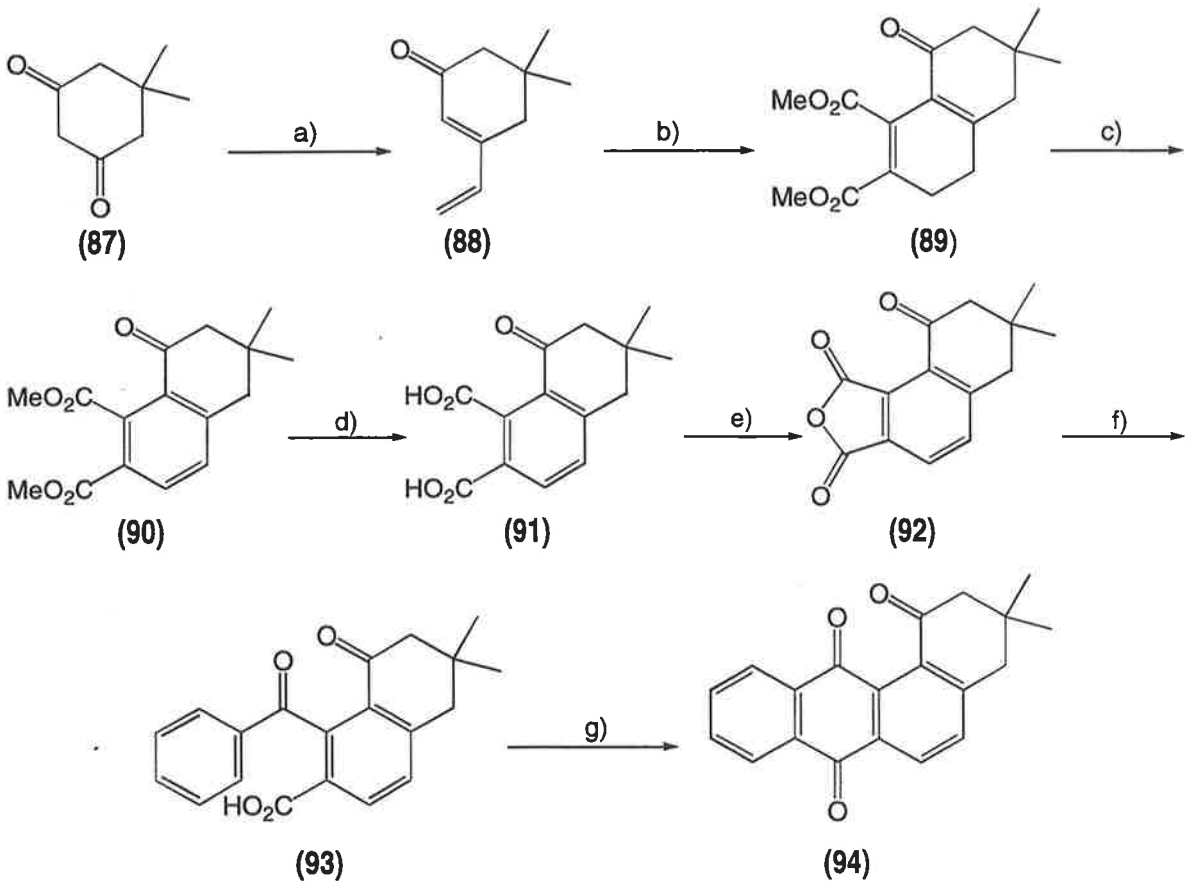

a) (i) HCl, EtOH, reflux, 16 hr, 59%; (ii) Mg, vinyl bromide, THF, reflux, 16 hr, (iii) 1M H_2SO_4, 10 min. 61%; b) dimethyl acetylenedicarboxylate, toluene reflux, 60 hr, 73%; c) NBS, CCl_3, reflux, 2 hr, 82%; d) 5% NaOH, reflux, 3 hr, 75%; e) acetic anhydride, reflux, 30 min. 90%; f) $AlCl_3$, benzene, reflux, 4 hr, 85%; g) H_3PO_4, 80°C, 5%.

Scheme 20. Formation of model angucyclinone **(94).**

Dienone **(88)** was made from dimedone **(87)** by conversion to the enol ether followed by a 1,2 Grignard addition of vinyl magnesium bromide. Rings A and B were created by a Diels-Alder condensation between dimethylacetylene dicarboxylate and dienone **(88)** followed by aromatization to yield the aromatic ester **(90)** which was converted through **(91)** to anhydride **(92)**. A Friedel-Crafts cyclisation between **(92)** and benzene gave two carboxylic acids e.g. **(93)**. Treatment of the acids with polyphosphoric acid, gave the required angucyclinone **(94)** in only 5% yield. The yield of the final reaction could not be improved, thus this synthetic route was abandoned.

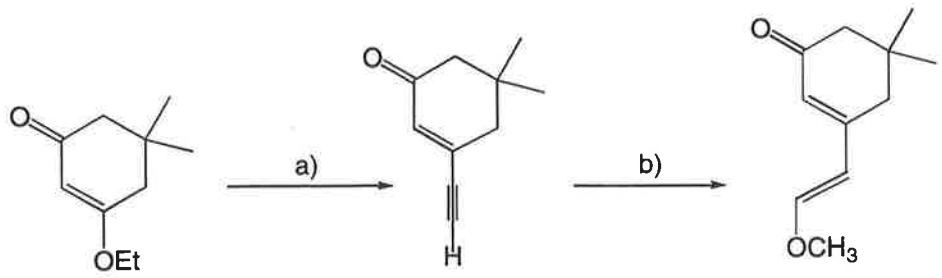

(95) **(96)** **(97)**

a) (i) $CeCl_3$, CH≡CMgBr, 20°C, 12 hr (ii) H_2SO_4, H_2O. CH_2Cl_2, 1 hr 85%; b) NMO, MeOH, benzene, 20°C, 96 hr, 83%

Scheme 21. Synthesis of methoxy activated dienone **(97).**

The second synthetic strategy was based on the Diels-Alder approach used by Guingard and Barretto in their synthesis of racemic ochromycinone **(3)**.[30] The polarized, methoxy activated dienone **(97)** was synthesized from the ethoxy enol **(96)** in two steps as shown in Scheme 21. Intermediates and products formed during the Diels-Alder condensations are shown in Scheme 22.

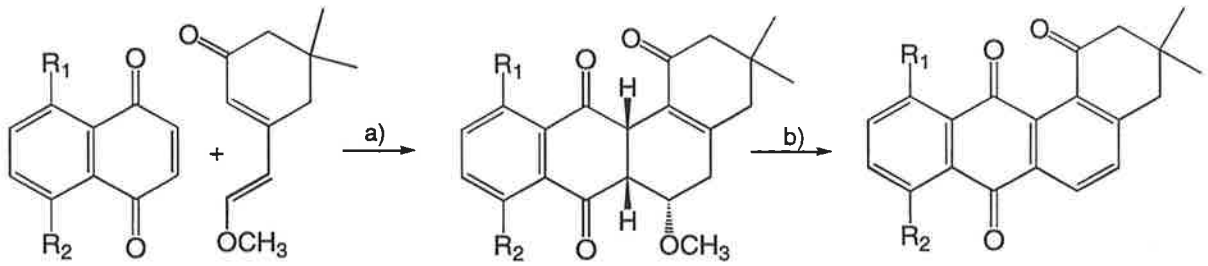

(98) $R_1 = R_2 = H$ **(97)** +/- **(99)** not isolated **(94)** $R_1 = R_2 = H$, 20%

(100) $R_1 = R_2 = OH$ +/- **(101)** $R_1 = R_2 = OH$, 27% **(102)** $R_1 = R_2 = OH$, 24%

a) toluene, reflux, 24 hr; b) DBU, CH_2Cl_2, air, 6 hr, 90%

Scheme 22. Synthesis of angucyclinone **(94)** and 8,11-hydroxy **(102)** by the Diels-Alder strategy.

Diels-Alder cyclisations with unsymmetrical 1,4-naphthoquinones such as juglone can lead to a mixture of products.[53] Standard Lewis acid conditions, utilizing boron triacetate, were used to catalyse and direct the facial selectivity of the Diels-Alder cyclisations between complexes **(103, 106)** and dienone **(97)** to form the adducts **(104, 107)**, which convert smoothly to fully aromatic **(105)** or **(108)** upon treatment with diazobicycloundecane (DBU) (Scheme 23).[30,54] X-ray crystallographic investigations confirm the relative stereochemistry and molecular structure of adduct **(107)** and angucyclinone **(108)** as that outlined in Scheme 23.#

Refer to Publications Section, paper no. 1, for Ortep generated graphical representations of **(107)** and **(108)**

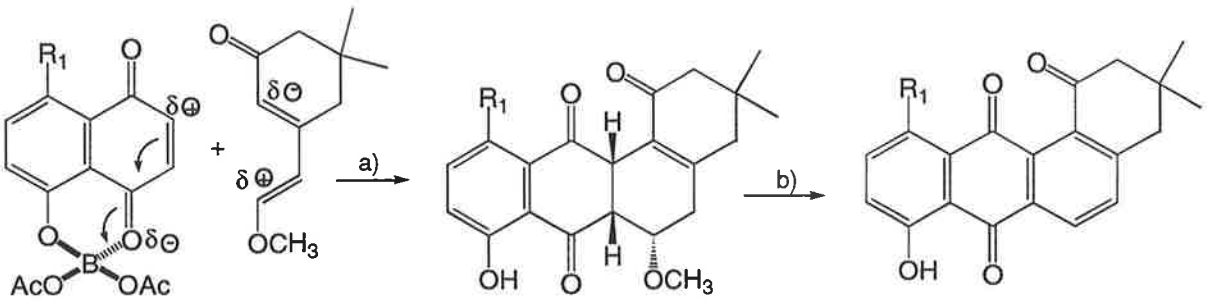

(103) R_1 = OMe **(97)** +/- **(104)** R_1 = OMe, 16% **(105)** R_1 = OMe, 30%

(106) R_1 = H +/- **(107)** R_1 = H, 59% **(108)** R_1 = H, 52%

a) CH_2Cl_2, 20°C, 2 hr; b) DBU, CH_2Cl_2, air, 20°C, 6 hr, 88%

Scheme 23. Synthesis of ochromycinone analogue **(108)** and 8-OH 11-OMe analogue **(105).**

The Diels-Alder synthetic strategies shown in Schemes 22 and 23 give the angucyclinones **(94,102,105,** and **108)** in 10 – 13% overall yield starting from dimedone (40 – 50% yields for the initial Diels-Alder reactions).

Current Aims

The aims of the present study are; (i) to synthesize the 11-hydroxy isomer of ochromycinone analogue **(108)** in order to explore structure function relationships of the D-ring, (ii) utilize the Diels-Alder adducts to initiate a synthetic methodology towards the more complex 12b,4a oxygen containing angucyclinones such as the sakyomycins **(5)**, (iii) to develop a synthetic methodology towards A and B-ring oxygenated angucyclinones and (iv) to explore the biological activities of angucyclinone analogues made.

Chapter 2. Synthesis of the 11-Hydroxy Ochromycinone Analogue

2.1. Introduction

The lack of any reported systematic structure/ function relationships in the angucyclinone family led us to investigate this feature. First, we require a simple synthesis of the 3 geminal dimethyl analog of ochromycinone where the phenolic functionality is in the 11 position **(109)**. The biological activity of this isomer and the previously synthesized isomer **(108)** will then be determined and compared.[#]

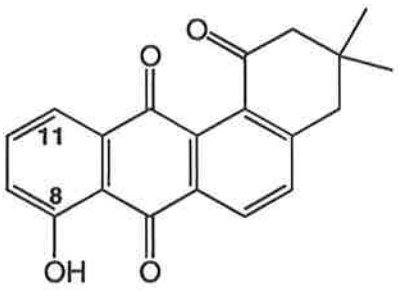

(108)

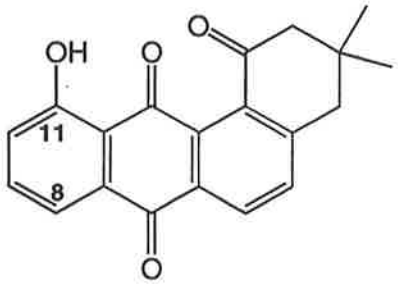

(109)

The most concise strategy for the construction of the 11 isomer **(109)** was the Lewis acid facilitated Diels-Alder condensation.[#] The opposite facial stereochemistry of **(109)** was generated by utilizing an appropriately polarized diene system **(111)** where upon condensation with juglone the facial selectivity would be reversed (Scheme 24).[39] The diene **(111)** was to be formed from the previously synthesized ketone **(88)** (Scheme 25).[52]

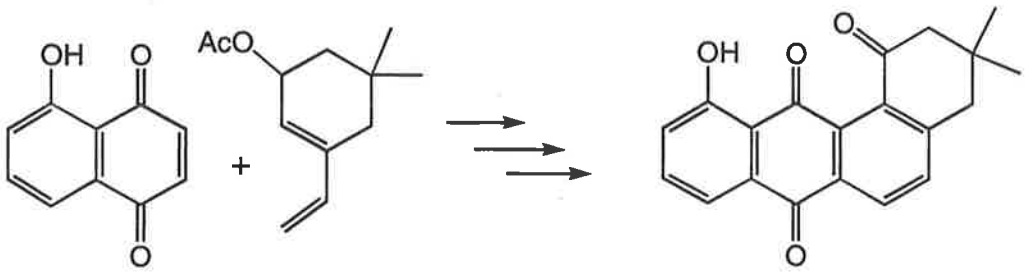

(34) **(111)** **(109)**

Scheme 24. Plan for the synthesis of the 11-hydroxy ochromycinone analogue **(109)**.

[#] Refer to Chapter 1.3, page 25

2.2. Reduction and Protection of Ketone (88)

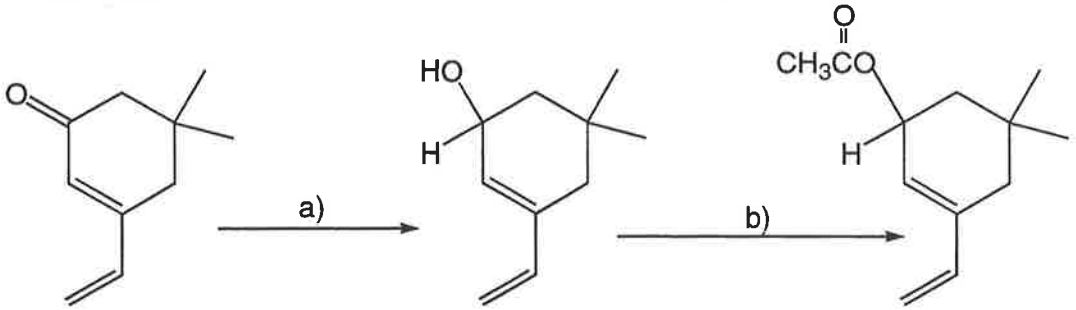

(88) **(110)** **(111)**

a) $CeCl_3$, $NaBH_4$, MeOH, 20°C, 30 min. 76%; b) CH_3COCl, pyridine, CH_2Cl_2, 20°C, 2 hr, 72%

Scheme 25. Synthesis of reactive dienol acetate **(111).**

The alcohol **(110)** was formed from the ketone **(88)** in good yield by utilizing the Luche reduction.[55] The Lewis acid [cerium (III) chloride] activates the carbonyl of the diene **(88)** which is then reduced specifically with sodium borohydride over a period of 15 minutes (Scheme 25). The doubly conjugated unsaturated ketone **(88)** requires the assistance of the Lewis acid ($CeCl_3$) not only to activate the carbonyl functionality towards reduction but also to effect the reduction of the carbonyl group rather than the diene centre.

The alcoholic product **(110)** is unstable and is best used immediately, however **(110)** can be stored at 0°C when dissolved in any dry solvent. Prolonged storage even at -20°C necessitates purification by chromatography before use. Flash chromatography of the stored mixture gives significant amounts of dimerised **(110)** as well as some polymeric material. The electron donating hydroxyl functionality does activate the product sufficiently for Diels-Alder reactions.[#] However, protection of the alcohol as the acetate **(111)** forms a more stable species.

The use of acetate **(111)** in the Diels-Alder condensation will lead to better stereospecificity (because of the steric bulk of the acetate) by favouring the formation of an *anti endo* transition state. In contrast, diene alcohol **(110)** cannot discriminate between the *anti* or *syn endo* transition states and therefore is likely to produce a mixture of diastrereomeric products upon condensation.[56]

[#] The condensation outcome of diene **(110)** and naphthoquinone will be discussed in Chapter 3.2

The mass spectrum of **(110)** indicated a molecular ion at *m/z* 152, which loses water; results consistent with the expected mass and fragmentation pattern of this alcohol. Other than the characteristic resonances of the geminal dimethyl group, the ^{1}H n.m.r. spectrum of **(110)** showed a broad singlet corresponding to the 2 vinylic hydrogen, followed by a doublet of doublets at 6.38 ppm coupled to the terminal CH_2 end of the vinyl group with coupling constants of 17.7 and 10.8 Hz. The larger of the two coupling constants is due to the interaction of the two *trans* hydrogens. The hydrogen of the hydroxyl group shows a broad singlet at 4.36 ppm.

The acetylation of **(110)** utilizing standard acetyl chloride/pyridine conditions gives the protected alcohol acetate **(111)** in 72% yield. This species was purified by flash chromatography and is more stable than the alcohol **(110).** The mass spectrum of **(111)** showed a molecular ion at *m/z* 194 which fragments competitively by the losses of acetic acid and CH_2CO. The ^{1}H n.m.r. spectrum of **(111)** is similar to that of **(110)**, except for the extra acetate methyl resonance at 2.15 ppm.

2.3. Boron Triacetate Facilitated Diels-Alder Cyclisation

Standard Diels-Alder cyclisations with unsymmetrical quinone starting materials such as juglone **(34)**, usually produce two regio-isomers.[54] The outcome of this cyclisation can be changed in favor of only one regioisomer when a non-symmetrical, polarized and activated diene system such as the "Danishefski diene" [essentially a trimethyl silyl trapped enolised α,β-unsaturated ketone] is used. This strategy was used by Danishefski to synthesize vineomycin B_2 aglycone using halogenated benzoquinones and siloxydienes.[57] More recently, a number of research groups have used a variation of the above method to construct angucycline aglycones by utilizing halogenated naphthoquinones in order to control the regiochemistry.[27, 36, 39, 47, 48] The pioneering work of Guingant and Baretto relied on the condensation of an electron deficient diene with juglone.[30] The lack of reactivity of the diene was counteracted by catalyzing the cyclisation with boron triacetate, which coupled to the 5-hydroxy substituent of juglone, directing the regioisomeric outcome of the reaction.

The Lewis acid of choice used in these cyclisations is either boron triacetate or tetra-O-acetyldiborate [see Brown and Stocky[58] for a discussion of the use of an oxy bridged borate structure versus a simple monomeric triacetate], however other Lewis acids such as trimethylborate can also be used.[59] Chiral Lewis acids are necessary when the dienophile is used to generate asymmetric induction through the complexing of the Lewis acid to the quinone.[31] In these cases the chiral Lewis acid is prepared from BH_3.THF and a chiral ligand.

Boron triacetate was prepared by heating boric acid in excess acetic anhydride.[60] Upon storage, boron triacetate converts into tetra-O-acetyl diborate. Boron triacetate can also be made *in situ* by the reaction between the BH_3.THF complex and three equivalents of glacial acetic acid.[54]

Reversal of the ground state polarization of the diene system (through the deletion of the methoxy functionality and reduction of the ketone to a protected alcohol) should reverse the regio-chemical outcome of the Diels-Alder condensation compared with that obtained in previous work.[53] This should produce the isomer having the phenolic functionality at position-11.

The regio-chemical outcome for the formation of the 11-hydroxy adduct **(113)** [which subsequently aromatises to give the angucyclinone **(109)**] is outlined in Scheme 26. Two regio-isomeric approaches of the diene to the boron triacetate-juglone complex are possible, but if the cycloaddition is kinetically controlled and concerted, the transition state with maximum interaction of the frontier orbitals should be the one that directs the formation of the product. The electron withdrawing impact of the interaction between the electron deficient boron and the oxygen of the carbonyl of complex **(112)** strongly polarizes the 2,3 double bond of the dienophile. The inductively electron donating acetate at position 1 of the racemic diene **(111)** also polarizes the molecule in such a way as to form the required 11-hydroxy adduct **(113)**.

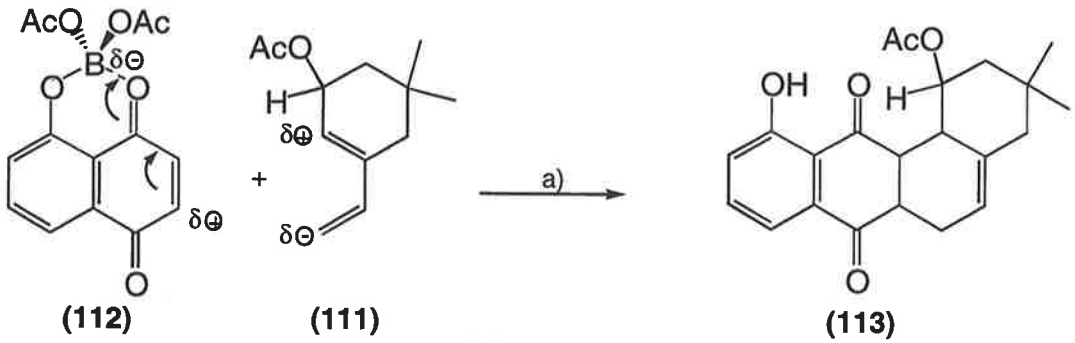

Scheme 26. Regiochemical outcome of the Lewis acid facilitated Diels-Alder reaction.

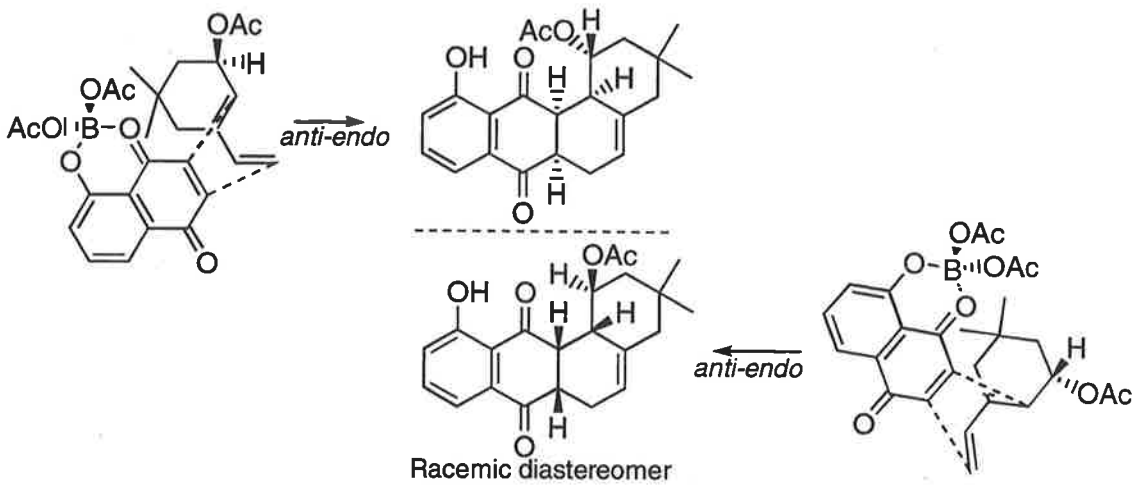

Scheme 27. *Anti endo* approach between the diene and dienophile rationalizing the stereochemistry of the adduct.

Due to the planar nature of dienophile **(112)**, the transition state of this reaction can be attained equally well from each plane. If only the symmetry allowed cycloaddition for the *endo* transition state is facile, the 1 acetate will take up an orientation which will minimize the steric interactions with the dienophile whilst maintaining the secondary-orbital interactions in the transition state. This predicts the formation of the single racemic diastereoisomer shown in Scheme 27, with an *anti* periplanar relationship between the 1 and 12b hydrogens. The cycloadduct **(113)** was isolated from the condensation reaction mixture with when the system is maintained under a nitrogen atmosphere. Subsequent purification by crystallization from dichloromethane/ diethyl ether gave **(113)** in 74% yield.

The gradient hetero nuclear quantum correlation (GHMQC) and the gradient heteronuclear multiple bond correlation (GHMBC) experiments (summarized in Appendix, NMR Section, Table 2) were used to confirm the framework and general structure features of adduct **(113)**. The GHMQC is a two dimensional, heteronuclear (atoms of different type) experiment used to determine which hydrogen atoms are directly attached to which carbon atoms. For example:

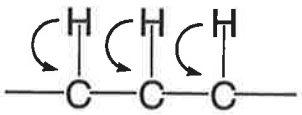

The GHMBC is a long range, two dimensional, heteronuclear experiment used to determine which hydrogen atoms are adjacent to which carbon atoms. For example:

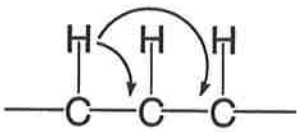

Correlated spectroscopy (COSY) experiments were used to elucidate coupling partners (Appendix, NMR Section, Table 1). The COSY experiment is a two dimensional homonuclear (atoms of the same type) experiment used to determine which hydrogen atoms are adjacent to each other (coupling partners). For example:

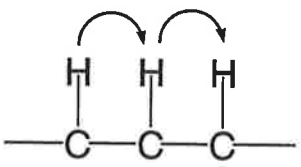

The ^{1}H n.m.r. spectrum of **(113)** showed very broad signals for H1, H6a, H12a, H12b: no coupling constant data were available for these signals. This makes interpretation using the vicinal Karplus correlation ambiguous and hence determination of the stereochemistry of the cycloadduct could not be made with certainty. Variable temperature experiments allowed for some sharpening of these signals, but ultimately failed to yield useful coupling data.

We attribute the broadening of these signals to rapid interconversion of the chair and boat forms of the A-ring of **(113)**. Theoretical calculations at the AM1 semi empirical level of theory reveal that the chair and boat forms of **(113)** lie within 3 kJ mol^{-1} of each other: the derived heats of formation were -743; and -740 kJ mol^{-1} respectively.[#]

Formation of a single diastereomer is confirmed from the ^{13}C n.m.r. spectrum of **(113)**, which shows sharp single peaks for all carbon resonances. Based on previous work of Frank *et* al, Carreno, and Larsen *et al*, the formation of a single racemic diastereomer is not unusual.[31, 33, 35, 56, 61]

Mass spectrometric analysis of the molecular ion at *m/z* 368 showed competitive losses of acetic acid and CH_2CO followed by the loss of a methyl radical. The infrared spectra shows carbonyl absorptions at 1731 (acetate carbonyl), 1703 and 1645 (peri OH-bonded carbonyl) cm^{-1}. We were unable to obtain crystals of **(113)** that were suitable for an X-ray study. However, since the regio and stereochemistry of the partially oxidized angucyclinone **(114)** [directly arising from **(113)** – see later] through an aerial oxidation is known, the relative stereochemistry of **(113)** is that depicted in Scheme 27.

[#] Calculations were performed by Dr D. K. Taylor on Silicon Graphics workstations, using the SPARTAN suite of programs; Wave function, Inc., 18401 Von Karman Avenue, Suite 370, Irvine, CA 92715, U.S.A.

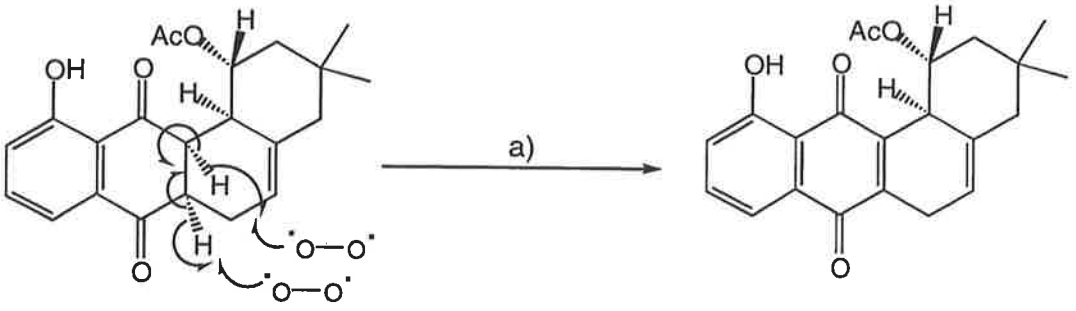

(113) **(114)**

a) SiO_2, O_2, 1 hr, 70%

Scheme 28. Aerial oxidation of **(119)** to give partially aromatized angucyclinone **(120).**

Absorption of adduct **(113)** onto silica, followed by exposure to air for 72 hr, cleanly oxidized the adduct into the fully B-ring aromatic angucyclinone **(115)** [see later in Scheme 29]. Shorter exposure to air (1 hr) led to the production of a partially oxidized angucyclinone product with a molecular ion two mass units lower than that of adduct **(113)**. The most likely mechanism for the partial oxidation of **(113)** is outlined in Scheme 28 where the point of unsaturation is the 6a,12a ring junction. This oxidation of the C-ring is analogous to similar oxidations in cognate systems.[36, 39, 33, 61] Elution of this product from the silica with dichloromethane followed by crystallization from dichloromethane / hexane gave pure angucyclinone **(114)** in 70% yield.

The structure of **(114)** was confirmed by n.m.r. techniques like those used for adduct **(113)**, including the GHMBC, GHMQC and COSY experiments summarized in Tables 1 and 2. The electron-impact positive-ion mass spectrum of **(114)** failed to give a molecular radical cation. However the negative ion electrospray ionization spectrum, gave a $(M-H)^-$ parent ion at *m/z* 365 which fragmented by loss of acetic acid.

Theoretical calculations at the AM1 semi empirical level of theory (carried out by Dr D. K. Taylor) reveal that the chair and boat forms of **(114)** lie within 10 kJ mol^{-1} of each other: the derived heats of formation were -663; and -653 kJ mol^{-1} respectively. The larger difference for the heats of formation of these two conformers [compared with those for **(113)**] is in accordance with the reduction in conformational mobility of rings A and B through the inclusion of the extra double bond in ring B. The ^1H n.m.r. spectrum reflects this result and good coupling information allowed the assignment of the stereo-chemistry of **(114)**.

The ^{1}H n.m.r. spectrum of **(114)** exhibits complex splitting patterns which are summarized in Table 1. The overall proton spectrum was that of a classical angucyclinone intermediate. There is a large coupling constant of 11.0 Hz between H12b and H1: Karplus correlation thus indicates an anti-periplanar relationship between the two axial protons approximating a dihedral angle of 180°. The splitting pattern of H1 (doublet of triplets) with the large coupling constant of 11.0 Hz to one of the H2 hydrogens suggests another anti-periplanar relationship with the axial proton of H2. The equatorial proton H2 has a 4 Hz coupling constant with H1 indicating a small dihedral angle of less than 45°.

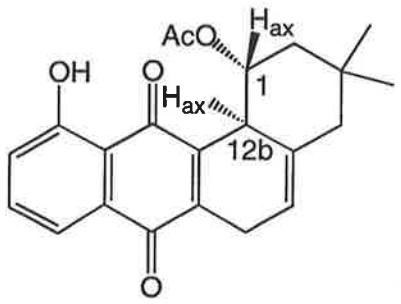

(114)

^{1}H ppm	Assign ment	Area	Multiplicity Coupling Constants	COSY	Long range COSY
12.0	C11-OH	1	s	-	-
7.61	H8	1	dd, 7.2, 1.2 Hz	H9, H10	H9, H10
7.58	H9	1	dt, 7.2, 1.2 Hz	H8, H10	H8, H10
7.23	H10	1	dd, 7.2, 1.2 Hz	H9, H8	H9, H8
5.64	H5	1	bs (7 Hz 1/2 W)	$H4_{ax}$, $H6_{ax}$, $H6_{eq}$	$H4_{ax}$, $H6_{ax}$, $H6_{eq}$,H12b
4.69	$H1_{ax}$	1	dt, 11.0, 4.0 Hz	$H2_{ax}$, $H2_{eq}$, H12b	$H2_{ax}$, $H2_{eq}$, H12b
3.67	$H12b_{ax}$	1	dddd, 11.0, 5.0 Hz	H1, $H6_{eq}$	H1, $H6_{eq}$, H5, $H6_{ax}$
3.41	$H6_{eq}$	1	bdm 25.0 Hz (7 Hz 1/2 W)	H5, $H6_{ax}$, H12b	H5, $H6_{ax}$, H12b, $H4_{eq}$
3.23	$H6_{ax}$	1	bdm 25.0 Hz (7 Hz 1/2 W)	H5, $H6_{eq}$, H12b	H5, $H6_{eq}$, H12b
2.05	$H4_{ax}$	1	bd, 26.0 Hz	$H4_{eq}$, H5	$H4_{eq}$, H5
2.01	$H4_{eq}$	1	bd, 26.0 Hz	$H4_{ax}$, $H6_{eq}$	$H4_{ax}$, $H6_{eq}$, $H2_{eq}$
1.87	$CH_{3\ acetate}$	3	s	-	-
1.79	$H2_{eq}$	1	dd, 11.0, 4.0 Hz	H1, $H2_{ax}$	$H4_{eq}$
1.73	$H2_{ax}$	1	t, 11.0 Hz	H1, $H2_{eq}$	CH_{3eq}
1.09	CH_{3ax}	3	s	-	-
0.95	CH_{3eq}	3	s	-	$H2_{ax}$

Table 1. Summary of ^{1}H n.m.r. data for **(114)**. The coupling constant of broad signals was calculated where possible from the with of the peak at half the amplitude and is referred to as n Hz ½ W (n = coupling constant).

\\

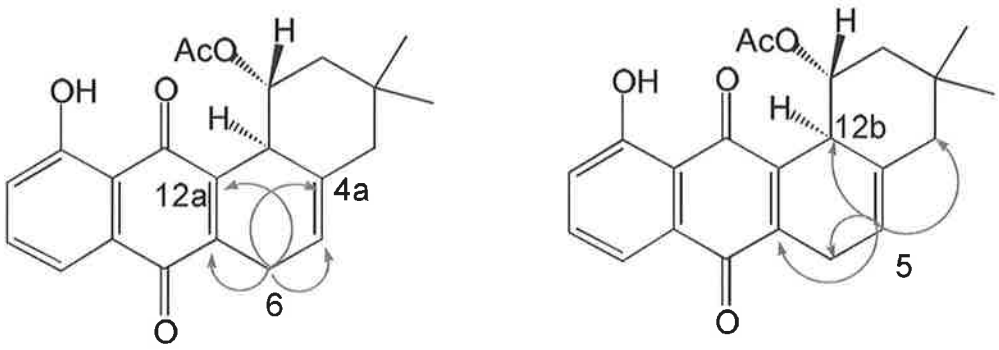

Figure 1. GHMBC correlations confirming location of unsaturation in **(114).**

The GHMBC correlations in **(114)** shown in Figure 1 confirm the location of the double bonds in the B-ring. All GHMBC and GHMQC ^{13}C experiments are summarized in Table 2. Carbon 6 correlates strongly to the four allylic carbons C4a, C5, C6a and C12a. Carbon 5 interacts with C4 and C6, the allylic C6a and finally C12b.

^{1}H ppm	Assign ment	HSQC ^{13}C ppm	Assign ment	HMBC ^{13}C
12.0	C11-OH	161.99	C11	-
7.61	H8	118.90	C8	C10, C11, C11a
7.58	H9	136.02	C9	C7, C10, C11a
7.23	H10	123.96	C10	C8, C11a
5.64	H5	118.98	C5	C4, C6a, C6, C12b
4.69	$H1_{ax}$	74.26	$C1_{ax}$	-
3.67	$H12b_{ax}$	41.98	$C12b_{ax}$	-
3.41	$H6_{eq}$	25.60	$C6_{eq}$	C4a, C6a, C5, C12a
3.23	$H6_{ax}$	25.60	$C6_{ax}$	C4a, C6a, C5, C12a
2.05	$H4_{ax}$	47.81	$C4_{ax}$	CH_{3eq}, C2, C3, C4a, C5, C12b
2.01	$H4_{eq}$	47.81	$C4_{eq}$	CH_{3eq}, C2, C3, C4a, C5, C12b
1.87	CH_3, $C1_{acetate}$	21.07	CH_3, $C1_{acetate}$	$C1_{acetate}$ (171.06)
1.79	$H2_{eq}$	46.09	$C2_{eq}$	CH_{3ax}, CH_{3eq}, C1, C3, C4, C12b
1.73	$H2_{ax}$	46.09	$C2_{ax}$	CH_{3ax}, CH_{3eq}, C1, C3, C12b
1.09	CH_{3ax}	31.86	CH_{3ax}	CH_{3eq}, C2, C4
0.95	CH_{3eq}	25.44	CH_{3eq}	CH_{3ax}, C2, C4

Table 4. Summary of ^{13}C n.m.r. data for **(114).**

The relative regio and stereochemistry of angucyclinone **(114)** was confirmed through the generation of a single X-ray crystallographic structure.[62] The computer generated perspective of **(114)** is shown in Figure 2. The phenolic hydroxyl was confirmed to be in position-11. The optical rotation of **(114)** was measured to be 0° confirming that the compound is racemic.

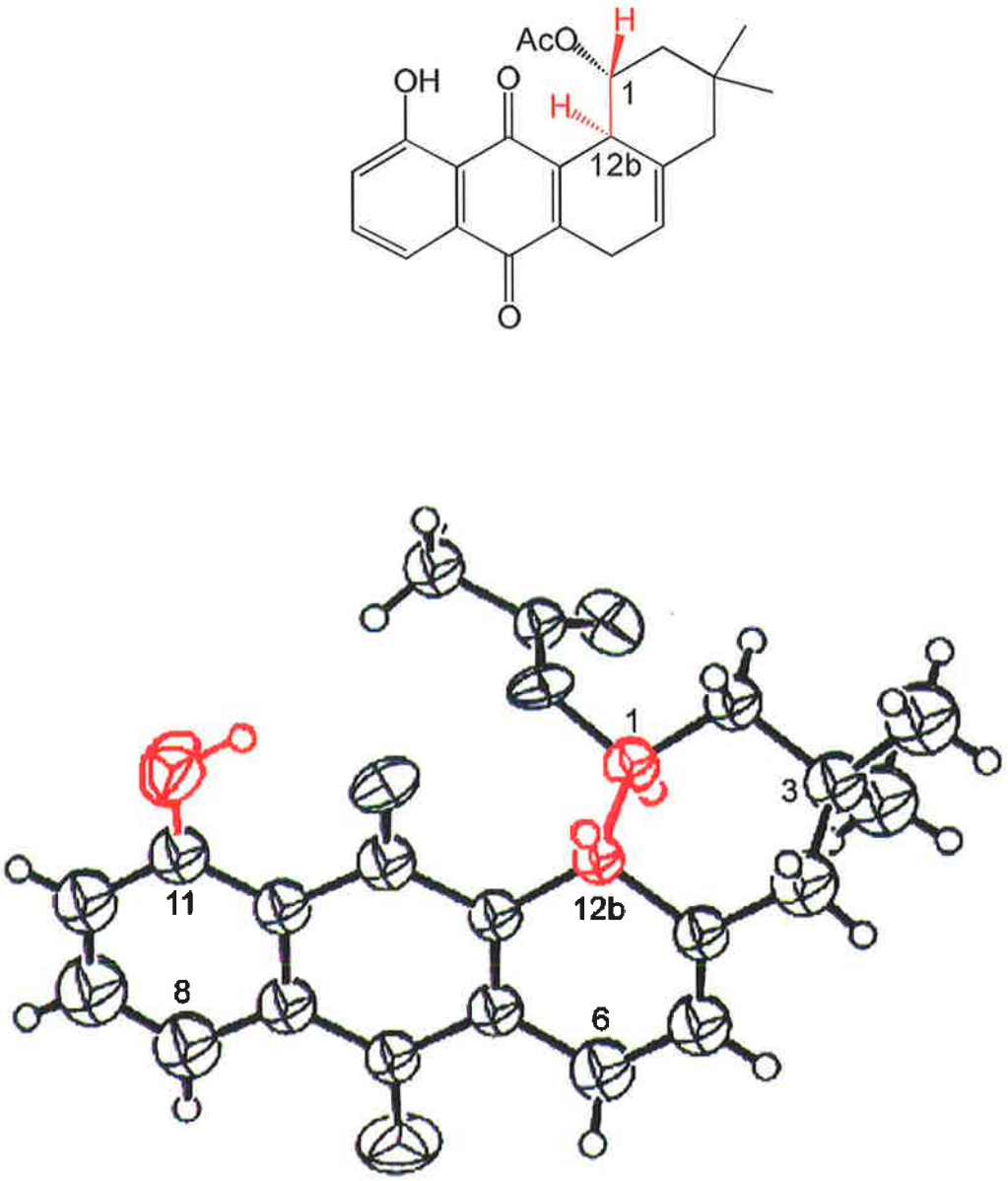

Figure 2. X-ray structure of angucyclinone **(114).**

2.4. Synthesis of the B-ring Aromatic Angucyclinone (115)

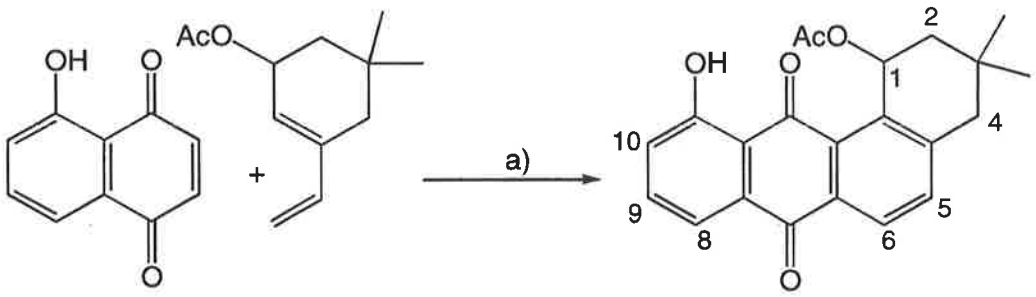

(34) **(111)** **(115)**

a) (i) $B(OAc)_3$, CH_2Cl_2, 20°C, 24 hr; (ii) SiO_2, O_2, 72 hr, 52%

Scheme 29. Synthesis of the B-ring aromatized angucyclinone intermediate **(115).**

Angucyclinone **(115)** was generated in 52% overall yield by complexing juglone **(34)** with boron triacetate and stirring the mixture with diene **(111)** for 24 hours (see Scheme 29). When the crude Diels-Alder adduct obtained from this reaction was absorbed onto silica, the solvent removed *in vacuo* and the solid mixture allowed to stand open to air for 72 hours, **(115)** was isolated in 52% yield (following chromatography) as bright orange crystals. A significant amount of unidentified polymeric material was also formed during the oxidation process. The key to generating the fully aromatic adduct **(115)** was the use of silica as an absorbent to provide a greater surface area for the aerial oxidation.

Structure confirmation of **(115)** was determined by as follows. The electron impact mass spectrum of **(115)** showed the molecular ion at *m/z* 364, together with fragmentation peaks arising from the sequential losses of acetic acid and a methyl radical. The infrared spectrum of **(115)** shows characteristic carbonyl absorptions at 1728 (acetate), 1664 (quinone carbonyl) and 1634 (*peri*-OH hydrogen bonded quinone carbonyl).

The ^1H and ^{13}C n.m.r. spectra are characteristic of aromatic **(115)**. The ^1H n.m.r. spectrum showed the characteristic sharp down field signal at 12.54 ppm due to the *peri* hydrogen bonded phenol and two coupled doublets at 8.29 and 7.54 ppm corresponding to the 6 and 5 hydrogens of the aromatic B-ring. The characteristic D-ring triplet and two sets of doublets of doublets (positions 9,8 and 10) at 7.63, 7.28, and 7.78 respectively are also present. The downfield triplet at 6.87 ppm corresponds to the acetate containing CH at position 1 which is coupled (two doublets of doublets) to the 2 CH_2 at 1.94 and 2.14 ppm. The resonances of

the 4 CH_2 hydrogens are at 2.65- 2.90 ppm as two doublets. The triplet splitting pattern of the H1 signal is a consequence of the 45° angle that H1 makes with both 2 CH_2 hydrogens. The geminal dimethyl signal is observed at 1.07 ppm, while the methyl of the acetate has a chemical shift at 1.98 ppm.

2.5. Deprotection and Oxidation of Angucyclinone (115)

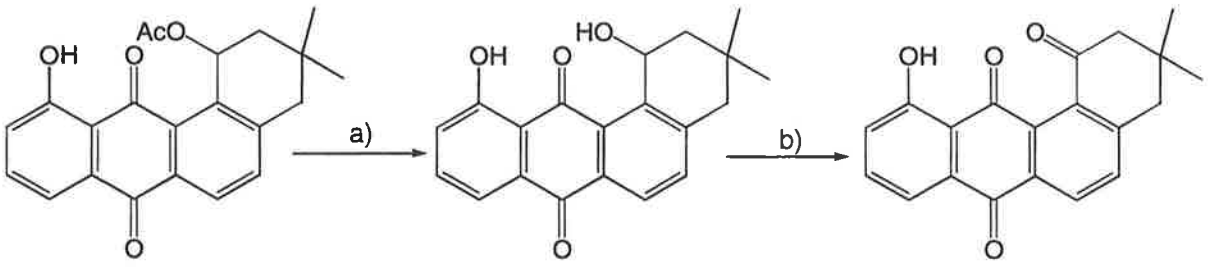

(115) **(116)** **(109)**

a) H_2O, 20% NaOH, THF, reflux, 24 hr, 82%; b) CH_2Cl_2, O_2, sun light, 48 hr, 77%

Scheme 30. Formation of target 11-hydroxyl isomer **(109).**

The next task was to hydrolyze the aromatic acetate **(115)** (Scheme 30) under basic conditions and oxidize the resultant alcohol **(116)** to give the target 11-hydroxy isomer **(109)** of the ochromycinone analogue **(108)** reported previously.[52]

Treatment of **(115)** with 20% aqueous sodium hydroxide solution in tetrahydrofuran at reflux for 24 hr gave the alcohol intermediate in a purified yield of 82%. Photo-oxygenation of 1-OH by the exposure of **(116)** in dichloromethane to sunlight for two days forms the 1 ketone in a purified yield of 77%. Similar treatment of **(115)** without isolating the intermediate alcohol gives **(109)** in quantitative yield.

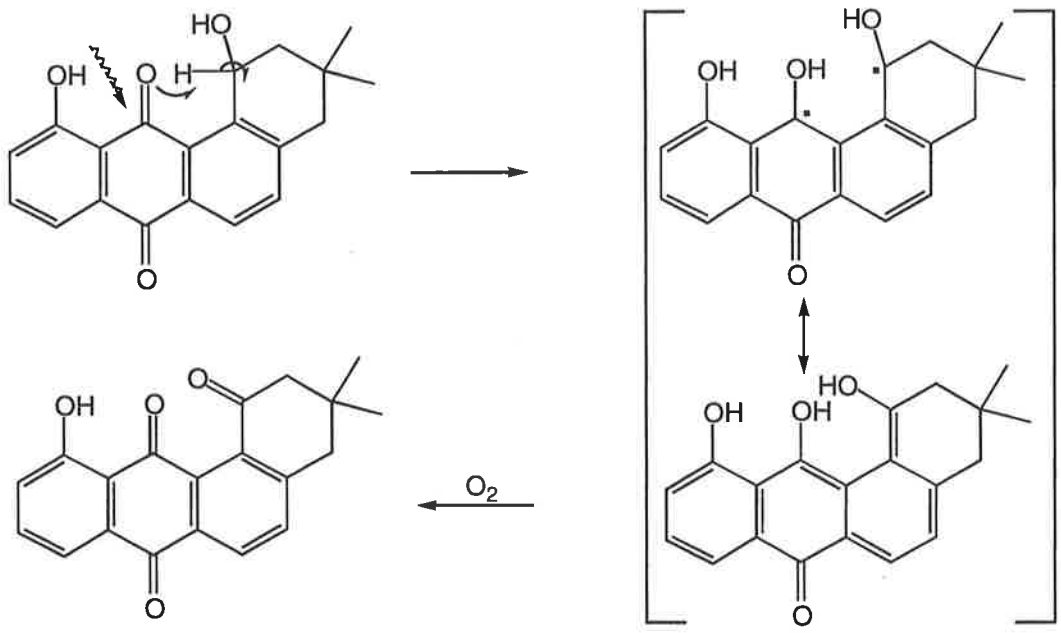

Scheme 31. Photo oxygenation of alcohol **(116).**

This key photo oxidation was first reported by Krohn following synthesis of a daunomycinone-rabelomycin hybrid.[2] The reaction is rationalized by the operation of a Norrish type II hydrogen abstraction of the excited carbonyl to yield a diradical.[63] A plausible mechanism utilizing a Norrish type II process for the photo-oxygenation of **(116)** is outlined in Scheme 31. The benzylic H of **(116)** must be in close proximity to the excited carbonyl group. The diradical will then rearrange to form the fully conjugated vinyl alcohol that tautomerizes to the 1-ketone followed by aerial oxidation to aromatize the B ring.

The EI mass spectrum of the 11-hydroxy angucyclinone **(109)** is shown in Figure 3. The prominent retro Diels-Alder process (loss of C_4H_8), followed by sequential losses of carbon monoxide are fragmentation routes also observed for the 8-hydroxy isomer **(108)**.[52]

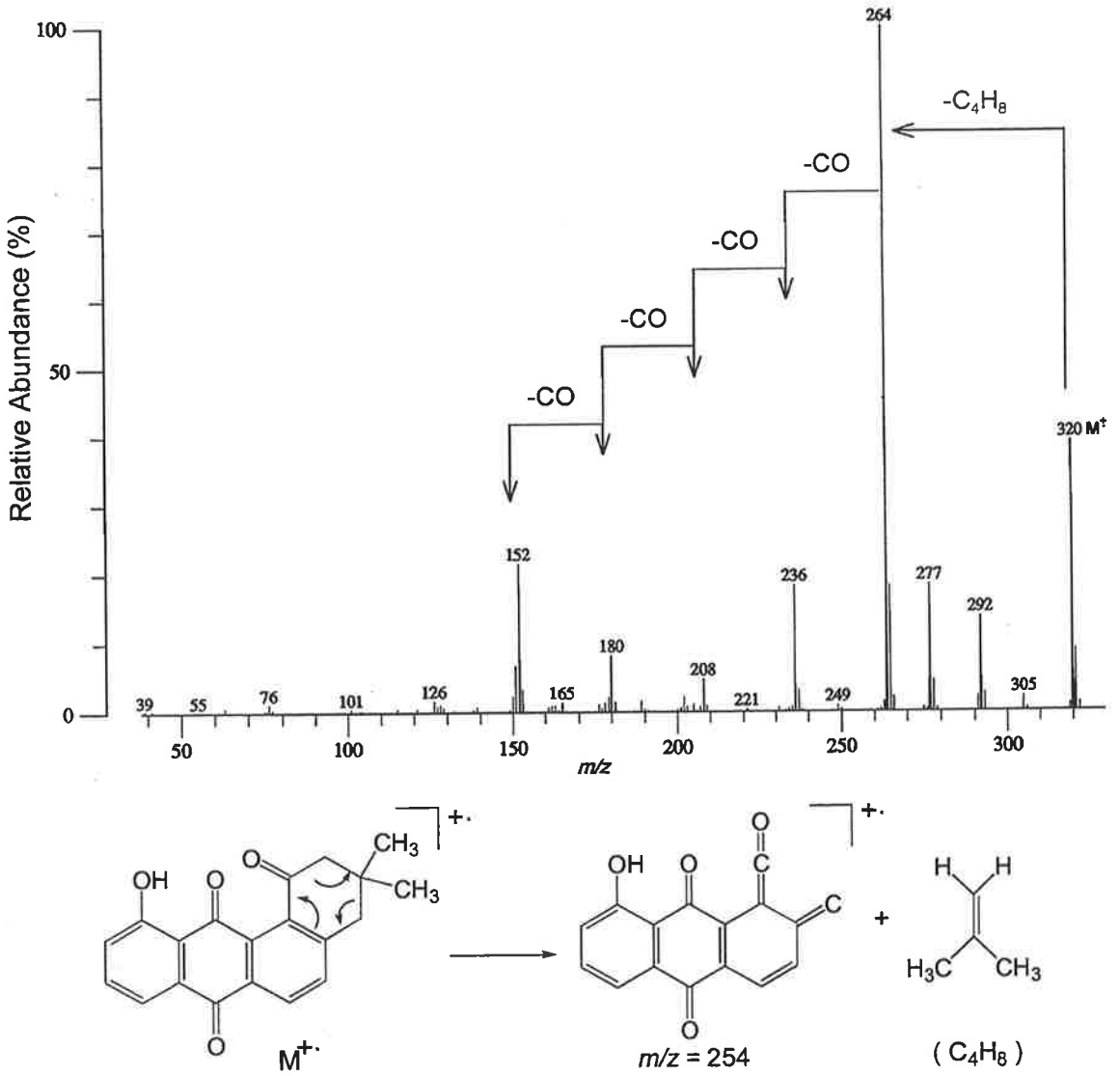

Figure 3. EI mass spectrum of the 11-hydroxy isomer **(109)** showing the retro Diels-Alder mechanism below the spectrum.

The ^{1}H and ^{13}C n.m.r. spectra of **(109)** are similar to those of other angucyclinones. The ^{1}H n.m.r. spectrum (Figure 4) shows the characteristic sharp downfield signal of the H-bonded 11-hydroxy group at 11.86 ppm. Position of this signal is subject to shielding caused by the nearby 1 carbonyl and is at a different and characteristic value compared with that of the 8-hydroxy isomer (12.28 ppm). The characteristic D-ring triplet and two sets of doublets of doublets are also present but exhibit a three fold increase in their coupling constant up to 8.4 Hz for **(109)** as compared to 3 Hz for the 8-hydroxy isomer **(108)**.[52] The two coupled doublets (8.0 Hz) of the B-ring hydrogens, and the three singlets of the A-ring hydrogens, are almost identical with those observed for isomer **(108)**.

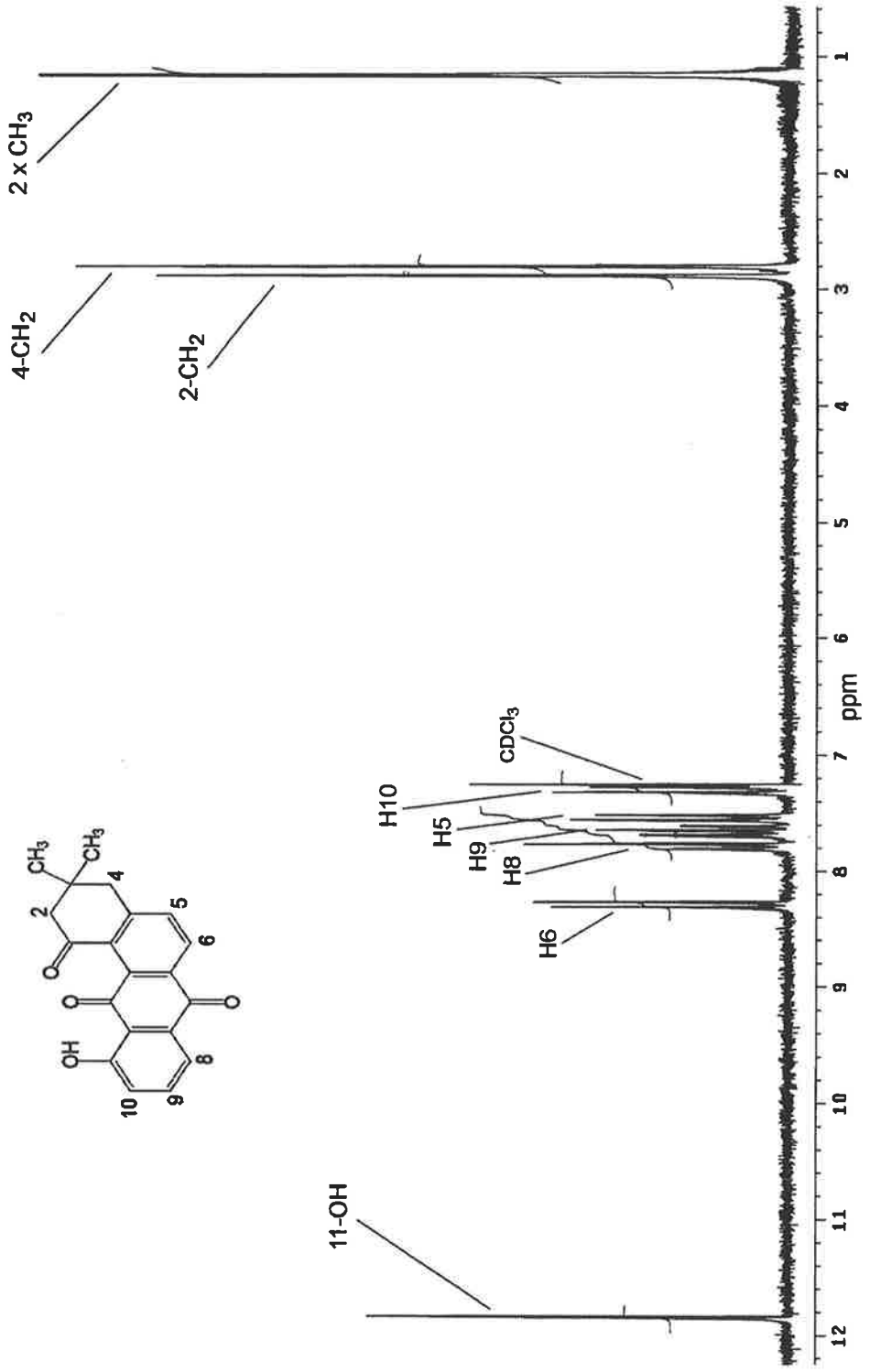

Figure 4. ^{1}H n.m.r. spectrum of the 11-hydroxy isomer **(109).**

2.6. Generation of C1-C12b Bond Fragmented Quinone (118)

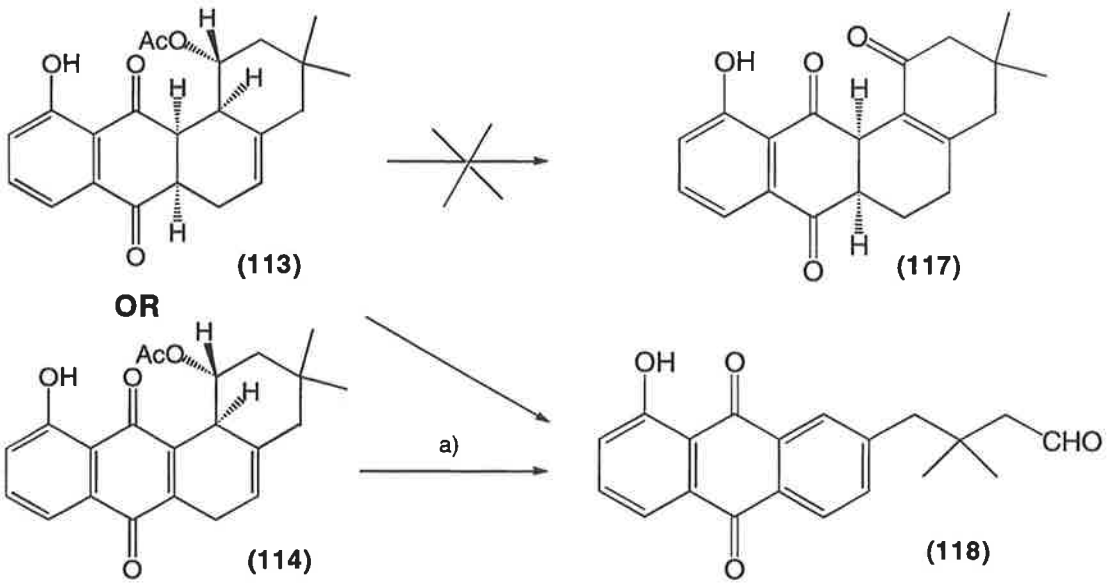

a) 1M MeO^- / MeOH, CH_2Cl_2, 20°C, 40 min., 67% from **(113)**, 70% from **(114)**

Scheme 32. Fragmentation of the C1-C12b bond.

Once the target 11-hydroxy isomer **(109)** was synthesized our attention was turned to the adducts **(113)** and **(114)**. It was hoped that removal of the acetate protecting group would give a free alcohol that could be gently oxidized to a ketone. Under mild acidic conditions, this ketone would then isomerize to the α,β-unsaturated isomer **(117)** having the double bond at the wanted 12b,4a ring junction suitably positioned for a possible dihydroxylation reaction across 12b,4a.[52]

Attempted deprotection of the acetate functionality in **(113)** using the standard procedure of stirring the compound with 1M sodium methoxide in dichloromethane gave an A-ring cleaved anthraquinone product **(118)** in a 67% yield (Scheme 32). This cleavage and aromatization also occurred with adduct **(114)** in 70% yield. A similar reaction has been observed for modified angucyclinones which contain an OMe at position 6 of the B-ring: clearly the loss of MeO^- (a good leaving group) assists this fragmentation.[33, 34, 47] Similar ring openings have been observed with several natural products (e.g. aquayamycin)[8] and establish a link to the related open chain products such as the frideomycins and vineomycin B_2.[1, 2] We envisage that the fragmentation to form **(118)** occurs during the aerial oxidation stage of the reaction

(Scheme 33), via an intermediate hydroperoxide [good leaving group] centred at position 6 of either **(113)** or **(114)**.

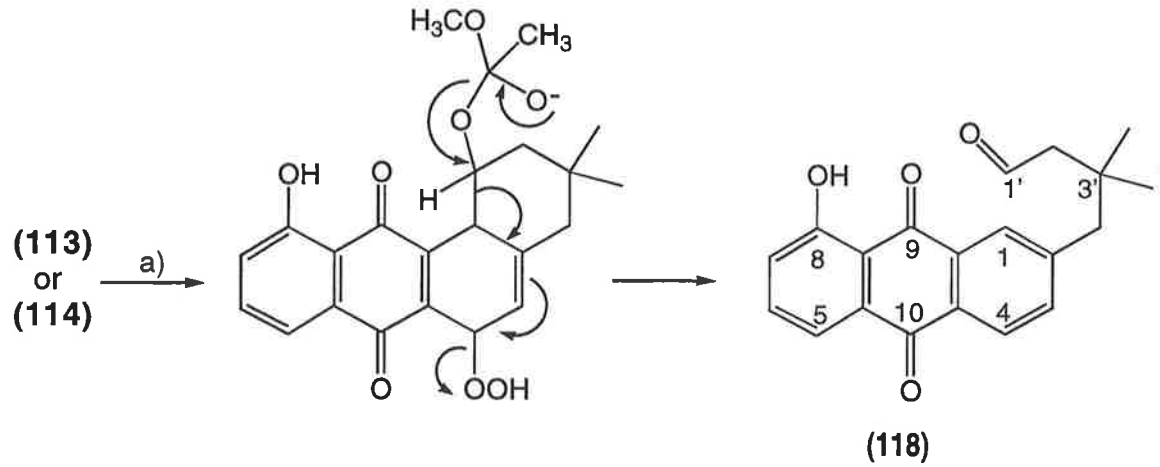

(118)

a) 1M MeO^- / MeOH, CH_2Cl_2, 20°C, 40 min., 67% from **(113)**, 70% from **(114)**

Scheme 33. Possible mechanism for the fragmentation of the C1-12b bond.

The ^1H n.m.r. spectrum of **(118)** reflects the planar nature of the anthraquinone framework. The quinone phenol group resonates as a sharp singlet at 12.6 ppm. The aromatic resonances show characteristic two doublets at 7.59, and 8.22 ppm [H3 and H4 7.8 Hz], together with a triplet and two doublet of doublets at 7.69, 7.31 and 7.83 ppm of H6, H7 and H5 respectively. The aldehyde hydrogen at position 1' resonates at 9.88 ppm as a triplet, coupled to the doublet at 2.33 ppm with a 3 Hz coupling constant. The last aromatic signal of H1 has a small long range 1.5 Hz coupling with H3. Mass spectrometric analysis of **(118)** gave a molecular ion at *m/z* 322 together with sequential loss of C_2H_4O (McLafferty rearrangement) and C_3H_4 (with accompanying H rearrangement) to give the base peak *m/z* 238.

In conclusion, the required 11-hydroxy isomer **(109)** was synthesized in moderate overall yield starting from commercially available juglone **(34)** and an easily prepared activated diene **(111)** using a boron triacetate catalyzed Diels-Alder reaction. The biological activity of **(109)** will be tested and compared to that of the 8-hydroxy isomer **(108)** [see later, page 92]. In addition an interesting quinone derivative **(118)** was synthesized through the known fragmentation of the C12b-C4a bond of **(113)** and **(114)** during the aerial oxidation stage of the reaction sequence.

Chapter 3. Attempted Oxygenation of the A,B Ring Junction

3.1. *Syn* Dihydroxylation Using Osmium Tetroxide

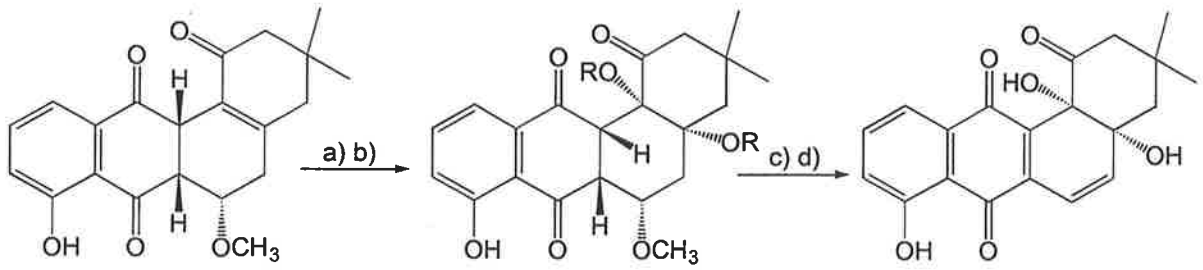

+/- (107) **+/- (119)** **+/- (120)**

a) Dihydroxylatyion b) Protection c) Oxidation d) Deprotection

Scheme 34. Synthesis of the aquayamycin like prototype **(120).**

A major aim of our study of angucyclinones is to effect a *cis* addition of two hydroxy groups across the 4a,12b double bond of **(107)** to make an aglycone aquayamycin-like prototype **(120)** (Scheme 34). Inspection of **(107)** reveals that the unsaturation is situated at the required ring junction and the most concise strategy for generating **(120)** is a *cis* dihydroxylation. Two questions have to be asked: (i) will a conventional dihydroxylating reagent react with a fully substituted, deactivated double bond? and (ii) will the *cis* addition occur from the correct plane of the molecule to give the required stereochemistry?

Examination of the molecular structure of adduct **(107)**, determined by X-ray analysis and chosen for the dihydroxylation trials, suggests that a dihydroxylating agent should approach from the less sterically hindered bottom plane.[52] This should give rise to a single diastereomer **(119)** which upon aromatisation should lose 3-chiral centres giving the racemic aquayamycin prototype **(120).** The deletion of chirality of the diene used to generate adduct **(107)** by the insertion of gem dimethyl functionality at position 3 has simplified the final stereochemical outcome of this reaction since it doesn't matter through which plane the dihydroxylation occurs, because formation of the two double bonds in the B ring will give the same racemic product.

The main method for introducing a *syn* diol functionality onto an alkene utilises osmium tetroxide [see Schröderfor a good review article[64]]. Traditionally this reagent was used in equimolar quantities using pyridine or acetone solvent.[64] However, the highly practical, and cost effective, contemporary method using catalytic quantities of OsO_4 and N-methylmorpholine N-oxide as the co-oxidant is now generally used.[65] Sharpless has pioneered his asymmetric dihydroxylation relying on the coordination of an optically pure basic ligand with OsO_4 to generate stereoselectivity.[66]

To summarise the general mode of action, the nucleophilic alkene adds to osmium tetroxide by a concerted process to give the osmium (VI) monoglycolate ester. This ester is subsequently hydrolysed by water to yield the diol and osmium monoglycolate. Co-oxidation of Os (VI) by a convenient agent such as N-methylmorpholine N-oxide or potassium ferrocyanide then regenerates the osmium tetroxide which can then enter a second hydroxylation cycle. The reactivity of osmium tetroxide towards nucleophilic attack can be enhanced by esterification with a heterocyclic base such as pyridine or cinuclidin.[66] Hydrolysis of the osmium (VI) monoglycolate ester can be accelerated using methyl sulfonamide ($MeSO_2NH_2$).[66]

Table 3 summarises the dihydroxylating conditions used on adduct **(107)**. All reactions led to the isolation of the stated amounts of the fully aromatic angucyclinone **(108)** and starting materials.

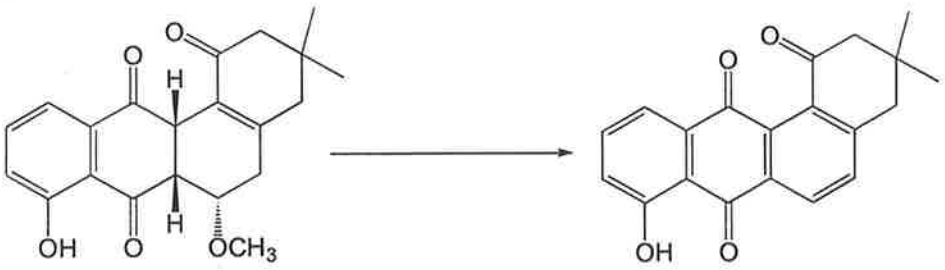

(107) **(108)**

Reactant	Solvent	Time/Temp.	Products
OsO_4 (1.1eq)	Pyridine	12 hr, 20°C	**(108)** 85%
OsO_4 (1.1eq)	Acetone	48 hr, 20°C	**(108)** 90%
OsO_4 (cat.), NMO	Acetone, t-butanol	24 hr, 20°C	**(107)** 30% **(108)** 50%
OsO_4, K_2CO_3, $K_3Fe(CN)_6$, chinuclidin, $CH_3SO_2NH_2$	Acetone, t-butanol	24 hr, 20°C	**(108)** 80%
mCPBA	Acetone	24 hr, 20°C	**(108)** 80%

Table 3. Attempted dihydroxylation conditions on adduct **(107)**.

The lack of reactivity of **(107)** towards OsO_4 based dihydroxylations can be attributed to the following causes: (i) The conjugation of the double bond to the carbonyl at position 1 has a strong electron-withdrawing effect thereby deactivating the double bond towards nucleophilic addition. Examples of successful dihydroxylations of alkene conjugated ketones in steroids have been reported but the harsh reaction conditions rely on long reaction times and basic solvents such as pyridine [i.e. trials using reported conditions led to aromatisation of the B-ring].[67, 68] (ii) The steric effect of the quaternary double bond may also retard dihydroxylation, especially from one face of **(107)**. (iii) Finally, the large quantities of fully aromatised angucyclinone **(108)** recovered from the reactions suggest that base catalysed elimination of methoxide and subsequent aromatisation is more favourable than dihydroxylation. There are many more reported[69-72] examples of dihydroxylations that utilise somewhat harsh acidic conditions which will cause aromatization through acid catalysed elimination of methanol. These have not been attempted.

This lack of reactivity of **(107)** towards dihydroxylation may be overcome by reducing the 1 ketone to an alcohol and converting this functionality to an acetate or trimethyl silyl ether; by so doing, electron donating groups are introduced which will induce the dihydroxilation to precede the aromatisation of the B ring.

3.2. Reduction of Adduct (107)

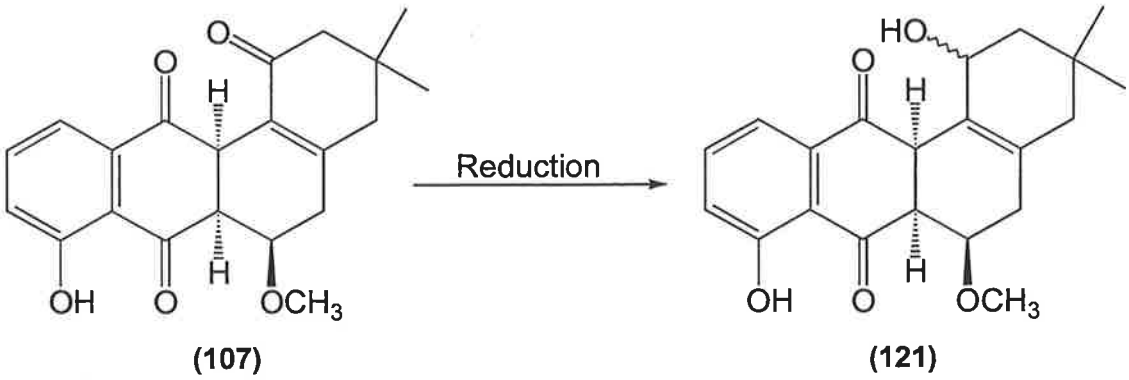

(107) **(121)**

Scheme 35. Reduction of adduct **(107).**

Addition of two hydroxy groups in a *cis* orientation across the 4a,12b double bond proved a difficult task for two reasons, (i) the double bond is tetrasubstituted and will therefore react sluggishly, and (ii) the carbonyl group at position 1 has a deactivating influence on the reaction. Conversion of the 1-carbonyl group into a hydroxyl (or a suitable derivative) may assist the *cis* dihydroxylation reaction. Two possible synthetic pathways exist to place the hydroxyl group at this position: (i) By condensing a diene having the hydroxy (or a suitable protecting group such as an acetate) already present in place of the ketone with juglone will generate a C-1 reduced Diels-Alder adduct. This strategy will be discussed in Section 3.3. (ii) Alternatively and more directly, the C-1 carbonyl of **(107)** may be reduced to alcohol **(121)** (Scheme 35); the stereochemistry at position 1 is not important since the alcohol will ultimately be re-oxidised to a ketone.

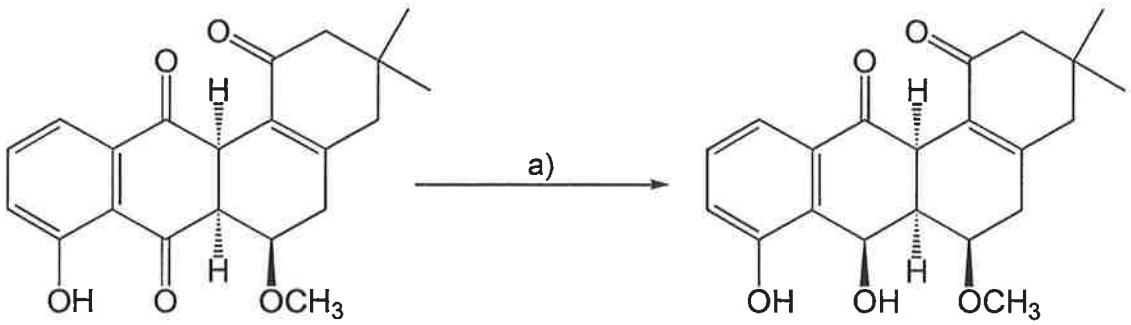

(107) **(122)**

a) $CeCl_3$, $NaBH_4$, ethanol, 20°C, 10 min. 54%

Scheme 36. Luche reduction of **(107)** to give the 7-hyroxy product **(122)**

Treatment of adduct **(107)** with anhydrous cerium (III) chloride and sodium borohydride in ethanol at ambient temperature for ten minutes gave a single product in 54% yield (Scheme 36). No starting material was recovered, and apart from the product, only polymeric material was detected by mass spectrometry. The reduced product gave a weak molecular ion by electron-impact mass spectrometry, but a pronounced MH^+ peak at *m/z 357* ($C_{21}H_{25}O_5$) was obtained by electrospray mass spectrometry (ESMS). The fragmentation pattern from the molecular cation indicates a loss of water followed by loss of methanol, however the observed retro Diels-Alder process [loss of C_4H_8 from the (MH^+ - H_2O) ion] shows that the product has retained the α,β–unsaturated 1 carbonyl functional group.

The reduction product also retains the ν_{max} value characteristic of an α,β–unsaturated carbonyl at either 1661 or 1677 cm^{-1} (see Chapter 5, "Experimental"), indicating that reduction does not occur at the 1 carbonyl. The lack of the characteristic *peri* OH [the 8-OH H-bonded to the 7 carbonyl] signal near 12 ppm in the ^1H n.m.r. spectrum suggests that the carbonyl at position 7 has been reduced, and that the reduction product is **(122)** or a stereoisomer.

The ^1H n.m.r. COSY, GHMQC and GHMBC data for the reduction product (reported in Appendix, NMR Section, Tables 5 and 6) together identify single hydrogens at the 6, 6a, 12a, and 7-positions and confirm the bond connectivity, and that position 7 is the site of reduction of **(107).**

A pictorial description of GHMBC experiments are shown in Figure 6: these show only the long range ^{1}H-^{13}C coupling partners of 6, 6a, 12a, and 7 hydrogens, and have been used to confirm the connectivity and site of reduction of alcohol **(122)**.

The long range ^{1}H-^{13}C correlation between the 7-hydrogen at the reduction centre and the nearby 6-methoxy and 8-phenol carbons suggests the 7 ketone as the site of reduction (Figure 6). Notice that the alternative 1-carbonyl reduction product **(121)** (Scheme 35) could not interact with the distant 6 and 8 carbons in the GHMBC experiments.

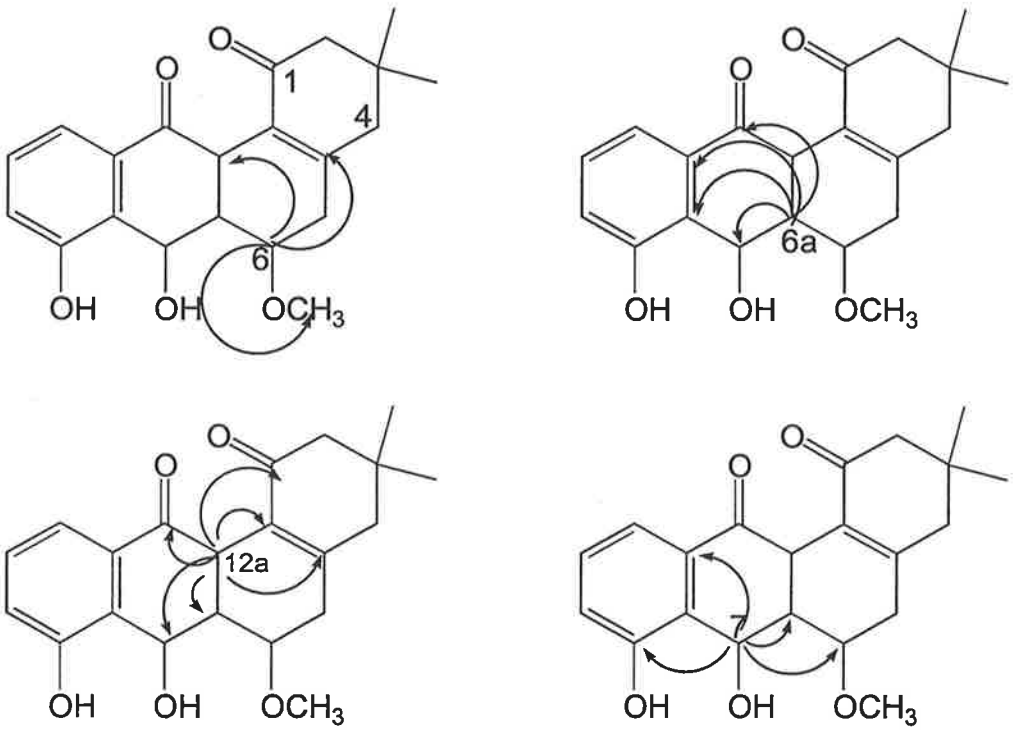

Figure 6

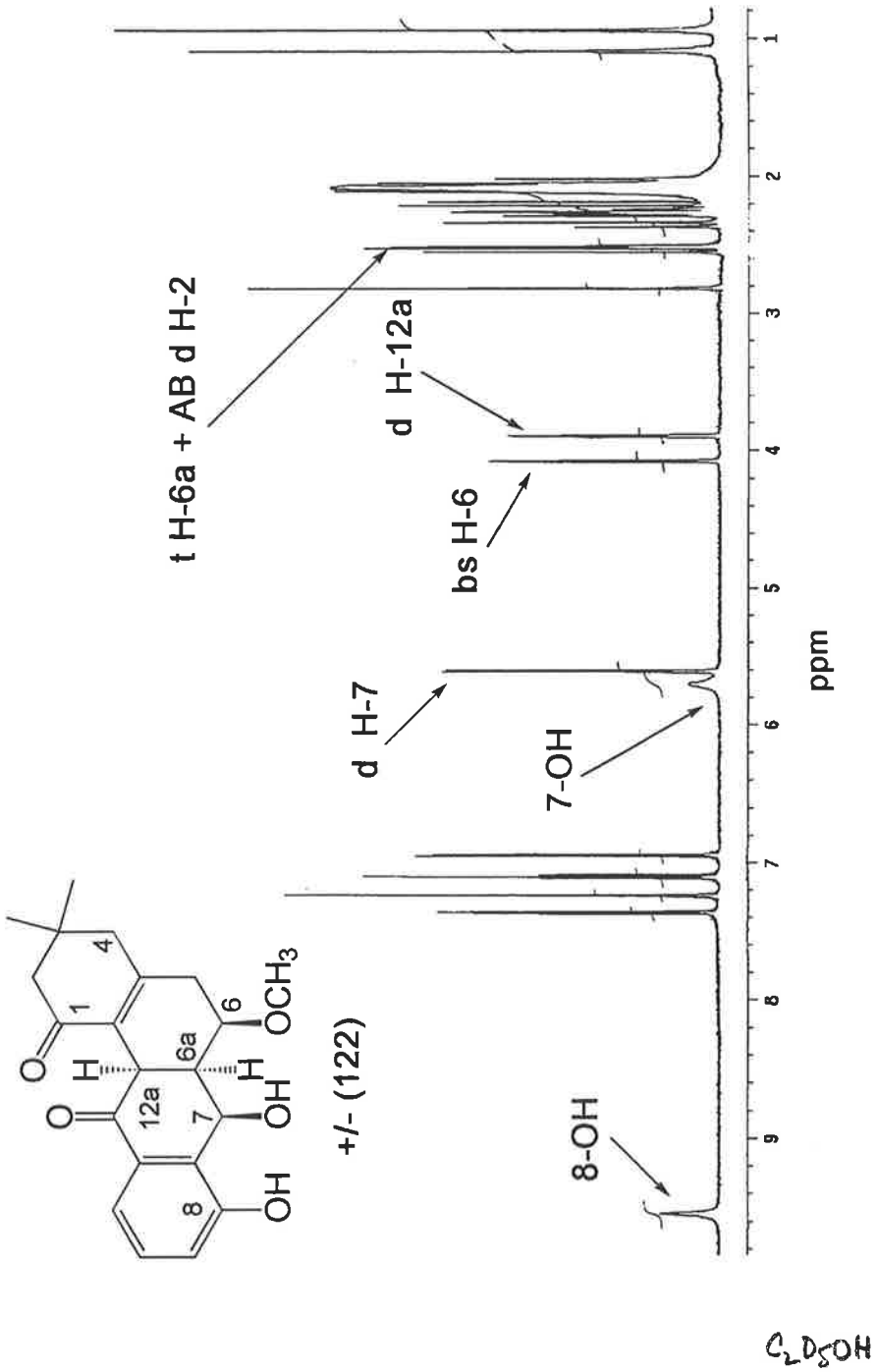

Figure 7. 600 MHz ^{1}H n.m.r. spectrum of diol **(122)** dissolved in deuterated ethanol.

The 600 MHz ^{1}H n.m.r. spectrum of diol **(122)** is shown in Figure 7. The first salient feature of this spectrum is the lack of the characteristic downfield signal near 12 ppm present in all angucyclinones or quinones having a hydroxyl functionality capable of H-bonding to a *peri* located carbonyl group. Thus, the H of the OH resonates at 9.57 ppm as a broad singlet. The other OH signal occurs at 5.75 ppm.

The doublet at 3.98 ppm [H12a coupled to H6a (6.0 Hz)] suggests a 35° dihedral angle between the two hydrogens. The triplet due to H 6a (2.70 ppm) shows a 6.0 Hz coupling to H12a and H7 with no coupling to the neighbouring H6, indicating a 90° angle between H6a and H7. The doublet at 5.77 ppm due to H7 (the CH containing the OH group i.e. the site of reduction) has a coupling constant of 6.0 Hz with H6a, indicating an axial-equatorial relationship with an approximate dihedral angle of 35°, suggesting a *cis* arrangement of H7 and H6a. The rest of the spectrum shows the geminal dimethyl resonances at 0.90 and 1.09 ppm; methoxy signal at 2.81 ppm; the overlying AB type doublets of the three methylene protons (2, 4, and 6) at 2.27-2.65 ppm; and the characteristic angucycline splitting pattern of the D ring at 7.06 – 7.39 ppm.

A nuclear Overhauser experiment (NOE), summarised in Figure 8, shows strong interaction of H7 with both H6a (9.9%) and H12a (7.0%) but no interaction between H7 and H6. Thus, H7 and H12a must be close to diaxial, which means that the 7-OH and 6-OMe substituents are on the same face of the molecule as indicated in Figure 8.

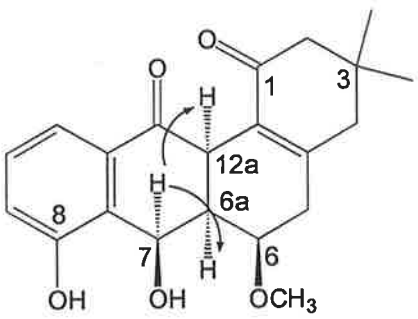

Figure 8. Summary of the NOE experiment of diol **(122)** used to assign the relative stereochemistry. Irradiation of H7 signal at 5.61 ppm excites 2.52 [H6a (9.9%)], 3.89 [H12a (7.0%)], and to a lesser degree 2.82 [H6 (0.74%)].

Figure 9 shows a computer generated ORTEP representation of the X-ray crystal structure of reduction product **(122)**.[82] The relative stereochemistry of the B and C rings of **(122)** was confirmed as that indicated in Figure 9. The measured optical rotation of **(122)** was found to be 0° degrees, indicating a racemic mixture.

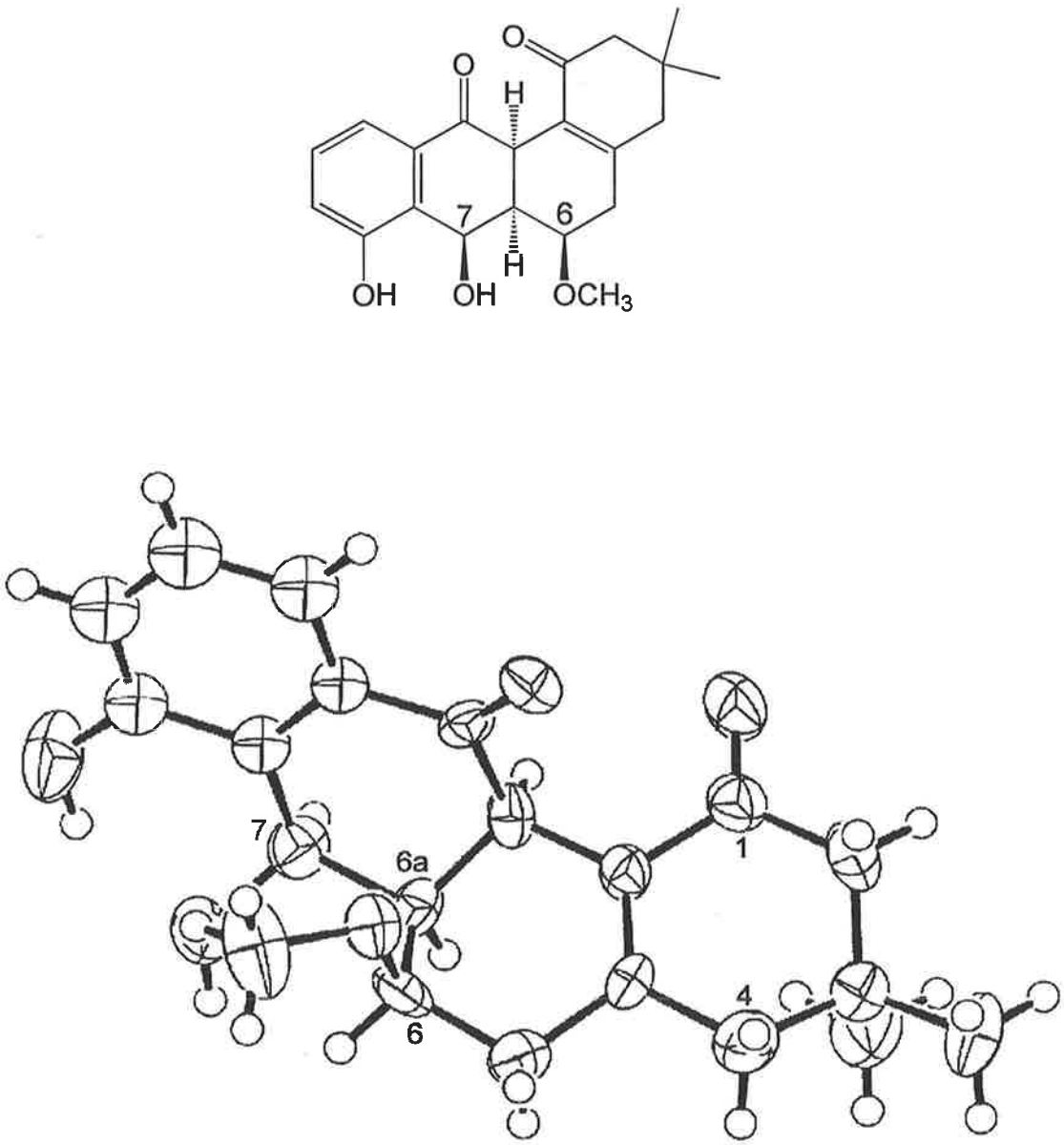

Figure. 9. Molecular structure for reduction product **(122)**.

Stereoselective carbonyl reductions utilising the Luche reagent [cerium (III) chloride and $NaBH_4$] have received considerable attention over the past two decades.[55] By analogy with stereoselective Luche reductions of α-diphenylphosphinoyl ketones,[73] 4-hydroxycyclopentenones[74] and other carbonyl-containing precursors,[55, 75] if initial complexation of the Ce^{III} atom is to the sterically less hindered face of **(107)** then the stereochemical relationship between 6-OMe and 7-OH after hydride delivery would be *trans*, whereas the reduction product **(122)** that was obtained has these two groups in a *cis* orientation.

The observed regiochemistry of this reduction can be rationalised by Ce^{III} binding preferentially to the more concave face in **(107)** [refer to X-ray of **(107)**][52] through strong binding to the 8-OH group [as indicated by n.m.r. spectroscopic studies],[76] and further binding to both 7-C=O and 6-OMe. Approach of the sodium borohydride is then to the sterically less hindered face and affords **(122)** with the observed *cis* stereochemistry. We predicted that **(122)** should also be formed if the borohydride reduction is carried out without the cerium(III) chloride. The observed regiochemistry should be maintained by the preferential interaction of the sodium borohydride with the acidic 8-hydroxy group of **(108)** rather than with the solvent.[55, 77] The 6-OMe substituent will direct the same stereochemistry by hydride delivery from the less hindered face in **(108)**. When the borohydride reduction was carried out without $CeCl_3$, precisely the same result was obtained as before.

In conclusion, a rapid regio- and stereo-specific hydride reduction of an angucyclinone intermediate has been described, with which it may be possible to synthesise angucyclinones with partially reduced C-rings, as are present in the anticancer agents elmycin A **(123)**[78] and angucyclinone D **(124)**.[79, #]

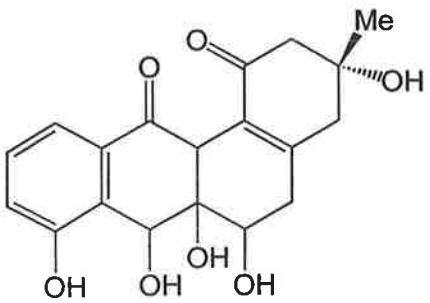

Elmycin A **(123)**

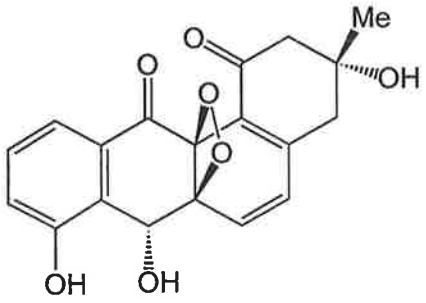

Angucylinone D **(124)**

The stereochemistries of **(123)** and **(124)** are unknown.

3.3. Attempted Formation of Model Alcohol (125)

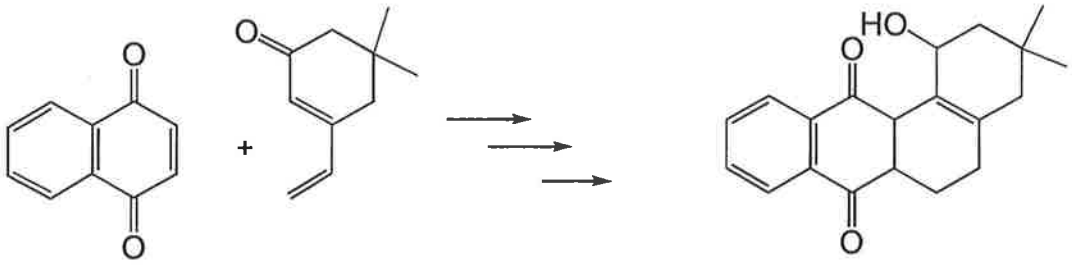

(98) **(88)** **(125)**

Scheme 37. Synthesis of model alcohol **(125).**

The model compound **(125)** contains an electron donating hydroxy substituent at position-1, which makes it a better candidate for an osmium tetroxide catalysed dihydroxylation. The absence of a 6-methoxy group will slow the base catalysed aromatisation experienced upon exposure of the molecule to dihydroxylating conditions.[#]

A synthetic route to **(125)** may employ a standard Diels-Alder condensation between 1,4-naphthoquinone and a diene lacking the methoxy substituent. The initial C4a-C5 double bond of the adduct may isomerise to the thermodynamically more stable 4a,12b α,β-unsaturated system (acid conditions may be required to facilitate this isomerization), which may then be reduced to give the model compound **(125)** (Scheme 37).[52] Sodium borohydride reduction of the 7-carbonyl will not occur because **(125)** lacks the 8-OH group in the D ring.[#]

The attempted cyclisation of diene **(88)**[52] and 1,4-naphthoquinone **(98)** was unsuccessful. This lack of reactivity can be attributed to the strong electron withdrawing effect exerted onto the diene by the carbonyl group of **(88).** Conversion of this deactivating carbonyl group into a Diels-Alder activating substituent can be accomplished in two ways: (i) protection of the carbonyl group as a ketal **(126)** (Scheme 38). The ketal **(127)** can then be readily converted back to the ketone in order to effect isomerization of the double bond to the required α,β-conjugated form.

[#] Refer to Chapter 3.1, page 47.

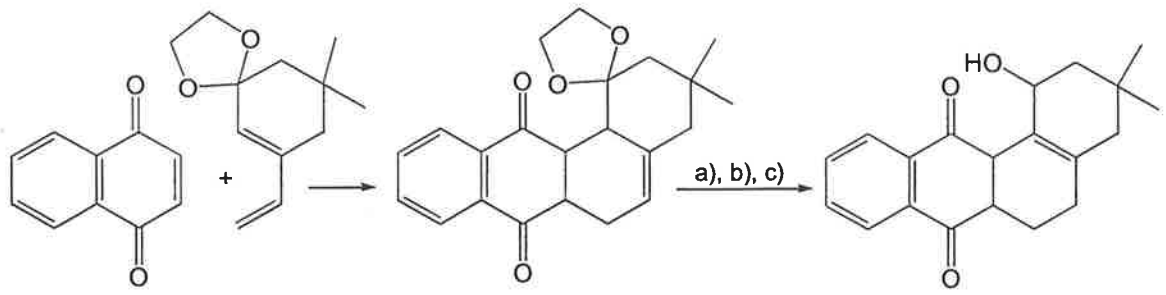

(98) **(126)** **(127)** **(125)**

a) Deprotection, b) Isomerisation, c) Reduction

Scheme 38. Synthetic strategy towards model **(125)** using an acetal protected diene **(126).**

Standard conditions of heating dienone **(88)** under reflux with ethane diol in benzene (with a catalytic amount of p-toluenesulfonic acid) failed to generate the cyclic acetal **(126)** and only starting materials were recovered.[80] Conversion of the hydroxyls of ethane diol into trimethyl silyl groups and the use of a bulky proton/trimethylsilyltriflate (Me_3SiOTf) under aprotic conditions constitutes a more reactive alternative to the dioxolanation.[81] However, under these conditions only a polymeric product having the cyclic acetal functionality was generated; the strongly acidic conditions which resulted by the use of Me_3SiOTf polymerised the diene **(126)**, so this synthetic pathway towards **(125)** was abandoned.

(ii) An alternative procedure would be to allow dienol **(110)**[#] to react with 1,4-naphthoquinone (Scheme 39). The desired product, alcohol **(128)** will then require careful oxidisation under acidic conditions to furnish the α,β-unsaturated ketone, which is then reduced to give the required product **(125).**

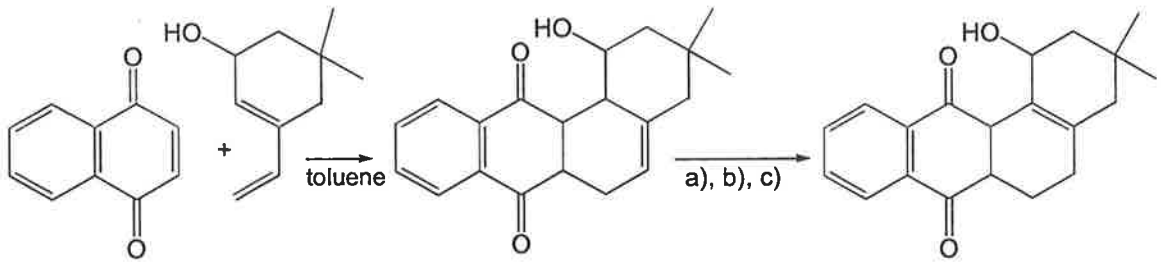

(98) **(110)** **(128)** **(125)**

a) Oxidation, b) Isomerisation, c) Reduction

Scheme 39. Synthesis of **(125)** utilising the reduced diene **(126).**

[#] Refer to Section 2.2, page 28.

Allowing the two starting materials to react under reflux in toluene yields the anthraquinone **(129)** as the major product in 34% purified yield. Anthraquinone **(129)** is presumably formed following dehydration and oxidation of the initial adduct **(128)**. Since this route does not constitute a viable synthesis of **(128)**, it is of no further application for the purpose of this project. Even so, the formation of **(129)** in 'one step' is both interesting and unusual; thus attempts were made to optimise the conditions of the reaction.

Formation of benz[*a*]anthraquinone (129)

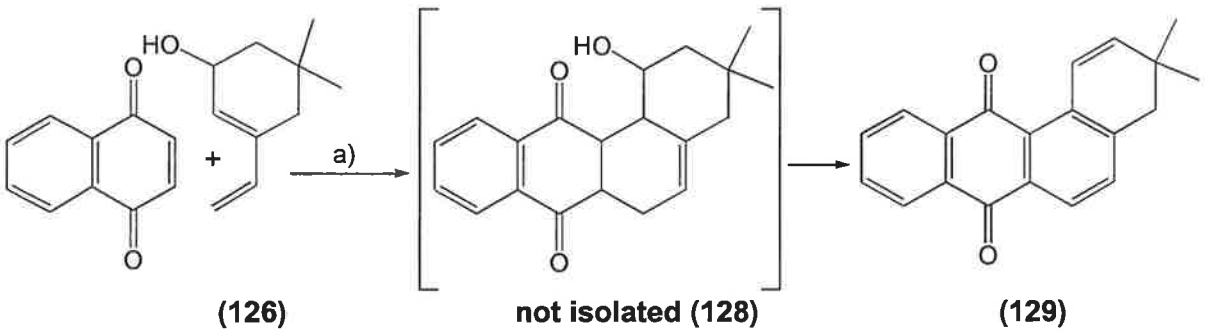

(126) **not isolated (128)** **(129)**

a) p-TSA, toluene, reflux, 72 hr, 52%

Scheme 40. 'One step' synthesis of anthraquinone **(129)**.

Heating 1,4-naphthoquinone and dienol **(126)** in toluene (containing a catalytic amount of p-toluenesulphonic acid) under reflux for 72 hours, followed by flash chromatography purification, and crystallisation from dichloromethane/hexane, gave pure **(129)** in 52% yield (Scheme 40). Under these reaction conditions the intermediate alcohol **(128)** was not detected.

The mass spectrum of **(129)** proved to be very simple: the only major fragmentation from the molecular ion at *m/z* 288 being pronounced loss of an allylic methyl radical. The almost planar nature of the benz[*a*]anthraquinone **(129)** was reflected in the ^{1}H n.m.r spectrum where the geminal dimethyl group produces a singlet at 1.11 ppm, and the 4 CH_2group gives a singlet at 2.83 ppm. Other resonances are standard and summarised in the experimental section (Chapter 5, page 99).

Chapter 4. Syntheses of A and B Ring Oxygenated Angucyclinones

4.1 Introduction

This last chapter of the quinone section of this thesis deals with developing a synthetic methodology towards: (i) Indirectly dihydroxylating and epoxidating the position-4a-12b ring junction to form aquayamycin **(4)** like analogs. (ii) Incorporating an α-hydroxy ketone functionality into the A-ring to form a model compound having two out of the 3 structural features of natural angucyclinone PD 116779 **(143)**. (iii) Explore the biological activities of promising angucyclinones made.

We have been unsuccessful in attempts to directly oxygenate the unsaturated 4a, 12b ring junction of adduct **(107)**[82] using direct *syn* dihydroxylating methods such as osmium tetroxide.[#] Professor D.W. Cameron of the University of Melbourne has suggested that condensing triene **(130)** with 1,4-naphthoquinone may produce an adduct **(131)** which might allow indirect access to oxygenating the 4a, 12b ring junction.[83] Scheme 41 outlines a speculative and challenging synthetic route through epoxide **(132)** that may be used to generate *bis* epoxide **(135)**, a possible precursor to a 4a,12b diol.

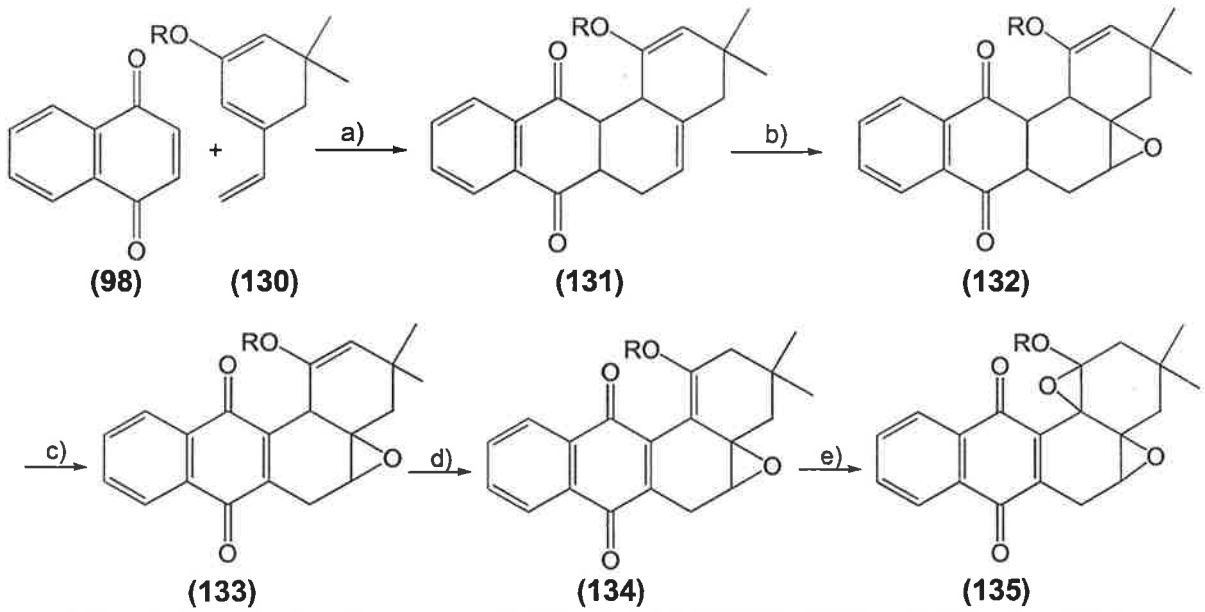

(98) **(130)** **(131)** **(132)** **(133)** **(134)** **(135)**

a) Diels-Alder cyclisation, b) mono epoxidation, c) partial oxidation, d) isomerization, e) epoxidation

Scheme 41. Proposed synthetic route towards diepoxide **(135)**.

[#] Refer to Chapter 3.1. page 45.

A Diels-Alder condensation between 1,4-naphthoquinone **(98)** and a protected enol form **(130)** of the diene **(88)** could form adduct **(131)**, which could be monoepoxidated to give **(132)** (Scheme 41). The mono epoxide **(132)** needs to be partially oxidised at the B,D ring junction to yield the quinone product **(133).**[62] The position 1,2 double bond of the enol acetate **(133)** may be isomerised to give **(134)** by hydrolysing and reforming the enol acetate at the more stable 1,12b position.[84] Treatment of **(134)** with a small highly reactive agent such as dimethyl dioxirane[85] should then form the diepoxide **(135)**.

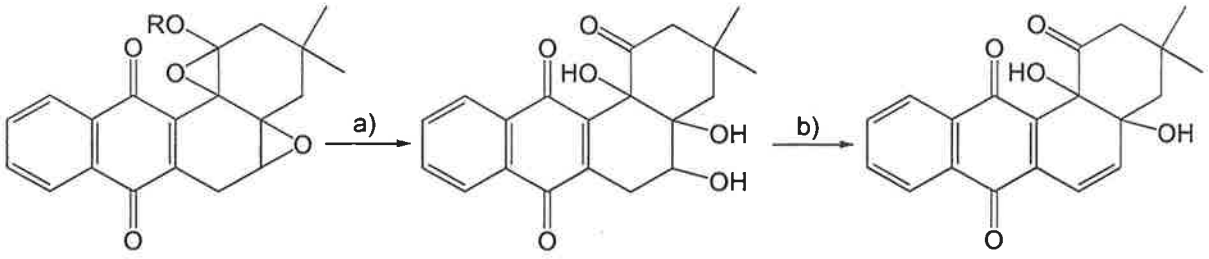

(135) **(136)** **(137)**

a) aqueous acid, b) aromatisation

Scheme 42. Synthesis of analogue **(137)** through acid catalysed epoxide ring opening of **(135).**

The aquayamycin analogue **(137)** might be formed by ring opening diepoxide **(135)** under mild aqueous acidic conditions (Scheme 42). The 4a,5 epoxide should open up in predictable fashion generating a diol, while the 1,12b epoxide could undergo ~~an acyloin reaction~~ rearrangement to form the α-hydroxy ketone **(136)**.having the hydroxyl at position 12b.[86] The triol **(136)** is expected to eliminate the secondary 5 alcohol in preference to the tertiary alcohol, to give the aquayamycin-like model compound **(137)**. The relative stereochemistry of the diol **(137)** is difficult to predict at this stage, but in the event of the generation of a *trans* diol perhaps one of the hydroxyl groups can be inverted to give the aquayamycin like *cis* diol.

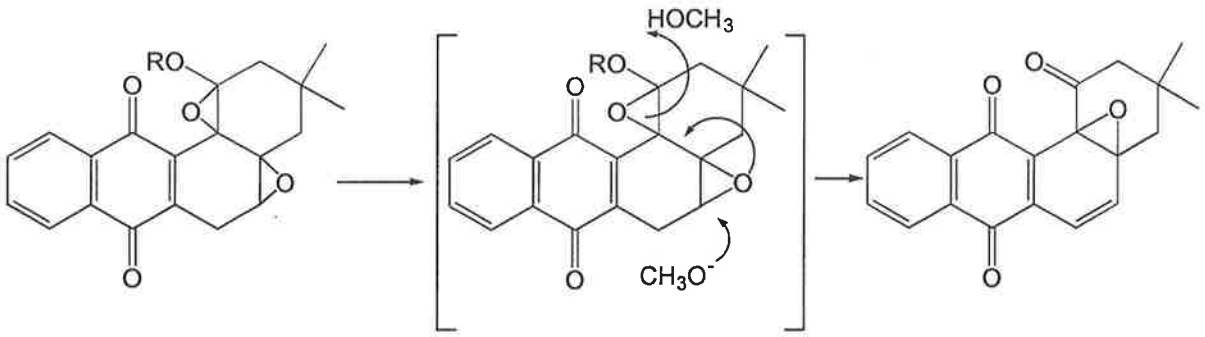

(135) **(138)**

Scheme 43. Synthesis of 4a,12b epoxide **(135)** by anhydrous epoxide opening and rearrangement.

An alternative protocol is shown in Scheme 43. Treating diepoxide **(135)** with a nucleophile, e.g. MeO^-, the more electrophilic position 4a,5 epoxide will be opened up generating an oxide anion which is in such an orientation capable of attacking and opening the A ring epoxide.[83] This will form a epoxide positioned at the 4a,12b ring junction and a labile hemi ketal at the 1 position which should hydrolyse to a ketone. Elimination of methoxide will aromatise the B ring forming **(138)** which can be converted to a *cis* diol (by transforming the epoxide to a halohydrin[87]). Model compound **(138)** contains the A,B ring junction epoxide present in the WP 3688-3 **(142)** type angucyclines.

Formation of an α-hydroxy ketone in the A ring could be accomplished as shown in Scheme 44. The initial Diels-Alder adduct **(132)** from Scheme 41 has the double bond in the A-ring placed in such a way that if this adduct is treated with excess dimethyl dioxirane or *meta*-chloroperbenzoic acid, followed by partial oxidation to introduce the C,D ring double bond, the diepoxide **(139)** may be formed. Aqueous acid catalysed opening of both epoxide rings, shown in Scheme 44, will then form a non-isolable hemi-ketal intermediate, which upon hydrolysis may form the diol **(140).**[86] Dehydration of **(140)** will yield the required α-hydroxy ketone **(141)**, a structural analogue of **(143).**

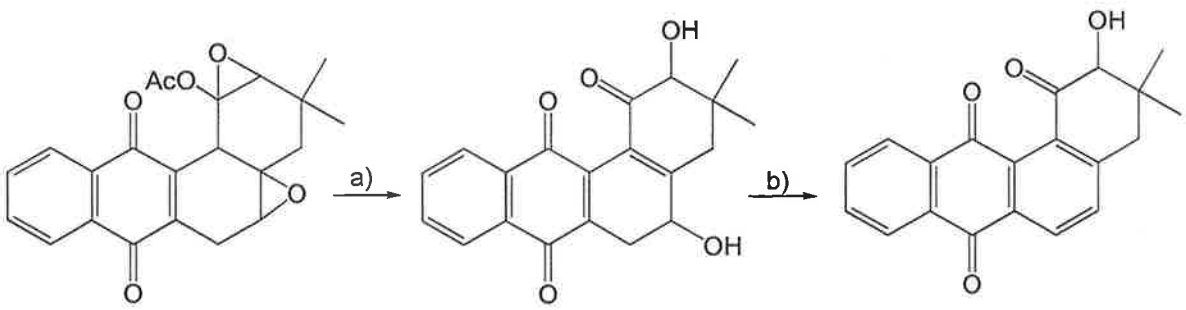

(139) **(140)** **(141)**

a) aqueous acid, b) aromatisation

Scheme 44. Synthesis of α-hydroxy ketone **(141).**

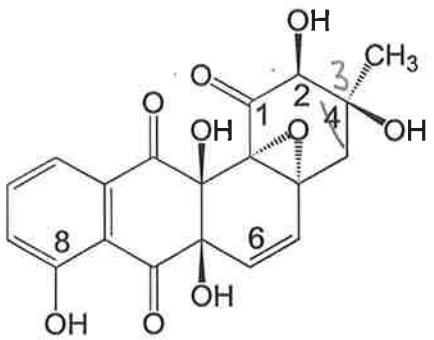

(142) WP 3688-3

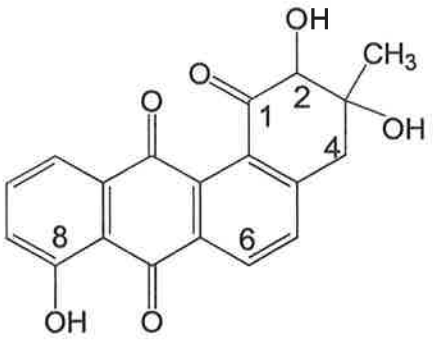

(143) PD 116779

WP 3688-3 **(142)** is a structurally interesting, novel, oxygen rich angucyclinone isolated from *Streptomyces phaeochromogenes* showing antibacterial activity and exhibiting an unusual C-4a,12b epoxidation plus a hydroxyl α to the C-1 ketone having all hydroxy groups on the same face of molecule.[88] PD 116779 **(143)** also contains the α-hydroxy ketone functionality in the A-ring without the extensive oxygenation of **(142)**.[89] The stereochemistries of the 2 and 4 hydroxy groups has not been defined.

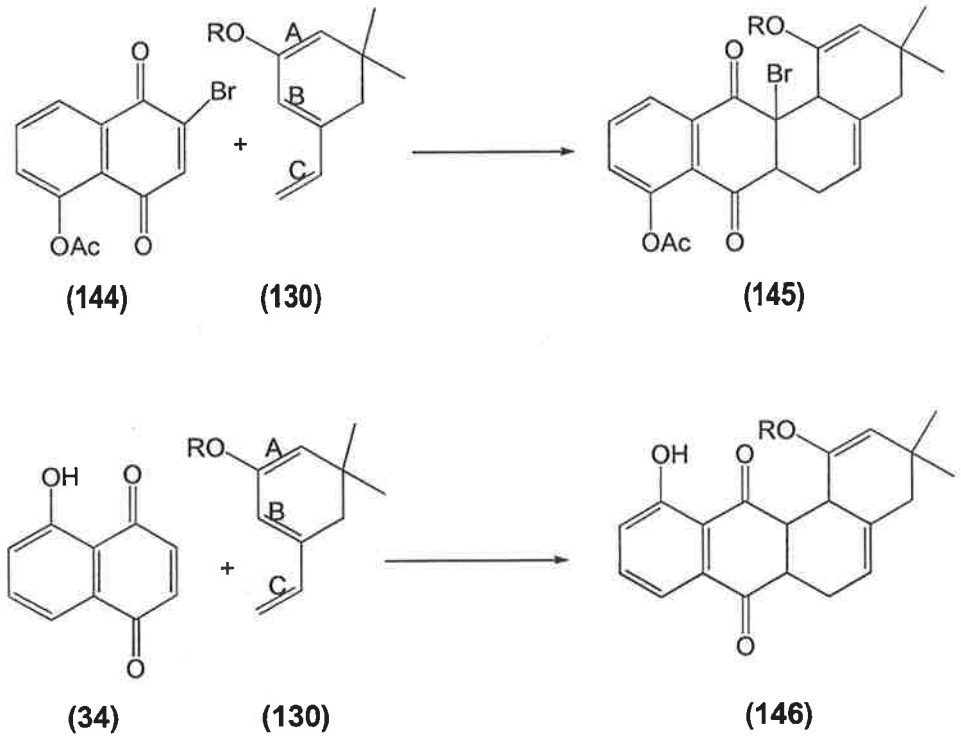

Scheme 45. Formation of the 8-acetoxy adduct **(145)** and an 11- hydroxy analogue **(146).**

Scheme 45 suggests how to synthesise both the 8 and 11 hydroxy precursors to model compounds **(137, 138,** and **140).** In principle, this can be accomplished by condensing the protected enol diene **(130)** with either juglone **(34)** or 2-bromo-5-acetoxy-1,4-naphthoquinone **(144)**.[47, 72] The ground state orbital polarisation of 2-bromo-4-acetoxy-1,4-naphthoquinone **(144)** and triene **(130)** is such that upon condensation, the 8 hydroxy adduct **(145)** should form. However, the reaction of **(130)** with the reversely polarised juglone **(34)**, should effect the opposite stereoselectivity to yield the 11-hydroxy analogue **(146)**.

4.2. Formation and Condensation of Triene (147) with Maleic Anhydride

The enol acetate **(147)** was chosen as the triene system to be used. This choice was based on the resonant electron-withdrawing characteristics of the acetate group to deactivate the A double bond towards Diels-Alder condensation and give the required regio-isomeric product. Protection of the enol with a silyl group (e.g. tert. butyl dimethyl silyl) will activate the A double bond towards a Diels-Alder reaction (due to the electron donating effect of this group) giving the unwanted regio-isomeric product formed by reaction withy the A and B double bonds.

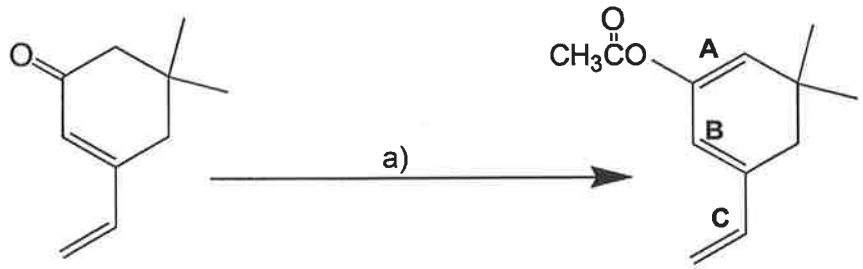

(88) **(147)**

a) (i) LDA, THF, -78°C, (ii) Acetic anhydride, pyridine, 95%

Scheme 46. Formation of enol acetate **(147)** from ketone **(88).**

The enol acetate **(147)** was conveniently prepared from **(88)** in quantitative yield by enolising the ketone starting material with freshly prepared lithium diisopropyl amide (LDA) at -78°C followed by trapping the enolate anion with a quenching solution of pyridine and acetic anhydride (Scheme 46). The acetate **(147)** is sensitive to moisture and is best stored at -20°C under anhydrous conditions.

The electron impact mass spectrum of **(147)** shows a $(MH)^+$ parent ion at *m/z* 193 with a sequential fragmentation pattern of loss of CH_2CO and CH_3 radical. The ^1H n.m.r. spectrum shown in Experimental on page 98 is consistent with the structure of **(147)**.

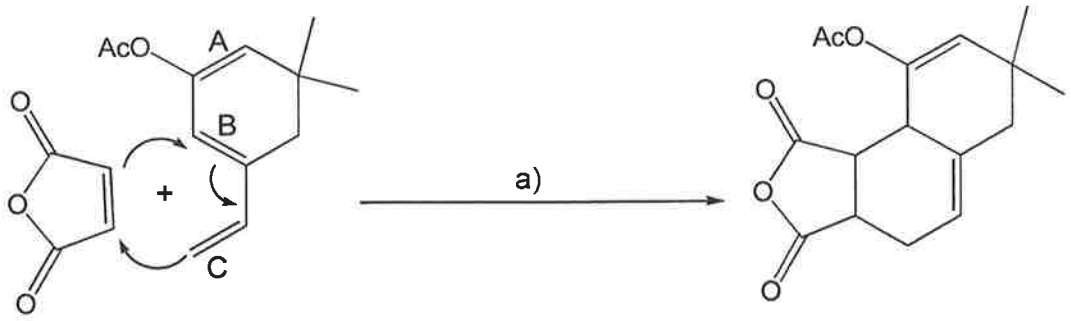

(148) **(147)** **(149)**

a) Toluene, reflux, 16 hr, 76%

Scheme 47. Formation of required model Diels-Alder adduct **(149).**

Maleic anhydride has been used by our research group as a simple model dienophile when the outcome of a condensation reaction is unknown.[91] When maleic anhydride **(148)** and enol acetate **(147)** were heated under reflux in toluene for 16 hours, the required Diels-Alder adduct **(149)** was obtained in 76% yield (Scheme 47). The regio-selectivity of the addition can be attributed to the deactivation of the A double bond of **(147)** by the electron-withdrawing capability of the acetate group.

The EI mass spectrum of **(149)** showed an MH^+ peak at *m/z* 291, together with loss of CH_2CO followed by 'CH_3 to give the base peak at *m/z* 234. GHMQC and GHMBC NMR experiments were used to confirm the framework and general structural features of adduct **(149)** (Summarised in Appendix, NMR section, Table 8). COSY and ROESY experiments were used to assign the relative stereochemistry of **(149)**: data are recorded in Table 4, and summarised below.

A ROESY correlation between protons H9a and 3a confirm a 1,3 diaxial spatial interaction implying that both of these hydrogens are on the same side of the molecule. The coupling constant of 6.6 Hz between H9a and 9b suggests a small dihedral angle approaching 45°. This result combined with the fact that ring closures in Diels-Alder reactions occur with *syn* orientation confirms the stereochemistry shown in Figure 10: the three hydrogens attached to the three chiral centres are all on the same side of the molecule. The structure of **(149)** is consistent with that resulting from an *endo* approach between the triene **(147)** and dienophile **(148)**.[62, 91]

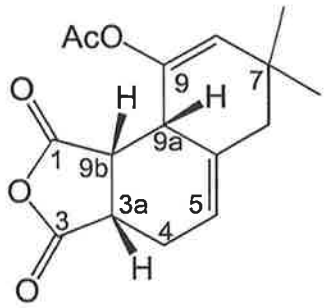

Figure 10. The relative stereochemistry of the B-ring of racemic **(149).**

^{1}H ppm	Assignment	Area	Multiplicity Coupling Constants	COSY	ROESY
5.79	H5	1	ddd, 7.2, 2.4, 2.2 Hz	$H4_{ax}$, $H4_{eq}$, H9a	$H6_{eq}$
5.65	H8	1	t, 1.0 Hz	$H6_{eq}$, H9a	CH_{3ax}, CH_{3eq},
3.57	$H9b_{eq}$	1	dd, 9.6, 6.6 Hz	H3, H9a	-
3.46	$H3a_{ax}$	1	ddd 9.6, 7.8, 1.8 Hz	$H4_{ax}$, $H4_{eq}$, H9a	H9a
3.27	$H9a_{ax}$	1	ddd 6.6, 2.2, 1.0 Hz	H5, H8, H10	CH_{3eq}, H3, $H4_{eq}$,
2.75	$H4_{ax}$	1	ddd 9.0, 7.2, 1.8 Hz	H3, $H4_{eq}$, H5	-
2.29	$H6_{ax}$	1	d, 13.8 Hz	$H6_{eq}$	CH_{3eq},
2.24	$H4_{eq}$	1	ddd 9.0, 7.8, 2.4 Hz	H3, $H4_{ax}$, H5	H9a
2.19	CH_3, acetate	3	s	-	-
2.11	$H6_{eq}$	1	dd, 13.8, 1.0 Hz	$H6_{ax}$, H8	CH_{3ax}, H5
1.06	CH_{3eq}	3	s	-	H_{6ax}, H8, H9a
0.93	CH_{3ax}	3	s	-	H_{6eq}, H8

Table 4. Summary of the ^{1}H n.m.r. experiments used to assign the relative stereochemistry of **(149).**

In conclusion, the reaction of enol acetate **(147)** with maleic anhydride **(148)** gave the required Diels-Alder adduct **(149)** arising from the condensation between bonds B/ C of **(147)** through an *endo* transition state. Based on this result, the triene system **(147)** is expected to condense with 1,4-naphthoquinones in a similar fashion.

4.3. Formation of the 11-Hydroxy Adduct (150)

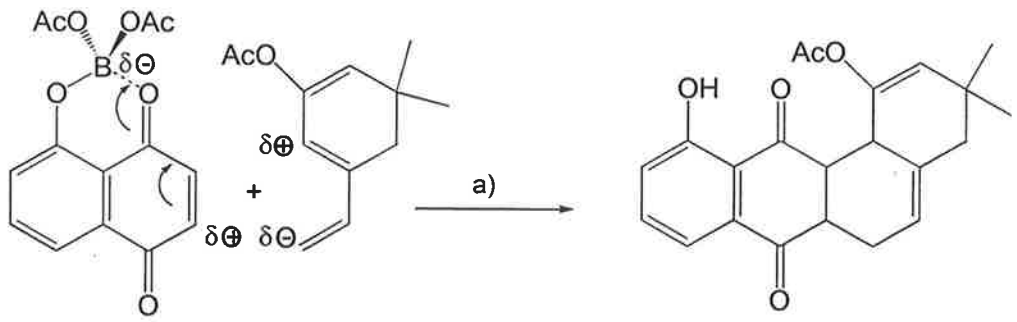

(112) **(147)** **(150)**

a) CH_2Cl_2, 20°C, 4 hr, 40%

Scheme 48. Regio-chemical outcome for the Lewis acid facilitated Diels-Alder reaction between **(112)** and **(147)**.

The Diels-Alder reaction between boron triacetate complexed juglone **(112)** and the triene **(147)** should produce adduct **(150)** to the exclusion of the other regio-isomer (Scheme 48).[52, 62] Under these conditions the required 11-hydroxy adduct **(150)** is formed, but in a yield of only 40%. Significant amounts of the B ring aromatic 1-ketone derivatives of **(150)** are also present in the product mixture. Hydrolysis of the enol acetate is being effected by either boron triacetate, or by acetic acid which is a by-product of the initial complexation reaction with juglone.

Because of the complex mixture formed by the reaction shown in Scheme 48, the reaction conditions were changed to delete the Lewis acid catalyst. In the absence of a Lewis acid catalyst, two regio-isomers could be formed as shown in Scheme 49. However juglone exhibits polarisation of the electrophilic double bond caused by the *peri* hydroxy substituent hydrogen bonding to one of the quinone carbonyls.[27, 36] This H-bonding is known to generate some facial regio-chemistry in Diels-Alder reactions,[36] suggesting that **(150)** should be the major regio-isomer produced by the reaction shown in Scheme 49.

When juglone **(34)** and triene **(147)** were heated under reflux in toluene for 24 hr under nitrogen, a 10:1 mixture of the 11-hydroxy **(150)** and 8-hydroxy **(151)** adducts were obtained. Flash chromatography on silica resulted in a 68% yield of the pure 11-hydroxy regio-isomer, a significant improvement over the yield obtained from the Lewis acid catalysed condensation reaction described above.

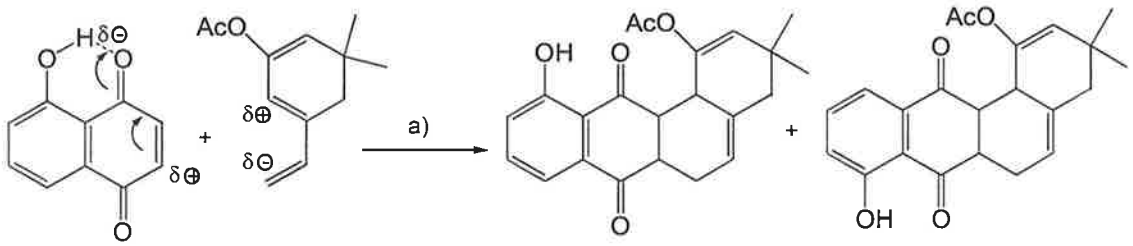

(34) **(147)** **(150)** 68% purified **(151)** 7.5% purified

a) Toluene, reflux, 24 hr, 83%

Scheme 49. The 11 and 8-hydroxy regio-chemical isomers **(150)** and **(151)** form in a 10:1 ratio.

Since both triene and dienophile are planar, the transition state can be attained equally well from each plane. Due to the orbital interactions in the transition state only the symmetry allowed *endo* cycloaddition will be facile. Thus **(150)** should be the racemic diastereomer shown in Figure 11: with the H6a, H12a and H12b all on the same side of the molecule.

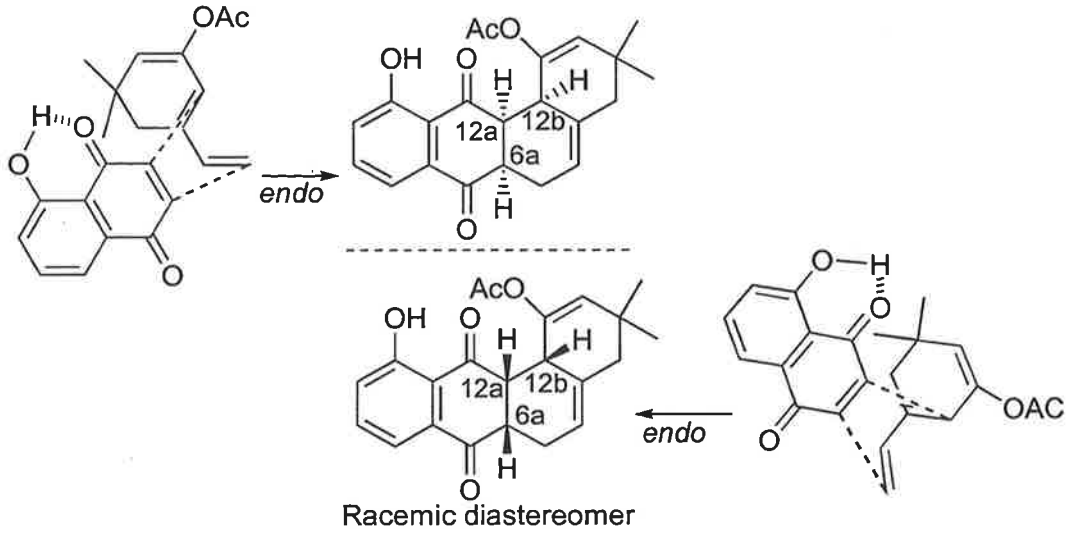

Figure 11. *Endo* approach between triene and juglone rationalizing stereochemistry of adduct.

Electrospray mass spectrometry of **(150)** under negative chemical ionisation conditions gave an $(M-H)^-$ ion at *m/z* 365, with the fragmentation sequence $[(M-H)^- - CH_2CO - H_2O]$. The framework and general structure features of **(150)** were confirmed by GHMQC and GHMBC NMR experiments (Summarised in Appendix, NMR section, Table 10). COSY and ROESY experiments were used to assign the stereochemistry of the B ring: These data are recorded in Table 5.

^1H ppm	Assign ment	Area	Multiplicity Coupling Constants	COSY	ROESY
11.72	C11-OH	1	s	-	H10
7.61	H9	1	t, 7.8 Hz	H8, H10	-
7.53	H8	1	dd, 7.8, 1.2 Hz	H9, H10	-
7.22	H10	1	dd, 7.8, 1.2 Hz	H8, H9	H8
5.43	H5	1	bs (½ W = 4.0 Hz)	$H4_{ax}$, $H6_{eq}$, $H6_{ax}$, H12b	$H4_{eq}$,
5.38	H2	1	t, 1.0 Hz	$H4_{eq}$, H12b	CH_{3ax}, CH_{3eq},
3.60	$H12a_{eq}$	1	t, 4.5 Hz	H6a, H12b	-
3.45	$H12b_{ax}$	1	bs (½ W = 4.0 Hz)	H2, H5, $H6_{ax}$, H12a	$H4_{ax}$, H6a
3.22	$H6a_{ax}$	1	ddd, 11.4, 6.6, 4.5 Hz	$H6_{ax}$,$H6_{eq}$, H12a	H12b
2.37	$H6_{eq}$	1	ddd, 11.6, 6.6, 4.0 Hz	H5,$H6_{ax}$, $H6a_{ax}$	-
2.33	$H4_{ax}$	1	dd, 14.0, 3.1 Hz	$H4_{eq}$, H5	CH_{3eq}, H12b
2.24	$H6_{ax}$	1	dddd, 11.6, 11.4, 3.8, 1.0 Hz	H5, H6eq, H6a, H12b	-
2.08	CH_3 acetate	3	s	-	-
2.06	$H4_{eq}$	1	dd, 14.0, 1.0 Hz	H2, $H4_{ax}$	CH_{3ax}, CH_{3eq}, H5
1.12	CH_{3eq}	3	s	-	H2, $H4_{ax}$, $H4_{eq}$,
1.06	CH_{3ax}	3	s	-	H2, $H4_{eq}$

Table 5. Summary of the ^1H n.m.r. experiments used to confirm the structure and the relative stereochemistry of adduct **(150).**

Adduct **(150)** exhibits many of the characteristic ^1H n.m.r. signals seen previously for other angucyclinone like adducts.[52, 62, 82] These are listed in Table 5. A ROESY correlation between H12b and 6a confirms a 1,3 pseudo diaxial interaction implying that both hydrogens are on the same side in the molecule. The equal coupling constant of 4.5 Hz between H12a and 12b; H12a and 6a suggests a small dihedral angle of less than 45° for both bonds. Thus the three hydrogens attached to the chiral carbons of the B ring are all on the same side of the molecule as shown in Figure 12.

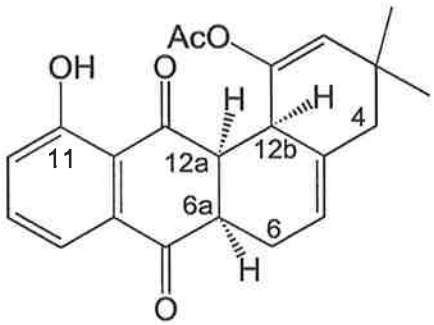

Figure 12. Relative stereochemistry of adduct **(150).**

The structure of the 11-hydroxy adduct **(150)** was confirmed by X-ray crystallography.[92] The computer generated representation is shown in Figure 13. The phenolic hydroxyl is in position 11 and the three hydrogens at chiral positions on the B-ring are all on the same side of the molecule. The stereochemistry is consistent with *endo* approach between the triene and juglone.

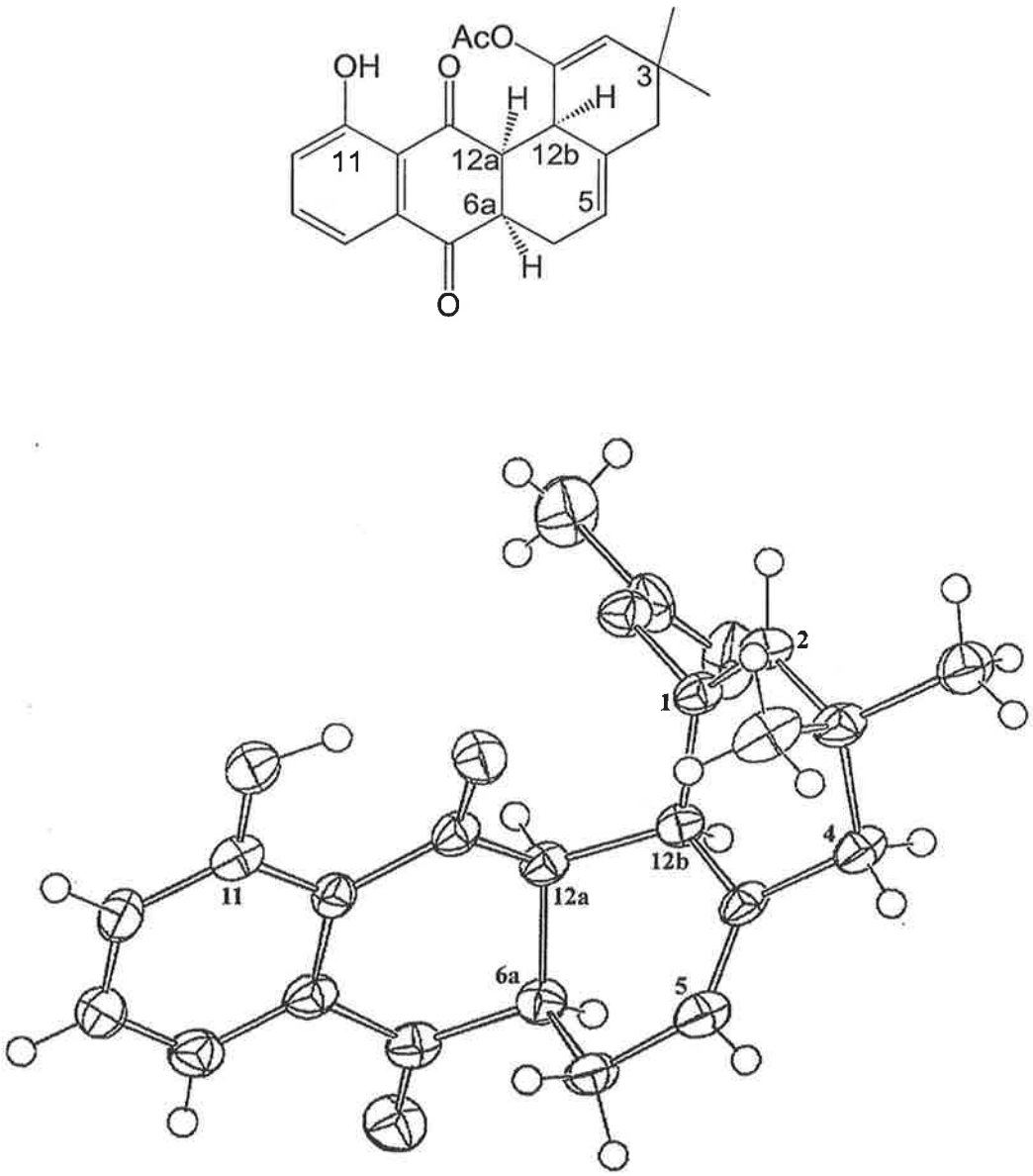

Figure 13. Molecular structure of 11-hydroxy adduct **(150).**

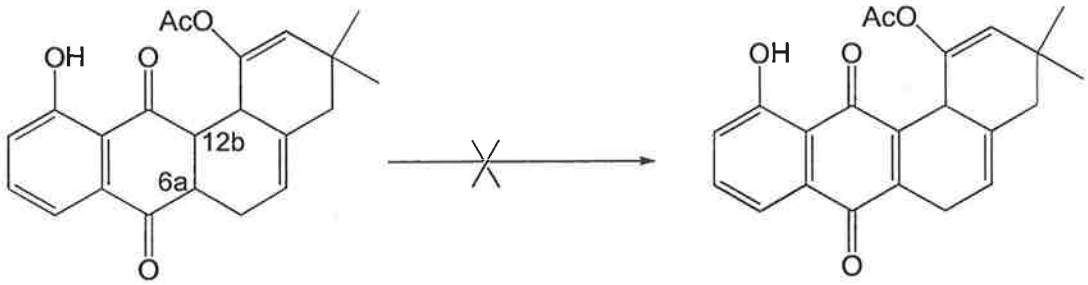

(150) **(152)**

Scheme 50. Failed oxidation of **(150)** to **(152).**

The next step in the synthesis towards a 4a,12b dihydroxylated angucyclinone (outlined in Scheme 50) consists of inserting a double bond (through a SiO_2facilitated aerial oxidation) at position 6a,12b of **(150)** to make quinone **(152)**.

In our previous work towards the synthesis of the isomeric 11-hydroxy analogue of ochromycinone **(109)**,[#] we reported the facile aerial oxidation of adduct **(113)** to quinone **(114)** by absorbing the condensation adduct onto silica and exposing the solid mixture to air.[62] Absorption of **(150)** onto silica and exposure to oxygen for 72 hr led to the total recovery of starting material.

Treatment of adduct **(150)** with freshly prepared manganese dioxide also failed to generate quinone **(152)**. This procedure was successfully employed by Larsen and O'Shea to perform an identical oxidation to generate a quinone from a Diels-Alder adduct as a step in their entry to the ring system of angucyclinones PD 116740 and TAN 1085.[42] In light of this failure our efforts were next directed to the 8-hydroxy Diels-Alder adduct **(153)** (Scheme 51). The inclusion of a bromine atom at the B/ C ring bridge may facilitate oxidation through a dehydrobromination reaction.[39, 40, 47]

[#] Refer to Chapter 2.3, page 34.

4.4. Formation of the 8-Acetoxy Adduct (153)

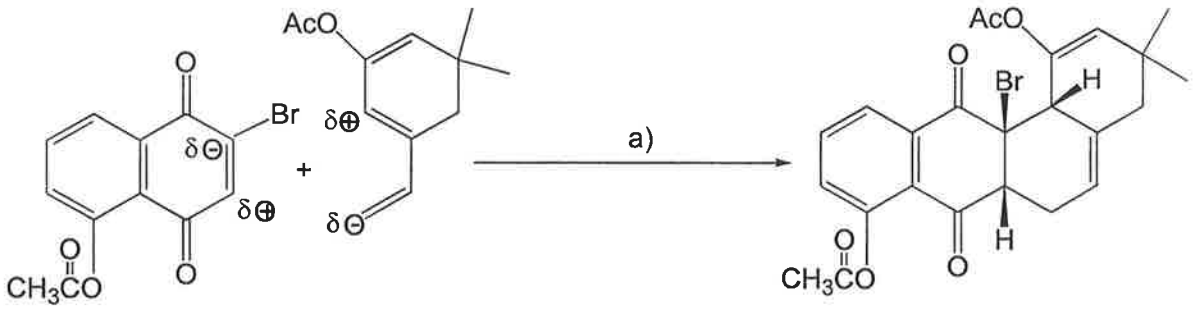

(144) **(147)** **+/- (153)**

a) Toluene, reflux, 24 hr, 92%

Scheme 51. Formation of 8-acetoxy adduct **(153).**

The reaction between 2-bromo-5-acetoxy-1,4-naphthoquinone **(144)** and triene **(147)** in toluene under reflux for 24 hr (and under nitrogen) gave the 8-hydroxy bromo adduct**(153)** in 92% yield. Purification of **(153)** is not necessary if used immediately in the next step of the synthesis. Adduct **(153)** can be stored at -20°C suspended in anhydrous ether. Following storage, **(153)** must be purified by flash chromatography on silica.

The regio-selectivity of this Diels-Alder process is caused by ground state polarisation of the dienophile being effected by the bromine and acetate substituents. The electron withdrawing bromine atom is responsible for reversely polarising the double bond of **(144)** while protection of the phenol (as acetate) prevents the hydrogen bonding between this group and the quinone carbonyl (otherwise responsible for competing polarisation in the other direction). The *endo* approach of the flat triene from above or below of the dienophilegives a racemate with the stereochemistry shown in Scheme 51.

The EI mass spectrum of **(153)** shows two MH^+ ions at *m/z* 487, 489. with the major fragmentation sequence being MH^+ - HBr - CH_2CO – CH_3CO_2H. The final loss of acetic acid is surprising, since this loss can only occur from the A ring after isomerization of the 1,2 double bond.

The connectivity and general structure features of **(153)** were confirmed by GHMQC and GHMBC NMR experiments (Summarised in Appendix, NMR section, Table 12). COSY and ROESY experiments were used to assign the stereochemistry of the B ring: These data are recorded in Table 6.

^{1}H ppm	Assign ment	Area	Multiplicity Coupling Constants	COSY	ROESY
8.00	H11	1	dd, 7.8, 1.2 Hz	H10, H9	-
7.75	H10	1	t, 7.8 Hz	H9, H11	-
7.37	H9	1	dd, 7.8, 1.2 Hz	H10, H11	-
5.54	H5	1	dt, 4.2, 2 Hz	$H6_{eq}$, $H6_{ax}$, H12b	CH_{3ax}, $H4_{eq}$, $H4_{ax}$,
5.40	H2	1	dd, 1.8, 1.5 Hz	$H4_{eq}$, H12b	CH_{3ax}, CH_{3eq},
3.97	$H12b_{ax}$	1	bs	H2, H5, $H6_{ax}$	$H4_{ax}$, H6a
3.62	$H6a_{ax}$	1	dd, 12.0, 6.0 Hz	$H6_{ax}$,$H6_{eq}$	H12b
2.45	$H6_{eq}$	1	ddd, 12.8, 6.0, 4.2, Hz	H5, $H6_{ax}$, H6a	-
2.40	$C8_{acetate}$	3	s	-	-
2.34	$H4_{ax}$	1	d, 12.9 Hz	$H4_{eq}$	CH_{3eq}, H5, H12b
2.30	$H6_{ax}$	1	m, 12.8, 12.0, 4.2 Hz	H5, H6eq, H6a, H12b	-
2.10	$C1_{acetate}$	3	s	-	-
2.06	$H4_{eq}$	1	dd, 12.9,1.8 Hz	H2, $H4_{ax}$	CH_{3ax}, CH_{3eq}, H5,
1.12	CH_{3eq}	3	s	-	H2, $H4_{ax}$, $H4_{eq}$,
1.04	CH_{3ax}	3	s	-	H2, $H4_{eq}$, H5

Table 6. Summary of ^{1}H n.m.r. experiments for bromo adduct **(153).**

The 1,3 diaxial ROESY interactions between the position- 4, 12b and 6a axial protons (2.30, 3.97, 3.6 ppm respectively) indicate that all hydrogens are on the same face of the molecule as shown in Figure 14.[#] The ROESY cross peak of the 1.12 ppm methyl resonance with only the axial H4 designates its stereochemistry as up. The equatorial H4 (down) resonating at 2.06 ppm, interacts with both methyl signals (1.12 and 1.04 ppm) of the 3-geminal methyl groups. This ROESY interaction implies that the equatorial H4 bisects the geminal dimethyl group at approximately 45°.

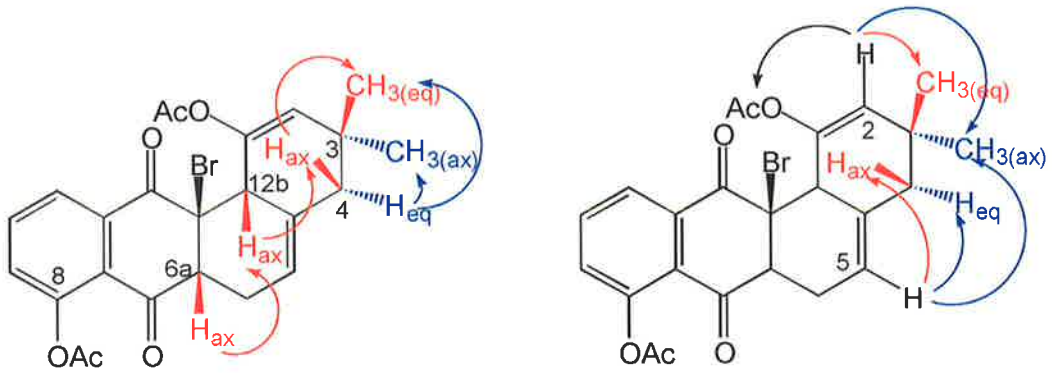

Figure 14. Graphical summary of the ROESY correlations used to assign the relative stereochemistry of racemic **(153)** at positions-3, 4, 6a, 12a, 12b (red arrows = correlations between protons on topside of molecule, blue arrows = correlations between protons on bottom side of molecule).

The structure of the 11-hydroxy adduct **(153)** was confirmed by X-ray crystallography.[92] The computer generated representation is shown in Figure 15. The D-ring acetate group was confirmed to be in position 8. The two hydrogens at the 6a and 12b chiral positions on the B-ring and the bromine atom are all on the same side of the molecule. The stereochemistry is consistent with *endo* approach between the triene and 2-bromo-5-acetoxy-1,4-naphthoquinone.

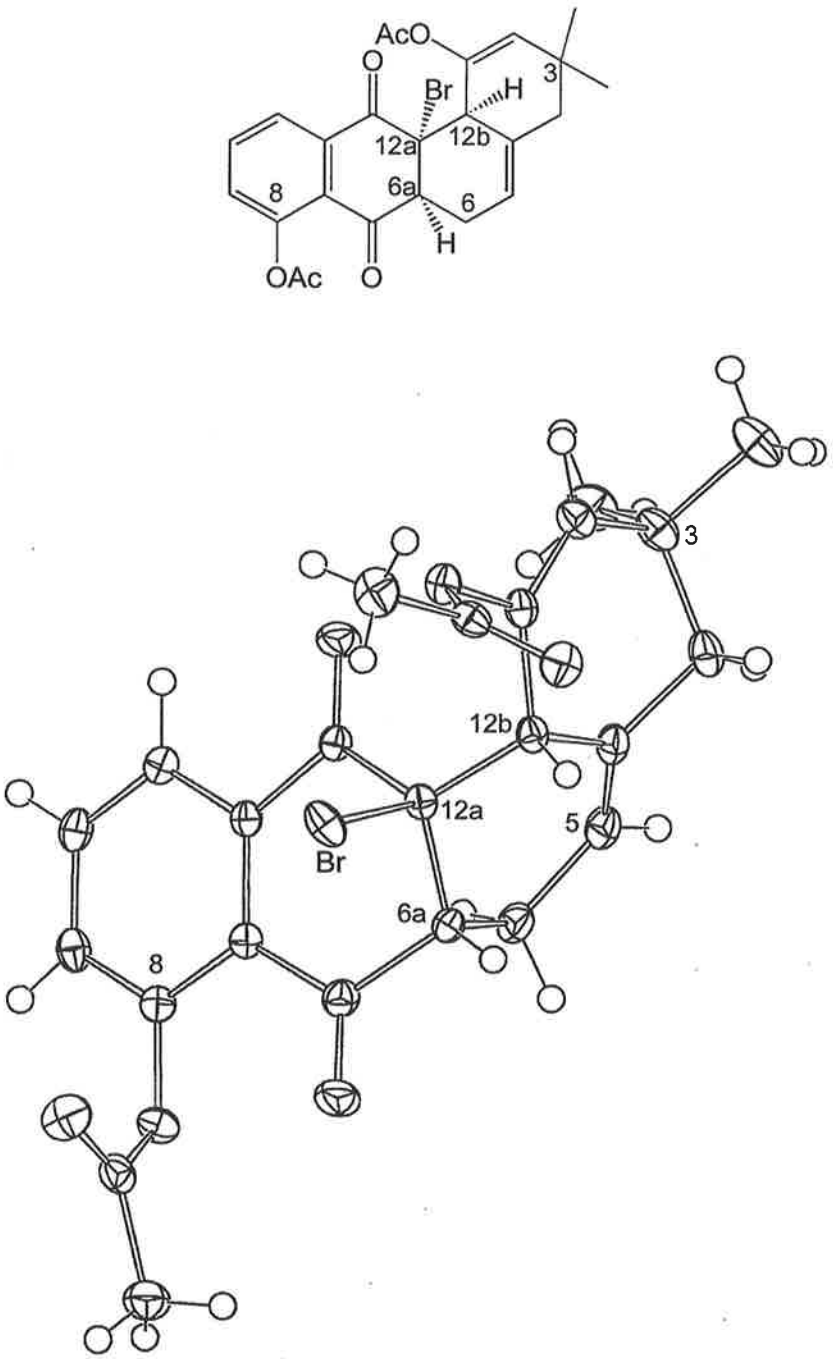

Figure 15. Molecular structure of the 8-acetoxy adduct **(153).**

4.5. Regio and Stereospecific Monoepoxidation of Adduct (153)

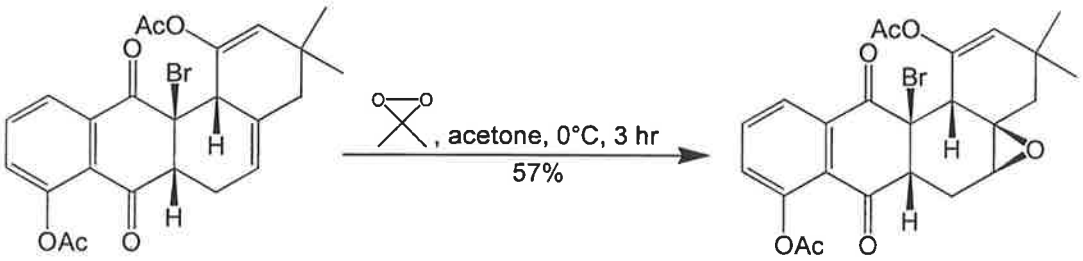

+/- (153) **+/- (154)**

Scheme 52. Regiospecific epoxidation of bromo adduct **(153).**

Treatment of **(153)** with a 1:1 molar anhydrous acetone solution of dimethyldioxirane (DMDO)[#, 85] at 0°C for 3 hr gave bromo epoxide **(154)** in a yield of 57% (Scheme 52). The product **(154)** is unstable and should be stored in diethyl ether -20°C.

The epoxidation of **(154)** is both regio and stereo-specific. The conditions of slow DMDO addition and high dilution of the reaction mixture lead to the preferential attack at the less hindered tri-substituted 4a,5 double bond. As the concentration of DMDO increases, so does the chance of attack at the more hindered (and deactivated) 1,2 double bond. One plane of the 4a,5 double bond of **(153)** is partially blocked by the axial methyl substituent of the C-3 *gem* dimethyl group [see to the X-ray structure of **(153)** in Figure 15]. It is this structural feature that directs the delivery of the epoxidating reagent from the less hindered, bromine containing, top plane of the molecule.

Epoxide **(154)** shows weak molecular ions at *m/z* 503, 505 when subject to EI ionisation. The major fragmentation pathway, $M^{+\cdot}$ - HBr - CH_2CO – CH_3CO_2H is similar with that of the precursor **(153).** The framework and general structure features of **(154)** were confirmed by the GHMQC and GHMBC NMR experiments (Summarised in Appendix, NMR section, Table 14), while a COSY, ROESY, NOE and coupling constant data were used to assign the relative stereochemistry of the A and B rings. The ^1H n.m.r. experiments are summarised in Table 7, while Figures 16 and 17 contain the graphical summary of the ROESY and NOE experiments.

DMDO was prepared following a modified method based on that of Adam and Hadjiarapoglue and standardised by completing a iodometric titration.[85]

^{1}H ppm	Assignment	Area	Multiplicity Coupling Constants	COSY	ROESY
7.95	H11	1	dd, 8.0, 1.2 Hz	H10, H9	-
7.76	H10	1	t, 8.0 Hz	H9, H11	-
7.37	H9	1	dd, 8.0, 1.2 Hz	H10, H11	-
5.53	H2	1	dd, 1.8, 1.2 Hz	H12b, $H4_{eq}$	CH_3,
3.79	$H12b_{ax}$	1	d, 1.8 Hz	H2	$H4_{ax}$, H6a
3.75	$H6a_{ax}$	1	dd, 13.2, 4.8 Hz	$H6_{ax}$,$H6_{eq}$	H12b
3.17	$H5_{eq}$	1	bs	$H6_{eq}$, $H6_{ax}$	CH_3, $H4_{ax}$, $H4_{eq}$
2.47	$H6_{eq}$	1	ddd, 15.0, 4.8, 2.7 Hz	H5, $H6_{ax}$, H6a	-
2.40	C8 acetate	3	s	-	-
2.20	$H4_{ax}$	1	d, 13.2 Hz	$H4_{eq}$	CH_3, H5, H12b
2.09	C1 acetate	3	s	-	CH_3
1.99	$H6_{ax}$	1	ddd, 15.0, 13.2, 1.2 Hz	H5, H6eq, H6a	-
1.30	$H4_{eq}$	1	dd, 13.2,1.2 Hz	H2, $H4_{ax}$	CH_3, H5,
1.15	$CH_{3(eq)}$	3	s	-	$C1_{acetate}$, H2, $H4_{ax}$, H12b
1.15	$CH_{3(ax)}$	6	s		$C1_{acetate}$, H2, $H4_{ax}$, $H4_{eq}$, H5

Table 7. Summary of ^{1}H n.m.r. experiments for epoxide **(154)**.

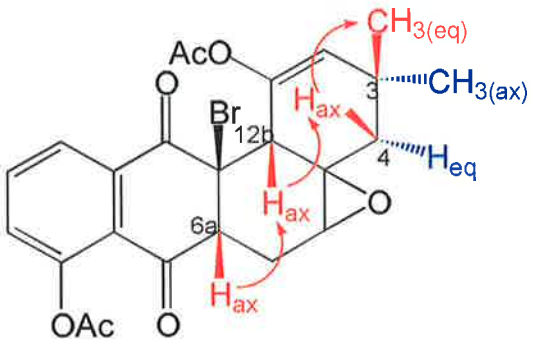

Figure 16. Graphical ROESY summary of **(154)**.

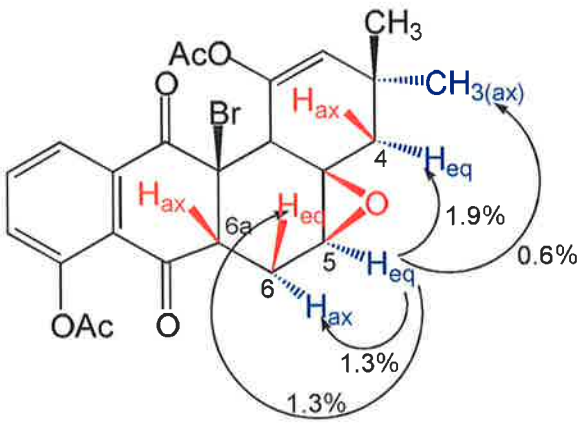

Figure 17. NOE on H-5 of **(154)**.

The spatial 1,3 diaxial ROESY interactions of protons H6a, 12b, and 4_{ax} (3.75, 3.79, and 2.20 ppm) confirm the relative stereochemistry at those sites as up, being all on the same side of the molecule (Figure 16).# The ROESY spectrum failed to resolve the stereochemistry of the epoxide, however irradiation of H5 (3.17 ppm) in a NOE experiment enhanced protons at positions - 4eq, CH_3(ax), 6ax and 6eq, by values specified in Fig 17.

The axial/ equatorial nomenclature has been used for convenience, in fact the protons of the A and B rings are pseudo axial/equatorial (i.e. the angle between $H6a_{ax}$ and $H6_{ax}$ is not exactly 180°)
Only one enantiomer of the racemate is shown in **Figures 16** and **17**.

experiment show that H5 is on the opposite side of the molecule to H6a, 12b, and 4_{ax}. Similar NOE enhancement of $H6_{ax}$ and $H6_{eq}$ suggests that H5 bisects the two hydrogens of the 6-methylene group.

The relative stereochemistry of the 6-hydrogens were assigned by interpreting the coupling constants and splitting patterns using the Karplus correlation. The large coupling constant of 13.2 Hz between H6a and H6 (3.75 and 1.99 ppm respectively) results from an anti-peri planar relationship between the two pseudo axial protons approximating a dihedral angle of 180°: thus the 1.99 ppm resonance is that of the axial hydrogen. The splitting pattern of $H6_{ax}$ is a ddd (appears to be a doublet of triplets) as a results of a geminal 15.0 Hz coupling to $H6_{eq}$ plus a small 1.2 Hz coupling to $H5_{eq}$. The 4.8 Hz coupling constant between $H6_{eq}$ and H6a indicates an approximate angle of 45°. Figure 18 is a computer generated drawing of epoxide **(154)** showing the average conformation and stereochemistry of the B-ring as shown by the NMR experiments.

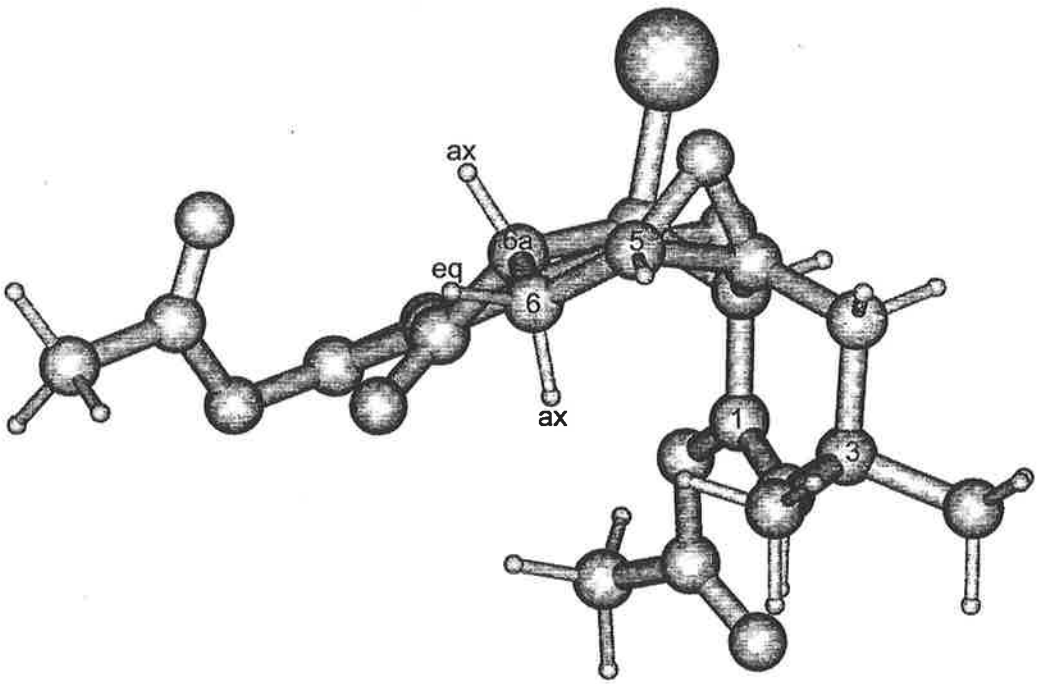

Figure 18. Perspective drawing of epoxide **(154)** showing conformation of the A and B rings.

4.6 Dehydrobromination of Adduct (153) and Epoxide (154)

Dehydrobromination of **(153)** under (i) mild acidic conditions led to recovery of starting material or (ii) basic conditions caused aromatisation to yield angucyclinone **(156)** and ochromycinone analogue **(108).**

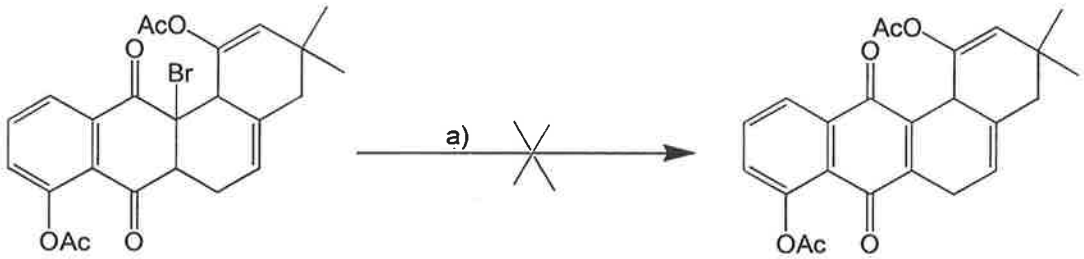

(153) **(155)**

a) SiO_2, Failed to react

Scheme 53. Failed silica gel induced dehydrobromination of bromo adduct **(153).**

Absorption of **(153)** onto silica and exposure to the atmosphere for 48 hr led to the total recovery of starting materials (Scheme 53).

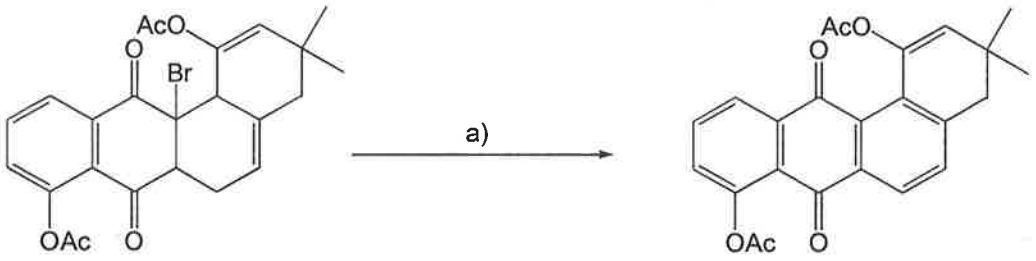

(153) **(156)**

a) DBU, dry benzene, 0°C, 44% **(156)** or DABCO, dry benzene, 0°C, 40% **(156)**

Scheme 54. Formation of the B-ring aromatic enol acetate **(156).**

Standard base catalysed dehydrobromination of **(153)** using either DBU or DABCO in dry benzene under nitrogen (found to be effective by Sulikovski in his earlier work[47]) also failed to give **(155):** in both cases, aromatisation gave **(156)**, $M^{+\cdot}$ = 404 as the major product (Scheme 54).

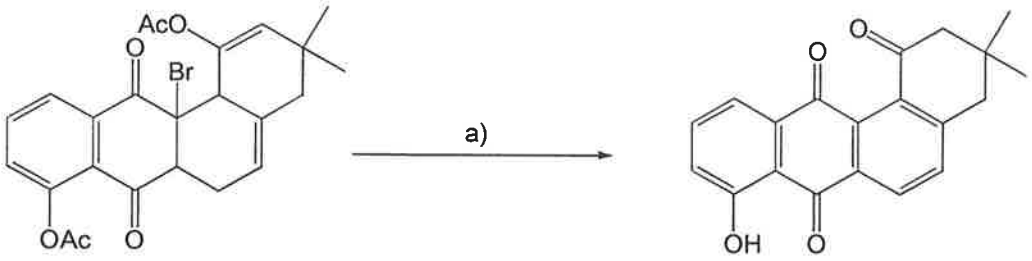

(153) **(108)**

a) 20% aq. NaOH, THF, 20°C, 48 hr, 20%

Scheme 55. One-pot formation of ochromycinone analogue **(108)** from **(153).**

Treatment of **(153)** with 20% aqueous sodium hydroxide solution in tetrahydrofuran at 20°C for 48 hours gave the aromatised and deprotected ochromycinone analogue **(108)** in poor yield (Scheme 55). The ^{1}H n.m.r. spectrum of **(108)** produced from **(153)** was identical to the spectrum of authentic **(108)** synthesised earlier.[52]

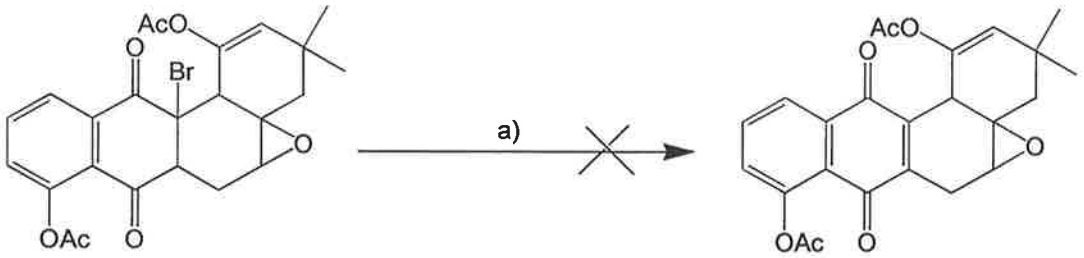

(154) **(157)**

a) SiO_2, Failed to react

Scheme 56. Failed silica gel induced dehydrobromination of epoxide **(154).**

Absorption of the mono epoxide **(154)** onto silica and exposure to the atmosphere for 48 hr led to the total recovery of starting materials (Scheme 56). The failure of this procedure is surprising since it is commonly used for such purposes.[39, 40]

Treatment of **(154)** with 1 equivalent of DBU in dry benzene under nitrogen also failed to form isolable **(157.)**. Several products were formed, one of which was the aromatic species **(156).** Employing less basic conditions of heating a solution of **(154)** in anhydrous pyridine at reflux for one minute (under nitrogen) and then allowing the solution to stand at 20°C for an additional thirty minutes, did generate a quinone product. Preliminary characterisation by NMR and MS seem to indicate the identity of this product as **(157)** shown in Scheme 56. This quinone product needs additional investigation: unfortunately time has run out.

4.7. Stereospecific *Bis*-Epoxidation of Adduct (158)

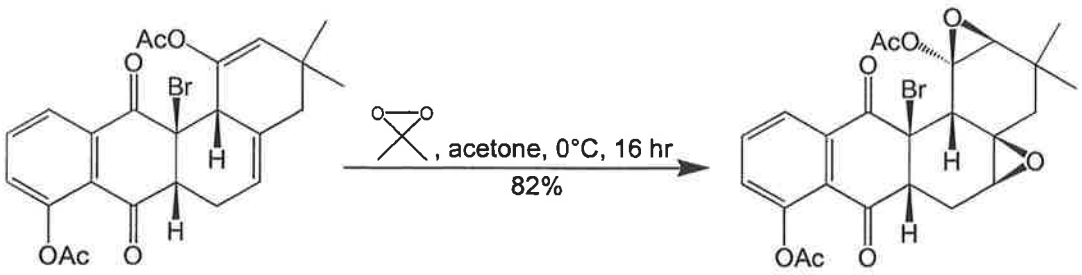

+/- (153) **+/- (158)**

Scheme 57. Regiospecific epoxidation of adduct **(153).**

Treatment of bromo adduct **(153)** with 2.5 equivalents of dimethyldioxirane (DMDO) in anhydrous acetone at 0°C for 16 hr gave the *bis*-epoxide **(158)** in 82% yield (Scheme 57). The *bis*-epoxide **(158)** is more stable at room temperature than the monoepoxide **(154)**, but it is best stored as a suspension in anhydrous diethyl ether at -20°C. We believe that the 4a,5 double bond is attacked first from the more accessible top side of the molecule (see X-ray structure of **(153)** in Figure 15), followed by the attack on the less nucleophilic, deactivated 1,2-double bond. The computer generated representation of the monoepoxide (Figure 18) clearly shows that the bottom side of the ring A is blocked and so formation of the 1,2-epoxide must involve attack of DMDO from the top face molecule to give **(158)** (Scheme 57).

Bis-epoxide **(158)** on electron impact ionisation gave molecular ions at *m/z* 519, 521 together with a fragmentation pattern [$M^{+\cdot}$ - CH_2CO – HBr – CH_3CO_2H] similar to that of **(153)** and **(154).** The framework and general structural features of **(158)** were confirmed by the GHMQC and GHMBC NMR experiments (Summarised in Appendix, NMR section, Table 16), while COSY, ROESY, NOE and coupling constant data were used to assign the relative stereochemistry of the A and B rings. The ^1H n.m.r. experiments are summarised in Table 8, while Figures 19 and 20 contain the graphical summary of the ROESY and NOE experiments.

^{1}H ppm	Assignment	Area	Multiplicity Coupling Constants	COSY	ROESY
7.96	H11	1	dd, 7.5, 1.2 Hz	H10, H9	-
7.78	H10	1	t, 7.5 Hz	H9, H11	-
7.40	H9	1	dd., 5, 1.2 Hz	H10, H11	-
3.76	$H12b_{ax}$	1	bs	H2	$H4_{ax}$, H6a
3.73	$H6a_{ax}$	1	dd, 12.6, 4.2 Hz	$H6_{ax}$,$H6_{eq}$	H12b
3.35	$H2_{eq}$	1	bs	$H12b_{ax}$	CH_{3ax}, CH_{3eq}
2.96	$H5_{eq}$	1	bs	$H6_{eq}$, $H6_{ax}$	CH_{3ax}, $H4_{eq}$
2.43	$H6_{eq}$	1	ddd, 14.0, 4.2, 2.4 Hz	H5, $H6_{ax}$, H6a	-
2.40	C8 acetate	3	s	-	-
2.27	$H4_{ax}$	1	d, 13.8 Hz	$H4_{eq}$	CH_{3eq}, H12b
1.96	$H6_{ax}$	1	ddd, 14.0, 12.6, 1.2 Hz	H5, $H6_{eq}$, H6a	-
1.95	C1 acetate	3	s	-	CH_{3eq}
1.20	CH_{3ax}	3	s	-	H2, $H4_{eq}$, $H5_{eq}$
1.15	CH_{3eq}	3	s	-	$C1_{acetate}$, H2, $H4_{ax}$, $H4_{eq}$,
0.71	$H4_{eq}$	1	d, 13.8 Hz	$H4_{ax}$	CH_{3eq}, CH_{3ax}, $H5_{eq}$

Table 8. Summary of ^{1}H n.m.r. experiments for *bis*-epoxide **(158)**.

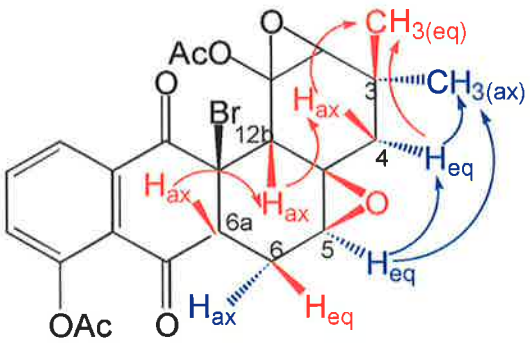

Figure 19. Graphical representation of the ROESY experiment on **(158)** [red arrows indicate interactions between hydrogens on the top side of molecule, while blue arrows represent bottom H's.]

A summary of the interpretation of the ROESY experiments is shown in Figure 19, in particular, the large 12.6 Hz coupling constant between H6a and H6 indicates a pseudo trans diaxial relationship (approximating a dihedral angle of 180°) meaning that the hydrogens are on opposite planes of the molecule [$H6a_{ax}$ is arbitrarily shown as up]. The other 6 methylene

ROESY interactions between $H6_{ax}$, $H12b_{ax}$, $H4_{ax}$ imply that these hydrogens are on the same side of **(158)**. The ROESY cross peak between $H4_{ax}$ and the methyl resonance at 1.15 ppm (plus the lack of a ROESY between $H4_{ax}$ and the other down facing methyl at 1.20 ppm) sets this methyl signal as being up [see Table 8 for H chemical shift values]. H5 is down (equatorial) due to: (i) the lack of the 1,3 diaxial ROESY interactions between H5 and the axial H12b or H6a and (ii) ROESY interaction between $H5_{eq}$, CH_{3ax}, and $H4_{eq}$.

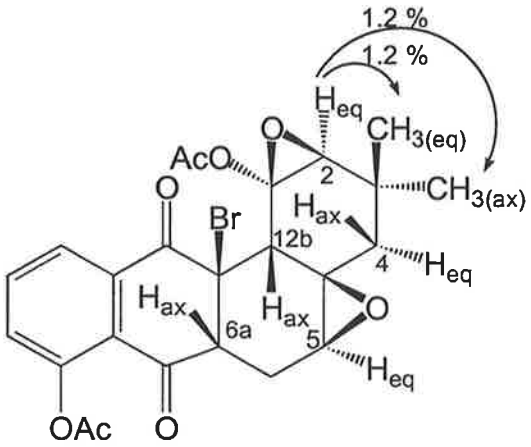

Figure 20. Results of NOE experiment on H4 showing the stereochemistry of **(158).**

Figure 20 shows the results of a NOE experiment on *bis*-epoxide **(158)** used to assign the relative stereochemistry of the 1,2 epoxide. Irradiation of H2 (3.35 ppm) led to the enhancement of both the 3 methyl groups (equally by 1.2%) implying that H2 bisects the two groups. The lack of any NOE enhancements (or 1,3 diaxial ROESY cross peaks) between H2, $H12b_{ax}$ or $H4_{ax}$ suggests that H2 is facing down [equatorial on the opposite plane of **(158)]**.

In conclusion, NMR data suggest that both of the epoxides of **(158)** are on the same side of the molecule as the 12a bromine group (Figure 20). Suitable crystals of **(158)** could not be obtained for an X-ray crystallographic study.

4.8. Synthesis of α-Hydroxy Ketone (161)

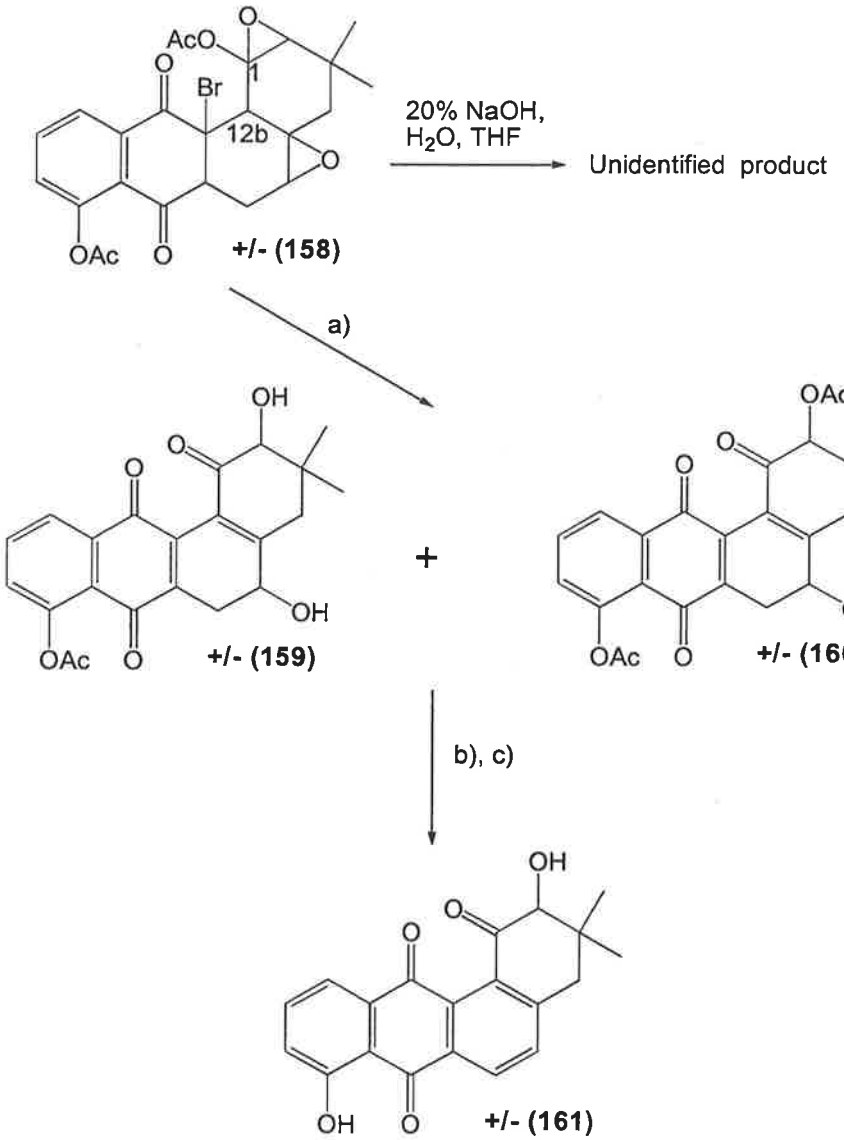

a) pTSA cat. THF, H_2O, reflux, 16 hr, 75%; b) Acetic acid, H_2SO_4 cat. 2 hr, 88%; c) THF, 20% NaOH, 3 hr, 78%

Scheme 58. Synthesis of the A-ring α-hydroxy ketone containing angucyclinone **(161).**

In principle, epoxide ring opening of **(158)**, followed by aromatisation/ hydrolysis should give the α-hydroxy ketone **(161)**.[86, 93] The reaction scheme is summarised in Scheme 58. Treating **(158)** with base should give the α-hydroxy ketone **(161)** in one step, however refluxing **(158)** in tetrahydrofuran and 20 % aqueous sodium hydroxide solution for 24 hours failed to give the required product **(161)** in acceptable yields.

By refluxing a mixture of the *bis*-epoxide **(158)** with a catalytic amount of p-toluene sulfonic acid in wet tetrahydrofuran for 16 hours led to the isolation of a 2:1 mixture of the intermediate diol **(159)** and the *bis* acetate **(160)** in about 75% overall yield. Compounds **(159)** and **(160)** can be separated by flash chromatography, but purification is unnecessary if these products are to be used in the next step of the synthesis. The crude mixture of**(159)** and **(160)** was dehydrated with acetic acid containing a catalytic amount of concentrated sulphuric acid to yield a mixture B ring oxidised angucyclinones in essentially quantitative yield. These intermediate angucyclinones (not isolated) were subject to base catalysed hydrolysis (20% aqueous sodium hydroxide in tetrahydrofuran for 3 hr at ambient temperature) to give the final A-ring α-hydroxy ketone **(161)** in 55% yield (purified) from the *bis*-epoxide **(158)**. The acid catalysed opening of *bis*-epoxide **(158)** to **(159)** and **(160)** is complex and will be dealt with in section 4.9.

The structure of the α-hydroxy ketone **(161)** was confirmed as follows. The 300 MHz ^{1}H n.m.r. spectrum (Figure 21) is that of a classical planar angucyclinone. The characteristic sharp down field signal due to the *peri*-hydroxy group resonates at 12.22 ppm, with two coupled doublets of H6 and H5 at 8.36 and 7.58 ppm (7.8 Hz). The H10 triplet (7.29 ppm) is coupled to the two overlapping doublets of H9 and H11 at 7.68 ppm (3.9 Hz). Other data are shown in Figure 21.

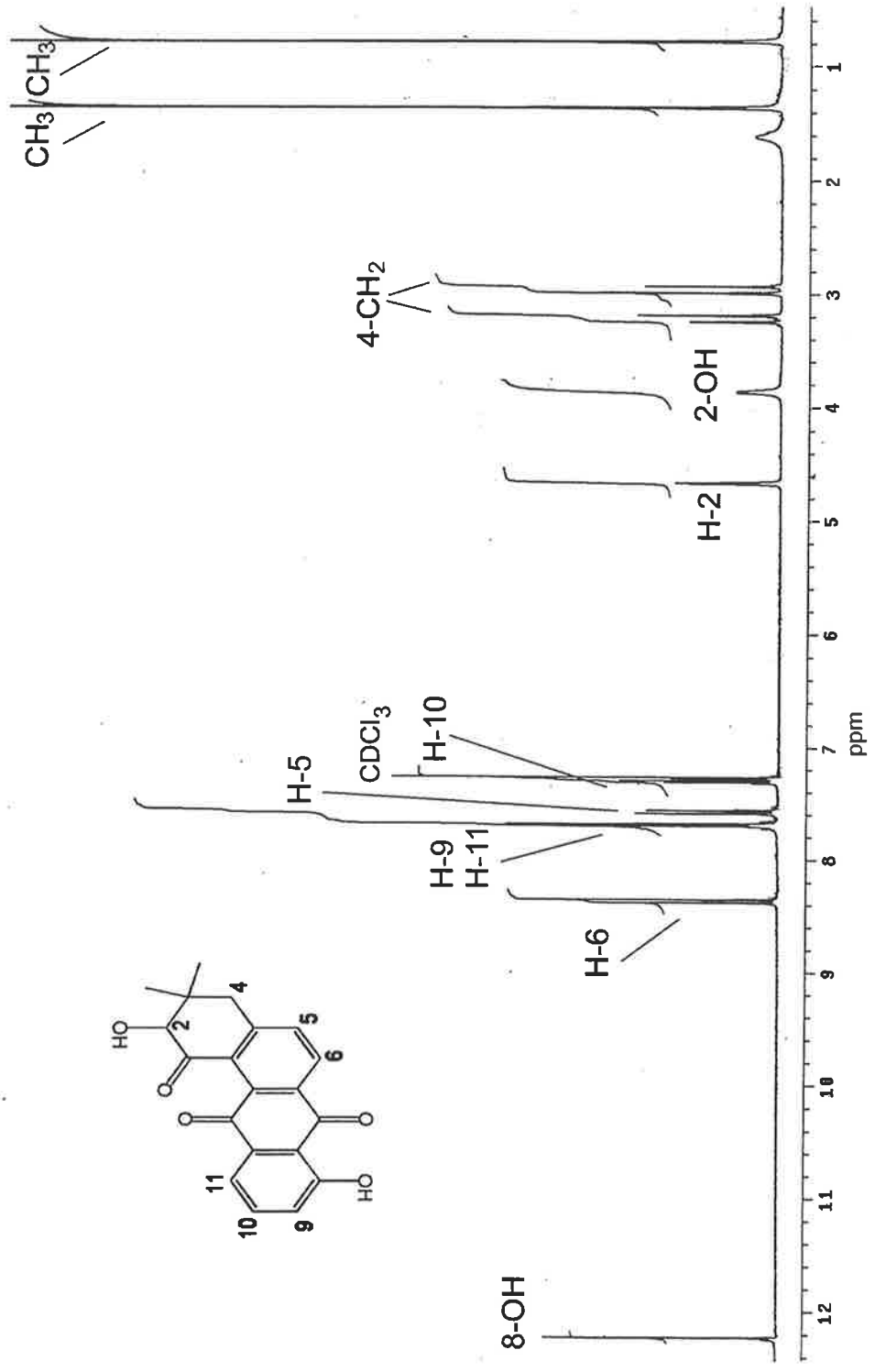

Figure 21. A 300 MHz 1H n.m.r. spectrum ($CDCl_3$) of the α–hydroxy ketone **(161).**

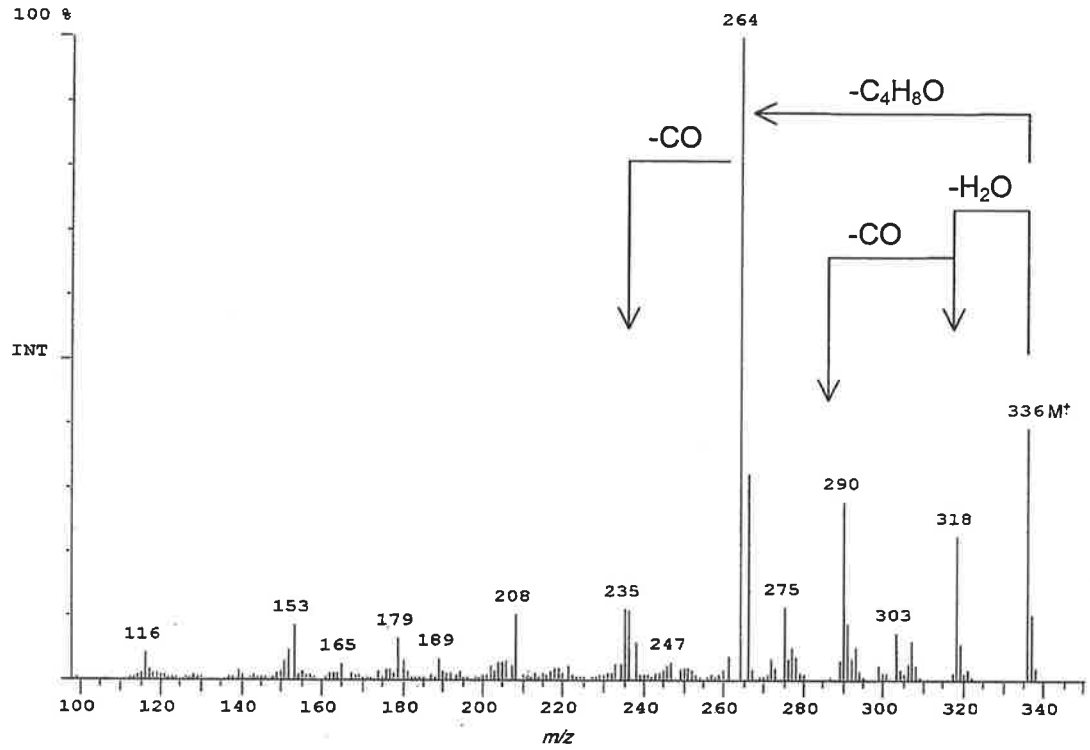

Figure 22. EI mass spectrum of α–hydroxy ketone **(161).**

The infrared carbonyl absorptions are at 1693 (α OH-carbonyl), 1660 (quinone carbonyl) and 1633 (peri OH bonded carbonyl) cm^{-1}. The electron impact mass spectrum is shown in Figure 22 and shows the molecular ion $C_{20}H_{16}O_5$ at *m/z* 336, with the main fragmentation being the characteristic retro Diels-Alder loss of C_4H_8O from the A ring..

In conclusion, the A ring containing α-hydroxy ketone angucyclinone **(161)** was synthesised in a 55% overall yield starting from the *bis*-epoxide **(158)** by acid catalysed epoxide opening together with B-ring aromatisation through dehydrobromination and water elimination. Angucyclinone **(161)** is structurally related to Pd 116779 **(143)** and WP 3688-3 **(142)** shown on page 61.

4.9. Structure Determination of Diol (159) and *bis*-Acetate (160)

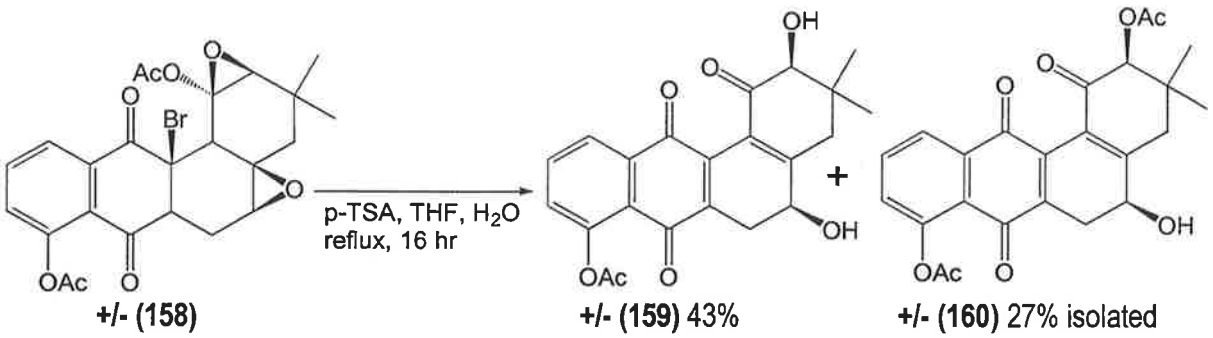

+/- (158) **+/- (159)** 43% **+/- (160)** 27% isolated

Scheme 59. Acid catalysed epoxide opening and partial oxidation of **(158).**

Subjecting *bis*-epoxide **(158)** to aqueous acid catalysed epoxide ring opening forms a non isolated triol having a hemi ketal functional group at position 1 which subsequently hydrolyses into an α-hydroxy ketone[86, 93] or undergoes a 1,2 acetate migration to form **(160).**[94] This complicated process will be discussed in detail later in this chapter. Dehydrobromination and elimination of water (at position 4a) then gives a mixture of the diol **(159)** and acetate **(160)** in a 75% yield. Purification by flash chromatography on silica gives pure **(159)** and **(160)** in 43% and 27% yields respectively.

Structure confirmation of the two products was as follows. Diol **(159)** shows weak molecular ion at *m/z* 396 when subject to EI ionisation. The major fragmentation pathway is $M^{+\cdot}$ - H_2O - CH_2CO – C_4H_8O – CO. Bis-acetate **(160)** exhibits a similar mass spectrum to **(159)** showing a weak molecular ion at *m/z* 438 when subject to EI ionisation, with the major fragmentation pathway being: M^+ - H_2O - CH_2CO – $C_6H_{10}O_2$ – CO. Both compounds undergo the characteristic retro Diel-Alder process being the loss of C_4H_8O for diol **(159)** and $C_6H_{10}O_2$ for *bis*-acetate **(160).** The infrared carbonyl absorptions for diol **(159)** were: 1772 (acetate carbonyl), 1749 (α-hydroxy carbonyl), 1671 and 1656 (quinone carbonyls). The infrared carbonyl absorptions for the closely related *bis*-acetate **(160)** were: 1770 (D ring acetate carbonyl), 1733 (A ring acetate carbonyl), 1689 (α-acetoxy carbonyl), 1650 and 1640 (quinone carbonyls).

The framework and general structural features of products **(159)** and **(160)** were confirmed by the GHMQC and GHMBC NMR experiments (Summarised in Appendix, NMR section, Table 18 and 20), while COSY, ROESY and coupling constant data were used to assign the relative stereochemistry of the A and B rings. Figures 23 and 24 graphically summarise the GHMBC experiment for **(159)** and **(160)**.

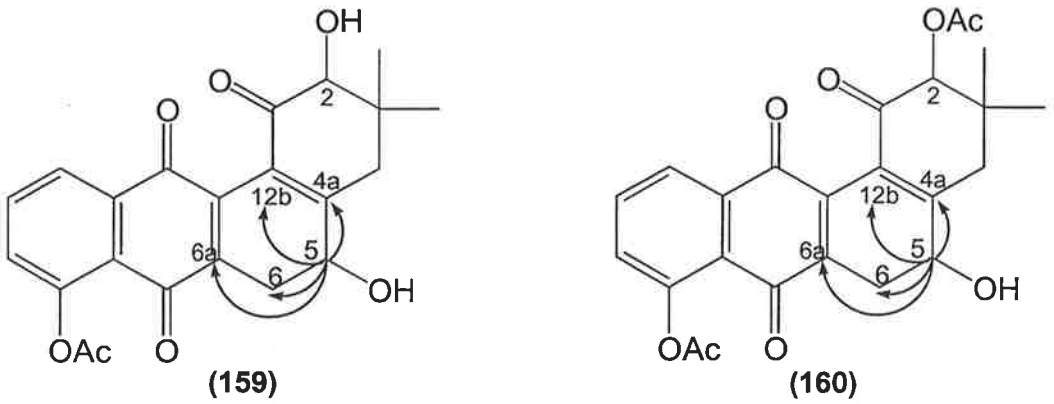

Figure 23. GHMBC correlations of H5 of diol **(159)** and *bis*-acetate **(160).**

Structural similarities of compounds **(159)** and **(160)** were evident from the GHMBC experiments. Both **(159)** and **(160)** show long range ^{1}H-^{13}C coupling between H5 (OH containing carbon) and a fully substituted double bond (C4a, C12b), a methylene carbon (C6), and one alkene carbon (C6a). These data confirm the positions of the hydroxyl groups in **(159)** and **(160)** as shown in Figure 23.

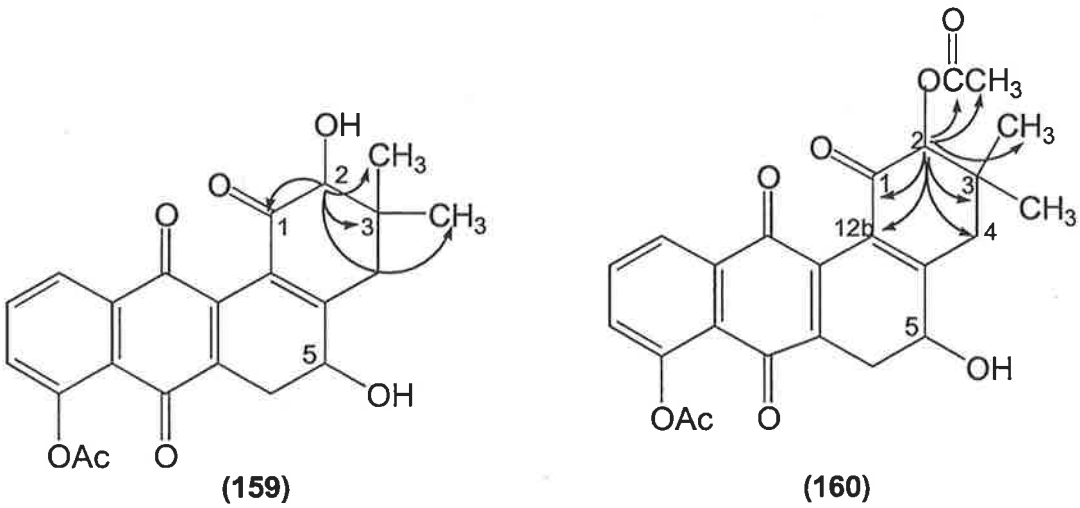

Figure 24. GHMBC correlations of H2 in diol **(159)** and *bis*-acetate **(160).**

GHMBC correlations of H2 of **(159)** are shown in Scheme 24, where H2 has ^{1}H-^{13}C long range coupling to the quaternary C3, the geminal dimethyl group and the 1 carbonyl. The *bis*-acetate **(160)** additionally correlates to the carbonyl and methyl group of the acetate substituent, the fully substituted C12b alkene and C4 methylene. The ^{1}H n.m.r experiments for diol (159) are summarised in Table 9, while figures 25 and 26

contain a graphical summary of the ROESY experiments used to assign the relative stereochemistry of the A and B rings.

^{1}H ppm	Assign ment	Area	Multiplicity Coupling Constants	COSY	ROESY
7.93	H11	1	dd, 7.8, 1.2 Hz	H10, H9	-
7.77	H10	1	t, 7.8 Hz	H9, H11	-
7.37	H9	1	dd, 7.8, 1.2 Hz	H10, H11	-
5.58	C5-OH	1	d, 6.0 Hz	$H5_{ax}$	$H4_{eq}$, $H6_{eq}$, $H6_{ax}$
4.44	$H5_{ax}$	1	ddd, 15.6, 6.6, 6.0 Hz	$H6_{ax}$,$H6_{eq}$ C5-OH	$H4_{ax}$
4.30	$H2_{ax}$	1	d, 4.2 Hz	C2-OH	CH_{3eq}, $H4_{ax}$
4.15	C2-OH	1	bd, 4.2 Hz	$H2_{ax}$	CH_{3ax}, $H4_{eq}$
3.22	$H6_{eq}$	1	dd, 16.8, 6.6 Hz	$H5_{ax}$, $H6_{ax}$	C5-OH
3.07	$H4_{eq}$	1	d, 20.0 Hz	$H4_{ax}$	CH_{3ax}, CH_{3eq}, C5-OH, C2-OH
2.47	$H4_{ax}$	1	d, 20.0 Hz	$H4_{eq}$	$H2_{ax}$, $H5_{ax}$
2.43	$CH_{3\ acet.}$	3	s	-	-
2.34	$H6_{ax}$	1	dd, 16.8, 15.6 Hz	$H6_{eq}$, $H5_{ax}$	CH_{3ax}, C5-OH
1.26	CH_{3eq}	3	s	-	CH_{3ax}, $H2_{ax}$, $H4_{eq}$, $H4_{ax}$
0.84	CH_{3ax}	3	s	-	CH_{3eq}, C2-OH, $H4_{eq}$, $H6_{ax}$

Table 9. Summary of ^{1}H n.m.r. experiments for diol **(159)**.

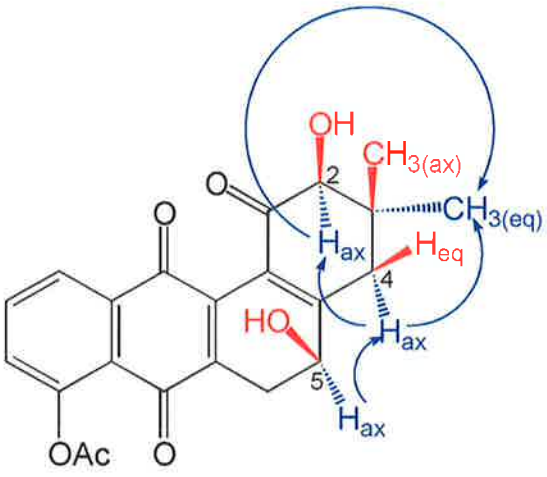

Figure 25.

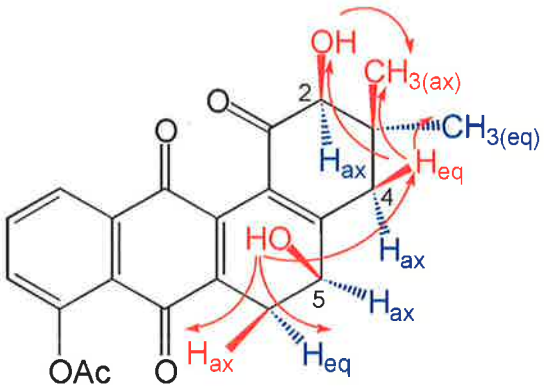

Figure 26.

Figure 25 summarises the spatial ROESY interactions (1,3 pseudo diaxial) of **(159)** confirming the relative stereochemistry of $H2_{ax}$, 4_{ax}, and 5_{ax} (4.30, 2.47, and 4.44 ppm) as on the same side of the molecule (arbitrarily drawn as down in blue). The ROESY cross peak between C-3 methyl (1.26 ppm), $H4_{ax}$ and $H2_{ax}$ assigns its stereochemistry as down (equatorial). ROESY interactions used to assign the up facing protons (red arrows) are summarised in Figure 26. In particular, the relative stereochemistry of the two hydroxyl

groups was confirmed to be *syn* by the 5-OH groups (5.58 ppm) interaction with $H4_{eq}$ (3.07 ppm), which additionally interacts with the 2-OH (4.15 ppm) implying that both hydroxyl groups are on the same side of the molecule. The up facing (axial) H6 was identified by coupling to the down facing $H5_{ax}$ (axial) with 15.6 Hz, indicating a large dihedral angle approximating 180° (pseudo trans diaxial). Other interpretations of the ^{1}H n.m.r spectrum of **(159)** are summarised in Table 9.

The ^{1}H n.m.r experiments for *bis*-acetate **(160)** are summarised in Table 10, while Figure 27 contains a graphical summary of the ROESY experiments used to assign the relative stereochemistry of the A and B rings.

^{1}H ppm	Assignment	Area	Multiplicity Coupling Constants	COSY	ROESY
7.91	H11	1	dd, 7.8, 1.2 Hz	H10, H9	-
7.65	H10	1	t, 7.8 Hz	H9, H11	-
7.27	H9	1	dd, 7.8, 1.2 Hz	H10, H11	-
5.42	$H2_{ax}$	1	s	-	CH_{3eq}, $H4_{ax}$
4.59	$H5_{ax}$	1	ddd, 11.4, 7.0, 5.4, Hz	$H6_{ax}$, $H6_{eq}$, C5-OH	$H4_{ax}$
3.23	$H6_{eq}$	1	dd, 16.8, 7.0 Hz	$H5_{ax}$, $H6_{ax}$	-
3.07	$H4_{eq}$	1	d, 20.2 Hz	$H4_{ax}$	CH_{3ax}, CH_{3eq}, C5-OH
2.81	C5OH	1	d, 5.4 Hz	$H5_{ax}$	$H4_{eq}$, $H6_{ax}$
2.58	$H4_{ax}$	1	bd, 20.2 Hz	$H4_{eq}$, CH_{3ax}	CH_{3eq}, $H2_{ax}$, $H5_{ax}$
2.43	$C8_{acetate}$	3	s	-	-
2.40	$H6_{ax}$	1	dd, 16.8, 11.4 Hz	$H6_{eq}$, $H5_{ax}$	C5-OH, CH_{3ax}
2.24	$C2_{acetate}$	3	s	-	CH_{3ax}, CH_{3eq}
1.21	CH_{3eq}	3	s	-	CH_{3ax}, $C1_{acetate}$, $H2_{ax}$, $H4_{ax}$, $H4_{eq}$
1.01	CH_{3ax}	3	bs	$H4_{ax}$	CH_{3eq}, $C1_{acetate}$, $H4_{eq}$

Table 10. Summary of ^{1}H n.m.r. experiments for *bis*-acetate **(160)**.

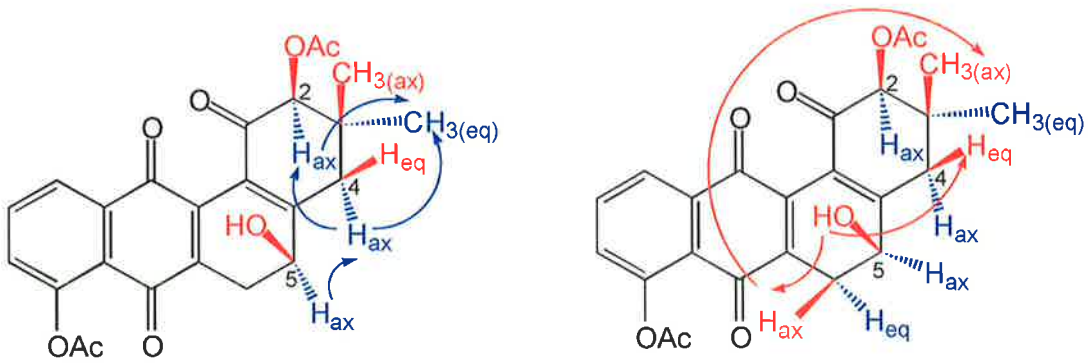

Figure 27. Graphical representation of the ROESY experiment on **(160)**.

The ROESY interactions of the *bis*-acetate **(160)** between: $H2_{ax}$ and 4_{ax} (5.42 and 2.58 ppm, 1,3 pseudo diaxial), $H4_{ax}$ and CH_{3eq} (1.21 ppm) indicate that these groups are on the side of the molecule, arbitrarily assigned as down (Figure 27). A weak ROESY cross peak between $H4_{ax}$ and $H5_{ax}$ suggest a *syn* relationship between the 2-acetate and 5-OH. This *syn* relationship is further confirmed by a ROESY cross peak between 5-OH (2.81 ppm), the up facing $H4_{eq}$ signal (3.07 ppm) and H6 (2.40 ppm). H6 was assigned as up (pseudo axial) based on the large 16.8 Hz coupling constant with $H5_{ax}$ which is facing down indicating a large 180° dihedral angle (*trans* relationship). The unusual long range ROESY cross peak between $H6_{ax}$ and CH_{3ax} (1.01 ppm) confirms that these two groups are on the same side of **(160)** and is further evidence for the *syn* orientation of the hydroxyl and acetate groups. Other interpretations of the ^1H n.m.r spectrum are summarised in Table 10.

The NMR data confirm the relative stereochemistry of both compounds, indicating that both the hydroxyl groups of **(159)**, and the hydroxyl and acetate group of **(160)** are on the same side of the molecule. Suitable crystals of both compounds could not be obtained for an X-ray crystallographic study.

Mechanism for the acid catalysed epoxide opening of (158)

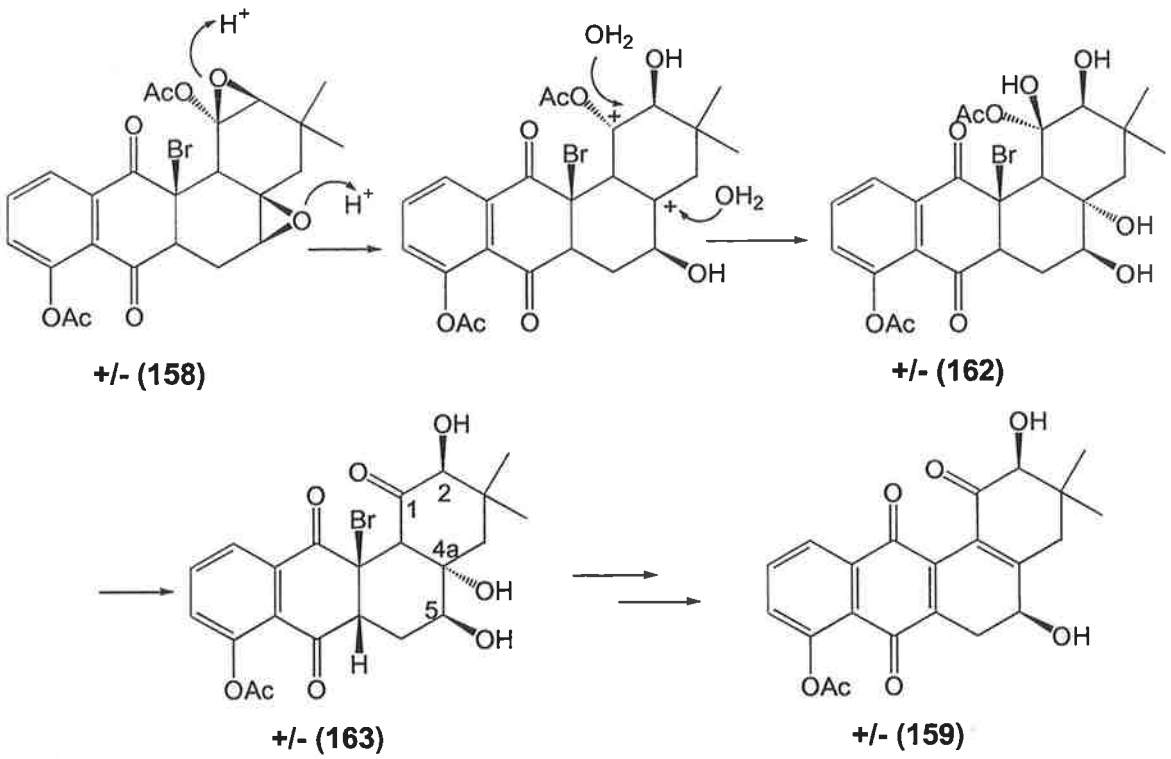

Scheme 60. Mechanism for the acid catalysed epoxide opening of **(158)**.

The observed *syn* stereochemistry between the two hydroxyl groups in **(159)** can only result from the epoxide opening pathway of *syn bis*–epoxide **(158)** shown in Scheme 60. Under acidic conditions the 4a,5 epoxide of **(158)** will protonate. Since the protonated intermediate has partial S_N1 character, water will add at the more substituted carbon of the epoxide ring. This reaction will therefore involve retention of configuration at the 5 position. Similar retention of configuration occurs at the 2 position where water similarly adds at the more substituted carbon of the epoxide. The ketal **(161)** hydrolyses under acidic conditions to form the α-hydroxy ketone **(162)**.[86, 93] Elimination of the 4a-OH followed by dehydrobromination will then form **(159)** having *syn* relative stereochemistry of the two hydroxyl groups.

The α-acyloxy ketone functional group present in the *bis*-acetate **(160)** is rationalised on being formed by the acid-catalysed enol ester epoxide rearrangement[94] outlined in Scheme 61.

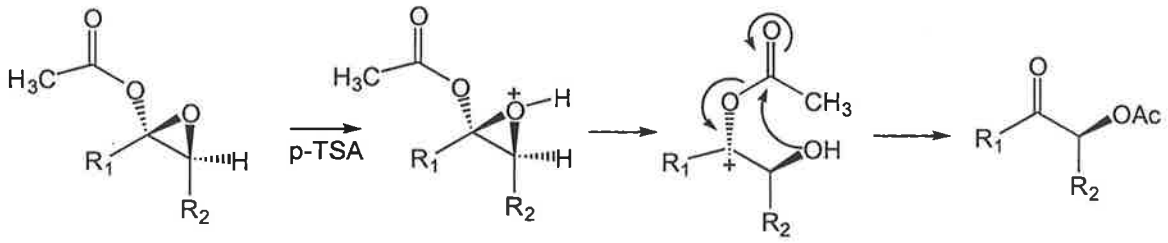

Scheme 61. Mechanism for the acid catalysed enol ester rearrangement used to form **(160)** with retention of configuration at position 2.

4.10. Anticancer Activity Determination

The selected angucyclinones listed in Table 11 have been tested for anticancer activity in the NCI in vitro screening panel testing with 54 human tumour cell lines.[144] Results are summarised in Table 11. Angucyclinones **(102)** and **(108)** show little activity, **(122)** shows some activity while **(114)** has anticancer activity against all the main groups of human cancers with IC values in the 10^{-5} to 10^{-4} Molar concentration range. The anticancer mode of action is unknown at this time.

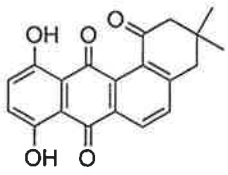

(102)

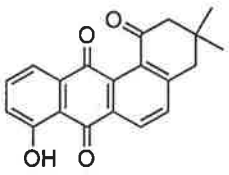

(108)

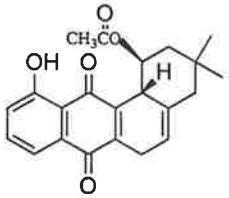

(114)

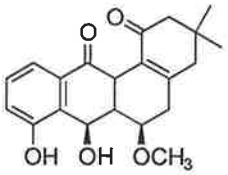

(122)

Cancer	(102)	(108)	(114)	(122)
Leukaemia	-	-	4	-
Lung	-	-	5	-
Colon	-	-	5	4-5
CNS	-	-	5	4-5
Melanoma	-	-	5	4-5
Ovarian	-	-	5	4-5
Renal	-	-	5	4-5
Prostate	-	-	5	-
Breast	-	-	4-5	4-5
Total	-	-	48	9

Table 11. LC 50 anticancer activities of selected angucyclinones **(102)**, **(108)**, **(114)** and **(122)**.

The above are data from the NCI testing program.[144] No value in the table indicates that the angucyclinones, although anticancer active, were deemed not sufficiently active in the first stage (testing against three tumour lines) of the NCI testing program, to warrant second stage testing. When figures are given in the table, these are a summary of the results for those angucyclinones, which were tested, in the second stage of the NCI testing program against 54 human tumours. Activities are given as LC 50 values, the minimum molar concentrations required to kill 50% of the cancer cells. In the table, these are shown as n as in 10^{-n} M. When there is no figure given, LC 50 is > 10^{-4} M. The data above indicate only cancer groupings not the individual cancers within a particular grouping. The figure in the last line of the table indicates the total number of cancers (out of 54) that each peptide is active against within the concentration range given. Compounds **(109)**, **(150)**, **(157)**, **(159)**, **(160)** and **(161)**, have been sent for testing but results are not yet available.

4.11. Unfinished work

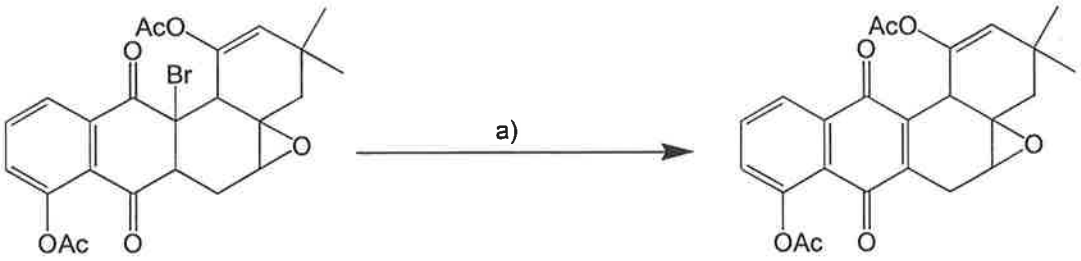

(154) **(157)**

a) pyridine, N_2, reflux 1 min. quantitative yield

Scheme 62. Dehydrobromination of **(154)** using mild basic conditions.

The dehydrobromination step outlined in Scheme 62, needs to be repeated. Preliminary characterisation by NMR and MS indicates that quinone **(157)** was formed but full characterisation is yet to be done.

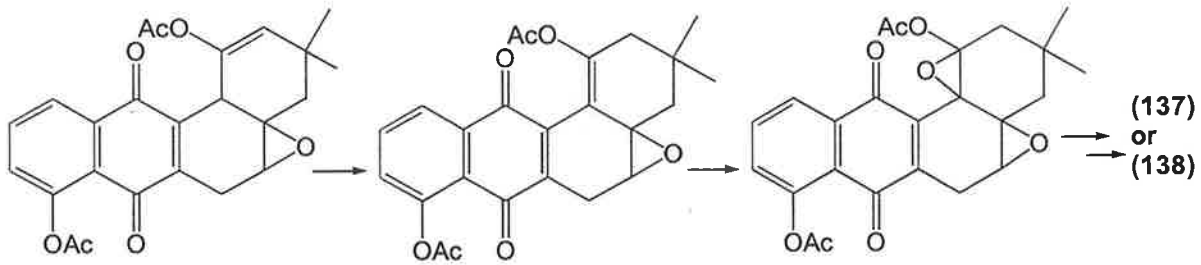

(157)

Scheme 63. Proposed synthetic pathway towards 4a,12b oxygenated analogues **(137)** or **(138)**.

The isomerization of **(157)** outlined in Scheme 63 is the next challenge, followed by the epoxidation of the isomerised double bond. Opening up the *bis*-epoxide by chemistry similar to that reported in this thesis[#] may then yield aquayamycin like analogues i.e. **(137)**.

[#] Refer to Section 4.8, page 82.

Chapter 5. Experimental

6.1. General Experimental

Melting points were determined on a Kofler hot-stage apparatus equipped with a Reichart microscope and are uncorrected. Infrared spectra were recorded on an ATI Mattson Genesis Series FTIR spectrometer as liquid films between sodium chloride plates, KBr disks, or in liquid cells using deuterochloroform as the solvent and are measured in cm^{-1}. Ultraviolet spectra were recorded on a Hewlett Packard 845A Diode Array spectrometer. ^{1}H and ^{13}C n.m.r. spectra were recorded on either a Varian Gemini-200, Varian Gemini-2000 or Varian 600 MHz spectrometers as solutions in deuterochloroform (unless stated to the contrary) using tetramethylsilane as an internal standard. Chemical shifts are recorded on the δ-scale in parts per million (ppm), followed by multiplicity, coupling constant(s) and assignment. In reporting spectral data the following abbreviations have been used: b, broad; s, singlet; d, doublet; t, triplet; q, quartet; p, pentet; m, multiplet. When reporting multiplets or AB doublets, the chemical shift at the centre of a signal is recorded. Electron impact (EI) mass spectra were recorded on VG ZAB 2HF, Finnigan GCQ or LCQ mass spectrometers as appropriate. The mass of relevant ions is listed followed by the particular fragmentation loss and the relative intensity of the peak. Only the molecular ion value and diagnostic fragmentation peaks are recorded. Thin layer chromatography (t.l.c) was performed on aluminium backed *Kieselgel* $60PF_{254}$ silica plates. Analytical t.l.c. plates were visualised using UV light (254 nm). Flash chromatography was performed using *Merck* $60PF_{254}$ silica gel (230-400 mesh). All solvents and reagents were purified using standard laboratory procedures[95] and each reaction was followed by t.l.c. whenever possible. Microanalyses were performed by the University of Otago, Dunedin, New Zealand and exact mass measurements were performed by the spectroscopy facility of the University of Tasmania, Australia.

Juglone (5-hydroxy-1,4-naphthoquinione) and 1,4-naphthoquinone were commercial samples and were chromatographed prior to use. 5-Acetoxy-2-bromo-1,4-naphthoquinonone was synthesised starting from 1,5-dihydroxynaphthalene by a reported technique.[96] 5,5-Dimethyl-3-ethoxy-2-cyclohexen-1-one **(87)** was synthesised from dimedone (5,5-dimethyl-1,3-cyclohexanedione).[52] Dimethyl dioxirane was prepared from acetone using the standard literature procedure described by Adam and Hadjiarapoglou and standardised by an iodometric titration.[85]

6.2. Synthesis of Nucleophilic Dienes

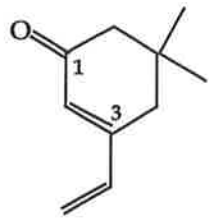

5,5-Dimethyl-3-vinyl-2-cyclohexen-1-one (88)

Vinyl bromide (5 cm^3) in anhydrous tetrahydrofuran (15 cm^3) was added dropwise, under nitrogen, at 40° C to a stirring mixture of magnesium turnings (1.5 g), tetrahydrofuran (15 cm^3) and a crystal of iodine at such a rate that the temperature does not exceed 45°C. The reaction mixture was allowed to stir at 40°C for 30 min., cooled to 0°C, 5,5-dimethyl-3-ethoxy-2-cyclohexen-1-one **(87)** (5.8 g) in anhydrous tetrahydrofuran (15 cm^3) was added over a 5 minute period and the mixture then heated at reflux for 16 hours. The mixture was cooled to 0°C, aqueous ammonium chloride (saturated, 10 cm^3) was added, the mixture was filtered, the reaction salts washed with dichloromethane (2 x 25 cm^3) and solvents removed *in vacuo*. The aqueous filtrate was dissolved in dichloromethane (50 cm^3), aqueous sulphuric acid (10 %, 25 cm) was added and mixture stirred at 20°C for 30 min, the organic layer separated and washed with aqueous sodium hydrogen carbonate (saturated, 50 cm^3), then water (50 cm^3) and aqueous sodium chloride (saturated, 25 cm^3), dried ($MgSO_4$), and the solvent removed *in vacuo* to give crude 5,5-dimethyl-3-vinylcyclohex-2-ene-1-one **(88)** (4.5 g, 87% yield). This material decomposes on standing and is best used immediately for the next step of the synthesis without purification. However **(88)** can be stored for short periods at 0°C dissolved in anhydrous dichloromethane or diethyl ether. Purification by flash chromatography on silica, eluding with hexane/diethyl ether (2:1) yields **(88)** (2.35 g, 45%) as a clear oil, b.p. 56-57°C at 0.4 mmHg.[52] λ_{max} nm (log ε) 264 (4.85). ν_{max} (neat) 3050, 1650 cm^{-1}. $^{-1}$H n.m.r. δ: 1.08 s (6H, 2 x CH_3); 2.29 s (2H, H6); 2.34 s (2H, H4); 5.45 d (1H, 10.8 Hz); 5.68 d (1H, 17.6 Hz); 5.97 s (1H, H2); 6.53 dd (1H, 17.6, 10.8 Hz). *m/z* 150 ($M^{+\cdot}$), 94; (-C_4H_8) 100%.

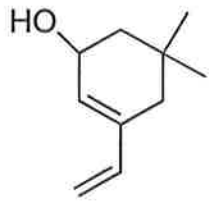

5,5-Dimethyl-3-vinyl-2-cyclohexen-1-ol (110)

Anhydrous cerium chloride (1.64 g, 6.66 mmol) was added to a solution of 5,5 dimethyl-3-ethoxycyclohex-2-en-1-one **(88)** (1 g, 6.66 mmol) in methanol (20 cm^3) and the mixture stirred for 20 min. at 20°C. Sodium borohydride (0.31 g, 7.99 mmol) was added portionwise over a 5 min. period at 20°C, the mixture stirred for a further 10 min., cooled to 0°C, hydrolysed with aqueous hydrochloric acid (10%, 10 cm^3), and extracted with diethyl ether (2 x 25 cm^3). The combined organic extracts were washed with water (25 cm^3), aqueous sodium hydrogen carbonate (saturated, 25 cm^3), water (25 cm^3), aqueous sodium chloride (saturated, 25 cm^3), dried ($MgSO_4$) and the solvent removed *in vacuo* to give crude 5,5-dimethyl-3-vinylcyclohex-2-ene-1-ol **(110)** (0.90 g, 89%). The product is unstable and is best used immediately. However **(110)** can be purified by flash chromatography on silica, eluting with hexane/diethyl ether (1:1) to give the product as a colourless oil (0.76 g, 76%), b.p. 44-45°C (0.1 mmHg). $M^{+\cdot}$ 152.1202, $C_{10}H_{16}O$ requires 152.1201. ν_{max} (neat) 3100-3600, 1641, 1606, 1453, 1351 cm^{-1}. ^1H n.m.r. δ: 0.91 s (3H, CH_3); 1.06 s (3H, CH_3); 1.29 dd (1H, 12.3, 9.3 Hz H6); 1.83 dd (1H, 12.3, 6 Hz H6); 1.95 s (2H, H4); 4.36 bs (1H, H1); 5.03 d (1H, 10.8 Hz); 5.19 d (1H, 17.7 Hz); 5.72 s (1H, H2); 6.38 dd (1H, 17.7, 10.8 Hz). ^{13}C n.m.r. δ: 26.01 (CH_3); 30.63 (C5); 31.37 (CH_3); 37.46 (C4); 45.37 (C6); 66.74 (C1); 112.78; 130.27; 136.76; 139.38. *m/z* 152 ($M^{+\cdot}$) 28; 135 (OH) 100%.

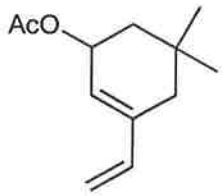

5,5-Dimethyl-3-vinyl-2-cyclohexanyl acetate (111)

Freshly distilled acetyl chloride (0.31 g, 3.90 mmol) was added dropwise to a mixture of 5,5-dimethyl-3-vinyl-2-cyclohexen-1-ol **(110)** (0.40g, 2.66 mmol), anhydrous pyridine (0.31 g, 3.90 mmol) in anhydrous dichloromethane (10 cm^3) at 0°C under nitrogen. The mixture was allowed to warm to 20°C, stirred at this temperature for 15 min., hydrolysed with water (10 cm^3), the organic layer separated and washed with aqueous sulphuric acid (10%, 3 x 10 cm^3), aqueous sodium hydrogen carbonate (saturated, 10 cm^3), water (10 cm^3), dried ($MgSO_4$), the solvent removed *in vacuo* to give crude 5,5-dimethyl-3-vinyl-2-cyclohexanyl acetate **(111)** (0.40 g, 79%). The product is best used immediately without purification, if storage is required, the sample must be purified (before use) by flash chromatography eluting with hexane/diethyl ether (4:1) to yield **(111)** as a clear oil (0.36 g, 72%), b.p. 194-195°C at 760 mm Hg. $M^{+\cdot}$ 194.1299, $C_{12}H_{18}O_2$ requires 194.1307. λ_{max} nm (log ε) 206 (4.72), 216 (4.68), 270 (3.86). ν_{max}(neat) 2954, 1735, 1607, 1372, 1240 cm^{-1}. ^1H n.m.r. δ: 0.94 s (3H, CH_3); 1.03 s (3H, CH_3); 1.42 dd (1H, 12.8, 8.6 Hz H6); 1.80 dd (1H, 12.8, 6.4 Hz H6); 1.96 s (2H, H4); 2.03 s (3H, CH_3); 5.03 d (1H, 10.8 Hz); 5.19 d (1H, 17.4 Hz); 5.42 m (1H, H1); 5.63 s (1H, H2); 6.35 dd (1H, 17.4, 10.8 Hz). ^{13}C n.m.r. δ: 21.21 (CH_3); 26.63 (CH_3); 30.23 (C5); 30.59 (CH_3); 37.45 (C4); 40.86 (C6); 69.68 (C1); 113.15; 125.64; 138.50; 139.02; 170.80 (CO). *m/z* 194 ($M^{+\cdot}$) 12; 152 (CH_2CO) 21; 135 ($CH_3CO_2\cdot$) 100%.

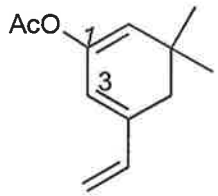

1-Acetoxy-3,3-dimethyl-5-vinylcyclohexa-1,5-diene

5,5-Dimethyl-3-vinyl-1,2-cyclohexadienyl acetate (147)

A hexane solution of freshly titrated butyl lithium (2.32 M, 3.32 cm^3) was concentrated *in vacuo*, the reaction flask flushed with nitrogen, the residue dissolved in anhydrous tetrahydrofuran (10 cm^3) and cooled to -78° C. Diisopropylamine (1.06 cm^3) in anhydrous tetrahydrofuran (10 cm^3) was added and the mixture stirred for 30 min. at -78° C. 5,5-Dimethyl-3-vinylcyclohex-2-ene-1-one **(88)** (1g) in anhydrous tetrahydrofuran (5 cm^3) was added, the mixture stirred for 45 min. at -78° C and quenched with acetic anhydride (1.22 cm^3), pyridine (0.14 cm^3) and anhydrous tetrahydrofuran (10 cm^3). The mixture was allowed to warm to 20° C over a period of 45 min., hexane (100 cm^3) and icewater (50 cm^3) were added, the organic layer was washed with cold aqueous sodium hydrogen carbonate (saturated, 2 x 50cm^3), cold water (50 cm^3), dried ($MgSO_4$) and the solvent removed *in vacuo* to give crude 5,5-dimethyl-3-vinyl-1,2-cyclohexadienyl acetate **(147)** (1.22 g, 95%). This crude product is best used immediately, however it can be stored at 0°C in either anhydrous diethyl ether or dichloromethane. If **(147)** is to be used following storage, it needs to be purified by flash chromatography eluting with hexane to give the pure product as a clear oil (0.92 g, 75%), b.p. 175°C at 760 mm Hg. $M^{+\cdot}$ 192.11502, $C_{12}H_{16}O_2$ requires 192.11503. λ_{max} nm (log ε), 247 (3.63), 277 (3.40). ν_{max} (neat) 2958, 1763, 1653, 1605, 1368 cm^{-1}. ^1H n.m.r. δ: 1.08 s (6H, 2 x CH_3); 2.15 s (3H, CH_3); 2.24 d (2H, 1.2 Hz, H4); 5.12 d (1H, 10.8 Hz); 5.23 d (1H, 1.2 Hz, H2); 5.28 d (1H, 17.4 Hz); 5.69 s (1H, H6); 6.41 dd (1H, 17.4, 10.8 Hz). ^{13}C n.m.r δ: 20.68 (CH_3); 28.05 (2 x CH_3); 31.99 (C5); 36.3 (CH_2); 113.30; 121.20; 122.73; 136.84 (C3); 137.59; 144.73 (C1); 168.91 (CO). *m/z* 193 $(M+H)^{+\cdot}$, 100; 177 (CH_4), 10; 151 (C_2H_2O), 22; 135 (C_2H_2O+CH_4), 47%.

6.3. Diels-Alder Cyclisation Reactions

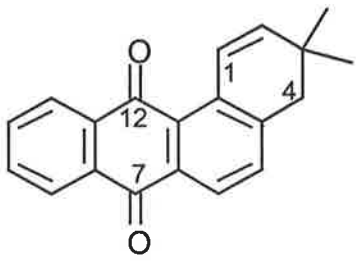

3,3-Dimethyl-3,4,7,12,-tetrahydrobenzo[*a*]anthracene-7,12-dione (129)

A mixture of 1,4-naphthoquinone (125 mg, 0.79 mmol), 5,5-dimethyl-3-vinylcyclohex-2-ene-1-ol **(110)** (120 mg, 0.79 mmol) and p-toluenesulphonic acid (1 mg) in anhydrous toluene (5 cm^3) was heated under reflux for 72 hr. The reaction mixture was allowed to cool to 20°C, the solvent removed *in vacuo* and the residue purified by flash chromatography on silica eluting with hexane/diethyl ether (gradient elution 11:1 to 1:1) to give 3,3-dimethyl-4-dihydrobenz[a]anthra-7,12-quinone **(129)** (120 mg, 52%). Crystallisation from dichloromethane/hexane gave **(129)** as pale yellow crystals (76 mg, 34%), m.p. 117-119°C. $M^{+\cdot}$ 288.1147, $C_{20}H_{16}O_2$ requires 288.1150. λ_{max} nm (log ε), 207 (4.19), 258 (4.29), 350 (3.46 shoulder). ν_{max} (nujol), 1666, 1590, 1562, 1376, 1311 cm^1. ^{1}H n.m.r. (300 mHz) δ: 1.11 s (6H, 2 x CH_3); 2.83 s (2H, H4); 6.18 d (1H, 10.8 Hz H2); 7.51 d (1H, 7.5 Hz, H5); 7.77 m (2H, H9, H10); 7.98 d (1H, 10.8 Hz, H1); 8.18 d (1H, 7.5 Hz H6); 8.26 m (2H, C8, H11). ^{13}C n.m.r. δ: 27.26 (2 x CH_3); 31.06 (C3); 44.05 (C4); 123.11 (CH); 126.52 (CH); 126.58 (CH); 127.33 (CH); 132.86 (C); 132.91 (C); 133.46 (C); 133.50 (C); 134.06 (CH); 135.31 (C); 135.54 (C); 143.93 (C); 144.00 (C); 145.00 (CH); 183.60 (CO); 184.11 (CO). *m/z* 288 ($M^{+\cdot}$) 90; 273 (CH_3) 100%.

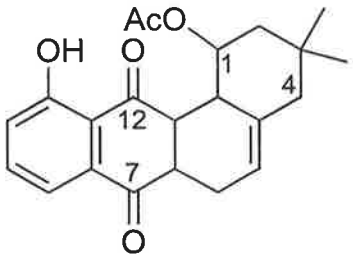

11-Hydroxy-3,3-dimethyl-7,12-dioxo-1,2,3,4,6,6a,7,12,12a,12b-decahydrobenzo[*a*]anthracen-1-yl acetate (113)

To a mixture of acetic acid (glacial, 0.32 g, 5.3 mmol) and tetrahydrofuran (2 cm^3) was added BH_3.THF (1.8 cm^3, 1.8 mmol) and the mixture stirred at 20°C for 1 hr. Removal of the solvent *in vacuo*, followed by trituration of the product with diethyl ether (5 cm^3) gave boron triacetate (0.32 g.) as white crystals, m.p. 118-120°C (lit.[58]). Fresh boron triacetate (332 mg, 1.76 mmol) in dry dichloromethane (5 cm^3) was added to a solution of 5-hydroxy-1,4-naphthoquinone (281 mg, 1.62 mmol) in dry dichloromethane (5 cm^3), the mixture allowed to stir at 0°C for 10 min. under nitrogen. 5,5-Dimethyl-3-vinyl-2-cyclohexanyl acetate **(111)** (376 mg, 1.94 mmol) in anhydrous dichloromethane (5 cm^3) was added, the reaction mixture warmed to 20°C and stirred for 16 hr. under nitrogen. The reaction mixture was diluted with dichloromethane (85 cm^3), washed with water (4 x 50 cm^3), aqueous sodium chloride (saturated, 50 cm^3) and dried ($MgSO_4$). The organic extract was concentrated to 2 cm^3 *in vacuo* and the crude adduct precipitated following dropwise addition of diethyl ether at 0°C. Crystallisation from dichloromethane/ diethyl ether gave pure -/+ 11-hydroxy-3,3-dimethyl-7,12-dioxo-1,2,3,4,6,6a,7,12,12a,12b-decahydrobenzo[*a*]anthracen-1-yl acetate **(113)** as yellow orange crystals (440 mg, 74%), m.p. 130-145°C. $M^{+\cdot}$ 368.1604, $C_{22}H_{24}O_5$ requires 368.1624. λ_{max} nm (log ε) 205 (4.33), 230 (4.53), 262 (3.92), 347 (3.95). ν_{max} ($CDCl_3$), 1731, 1703, 1645, 1455, 1247, 1246 cm^1. ^1H n.m.r. (assignments from 600MHz COSY and GHMBC) δ: 0.82 s (3H, CH_3); 0.91 s (3H, CH_3); 1.08 t (1H, 11.4 Hz, H2); 1.71 s (3H, $COCH_3$); 1.76 dd (1H, 4.1, 11.4 Hz, H2); 1.92 bs (2H, H4); 2.17 bdd (1H, 6.9, 18.0 Hz, H6); 2.7 bt (1H, 6.9 Hz, H12b); 2.85 bdd (1H, 3.0, 18.0 Hz, H6); 3.4 dt (1H, 3.0, 6.9 Hz, H6a); 3.50 t (1H, 6.9 Hz, H12a); 4.58 bs (1H, H1); 5.58 bs (1H, H5); 7.22 dd (1H, 7.8, 1.2 Hz, H10); 7.53 dd (1H, 7.8, 1.2 Hz, H8); 7.61 t (1H, 7.8 Hz, H10); 12.15 s (1H, OH). ^{13}C n.m.r. (600MHz GHMQC) δ: 20.63 ($COCH_3$); 24.58 (CH_3); 31.39 (CH_3); 32.39 (C3); 43.76 (CH, C12b); 44.95 (CH_2, C2); 45.51 (CH_2, C6); 47.72 (CH, C6a); 48.30 (CH, C12a); 49.08 (CH_2,C4); 71.28 (C1); 118.11 (ArH, C8); 118.30 (C11a); 121.64 (CH, C5); 123.48 (ArH, C10); 133.78 (C4a); 135.0

(C7a); 136.73 (ArH, C9); 160.90 (C11); 168.90 ($COCH_3$); 196.43 (CO, C7); 206.40 (CO, C12). *m/z* 368 ($M^{+\cdot}$) 12; 324 (CH_3CHO) 16; 309 (CH_3CO_2) 100; 294 ($CH_3CO_2\cdot + CH_3$) 25; 279 ($CH_3CO_2\cdot + CH_3 + CH_3$) 30%.

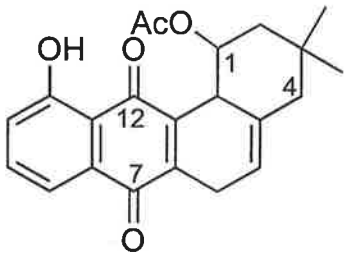

11-Hydroxy-3,3-dimethyl-7,12-dioxo-1,2,3,4,6,7,12,12b-octahydrobenzo[*a*]anthracen-1-yl acetate (114)

To a solution of 11-hydroxy-3,3-dimethyl-7,12-dioxo-1,2,3,4,6,6a,7,12,12a,12b-decahydrobenzo-[*a*]anthracen-1-yl acetate **(113)** (100 mg, 0.27 mmol) in dichloromethane (10 cm^3) was added silica gel (5 g), the solvent removed *in vacuo* and the solid mixture allowed to stand at 25°C for 1 hr open to the atmosphere. The solid was extracted with dichloromethane (4 x 50 cm^3), filtered, the solvent removed *in vacuo* and the residue crystallised from dichloromethane/ hexane (1:1) to give 11-hydroxy-3,3-dimethyl-7,12-dioxo-1,2,3,4,6,7,12,12b-octahydrobenzo[*a*]anthracen-1-yl acetate **(114)** as fine orange needles (70 mg, 70%), m.p. 137-139°C. Found C, 71.78%; H, 6.05%; $C_{22}H_{22}O_5$requires C, 72.11%; H, 6.05%. λ_{max} nm (log ε) 210 (4.44); 248 (4.00); 275 (3.99); 410 (3.62). ν_{max} ($CDCl_3$) , 1728, 1660, 1635, 1615, 1340, 1288 cm^{-1}. ^1H n.m.r. (assignments from 600MHz COSY and GHMBC) δ: 0.95 s (3H, CH_3); 1.09 s (3H, CH_3); 1.73 t (1H, 11.0 Hz, H2); 1.79 dd (1H, 4.0, 11.0 Hz, H2); 1.87 s (3H, CH_3CO_2); 2.01 bd (1H, 26.0 Hz, H4); 2.05 bd (1H, 26.0 Hz, H4); 3.23 bdm (1H, 7.0 Hz at ½ W, 25.0 Hz, H6); 3.41 bdm (1H, 7.0 Hzat ½ W, 25.0 Hz, H6); 3.67 bm (1H, 11.0 Hz at 1/2 W, H12b); 4.69 dt (1H, 4.0, 11.0 Hz, H1); 5.64 bs (1H, 7 Hz at ½ W, H5); 7.23 dd (1H, 1.2, 7.2 Hz, H10); 7.58 dt (1H, 1.2, 7.2 Hz, H9); 7.61 dd (1H, 1.2, 7.2 Hz, H8); 12.03 s (1H, H11 OH). ^{13}C n.m.r. (600MHz GHMQC) δ: 21.07 (CH_3CO); 25.44 (CH_3); 25.60 (CH_2, C6); 31.86 (CH_3); 33.13 (C3); 41.98 (CH, C12b); 46.09 (CH_2, C2); 47.87 (CH_2, C4); 74.26 (C1); 114.91 (C11a); 118.90 (CH, C5); 118.98 (ArH, C8); 123.96 (ArH, C10); 132.00 (C7a); 133.19 (C4a); 136.00 (ArH, C9); 142.18 (C12a); 143.70 (C6a); 160.99 (C11); 170.58 (COAc); 183.50 (CO, C7); 189.88 (CO, C12). HO^- negative ion ms,*m/z* 365 ($M\text{-}H^-$) 305 (CH_3CO_2H) 100; 290 ($CH_3CO_2H + CH_3$) 70%.

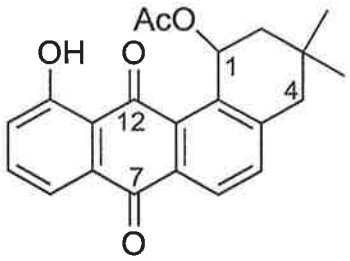

11-Hydroxy-3,3-dimethyl-7,12-dioxo-1,2,3,4,7,12-hexahydrobenzo[*a*]anthracen-1-yl acetate (115)

To a solution of 11-hydroxy-3,3-dimethyl-7,12-dioxo-1,2,3,4,6,7,12,12b-octahydro-benzo[*a*]anthracen-1-yl acetate **(114)** (100 mg, 0.27 mmol) in dichloromethane (10 cm^3) was added silica gel (5 g), the solvent removed *in vacuo* and the solid stored at 25°C for 72 hr open to the atmosphere. The solid mixture was extracted with dichloromethane (4 x 50 cm^3), filtered, the solvent removed *in vacuo* and the residue crystallised from dichloromethane/ diethyl ether (1:1) to give 11-hydroxy-3,3-dimethyl-7,12-dioxo-1,2,3,4,7,12,12b-octahydrobenzo[*a*]anthracen-1-yl acetate **(115)** as fine orange crystals (50 mg, 51%), m.p. 148-150°C (sublimes). $M^{+\cdot}$ 364.1315, $C_{22}H_{20}O_5$ requires 364.1317. λ_{max} nm (log ε) 220 (4.40); 262 (4.48); 284 (4.06); 358 (3.58), and 405 (3.68). ν_{max} (KBr), 1728, 1664, 1634, 1584, 1295, 1241 cm^{-1}. ^1H n.m.r. (200 MHz) δ: 1.07 s (6H, 2 x CH_3); 1.94 dd (1H, 5.6, 14.0 Hz, H2); 1.98 s (3H, CH_3); 2.14 dd (1H, 5.6, 14.0 Hz, H2); 2.69 d (1H, 17.0 Hz, H4); 2.86 d (1H, 17.0 Hz, H4); 6.87 t (1H, 5.6 Hz, H1); 7.28 dd (1H, 1.2, 9,2 Hz, H10); 7.54 d (1H, 8.0 Hz, H5); 7.63 t (1H, 9.2 Hz, H9); 7.76 dd (1H, 1.2, 9.2 Hz, H8); 8.28 d (1H, 8.0 Hz, H6); 12.54 s (1H, ArOH, H11). ^{13}C n.m.r. (200MHz) δ: 20.92 ($COCH_3$); 28.27 (CH_3); 28.65 (CH_3); 28.77 (C3); 41.54 (C2); 45.35 (C4); 68.72 (C1); 117.12 (C11a); 118.86 (C8); 124.70 (C10); 127.86 (C6); 132.20 (C12b); 132.63 (C7a); 134.12 (C4a); 135.96 (C12a); 136.03 (C5); 136.30 (C9); 146.09 (C6a); 162.43 (C11); 170.50 (CO); 182.40 (C7); 190.60 (C12). *m/z* 364 ($M^{+\cdot}$) 15; 321 (CH_3CO) 30; 304 (CH_3CO_2H) 58; 289 (CH_3CO_2H + CH_3) 100%.

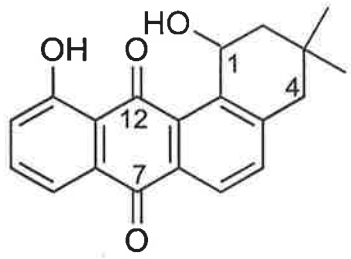

1,11-Dihydroxy-3,3-dimethyl-7,12-dioxo-1,2,3,4,7,12-hexahydrobenz[*a*]anthracene (116)

A mixture of 11-hydroxy-3,3-dimethyl-7,12-dioxo-1,2,3,4,7,12-hexahydrobenzo[*a*]anthracen-1-yl acetate **(115)** (30 mg, 0.08 mmol), sodium hydroxide (30 mg) and moist tetrahydrofuran (15 cm^3) was heated under reflux for 24 hr, cooled to 25°C, aqueous hydrochloric acid (10%, 2cm^3) added and the solvent removed *in vacuo*. The residue was extracted with diethyl ether (2 x 20cm^3), the combined organic extract was washed with aqueous hydrogen chloride (10%, 10 cm^3), water (10 cm^3), aqueous sodium chloride (saturated, 10 cm^3), dried ($MgSO_4$) and solvent removed *in vacuo*. Crystallisation of the residue from dichloromethane/ diethyl ether (1:1) gave 1,11-dihydroxy-3,3-dimethyl-7,12-dioxo-1,2,3,4,7,12-hexahydrobenzo-[*a*]anthracene **(116)** as orange crystals (21 mg, 82%), m.p. 154-156 °C. $M^{+\cdot}$ 322.1219, $C_{20}H_{16}O_4$ requires 322.1206. λ_{max} nm (log ε) 210 (4.35); 260 (4.18); 400 (3.46). ν_{max} (KBr), 3538, 1668, 1635, 1583, 1454, 1363, 1305, 1224 cm^{-1}. ^1H n.m.r. (300 MHz) δ: 1.00 s (3H, CH_3); 1.17 s (3H, CH_3); 1.95 dd (1H, 6.0, 15.8 Hz, H2); 2.01 ddd (1H, 1.2,6.0, 15.8 Hz, H2); 2.68 d (1H, 17.1 Hz, H4); 2.86 d (1H, 17.1 Hz, H4); 4.70 t (1H, 6.0 Hz, H1); 7.31 dd (1H, 1.0, 8.1 Hz, H10); 7.55 d (1H, 8.1 Hz, H5); 7.67 t (1H, 8.1 Hz, H9); 7.80 dd (1H, 1.0, 8.1 Hz, H8); 8.25 d (1H, 8.1 Hz, H6); 12.55 s (1H, ArOH, H11). ^{13}C n.m.r. (200 MHz) δ: 28.04 (CH_3); 28.85 (CH_3); 29.17 (C3); 43.99 (C2); 45.97 (C4); 65.03 (C1); 117.23 (C11a); 119.20 (C8); 124.84 (C10); 127.32 (C6); 131.46 (C12b); 132.67 (C7a); 134.40 (C4a); 136.86 (C9); 136.91 (C5); 141.92 (C12a); 145.41 (C6a); 162.79 (C11); 182.55 (C7); 193.03 (C12). *m/z* 322 ($M^{+\cdot}$) 40; 307 (CH_3) 30; 304 (H_2O) 45; 289 (H_2O + CH_3) 100, 248 (H_2O + C_4H_8) 40%.

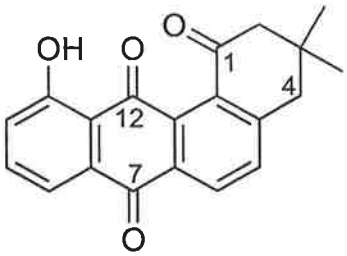

11-Hydroxy-3,3-dimethyl-1,2,3,4-tetrahydrobenzo[*a*]anthracene-1,7,12-trione (109)

1,11-Dihydroxy-3,3-dimethyl-7,12-dioxo-1,2,3,4,7,12-hexahydrobenzo[*a*]anthracene **(116)** (30 mg, 0.093 mmol) in deuterated chloroform (4 cm^3) was placed an NMR tube and exposed to light from a sunlamp for 48 hr. The solvent was removed *in vacuo* and the residue purified by flash chromatography eluting with hexane /diethyl ether (2:1) to give 11-hydroxy-3,3-dimethyl-1,2,3,4-tetrahydrobenzo[*a*]anthracene-1,7,12-trione **(109)** which crystallised from dichloromethane/ diethyl ether (1:1) as deep orange crystals (23 mg, 77%). m.p. 185.5-187.5°C. $M^{+\cdot}$ 320.1046, $C_{20}H_{16}O_4$ requires 320.1049. Found C, 74.65% ; H, 4.80%; $C_{20}H_{16}O_4$ requires C, 74.99%; H, 5.04%. λ_{max} (log ε) nm, 206 (4.28); 265 (4.23); 405 (3.41). ν_{max} (KBr), 2965, 1693, 1664, 1641, 1585, 1451 cm^{-1}. ^1H n.m.r. (200 MHz) δ: 1.15 s (6H, 2 x CH_3); 2.80 s (2H, H4); 2.89 s (2H, H2); 7.30 dd (1H, 1.4, 8.4 Hz, H10); 7.54 d (1H, 8.0 Hz, H5); 7.65 t (1H, 8.4 Hz, H9); 7.79 dd (1H, 1.4, 8.4 Hz, H8); 8.30 d (1H, 8.0 Hz, H6); 11.86 s (1H, ArOH, H11). ^{13}C n.m.r. (200 MHz) δ: 29.10 (2 x CH_3); 34.74 (C3); 44.19 (C2); 53.41 (C4); 116.89 (C11a); 119.23 (C8); 124.47 (C10); 129.50 (C6); 132.64 (C7a); 134.25 (C5); 136.34 (C9); 148.90 (C12b); 161.86 (C11); 181.88 (C7); 187.74 (C12); 199.33 (C1). *m/z* 320 ($M^{+\cdot}$) 50; 305 (CH_3) 5; 292 (CO) 10; 277 (CH_3 + CO) 15; 264 (C_4H_8) 100%.

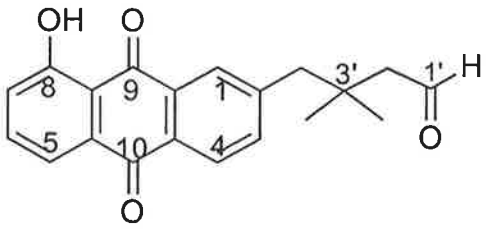

4-(8-Hydroxy-9,10-dioxo-9,10-dihydro-2-anthracenyl)-3,3-dimethylbutanal (118)

Sodium methoxide (1M, 3cm^3) was added dropwise to a solution of 11-hydroxy-3,3-dimethyl-7,12-dioxo-1,2,3,4,6,6a,7,12,12a,12b-decahydrobenzo[*a*]anthracen-1-yl acetate **(113)** (10 mg, 0.03 mmol) in dry dichloromethane (2 cm^3) at 0°C under nitrogen. The reaction mixture was allowed to warm to 20°C and stirred for 40 min., diluted with dichloromethane (10 cm^3), washed with aqueous hydrogen chloride (10%, 4 x 10 cm^3), water (10 cm^3), dried ($MgSO_4$) and solvent removed *in vacuo*. Flash chromatography on silica eluting with dichloromethane/ acetone (99:1) gave 4-(8-hydroxy-9,10-dioxo-9,10-dihydro-2-anthracenyl)-3,3-dimethylbutanal **(118)**, which crystallised from dichloromethane as fine yellow crystals (7 mg, 68%). m.p. 101-103°C. Found C, 74.52% ; H, 5.63%, $C_{20}H_{18}O_4$ requires C, 74.64%; H, 5.54%. λ_{max} nm (log ε) 208 (4.20); 261 (4.24); 285 (3.85); 400 (3.36). ν_{max} (KBr) 3500, 2917, 1715, 1668, 1637, 1594, 1455 cm^{-1}. ^{1}H n.m.r. (300 MHz COSY) δ: 1.13 s (6H, 2 x CH_3); 2.33 d (2H, 3.0 Hz, H2'); 2.85 s (2H, H4'); 7.31 dd (1H, 0.6, 7.8 Hz, H7); 7.59 dd (1H, 1.5, 8.1 Hz, H3); 7.69 t (1H, 7.8 Hz, H6); 7.83 dd (1H, 0.6, 7.8 Hz, H5); 8.07 d (1H, 1.5 Hz, H1); 8.22 d (1H, 8.1 Hz, H4); 9.88 t (1H, 3.0 Hz, H1'); 12.6 s (1H, OH). ^{13}C n.m.r. δ: 27.25 (2 x CH_3); 29.63; 48.54 ; 54.30; 116.28; 119.53; 124.33; 127.35; 128.60; 132.13; 136.50; 136.80; 136.89; 145.45; 162.70; 181.30; 198.23; 202.11. *m/z* 322 ($M^{+\cdot}$) 18; 278 (CH_3CHO) 86; 238 ($CH_3CHO + C_3H_4$) 100.

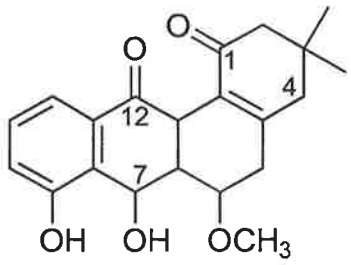

7,8-Dihydroxy-6-methoxy-3,3-dimethyl-1,2,3,4,5,6,6a,7,12,12a-decahydrobenzo[*a*]anthracene-1,12-dione (122)

Anhydrous cerium (III) chloride (150 mg, 0.60 mmol) was added to a solution of 8-hydroxy-6-methoxy-3,3-dimethyl-1,2,3,4,,5,6,6a,7,12,12a-decahydrobenzo[*a*]anthracene-1,7,12-trione **(107)** (140 mg, 0.40 mmol) in ethanol (25 cm^3) and the mixture stirred for 20 min. at 20°. Sodium borohydride (30 mg, 0.80 mmol) was added portionwise over a 5 min. period, the mixture stirred for 10 min. and then cooled to 0°C. Aqueous hydrogen chloride (10%, 5 cm^3) was added, then water (25 cm^3) and the mixture was extracted with ethyl acetate (2 x 25cm^3). The combined organic extract was washed with water (3 x 25 cm^3), dried ($MgSO_4$), the solvent removed *in vacuo* and the residue crystallised from ethanol to give 7,8-dihydroxy-6-methoxy-3,3-dimethyl-1,2,3,4-5,6,6a,7,12,12a-decahydrobenzo[*a*]anthracene-1,2-dione **(122)** as fine white needles (75 mg, 54%). m.p. 270°C (dec.). Found C, 70.47% ; H, 6.76%, $C_{21}H_{24}O_5$ requires C, 70.77%; H, 6.79%. λ_{max} nm (log ε) 212 (4.50); 249 (4.33); 312 (3.59). ν_{max} (nujol) 3362, 3218, 1677, 1661, 1639, 1610, 1583 cm^{-1}. ^1H n.m.r. (300 MHz COSY and 600 MHz GHMBC) δ: 1.10 s (3H, CH_3); 1.25 s (3H, CH_3); 2.27 d (1H, 18.0 Hz H4); 2.31 d (1H, 15.0 Hz, H2); 2.43 d (1H, 18.0 Hz, H4); 2.51 bs (2H, H5); 2.65 d (H, 15.0 Hz, H2); 2.70 t (1H, 6.0 Hz, H6a); 2.94 s (3H, OCH_3); 3.98 d (1H, 6.0 Hz, H12a); 4.25 bs (1H, H6); 5.77 d (1H, 6.0 Hz, H7); 7.06 d (1H, 7.8 Hz, H9); 7.24 t (1H, 7.8 Hz, H10); 7.39 d (1H, 7.8 Hz, H11). ^{13}C n.m.r. (600 MHz GHMQC) δ: 28.18 (CH_3); 30.29 (CH_3); 34.85 (C3); 39.21 (CH_2, C5); 43.03 (CH, C12a); 46.46 (CH_2, C4); 47.08 (CH, C6a); 52.41 (CH_2, C2); 57.43 (OCH_3); 69.31 (CH, C7); 73.86 (CH, C6); 118.15 (ArH, C11); 121.79 (ArH, C9); 128.82 (C7a); 129.34 (ArH, C10), 131.27 (C12b); 135.32 (C11a); 154.82 (C4a); 157.87 (C8); 197.37 (C12); 199.95 (C1). *m/z* (ES ms) 357 $(M+H)^+$ 100; 339 (H_2O) 50; 307 (H_2O + CH_3OH) 20: 283 (H_2O + C_4H_8) 45%.

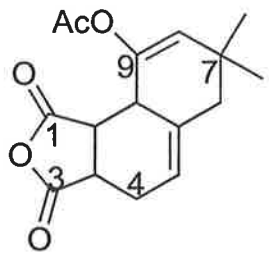

(+/-) 7,7-Dimethyl-1,3-dioxo-1,3,3a,4,6,7,9a,9b-octahyrobenzo[e]sobenzofuran-9-yl acetate (149)

A mixture of maleic anhydride (110 mg, 1.12 mmol) and 5,5-dimethyl-3-vinyl-1,2-cyclohexadienyl acetate **(147)** (215 mg, 1.12 mmol) in dry toluene (10 cm^3) was heated at reflux for 24 hours under nitrogen. The reaction mixture was cooled to 20°C, the solvent removed *in vacuo* and the residue crystallised from diethyl ether to give 7,7-dimethyl-1,3-dioxo-1,3,3a,4,6,7,9a,9b-octahydrobenzo[e]sobenzofuran-9-yl acetate **(149)** as colourless crystals (250 mg 76%), m.p. 158-199°C. Found C, 66.02%; H, 6.40%, $C_{16}H_{18}O_5$requires C, 66.00%; H, 6.53%. ν_{max} (nujol); 1841, 1776, 1745, 1691, 1461, 1376, 1201 cm^{-1}. ^1H n.m.r. (600mHz COSY and GHMBC) δ: 0.93 s (3H, CH_3); 1.06 s (3H, CH_3); 2.11 dd (1H, 1.0, 13.8, Hz H6); 2.19 s (3H, CH_3); 2.24 ddd (1H, 2.4, 7.8, 9.0 Hz, H4); 2.29 d (1H, 13.8 Hz, H6); 2.75 ddd (1H, 1.8, 7.2, 9.0 Hz H4); 3.27 ddd (1H, 1.0, 2.2, 6.6 Hz, H9a); 3.46 ddd (1H, 1.8, 7.8, 9.6 Hz, H3); 3.57 dd (1H, 9.6, 6.6 Hz, H10); 5.65 t (1H, 1.0 Hz, H8); 5.79 m (1H, 7.2, 2.4, 2.2 Hz, H5). ^{13}C n.m.r. δ: 21.14 (CH_3, acetate); 24.32 (CH, C4); 28.54 (CH_3); 29.53 (CH_3); 31.89 (C7); 36.20 (CH, C9a); 40.72 (CH, C3); 41.74 (CH, C10); 44.14 (CH, C6); 121.61 (C5); 127.99 (C8); 138.65 (C5a); 143.19 (C9); 169.59 (CO, acetate); 169.88 (CO, C2); 173.98 (CO, C1). *m/z* 291 $(MH)^+$ 10; 249 (CH_2CO) 54; 233 (CH_2CO + CH_3) 100%.

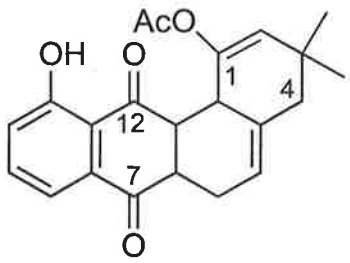

11-Hydroxy-3,3-dimethyl-7,12-dioxo-3,4,6,6a,7,12,12a,12b-octahydrobenzo[*a*]anthracen-1-yl acetate (150)

A mixture of 5-hydroxy-1,4-naphthoquinone (317 mg, 1.82 mmol) and 5,5-dimethyl-3-vinyl-1,2-cyclohexadienyl acetate **(147)** (350 mg, 1.82 mmol) in dry toluene (60 cm^3) was heated under reflux and nitrogen for 24 hours. The reaction mixture was allowed to cool to 20°C, the solvent concentrated to 2 cm^3 *in vacuo* and the product precipitated following dropwise addition of diethyl ether at 0°C (550 mg, 83%). Purification by flash chromatography on silica eluting with hexane/ diethyl ether (2:1), followed by crystallisation from dichloromethane/diethyl ether gave pure 11-hydroxy-3,3-dimethyl,-7,12-dioxo-3,4,6,6a,7,12,12a,12b-octahydrobenzo[*a*]anthracen-1-yl acetate **(150)** as white crystals (450 mg 68%), m.p. 188-190°C. Found C, 71.98%; H, 6.05%, $C_{22}H_{22}O_5$ requires C, 72.12%; H, 6.20%. λ_{max} nm (log ε), 260 shoulder (3.72), 350 (3.75). ν_{max} (KBr), 1741, 1695, 1673, 1653, 1450, 1270, 1251, 1220, 1162 nm. ^{1}H n.m.r. (600mHz COSY and GHMBC) δ: 1.06 s (3H, CH_3); 1.12 s (3H, CH_3); 2.06 dd (1H, 1.0, 14.0 Hz, H4); 2.08 s (3H, CH_3 acetate); 2.24 tm (1H, 1.0, 3.8, 11.4, 11.6 Hz, H6); 2.33 dd (1H, 3.1, 14.0 Hz, H4); 2.37 dm (1H, 3.6, 6.6, `11.4 Hz, H6); 3.21 ddd (1H, 4.5, 6.6, 11.4 Hz, H6a); 3.45 bs (1H, 4.5 Hz at ½ W, H12b); 3.6 t (1H, 4.5 Hz, H12a); 5.38 t (1H, 1.0 Hz, H2); 5.43. bs (1H, 4.0 Hz at ½ W, H5); 7.22 dd (1H, 1.2, 7.8 Hz, H10); 7.53 dd (1H, 1.2, 7.8 Hz, H8); 7.61 t (1H, 7.8 Hz, H9); 11.72 s(1H, H11 OH). ^{13}C n.m.r. δ: 21.00 (CH_3, acetate); 26.57 (C6); 27.52 (CH_3); 30.51 (CH_3); 32.58 (C3); 37.93 (C12b); 45.93 (C12a); 46.04 (C4), 48.39 (C6a); 117.24 (C4a); 118.56 (C8); 118.82 (C5); 123.76 (C2); 124.29 (C10); 132.79 (C7a); 134.04 (C11a); 136.65 (C9); 145.43 (C1); 161.02 (C11); 169.41 (CO, acetate); 197.99 (C12, CO); 202.67 (C7, CO). *m/z* 365 $(M-H)^-$ 14; 323 (CH_2CO) 75; 305 ($CH_2CO + H_2O$) 25%.

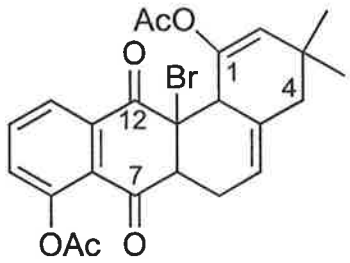

1-Acetoxy-12a-bromo-3,3-dimethyl-7,12-dioxo -3,4,6,6a,7,12,12a,12b-octahydrobenzo[a]anthracen-8-yl acetate (153)

A mixture of 5-acetoxy-2-bromo-1,4-napthoquinone (1.54 g, 5.23 mmol) and 5,5-dimethyl-3-vinyl-1,2-cyclohexadienyl acetate **(147)** (1 g, 5.23 mmol) in anhydrous toluene (80 cm^3) was heated at reflux for 24 hours under nitrogen. The reaction mixture was allowed to cool to 20°C, the solvent removed *in vacuo* to afford **(153)** (2.33 g, 92%) as an orange yellow glass. The product is best used immediately without purification. Purification by flash chromatography on silica eluting with dichloromethane/ acetone (98:2), followed by crystallisation from isopropanol/diethyl ether (1:1) gave 1-acetoxy-12a-bromo-3,3-dimethyl,-7,12-dioxo -3,4,6,6a,7,12,12a,12b-octahydrobenzo[a]anthracen-8-yl acetate **(153)** as colourless crystals which decolourised quickly to orange upon exposure to air (1.63 g 63%), m.p. 112°C decomposes. The product is unstable but may be stored at -20°C. Found C, 58.98%; H, 4.59%, requires $C_{24}H_{23}O_6Br$ C, 59.15%; H, 4.76%. λ_{max} nm (log ε) 258 shoulder (3.60), 312 (3.37). ν_{max} (nujol) 1773, 1751, 1704, 1589, 1233, 1217, 1180 cm. ^1H n.m.r. δ: (600 mHz COSY and GHMBC) 1.04 s (3H, CH_3); 1.12 s (3H, CH_3); 2.10 s (3H, C1 acetate); 2.06 dd (1H, 1.8, 12.9 Hz, C4); 2.30 m (1H, 4.2, 12.0, 12.8 Hz, H6); 2.34 bd (1H, 12.9 Hz, C4); 2.40 s (3H, C8 acetate); 2.45 ddd (1H, 4.2, 6.0, 12.8 Hz, H6); 3.62 dd (1H, 6.0, 12.0 Hz, H6a); 3.97 bs (1H, H12b); 5.40 dd (1H, 1.5, 1.8 Hz, H2); 5.54 td (1H, 2.0, 4.2 Hz, H5); 7.37 dd (1H, 1.2, 7.8 Hz, C9); 7.75 t (1H, 7.8 C10); 8.00 dd (1H, 1.2, 7.8 Hz, C11). ^{13}C n.m.r. δ: 20.98 (CH_3, acetate); 21.90 (CH_3, acetate); 26.94 (CH3); 28.13 (C6); 30.14 (CH3); 32.16 (C3); 45.79 (C12b); 46.74 (C4); 59.3 (C6a); 62.32 (CBr, C12a); 119.46 (C5); 122.87 (C7a); 126.02 (C11); 127.10 (C2); 129.10 (C9); 133.64 (C4a); 134.11 (C11a); 135.05 (C10); 143.80 (C1); 149.62 (C8); 169.15 (CO, acetate); 170.36 (CO, acetate); 187.99 (CO, C12); 193.45 (CO, C7). *m/z* 487 (MH^+) 10 and 489 (MH^+) 10; 427, 429 (CH_3CO_2H) 22; 407 (HBr) 43; 387, 389 (CH_3CO_2H + CH_2CO) 53; 365 (HBr + CH_2CO) 86; 347 (HBr + CH_3CO_2H) 100; 305 (CH_3CO_2H + CH_2CO + HBr) 58%.

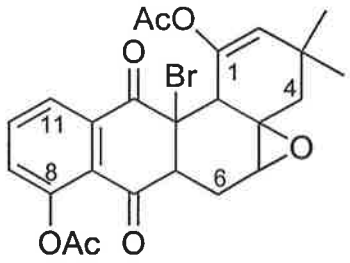

(+/-) 1-(Acetoxy)-12a-bromo-3,3-dimethyl-7,12-dioxo-3,5a,6,6a,7,12,12a,12b –octahydro-4H-benzo[1,2]anthra[2,3-b]oxiren-8-yl acetate (154)

A solution of freshly prepared dimethyl dioxirane in acetone (0.036 M, 30 cm^3) was added to a solution of 1-acetoxy-12a-bromo-3,3-dimethyl-7,12-dioxo-3,4,6,6a,7,12,12a,12b-octahydrobenzo[*a*]anthracen-8-yl acetate **(153)** (700 mg, 1.4 mmol) in distilled acetone (20 cm^3), at 0°C, using a syringe pump over a period of 3 hr and the mixture allowed to stir at 0°C for a further 1 hr under nitrogen. [note: The addition of dimethyl dioxirane was stopped at the first sign of detection of the *bis*-epoxide **(158)** by TLC.] The reaction mixture was warmed to 20°C, dried ($MgSO_4$), the solvent removed *in vacuo*, and the product purified by flash chromatography eluting with dichloromethane/acetone (98:1) to give the starting material **(153)** (200 mg, 29%), the *bis*-epoxide **(158)** (94 mg, 13%) and 1-(acetoxy)-12a-bromo-3,3-dimethyl-7,12-dioxo-3,5a,6,6a,7,12,12a,12b–octahydro-4H-benzo[1,2]anthra[2,3-b]oxiren-8-yl acetate **(154)** (400 mg, 57%) which was crystallised from dichloromethane/ hexane (1:1) as colourless crystals m.p. 89°C with decomposition (product is unstable and best stored at -20°C). $M^{+\cdot}$ 505.0682: $C_{24}H_{24}O_7Br$ requires 505.0685. λ_{max} nm (log ε) 263 shoulder (4.04), 313 (3.75), 337 shoulder (3.11). ν_{max} ($CDCl_3$) 1768, 1708, 1594, 1469, 1369, 1193 br, 1095 cm^{-1}. ^1H n.m.r. (600 mHz COSY and GHMBC) δ: 1.15 s (6H, 2 x CH_3); 1.30 dd (1H, 1.2, 13.2 Hz, H4); 1.99 ddd (1.2, 13.2, 15.0 Hz, H6); 2.09 s (3H, CH_3, acetate); 2.20 d (1H, 13.2 Hz, H4); 2.40 s (3H, CH_3, acetate) 2.47 ddd (1H, 2.7, 4.8, 15.0 Hz, H6); 3.17 bs (1H, H5) 3.75 dd (1H, 4.8, 13.2 Hz, H6a) 3.79 d (1H, 1.8 Hz, H12b); 5.53 dd (1H, 1.2, 2.0 Hz, H2); 7.37 dd (1H, 1.2, 8.0 Hz, H9); 7.76 t (1H, 8.0 Hz, H10); 7.95 dd (1H, 1.2, 8.0 Hz, H11). ^{13}C n.m.r. δ: 21.05 (CH_3, C8 acetate); 21.79 (CH_3, C1 acetate); 26.90 (CH_3); 28.44 (C6); 30.00 (CH_3); 31.24 (C3); 45.60 (C12b); 46.27 (C4); 54.74 (C6a); 59.32 (C4a); 59.61 (C5); 60.19 (CBr, C12a); 122.67 (C7a); 125.94 (C11); 126.91 (C2); 130.05 (C9); 134.82 (C11a); 135.27 (C10); 143.71 (C1); 149.35 (C8); 169.23 (CO, C8 acetate); 170.08 (CO, C1 acetate); 189.26 (CO, C12); 193.09 (CO, C7). *m/z* 503 (M^+) 3 and 505 (M^+) 3; 461, 463 (CH_2CO) 10; 459, 461 (CH_3CO_2H) 10; 423 (HBr) 11; 381 (CH_2CO + HBr) 15; 363 (HBr + CH_3CO_2H) 100; 321 (HBr + CH_3CO_2H + CH_2CO) 32%.

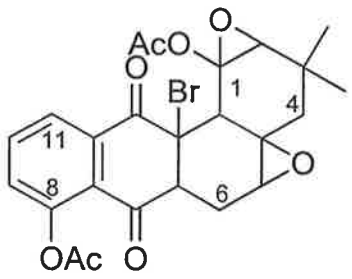

8-(Acetoxy)-12a-bromo-3,3-dimethyl-7,8-dioxo-3,4,4a,5,6,6a,7,12,12a,12b-decahydro-1aH-benzo[6,7]oxireno-[2',3',:10,10a]phenanthro[3,4-b]oxiren-12-yl acetate (158)

A solution of freshly prepared dimethyl dioxirane in acetone (81 cm^3, 0.036 M, 3.0 mmol) was added to a solution of 1-acetoxy-12a-bromo-3,3-dimethyl-7,12-dioxo-3,4,6,6a,7,12,12a,12b-octahydrobenzo-[*a*]anthracen-8-yl acetate **(153)** (586 mg, 1.2 mmol) in distilled acetone (20 cm^3) and allowed to stir at 0°C for 16 hr under nitrogen. The reaction mixture was warmed to 20°C, dried ($MgSO_4$) and the solvent removed *in vacuo* to give 8-(acetoxy)-12a-bromo-3,3-dimethyl-7,8-dioxo-3,4,4a,5,6,6a,7,12,12a,12b-decahydro-1aH-benzo[6,7]oxireno-[2',3',:10,10a]phenanthro[3,4-b]oxiren-1-yl acetate **(158)** (567mg, 91%), which was crystallised from dichloromethane/diethyl ether (1:1) as colourless crystals (512 mg, 82%), m.p. 111°C with decomposition. The product is unstable and best stored at -20°C. Found C, 55.35%; H, 4.26%, $C_{24}H_{23}O_8Br$ requires C, 55.51%; H, 4.46%. λ_{max} nm (log ε) 267 shoulder (3.72), 314 (3.45), 342 shoulder (2.87). $\nu_{max.}$ ($CDCl_3$), 1770 br, 1708, 1594, 1432, 1369, 1263, 1193 br cm^{-1}. ^1H n.m.r. (600 mHz COSY and GHMBC) δ: 0.71 d (1H, 13.8 Hz, H4); 1.25 s (3H, CH_3); 1.20 s (3H, CH_3); 1.95 s (3H, CH_3, C1 acetate); 1.96 ddd (1H, 1.2, 12.6, 14.0 Hz, H6); 2.27 d (1H, 13.8 Hz, H4); 2.40 s (3H, CH_3, C8 acetate); 2.43 ddd (1H, 2.4, 4.2, 14.0 Hz, H6); 2.96 bs (1H, H5); 3.35 bs (1H, H2); 3.73 dd (1H, 4.2, 12.6 Hz, H6a); 3.76 bs (1H, H12b); 7.40 dd (1H, 1.2, 7.5 Hz, H9); 7.78 t (1H, 7.5 Hz, H10); 7.96 dd (1H, 1.2, 7.5 Hz, H11). ^{13}C n.m.r. δ: 20.97 (CH_3, C8 acetate); 22.43 (CH_3); 22.51 (CH_3, C1 acetate); 27.71 (CH_3); 28.05 (C6); 31.40 (C3); 41.44 (C4); 45.83 (C12b); 54.58 (C6a); 56.99 (C4a); 60.68 (C5); 61.13 (CBr, C12a); 67.04 (C2); 83.78 (C1); 122.68 (C7a); 125.70 (C11); 130.30 (C9); 134.66 (C11a); 135.23 (C10); 149.57 (C8); 169.13 (CO, C8 acetate); 169.57 (CO, C1 acetate); 189.34 (CO, C12); 192.41 (CO, C7). *m/z* 519 ($MH^{+\cdot}$) 4 and 521 ($MH^{+\cdot}$) 4%; 477 and 479 (CH_2CO) 5; 459 and 461 (CH_3CO_2H) 5%; 379 (CH_3CO_2H + HBr) 50; 337 (CH_3CO_2H + HBr + CH_2CO) 100; 319 (CH_3CO_2H + HBr + CH_2CO + H_2O) 30%.

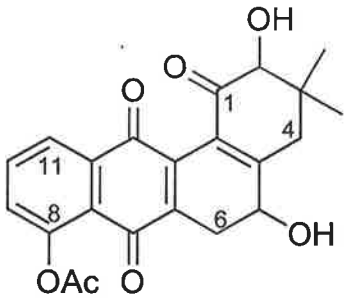

2,5-Dihydroxy-3,3-dimethyl-1,2,5,7,12-pentaoxo-1,2,3,4,5,6,7,12-octahydrobenzo[*a*]anthracen-8-yl acetate (159)

A mixture of 8-(acetoxy)-12a-bromo-3,3-dimethyl-7,8-dioxo-3,4,4a,5,6,6a,6,12,12a,12b-decahydro-1aH-benzo[6,7]oxireno-[2',3',:10,10a]phenanthro[3,4-b]oxiren-12-yl acetate **(158)** (400 mg, 0.77 mmol), water (5 cm^3), tetrahydrofuran (80 cm^3) and p-toluene sulfonic acid (5 mg) was heated under reflux for 16 hr. The solvent was removed *in vacuo,* dichloromethane (100 cm^3) was added, and the mixture was washed with water (50 cm^3), aqueous sodium chloride (saturated, 50 cm^3), dried ($MgSO_4$) and the solvent removed *in vacuo.* The crude mixture can be used in the next step of the synthesis without purification however separation of the two major components was accomplished by flash chromatography on silica eluting with dichloromethane/acetone (9:1) to give 2,5-dihydroxy-3,3-dimethyl-1,2,5,7,12-pentaoxo-1,2,3,4,5,6,7,12-octahydrobenzo[a]anthra-cen-8-yl acetate **(159)** (130 mg 43%) and 2-acetoxy-5-hydroxy-3,3-dimethyl-1,2,5,7,12-pentaoxo-1,2,3,4,5,6,7,12-octahydrobenzo-[a]anthracen-8-yl acetate **(160)** (90 mg 27%).

Diol **(159)** was crystallised from ethanol as light orange crystals (112 mg 37%), m.p. 184°C with decomposition. This product is best stored at -20°C. Found C, 66.79%; H, 5.07%, requires $C_{22}H_{20}O_7$ C, 66.66%; H, 5.09%. λ_{max} nm (log ε) 250 (4.31), 284 shoulder (4.00), 345 (3.68). $\nu_{max.}$ (nujol); .3436, 1772, 1769, 1749, 1671, 1656, 1589, 1274, 1184 cm^{-1}. ^1H n.m.r. (600 mHz COSY and GHMBC) δ: 0.84 s (3H, CH_3); 1.26 s (3H, CH_3); 2.34 d (1H, 15.6, 16.8 Hz, H6); 2.43 s (3H, CH_3, C8 acetate); 2.47 d (1H, 20.0 Hz, H4); 3.07 d (1H, 20.0 Hz, H4); 3.22 dd (1H, 6.6, 16.8 Hz, H6); 4.15 bd (1H, 4.2 Hz, C2-OH); 4.30 d (1H, 4.2 Hz, H2); 4.44 ddd (1H, 6.0, 6.6, 15.6 Hz, H5); 5.58 d (1H, 6.0 Hz, C5-OH); 7.37 dd (1H, 1.2, 7.8 Hz, H9); 7.77 t (1H, 7.8 Hz, H10); 7.93 dd (1H, 1.2, 7.8 Hz, H11). ^{13}C n.m.r. (600 mHz GHMQC) δ; 18.34 (CH_3), 20.12 ($COCH_3$), 26.85 (CH_3), 27.76 (C6), 37.85 (C4), 39.00 (C3), 66.62 (C5), 78.91 (C2), 122.23 (C7a), 123.74 (C11), 124.52 (C12b), 128.28 (C9), 133.56 (C11a), 133.76 (C10), 137.44 (C6a), 141.20 (C12a), 148.26 (C8), 165.98 (C4a), 168.21 (CO-acetate),

179.86 (C12), 180.67 (C7), 196.03 (C1). m/z 396 ($M^{+\cdot}$) 2; 378 (H_2O) 9; 336 (H_2O + CH_2CO) 60; 318 (H_2O + CH_2CO + H_2O) 40; 290 (H_2O + CH_2CO + H_2O + CO) 40; 264 (H_2O + CH_2CO + C_4H_8O) 100; 236 (H_2O + CH_2CO + C_4H_8O + CO) 20%.

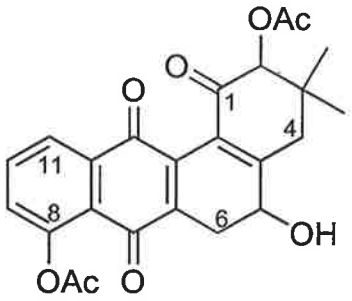

2-Acetoxy-5-hydroxy-3,3-dimethyl-1,2,5,7,12-pentaoxo-1,2,3,4,5,6,7,12-octahydrobenzo[*a*]anthracen-8-yl acetate (160).

The bis-acetate **(160)** was purified by crystallisation from chloroform/diethyl ether to give **(160)** as light orange crystals (74 mg 22%), m.p. 164-166°C. The product is unstable and best stored at -20°C. Found C, 65.46%; H, 5.12%, $C_{24}H_{22}O_8$, requires C, 65.75%; H, 5.06%. λ_{max} nm (log ε) 249 (4.08), 280 shoulder (3.81), 345 (3.46). ν_{max}. (nujol), 3474, 1770, 1733, 1689, 1650 br, 1640, 1587, 1243, 1193 cm^{-1}. ^1H n.m.r. (600 mHz COSY and GHMBC) δ: 1.01 s (3H, CH_3); 1.21 s (3H, CH_3); 2.24 (3H, CH_3, C2 acetate); 2.40 dd (1H, 11.4, 16.8 Hz, H6); 2.43 s (3H, CH_3, C8 acetate); 2.58 bd (1H, 20.2 Hz, H4); 2.81 d (1H, 5.4 Hz, C5 OH); 3.07 d (1H, 20.2 Hz, H4); 3.23 dd (1H, 7.0, 16.8 Hz, H6); 4.59 ddd (1H, 5.4, 7.0, 11.4 Hz, H5); 5.42 s (1H, H2); 7.27 dd (1H, 1.2, 7.8 Hz, H9); 7.65 t (1H, 7.8 Hz, H10); 7.91 dd (1H, 1.2, 7.8 Hz, H11). ^{13}C n.m.r. (600 mHz GHMQC) δ; 20.70 (CH_3), 20.74 ($COCH_3$), 21.09 ($COCH_3$), 27.48 (CH_3), 28.76 (C6), 38.30 (C4), 39.42 (C3), 68.17 (C5), 80. 96 (C2), 122.92 (C7a), 125.28 (C11), 126.79 (C12b), 129.02 (C9), 134.34 (C11a), 134.80 (C10), 138.35 (C6a), 141.74 (C12a), 149.10 (C8), 163.22 (C4a), 169.54 (CO acetate), 170.52 (COacetate), 180.43 (C12), 181.63 (C7), 190.41 (C1). m/z 438 ($M^{+\cdot}$) 1; 396 (CH_2CO) 25; 378 ($C_2H_4O_2$), 24; 360 ($C_2H_4O_2$ + H_2O) 20; 336 ($C_2H_4O_2$ + CH_2CO) 100; 318 ($C_2H_4O_2$ + CH_2CO + H_2O) 60; 264 (C_2H_2O + H_2O + $C_6H_{10}O_2$) 54; 244 ($C_2H_4O_2$ + CH_2CO + H_2O + C_4H_8O) 50%.

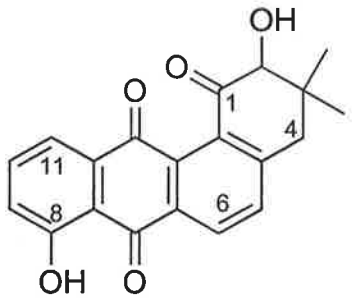

2,8-Dihydroxy-3,3-dimethyl-1,7,12,trioxo-1,2,3,4,7,12-hexahydrobenzo[*a*]anthracene (161)

The crude mixture of diol **(159)** and the bis-acetate **(160)** (100 mg) obtained from the previous step of the synthesis was dissolved in excess acetic acid (glacial, 10 cm^3), a catalytic amount of concentrated sulphuric acid (98%, 0.2 cm^3) was added and the mixture stirred for 2 hours at 20°C. The reaction mixture was diluted with diethyl ether (100 cm^3), cooled to 0°, neutralised with aqueous sodium hydroxide (20%, 35 cm^3), the organic layer separated, washed with water (2 x 50 cm^3) the solvent removed *in vacuo*, tetrahydrofuran (30 cm^3) was added, followed by aqueous sodium hydroxide (20%, 5 cm^3) and the mixture stirred at 20°C for 3 hr. The mixture was cooled to 0°C, neutralised with aqueous hydrogen chloride (10%, 55 cm^3) and the solvent removed *in vacuo*. The aqueous mixture was extracted with dichloromethane (2 x 50 cm^3), washed with aqueous hydrogen chloride (1M, 25 cm^3), water (50 cm^3), aqueous sodium chloride (saturated, 50 cm^3), dried ($MgSO_4$) and the solvent removed *in vacuo* to give 2,8-dihydroxy-3,3-dimethyl-1,7,12,trioxo-1,2,3,4,7,12-hexahydro-benzo[*a*]anthracene (82 mg, 96%) **(161)**, which was crystallised from hot ethanol/methanol (1:1) as fine yellow orange crystals (66 mg, 78%) m.p. 172°C with decomposition. $M^{+\cdot}$ 336.0991 $C_{20}H_{16}O_5$ requires 336.0997. λ_{max} nm (log ε) 265 (3.96), 400 (3.21). ν_{max}. (nujol), 3440, 1693, 1666, 1633,, 1589, 1348, 1284 cm^{-1}. ^1H n.m.r. (300mHz) δ: 0.78 s (3H, CH_3), 1.35 s (3H, CH_3), 2.95 d (1H, 17.4 Hz, H4), 3.21 d (1H, 17.4 Hz, H4), 3.88 bs (1H, C2-OH), 4.65 s (1H, 2H), 7.29 t (1H, 3.9 Hz, H10), 7.57 d (1H, 7.8 Hz, H5), 7.68 bd (2H, 3.9 Hz, H9, H11), 8.36 d (7.8 Hz, H6), 12.22 s (1H, C8-OH). ^{13}C n.m.r. (300mHz) δ: 18.49 (CH3), 27.52 (CH3), 42.38 (C3), 43.34 (C4), 80.89 (C2), 115.04, 119.28, 123.44, 129.88, 132.87, 133.32, 133.56, 134.94, 136.89, 136.90, 149.36, 163.81 (C8-OH), 182.50, 186.91, 198.78. *m/z* 336 ($M^{+\cdot}$) 45; 318 (H_2O) 20; 290 (H_2O + CO) 30; 264 (C_4H_8O) 100; 236 (C_4H_8O + CO) 15%.

Appendix

High Field NMR Data

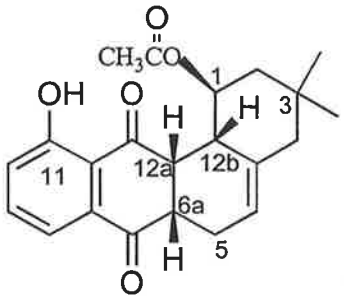

(113)

^{1}H PPM	ASSIGNMENT	AREA	MULTIPLICITY COUPLING CONSTANTS	COSY
12.15	C11-OH	1	s	-
7.61	H9	1	t, 7.8 Hz	H8, H10
7.53	H8	1	dd, 7.8, 1.2 Hz	H9, H10
7.22	H10	1	dd, 7.8, 1.2 Hz	H8, H9
5.58	H5	1	bs	H4, $H6_{ax}$, $H6_{eq}$, 12b
4.58	$H1_{ax}$	1	bs	$H2_{ax}$, $H2_{eq}$
3.50	$H12a_{eq}$	1	t, 6.9 Hz	H6a, H12b
3.40	$H6a_{ax}$	1	dt, 6.9, 3.0 Hz	$H6_{eq}$, $H6_{ax}$, H12a
2.85	$H6_{eq}$	1	bdd, 18.0, 3.0 Hz	H5, $H6_{ax}$,H6a
2.70	$H12b_{ax}$	1	bt, 6.9 Hz	$H2_{eq}$, H5, $H12a_{eq}$
2.17	$H6_{ax}$	1	bdd, 18.0, 6.9 Hz	H5, $H6_{eq}$, $H6a_{ax}$
1.92	H4	2	bs	H5
1.76	$H2_{eq}$	1	dd, 11.4, 4.1 Hz	$H1_{ax}$, $H2_{ax}$
1.71	CH_3 acetate	3	s	-
1.08	$H2_{ax}$	1	t, 11.4 Hz	$H1_{ax}$, $H2_{eq}$
0.91	CH_{3eq}	3	s	-
0.82	CH_{3ax}	3	s	-

Table 1. Summary of ^{1}H n.m.r. data for adduct **(113).**

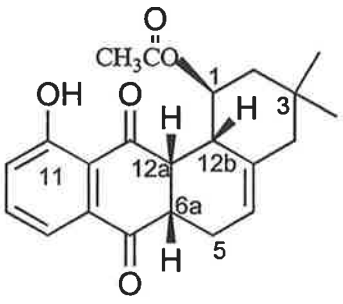

(113)

^{1}H PPM	ASSIGN MENT	HSQC ^{13}C PPM	ASSIGN MENT	HMBC ^{13}C
12.15	C11-OH	160.90	C11	-
7.61	H9	136.73	C9	C7a, C11
7.53	H8	118.11	C8	C7, C10, C11a
7.22	H10	123.48	C10	C8, C11a, C11
5.58	H5	121.64	C5	C12b
4.58	$H1_{ax}$	71.28	C1	-
3.50	$H12a_{eq}$	48.30	C12a	C1, C7, C12, C12b
3.40	$H6a_{ax}$	47.72	C6a	-
2.85	$H6_{eq}$	45.51	C6	-
2.70	$H12b_{ax}$	43.76	C12b	-
2.17	$H6_{ax}$	45.51	C6	C5, C7
1.92	H4	49.03	C4	CH_{3eq}, C3, C4a, C5, 12b
1.76	$H2_{eq}$	44.95	C2	-
1.71	CH_3, $C1_{acetate}$	20.63	CH_3	$C1_{acetate}$ (169.41)
1.08	$H2_{ax}$	44.98	C2	CH_{3eq}, C1, C3
0.91	CH_{3eq}	31.39	CH_{3eq}	CH_{3ax}, C2, C3, C4
0.82	CH_{3ax}	24.58	CH_{3ax}	CH_{3eq}, C2, C3, C4

Table 2. Summary of ^{13}C n.m.r. data for adduct **(113).**

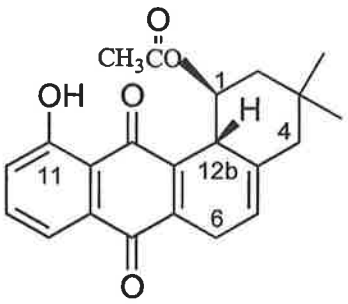

(114)

^{1}H ppm	Assign ment	Area	Multiplicity Coupling Constants	COSY	Long range COSY
12.0	C11-OH	1	s	-	-
7.61	H8	1	dd, 7.2, 1.2 Hz	H9, H10	H9, H10
7.58	H9	1	dt, 7.2, 1.2 Hz	H8, H10	H8, H10
7.23	H10	1	dd, 7.2, 1.2 Hz	H9, H8	H9, H8
5.64	H5	1	bs (7 Hz 1/2 W)	$H4_{ax}$, $H6_{ax}$, $H6_{eq}$	$H4_{ax}$, $H6_{ax}$, $H6_{eq}$,H12b
4.69	$H1_{ax}$	1	dt, 11.0, 4.0 Hz	$H2_{ax}$, $H2_{eq}$, H12b	$H2_{ax}$, $H2_{eq}$, H12b
3.67	$H12b_{ax}$	1	dddd, 11.0, 5.0 Hz	H1, $H6_{eq}$	H1, H5, $H6_{ax}$
3.41	$H6_{eq}$	1	bdm 25.0 Hz, 7 Hz at 1/2 W	H5, $H6_{ax}$, H12b	$H4_{eq}$
3.23	$H6_{ax}$	1	bdm 25.0 Hz, 7 Hz at 1/2 W	H5, $H6_{eq}$, H12b	H12b
2.05	$H4_{ax}$	1	bd, 26.0 Hz	H4eq, H5	H5
2.01	$H4_{eq}$	1	bd, 26.0 Hz	H4ax, H6eq	$H2_{eq}$
1.87	$CH_{3\ acetate}$	3	s	-	-
1.79	$H2_{eq}$	1	dd, 11.0, 4.0 Hz	H1, $H2_{ax}$	$H4_{eq}$
1.73	$H2_{ax}$	1	t, 11.0 Hz	H1, $H2_{eq}$	CH_{3eq}
1.09	CH_{3ax}	3	s	-	-
0.95	CH_{3eq}	3	s	-	$H2_{ax}$

Table 3. Summary of ^{1}H n.m.r. data for **(114)**.

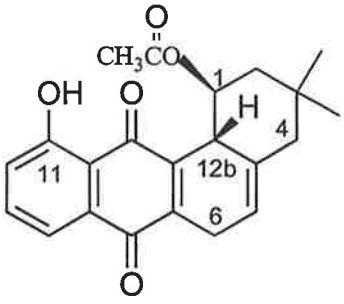

(114)

^{1}H ppm	Assignment	HSQC ^{13}C ppm	Assignment	HMBC ^{13}C
12.03	C11-OH	161.99	C11	-
7.61	H8	118.90	C8	C10, C11, C11a
7.58	H9	136.02	C9	C7, C10, C11a
7.23	H10	123.96	C10	C8, C11a
5.64	H5	118.98	C5	C4, C6a, C6, C12b
4.69	$H1_{ax}$	74.26	$C1_{ax}$	-
3.67	$H12b_{ax}$	41.98	$C12b_{ax}$	-
3.41	$H6_{eq}$	25.60	$C6_{eq}$	C4a, C6a, C8, C12a
3.23	$H6_{ax}$	25.60	$C6_{ax}$	C4a, C6a, C8, C12a
2.05	$H4_{ax}$	47.81	$C4_{ax}$	CH_{3eq}, C2, C3, C4a, C5, C12b
2.01	$H4_{eq}$	47.81	$C4_{eq}$	CH_{3eq}, C2, C3, C4a, C5, C12b
1.87	CH_3, $C1_{acetate}$	21.07	CH_3, $C1_{acetate}$	$C1_{acetate}$ (171.06)
1.79	$H2_{eq}$	46.09	$C2_{eq}$	CH_{3ax}, CH_{3eq}, C1, C3, C4, C12b
1.73	$H2_{ax}$	46.09	$C2_{ax}$	CH_{3ax}, CH_{3eq}, C1, C3, C12b
1.09	CH_{3ax}	31.86	CH_{3ax}	CH_{3eq}, C2, C4
0.95	CH_{3eq}	25.44	CH_{3eq}	CH_{3ax}, C2, C4

Table 4. Summary of ^{13}C n.m.r. data for **(114)**.

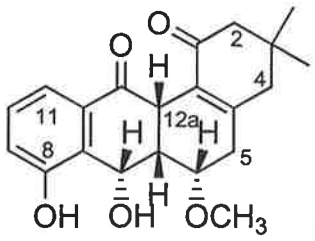

(122)

^{1}H ppm	Assign ment	Area	Multiplicity Coupling Constants	COSY
7.39	H11	1	d, 7.8 Hz	H10
7.24	H10	1	t, 7.8 Hz	H9, H11
7.06	H9	1	d, 7.8 Hz	H11
5.77	$H7_{eq}$	1	d, 6.0 Hz	H6a
4.25	$H6_{eq}$	1	bs	-
3.98	$H12a_{eq}$	1	d, 6.0 Hz	H6a
2.94	C6-OCH_3	3	-	-
2.70	$H6a_{ax}$	1	t, 6.0 Hz	H7, H12a
2.65	$H2_{ax}$	1	d, 15.0 Hz	$H2_{eq}$
2.51	H5	2	bs	-
2.43	$H4_{eq}$	1	d, 18.0 Hz	$H4_{ax}$
2.31	$H2_{eq}$	1	d, 15.0 Hz	$H2_{ax}$
2.27	$H4_{ax}$	1	d, 18.0 Hz	$H4_{eq}$
1.25	CH_{3ax}	3	s	-
1.10	CH_{3eq}	3	s	-

Table 5. Summary of ^{1}H n.m.r. data for alcohol **(122)**

^{1}H ppm	Assign ment	HSQC ^{13}C ppm	Assignmen t	HMBC ^{13}C
7.39	H11	118.15	C11	C9, C10, C12
7.24	H10	129.34	C10	C8, C9, C11a, C11
7.06	H9	121.79	C9	C8, C10, C11
5.77	$H7_{eq}$	69.31	$C7_{eq}$	C6, C6a, C8, C10, C11a
4.25	$H6_{eq}$	73.86	$C6_{eq}$	C4a, OCH_3, C12a
3.98	$H12a_{eq}$	43.03	$C12a_{eq}$	C1, C4a, C6, C6a, C7, C12, C12a
2.94	C6-OCH_3	57.43	C6-OCH_3	C6
2.70	$H6a_{ax}$	47.08	$C6a_{ax}$	C7, C7a, C12, C12a
2.65	$H2_{ax}$	52.41	$C2_{ax}$	CH_{3ax}, CH_{3eq}, C1, C3, C4
2.51	H5	39.21	C5	C4a, C6, C6a, C12b
2.43	$H4_{eq}$	46.46	$C4_{eq}$	CH_{3ax}, CH_{3eq}, C2, C3, C4a, C5, C12b
2.31	$H2_{eq}$	52.41	$C2_{eq}$	CH_{3ax}, CH_{3eq}, C1, C3, C4
2.27	$H4_{ax}$	46.46	$C4_{ax}$	CH_{3ax}, CH_{3eq}, C2, C3, C4a, C5, C12b
1.25	CH_{3ax}	28.18	CH_{3ax}	CH_{3ax}, C2, C3, C4
1.10	CH_{3eq}	30.29	CH_{3eq}	CH_{3eq}, C2, C3, C4

Table 6. Summary of ^{13}C n.m.r. data for alcohol **(122).**

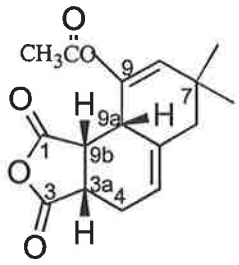

(149)

^{1}H ppm	Assignment	Area	Multiplicity Coupling Constants	COSY	ROESY
5.79	H5	1	ddd, 7.2, 2.4, 2.2 Hz	$H4_{ax}$, $H4_{eq}$, H9a	$H6_{eq}$
5.65	H8	1	t, 1.0 Hz	$H6_{eq}$, H9a	CH_{3ax}, CH_{3eq},
3.57	$H9b_{eq}$	1	dd, 9.6, 6.6 Hz	H3, H9a	-
3.46	$H3a_{ax}$	1	ddd 9.6, 7.8, 1.8 Hz	$H4_{ax}$, $H4_{eq}$, H9a	H9a
3.27	$H9a_{ax}$	1	ddd 6.6, 2.2, 1.0 Hz	H5, H8, H10	CH_{3eq}, H3, $H4_{eq}$,
2.75	$H4_{ax}$	1	ddd 9.0, 7.2, 1.8 Hz	H3, $H4_{eq}$, H5	-
2.29	$H6_{ax}$	1	d, 13.8 Hz	$H6_{eq}$	CH_{3eq},
2.24	$H4_{eq}$	1	ddd 9.0, 7.8, 2.4 Hz	H3, $H4_{ax}$, H5	H9a
2.19	CH_3, acetate	3	s	-	-
2.11	$H6_{eq}$	1	dd, 13.8, 1.0 Hz	$H6_{ax}$, H8	CH_{3ax}, H5
1.06	CH_{3eq}	3	s	-	H_{6ax}, H8, H9a
0.93	CH_{3ax}	3	s	-	H_{6eq}, H8

Table 7. Summary of ^{1}H n.m.r. data for lactone **(149).**

^{1}H ppm	Assignment	HSQC ^{13}C	Assignment	HMBC ^{13}C
5.79	H5	121.60	C5	-
5.65	H8	127.96	C8	CH_{3ax}, CH_{3eq}, C6, C7, C9
3.57	$H10_{eq}$	41.74	C10	C1, C2, C3, C4, C5a, C9a
3.46	$H3_{ax}$	40.72	C3	C1, C2, C4, C5, C10
3.27	$H9a_{ax}$	36.20	C9a	-
2.75	$H4_{ax}$	24.32	C4	C1, C3, C5, C5a
2.29	$H6_{ax}$	44.17	C6	CH_{3ax}, C1, C5, C5a
2.24	$H4_{eq}$	24.32	C4	-
2.19	CH_3, $C9_{acetate}$	21.17	CH_3, $C9_{acetate}$	$C9_{acetate}$ (169.59), C9
2.11	$H6_{eq}$	44.17	C6	CH_{3ax}, CH_{3eq}, C5, C7, C5a, C8, C9a
1.06	CH_{3eq}	29.53	CH_{3eq}	CH_{3ax}, C6, C7, C8, C9
0.93	CH_{3ax}	28.54	CH_{3ax}	CH_{3eq}, C6, C7, C8, C9

Table 8. Summary of ^{13}C n.m.r. data for lactone **(149).**

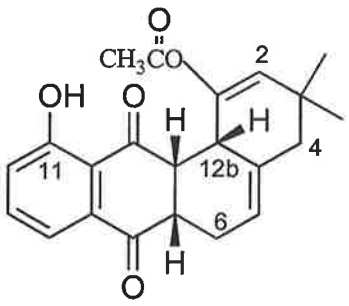

(147)

^{1}H ppm	Assignment	Area	Multiplicity Coupling Constants	COSY	ROESY
11.72	C11-OH	1	s	-	H10
7.61	H9	1	t, 7.8 Hz	H8, H10	-
7.53	H8	1	dd, 7.8, 1.2 Hz	H9, H10	-
7.22	H10	1	dd, 7.8, 1.2 Hz	H8, H9	H8
5.43	H5	1	bs (4.0 Hz ½ W)	$H4_{ax}$, $H6_{eq}$, $H6_{ax}$, H12b	$H4_{eq}$,
5.38	H2	1	t, 1.0 Hz	$H4_{eq}$, H12b	CH_{3ax}, CH_{3eq},
3.60	$H12a_{eq}$	1	t, 4.5 Hz	H6a, H12b	-
3.45	$H12b_{ax}$	1	bs (4.0 Hz at ½ W)	H2, H5, $H6_{ax}$, H12a	$H4_{ax}$, H6a
3.22	$H6a_{ax}$	1	ddd, 11.4, 6.6, 4.5 Hz	$H6_{ax}$, $H6_{eq}$, H12a	H12b
2.37	$H6_{eq}$	1	ddd, 11.6, 6.6, 4.0 Hz	H5, $H6_{ax}$, $H6a_{ax}$	-
2.33	$H4_{ax}$	1	dd, 14.0, 3.1 Hz	$H4_{eq}$, H5	CH_{3eq}, H12b
2.24	$H6_{ax}$	1	dddd, 11.6, 11.4, 3.8, 1.0 Hz	H5, H6eq, H6a, H12b	-
2.08	CH_3 acetate	3	s	-	-
2.06	$H4_{eq}$	1	dd, 14.0, 1.0 Hz	H2, $H4_{ax}$	CH_{3ax}, CH_{3eq}, H5
1.12	CH_{3eq}	3	s	-	H2, $H4_{ax}$, $H4_{eq}$,
1.06	CH_{3ax}	3	s	-	H2, $H4_{eq}$

Table 9. Summary of ^{1}H n.m.r. data for adduct **(147)**.

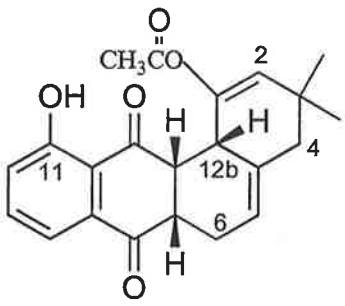

(147)

^{1}H ppm	Assignment	HSQC ^{13}C ppm	Assignment	HMBC ^{13}C
11.72	C11-OH	161.02	C11	C8, C9, C10, C11
7.61	H9	136.65	C9	C9, C11, C11a
7.53	H8	118.55	C8	C10, C12
7.22	H10	124.29	C10	C11, C8,
5.43	H5	118.82	C5	C4, C6a, C12a, C12b
5.38	H2	123.78	C2	CH_{3eq}, C1, C3, C4, C12a, C12b
3.60	$H12a_{eq}$	45.93	C12a	C6, C6a, C7, C11a, C12, 12b
3.45	$H12b_{ax}$	37.93	C12b	-
3.22	$H6a_{ax}$	48.39	C6a	C6, C7, C7a, C11, C12a, C12b
2.37	$H6_{eq}$	26.57	C6	C3, C4, C5, C8, C12a
2.33	$H4_{ax}$	46.04	C4	CH_{3ax}, C3, C4a
2.24	$H6_{ax}$	26.57	C6	C5, C8
2.08	CH_3,$C1_{acetate}$	21.00	CH_3, $C1_{acetate}$	$C1_{acetate}$ (169.41)
2.06	$H4_{eq}$	46.04	C4	CH_{3eq}, C2, C3, C4a, C12b
1.12	CH_{3eq}	30.51	CH_{3eq}	CH_{3ax}, C1, C2, C3, C4,
1.06	CH_{3ax}	27.52	CH_{3ax}	CH_{3eq}, C2, C3, C4

Table 10. Summary of ^{13}C n.m.r. data for adduct **(147).**

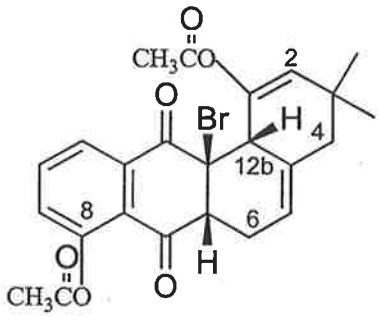

(153)

^{1}H ppm	Assignment	Area	Multiplicity Coupling Constants	COSY	ROESY
8.00	H11	1	dd, 7.8, 1.2 Hz	H10, H9	-
7.75	H10	1	t, 7.8 Hz	H9, H11	-
7.37	H9	1	dd, 7.8, 1.2 Hz	H10, H11	-
5.54	H5	1	dt, 4.2, 2 Hz	$H6_{eq}$, $H6_{ax}$, H12b	CH_{3ax}, $H4_{eq}$, $H4_{ax}$,
5.40	H2	1	dd, 1.8, 1.5 Hz	$H4_{eq}$, H12b	CH_{3ax}, CH_{3eq},
3.97	$H12b_{ax}$	1	bs	H2, H5, $H6_{ax}$	$H4_{ax}$, H6a
3.62	$H6a_{ax}$	1	dd, 12.0, 6.0 Hz	$H6_{ax}$, $H6_{eq}$	H12b
2.45	$H6_{eq}$	1	ddd, 12.8, 6.0, 4.2, Hz	H5, $H6_{ax}$, H6a	-
2.40	$C8_{acetate}$	3	s	-	-
2.34	$H4_{ax}$	1	d, 12.9 Hz	$H4_{eq}$	CH_{3eq}, H5, H12b
2.30	$H6_{ax}$	1	m, 12.8, 12.0, 4.2 Hz	H5, H6eq, H6a, H12b	-
2.10	$C1_{acetate}$	3	s	-	-
2.06	$H4_{eq}$	1	dd, 12.9, 1.8 Hz	H2, $H4_{ax}$	CH_{3ax}, CH_{3eq}, H5,
1.12	CH_{3eq}	3	s	-	H2, $H4_{ax}$, $H4_{eq}$,
1.04	CH_{3ax}	3	s	-	H2, $H4_{eq}$, H5

Table 11. Summary of ^{1}H n.m.r. data for bromo adduct **(153).**

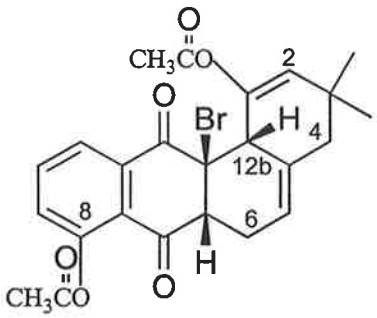

(153)

^{1}H ppm	Assign ment	HSQC ^{13}C ppm	Assign ment	HMBC ^{13}C
8.00	H11	126.02	C11	C7a, C8, C9, C10, C12,
7.75	H10	135.05	C10	C7a, C8, C9, C11, C11a
7.37	H9	129.97	C9	C7a, C8, C11,
5.54	H5	119.46	C5	C4, C6, C6a, C12b
5.40	H2	127.10	C2	CH_{3ax}, CH_{3eq}, C1, C3, C4, C12b
3.97	$H12b_{ax}$	45.78	C12b	C1, C4a, C12, C12a
3.62	$H6a_{ax}$	59.37	C6a	C5, C6, C7, C7a, C12, C12a, C12b
2.45	$H6_{eq}$	28.13	C6	C5, C6a, C12a, C4a
2.40	CH_3, $C8_{acetate}$	20.98	CH_3, $C8_{acetate}$	$C8_{acetate}$ (169.15)
2.34	$H4_{ax}$	46.74	C4	CH_{3ax}, C3, C4a, C5, C12b
2.30	$H6_{ax}$	28.13	C6	C4a, C5, C6a, C7
2.10	CH_3, $C1_{acetate}$	21.90	CH_3, $C1_{acetate}$	$C1_{acetate}$ (170.36), C2
2.06	$H4_{eq}$	46.74	C4	CH_{3ax}, CH_{3eq}, C3, C4a, C5, C12a, C12b
1.12	CH_{3eq}	30.14	CH_{3eq}	CH_{3ax}, C1, C2, C3, C4, C4a,
1.04	CH_{3ax}	26.94	CH_{3ax}	CH_{3eq}, C1, C2, C3, C4,

Table 12. Summary of ^{13}C n.m.r. data for bromo adduct **(153).**

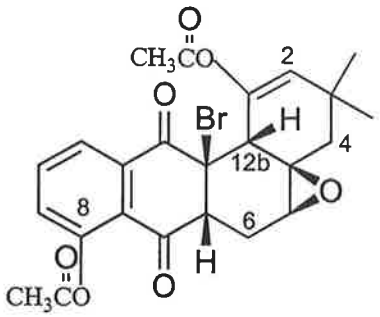

(154)

^{1}H ppm	Assignment	Area	Multiplicity Coupling Constants	COSY	ROESY
7.96	H11	1	dd, 7.5, 1.2 Hz	H10, H9	-
7.78	H10	1	t, 7.5 Hz	H9, H11	-
7.40	H9	1	dd., 5, 1.2 Hz	H10, H11	-
3.76	$H12b_{ax}$	1	bs	H2	$H4_{ax}$, H6a
3.73	$H6a_{ax}$	1	dd, 12.6, 4.2 Hz	$H6_{ax}$,$H6_{eq}$	H12b
3.35	$H2_{eq}$	1	bs	$H12b_{ax}$	CH_{3ax}, CH_{3eq}
2.96	$H5_{eq}$	1	bs	$H6_{eq}$, $H6_{ax}$	CH_{3ax}, $H4_{eq}$
2.43	$H6_{eq}$	1	ddd, 14.0, 4.2, 2.4 Hz	H5, $H6_{ax}$, H6a	-
2.40	C8 acetate	3	s	-	-
2.27	$H4_{ax}$	1	d, 13.8 Hz	$H4_{eq}$	CH_{3eq}, H12b
1.96	$H6_{ax}$	1	ddd, 14.0, 12.6, 1.2 Hz	H5, $H6_{eq}$, H6a	-
1.95	C1 acetate	3	s	-	CH_{3eq}
1.20	CH_{3ax}	3	s	-	H2, $H4_{eq}$, $H5_{eq}$
1.15	CH_{3eq}	3	s	-	$C1_{acetate}$, H2, $H4_{ax}$, $H4_{eq}$,
0.71	$H4_{eq}$	1	d, 13.8 Hz	$H4_{ax}$	CH_{3eq}, CH_{3ax}, $H5_{eq}$

Table 13. Summary of ^{1}H n.m.r. data for epoxide **(154).**

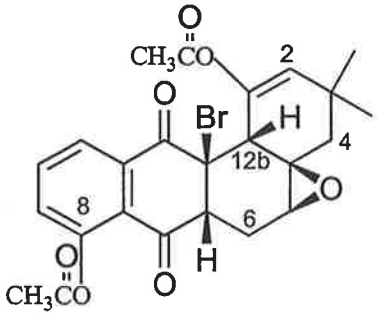

(154)

^{1}H ppm	Assignment	HSQC ^{13}C ppm	Assignment	HMBC ^{13}C
7.95	H11	125.94	C11	C7a, C9, C12,
7.76	H10	135.27	C10	C8, C11a
7.37	H9	130.05	C9	C7a, C8, C11,
5.53	H2	126.91	C2	CH_3 (30.0, 26.9), C1, C12b
3.79	$H12b_{ax}$	45.60	C12a	C1, C2, C4a, C5, C12
3.75	$H6a_{ax}$	54.74	C6a	C5, C6, C7, C7a, C12,
3.17	$H5_{eq}$	59.61	C5	C6a, C6
2.47	$H6_{eq}$	28.44	C6	C5, C12a, C4a
2.40	CH_3, $C8_{acetate}$	21.05	CH_3, $C8_{acetate}$	$C8_{acetate}$ (169.23)
2.20	$H4_{ax}$	46.27	C4	C2, C3, CH_3 (30.0, 26.9), C4a, C12b
2.09	CH_3, $C1_{acetate}$	21.79	CH_3, $C1_{acetate}$	$C1_{acetate}$ (170.08)
1.99	$H6_{ax}$	28.44	C6	C6a, C7
1.30	$H4_{eq}$	46.27	C4	C2, C3, CH_3 (30.0, 26.9), C4a, C12b,
1.15	$2XCH_3$	30.00 26.90	CH_3 CH_3	C2, C3, CH_3 (30.0 26.9), C4, C4a,

Table 14. Summary of ^{13}C n.m.r. data for epoxide **(154).**

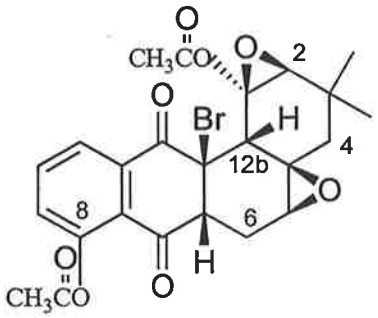

(158)

^{1}H ppm	Assignment	Area	Multiplicity Coupling Constants	COSY	ROESY
7.96	H11	1	dd, 7.5, 1.2 Hz	H10, H9	-
7.78	H10	1	t, 7.5 Hz	H9, H11	-
7.40	H9	1	dd., 5, 1.2 Hz	H10, H11	-
3.76	$H12b_{ax}$	1	bs	H2	$H4_{ax}$, H6a
3.73	$H6a_{ax}$	1	dd, 12.6, 4.2 Hz	$H6_{ax}$,$H6_{eq}$	H12b
3.35	$H2_{eq}$	1	bs	$H12b_{ax}$	CH_{3ax}, CH_{3eq}
2.96	$H5_{eq}$	1	bs	$H6_{eq}$, $H6_{ax}$	CH_{3ax}, $H4_{eq}$
2.43	$H6_{eq}$	1	ddd, 14.0, 4.2, 2.4 Hz	H5, $H6_{ax}$, H6a	-
2.40	C8 acetate	3	s	-	-
2.27	$H4_{ax}$	1	d, 13.8 Hz	$H4_{eq}$	CH_{3eq}, H12b
1.96	$H6_{ax}$	1	ddd, 14.0, 12.6, 1.2 Hz	H5, $H6_{eq}$, H6a	-
1.95	C1 acetate	3	s	-	CH_{3eq}
1.20	CH_{3ax}	3	s	-	H2, $H4_{eq}$, $H5_{eq}$
1.15	CH_{3eq}	3	s	-	$C1_{acetate}$, H2, $H4_{ax}$, $H4_{eq}$,
0.71	$H4_{eq}$	1	d, 13.8 Hz	$H4_{ax}$	CH_{3eq}, CH_{3ax}, $H5_{eq}$

Table 15. Summary of ^{1}H n.m.r. data for *bis*-epoxide **(158).**

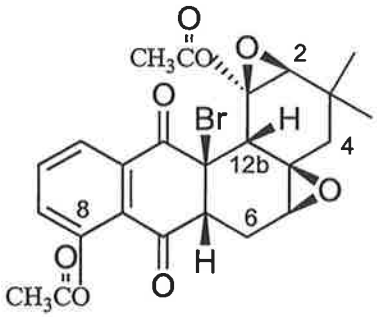

(158)

^{1}H ppm	Assignment	HSQC ^{13}C ppm	Assignment	HMBC ^{13}C
7.96	H11	125.70	C11	C7a, C9, C12,
7.78	H10	135.23	C10	C7a, C8, C11, C11a
7.40	H9	130.30	C9	C7a, C8, C11,
3.76	$H12b_{ax}$	45.43	C12b	C1, C2, C4a, C5, C6a, C12, C12a
3.73	$H6a_{ax}$	54.88	C6a	C6, C7, C7a, C12, C12a
3.35	H2	67.04	C2	CH_{3eq}, C1, C3, C4,
2.96	$H5_{eq}$	60.68	C5	C6a, C6
2.43	$H6_{eq}$	28.05	C6	C12a, C4a
2.40	CH_3, $C8_{acetate}$	20.97	CH_3, $C8_{acetate}$	$C8_{acetate}$ (169.13)
2.27	$H4_{ax}$	41.44	C4	CH_{3ax}, CH_{3eq}, C3, C4a, C5
1.96	$H6_{ax}$	28.05	C6	C6a, C7
1.95	CH_3, $C1_{acetate}$	22.51	CH_3, $C1_{acetate}$	C1, $C1_{acetate}$ (169.57)
1.20	CH_{3ax}	22.43	CH_{3ax}	CH_{3eq}, C2, C3, C4
1.15	CH_{3eq}	27.71	CH_{3eq}	CH_{3ax}, C1, C2, C3, C4, C4a
0.71	$H4_{eq}$	41.44	C4	CH_{3ax}, C2, C3, C4a, C5, C12b

Table 16. Summary of ^{13}C n.m.r. data for *bis*-epoxide **(158).**

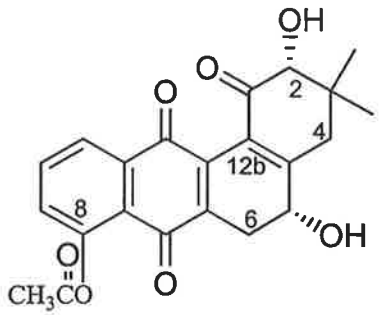

(159)

^1H ppm	Assignment	Area	Multiplicity Coupling Constants	COSY	ROESY
7.93	H11	1	dd, 7.8, 1.2 Hz	H10, H9	-
7.77	H10	1	t, 7.8 Hz	H9, H11	-
7.37	H9	1	dd, 7.8, 1.2 Hz	H10, H11	-
5.58	C5-OH	1	d, 6.0 Hz	$H5_{ax}$	$H4_{eq}$, $H6_{eq}$, $H6_{ax}$
4.44	$H5_{ax}$	1	ddd, 15.6, 6.6, 6.0 Hz	$H6_{ax}$, $H6_{eq}$ C5-OH	$H4_{ax}$
4.30	$H2_{ax}$	1	d, 4.2 Hz	C2-OH	CH_{3eq}, $H4_{ax}$
4.15	C2-OH	1	bd, 4.2 Hz	$H2_{ax}$	CH_{3ax}, $H4_{eq}$
3.22	$H6_{eq}$	1	dd, 16.8, 6.6 Hz	$H5_{ax}$, $H6_{ax}$	C5-OH
3.07	$H4_{eq}$	1	d, 20.0 Hz	$H4_{ax}$	CH_{3ax}, CH_{3eq}, C5-OH, C2-OH
2.47	$H4_{ax}$	1	d, 20.0 Hz	$H4_{eq}$	$H2_{ax}$, $H5_{ax}$
2.43	$CH_{3\ acet.}$	3	s	-	-
2.34	$H6_{ax}$	1	dd, 16.8, 15.6 Hz	$H6_{eq}$, $H5_{ax}$	CH_{3ax}, C5-OH
1.26	CH_{3eq}	3	s	-	CH_{3ax}, $H2_{ax}$, $H4_{eq}$, $H4_{ax}$
0.84	CH_{3ax}	3	s	-	CH_{3eq}, C2-OH, $H4_{eq}$, $H6_{ax}$

Table 17. Summary of ^1H n.m.r. data for diol **(159)**.

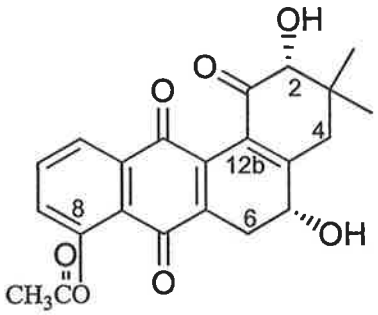

(159)

^{1}H ppm	Assignment	HSQC ^{13}C ppm	Assignment	HMBC ^{13}C
7.93	H11	123.74	C11	C7a, C9, C12,
7.77	H10	133.76	C10	C8, C11a
7.37	H9	128.24	C9	C7a, C8, C11,
5.58	C5-OH	-	C5-OH	C5, C5a, C6
4.44	$H5_{ax}$	66.62	C5	C2, C4a, C6, C6a, C12b
4.30	$H2_{ax}$	78.91	C2	CH_{3ax}, CH_{3eq}, C1, C3
4.15	C2-OH	-	C2-OH	C1, C2, C3
3.22	$H6_{eq}$	27.76	C6	C5, C5a, C6a, C7, C12a
3.07	$H4_{eq}$	37.85	C4	CH_{3ax}, C2, C3, C4a, C5, C12b
2.47	$H4_{ax}$	37.85	C4	CH_{3ax}, CH_{3eq}, C3, C4a, C12b
2.43	CH_3, $C8_{acetate}$	20.15	CH_3, $C8_{acetate}$	$C8_{acetate}$ (168.21)
2.34	$H6_{ax}$	27.76	C6	C4a, C5, C6a, C12a, C12b
1.26	CH_{3eq}	26.85	CH_{3eq}	CH_{3ax}, C2, C3, C4, C4a
0.84	CH_{3ax}	18.24	CH_{3ax}	CH_{3eq}, C2, C3, C4

Table 18. Summary of ^{13}C n.m.r. data for diol **(159).**

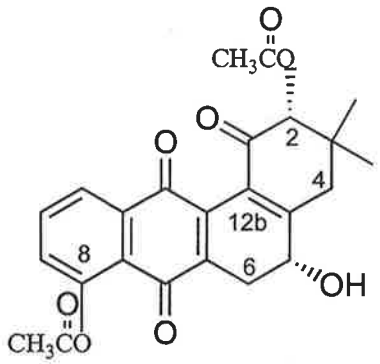

(160)

^{1}H ppm	Assignment	Area	Multiplicity Coupling Constants	COSY	ROESY
7.91	H11	1	dd, 7.8, 1.2 Hz	H10, H9	-
7.65	H10	1	t, 7.8 Hz	H9, H11	-
7.27	H9	1	dd, 7.8, 1.2 Hz	H10, H11	-
5.42	$H2_{ax}$	1	s	-	CH_{3eq}, $H4_{ax}$
4.59	$H5_{ax}$	1	ddd, 11.4, 7.0, 5.4, Hz	$H6_{ax}$, $H6_{eq}$, C5-OH	$H4_{ax}$
3.23	$H6_{eq}$	1	d, 16.8, 7.0 Hz	$H5_{ax}$, $H6_{ax}$	-
3.07	$H4_{eq}$	1	d, 20.2 Hz	$H4_{ax}$	CH_{3ax}, CH_{3eq}, C5-OH
2.81	C5-OH	1	d, 5.4 Hz	$H5_{ax}$	$H4_{eq}$, $H6_{ax}$
2.58	$H4_{ax}$	1	bd, 20.2 Hz	$H4_{eq}$, CH_{3ax}	CH_{3eq}, $H2_{ax}$, $H5_{ax}$
2.43	$C8_{acetate}$	3	s	-	-
2.40	$H6_{ax}$	1	dd, 16.8, 11.4 Hz	$H6_{eq}$, $H5_{ax}$	C5-OH, CH_{3ax}
2.24	$C2_{acetate}$	3	s	-	CH_{3ax}, CH_{3eq}
1.21	CH_{3eq}	3	s	-	CH_{3ax}, $C1_{acetate}$, $H2_{ax}$, $H4_{ax}$, $H4_{eq}$
1.01	CH_{3ax}	3	bs	$H4_{ax}$	CH_{3eq}, $C1_{acetate}$, $H4_{eq}$

Table 19. Summary of ^{1}H n.m.r. data for bis-epoxide **(160).**

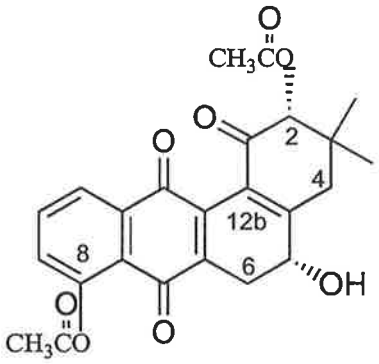

(160)

^{1}H ppm	Assignment	HSQC ^{13}C ppm	Assignment	HMBC ^{13}C
7.91	H11	125.28	C11	C7, C7a, C8, C9, C11a, C12,
7.65	H10	134.80	C10	C7a, C8, C9, C10, C11
7.27	H9	129.02	C9	C7, C7a, C8, C11,
5.42	$H2_{ax}$	80.96	C2	CH_{3eq}, C1, $C2_{acetate}$, $C2_{acetate}$ (170.52), C3, C4, C12b
4.59	$H5_{ax}$	68.17	C5	C4a, C6, C6a, C12b
3.23	$H6_{eq}$	28.76	C6	C4a, C5, C6a, C7, C12b
3.07	$H4_{eq}$	39.42	C4	CH_{3ax}, C1, C2, C3, C4a, C5, C12b
2.81	C5-OH	-	C5-OH	C4a, C5, C6
2.58	$H4_{ax}$	39.42	C4	CH_{3eq}, $CH3_{ax}$, C1, C3, C4a, C5, C12b
2.43	CH_3, $C8_{acetate}$	21.09	CH_3, $C8_{acetate}$	$C8_{acetate}$ (169.54)
2.40	$H6_{ax}$	28.76	H6ax	C4a, C5, C6a, C7, C12, C12a, C12b
2.24	CH_3, $C2_{acetate}$	20.74	CH_3, $C2_{acetate}$	$C2_{acetate}$ (170.52)
1.21	CH_{3eq}	27.48	CH_{3eq}	CH_{3ax}, C1, C2, C3, C4, C5
1.01	CH_{3ax}	20.70	CH_{3ax}	CH_{3eq}, C2, $C2_{acetate}$, C3

Table 20. Summary of ^{13}C n.m.r. data for bis-epoxide **(160).**

Crystallographic data for (114)

Formula	$C_{22}H_{22}O_5$	D_c (g cm^{-3})	1.305
M	366.4	F (000)	776
Crystal system	orthorhombic	μ_{max} (cm^{-1})	0.86
Space group	P 212121	unique reflns measured	2475
a (Å)	14.498(8)	θ_{max} (deg)	27.5
b (Å)	17.814(7)	reflections used	788
c (Å)	7.222(5)	R	0.097
V (Å^3)	1865(1)	R_w	0.090
Z	4	ρ_{max} (e Å-3)	0.35

Fractional atomic coordinates for (114)

Atom	x	y	z
O(1)	0.0527(6)	-0.1923(5)	0.208(1)
O(1a)	0.0905(7)	-0.2146(6)	0.509(2)
O(7)	0.3531(8)	0.0126(6)	-0.048(2)
O(11)	-0.0566(7)	0.0247(6)	-0.091(2)
O(12)	0.0168(6)	-0.1064(6)	-0.106(1)
C(1)	0.133(1)	-0.2340(8)	0.143(2)
C(1a)	0.043(1)	-0.1858(9)	0.395(2)
C(1b)	-0.030(1)	-0.1325(8)	0.436(2)
C(2)	0.108(1)	-0.3198(8)	0.170(2)
C(3)	0.195(1)	-0.367(1)	0.081(3)
C(3a)	0.158(1)	-0.448(1)	0.053(3)
C(3b)	0.262(1)	-0.369(1)	0.231(3)
C(4)	0.230(1)	-0.339(1)	-0.104(3)
C(4a)	0.247(1)	-0.2552(8)	-0.090(2)
C(5)	0.328(1)	-0.2232(8)	-0.088(2)
C(6a)	0.262(1)	-0.0935(8)	-0.052(2)
C(6)	0.347(1)	-0.1418(9)	-0.054(3)
C(7)	0.274(1)	-0.0127(9)	-0.051(2)
C(7a)	0.196(1)	0.0366(9)	-0.054(2)
C(8)	0.205(1)	0.115(1)	-0.043(3)
C(9)	0.125(1)	0.157(1)	-0.051(3)
C(10)	0.040(1)	0.129(1)	-0.068(3)
C(11)	0.026(1)	0.0522(9)	-0.074(3)
C(11a)	0.105(1)	0.0048(8)	-0.068(2)
C(12)	0.093(1)	-0.0774(9)	-0.078(2)
C(12a)	0.178(1)	-0.1251(8)	-0.055(2)
C(12b)	0.1616(1)	-0.2093(8)	-0.050(2)

Crystallographic data for (122)

Formula	$C_{21}H_{24}O_5$	F (000)	760
M	356.4	μ (cm^{-1})	0.90
Crystal system	orthorhombic	Crystal size (mm)	0.08 x 0.16 x 0.65
Space group	P 212121	unique reflns measured	1878
a (Å)	11.798(4)	θ_{max} (deg)	25
b (Å)	14.115(4)	Criterion of obs.	$I \geq 2.0\sigma(I)$
c (Å)	11.108(7)	reflections used	840
V (Å^3)	1849(1)	R	0.058
Z	4	Rw	0.045
D_c (g cm^{-3})	1.280	ρ_{max} (e Å-3)	0.21

Fractional atomic coordinates for (122)

Atom	x	y	z
O(1)	0.5395(5)	-0.1398(5)	0.2142(6)
O(6)	0.1902(4)	0.0723(4)	0.0821(6)
O(7)	0.0473(4)	0.0302(4)	0.3540(5)
O(8)	-0.0970(5)	-0.1019(5)	0.3144(6)
O(12)	0.3336(4)	-0.1198(4)	0.0319(5)
C(1)	0.5409(8)	-0.0564(7)	0.1887(8)
C(2)	0.6474(7)	-0.0069(7)	0.1416(9)
C(3)	0.6580(7)	0.0964(7)	0.1820(10)
C(3a)	0.7608(7)	0.0408(7)	0.120(1)
C(3b)	0.6726(8)	0.1005(8)	0.318(1)
C(4)	0.5497(8)	0.1471(6)	0.1446(8)
C(4a)	0.4410(7)	0.0949(7)	0.1753(8)
C(5)	0.3377(8)	0.1584(6)	0.184(1)
C(6)	0.2268(7)	0.1042(7)	0.1979(10)
C(6a)	0.2423(7)	0.0206(6)	0.2824(8)
C(6b)	0.0793(8)	0.0982(8)	0.0483(9)
C(7)	0.1346(6)	-0.0337(6)	0.3199(8)
C(7a)	0.0915(6)	-0.0994(6)	0.2247(8)
C(8)	-0.0253(7)	-0.1312(7)	0.2295(8)
C(9)	-0.0620(7)	-0.1911(7)	0.1391(9)
C(10)	0.0066(8)	-0.2237(7)	0.0519(9)
C(11)	0.1188(7)	-0.1960(6)	0.0458(9)
C(11a)	0.1588(6)	-0.1333(6)	0.1337(7)
C(12)	0.2785(7)	-0.1025(6)	0.1215(8)
C(12a)	0.3291(6)	-0.0474(6)	0.2261(7)
C(12b)	0.4365(6)	0.0021(6)	0.1941(7)

Crystallographic data for (153)

Formula	$C_{24}H_{23}BrO_6$	F (000)	1000
M	487.35	μ (cm^{-1})	19.52
Crystal system	orthorhombic	Crystal size (mm)	0.3 x 0.25 x 0.2
Space group	P_{z1}/c	θ_{max} (deg)	74.4
a (Å)	8.8741(4)	Criterion of obs.	$I \geq 2.0\ \sigma(I)$
b (Å)	20.104(1)	reflections used	8192
c (Å)	12.2989(6)	$T_{min, max}$	0.71, 0.80
V (Å^3)	2149(3)	R	0.058
Z	4	Rw	0.045

Fractional atomic coordinates for (153)

Atom	x	y	z
O(1)	0.1772(1)	0.90493(6)	0.13924(7)
O(1a)	0.0263(1)	0.92220(5)	-0.02944(8)
O(7)	0.3612(1)	0.63350()	0.13715(8)
O(8)	0.6019(1)	0.59310(4)	0.29498(7)
O(8a)	0.72223(1)	0.63791(5)	0.16780(8)
O(12)	0.3220(1)	0.85978(5)	0.35955(8)
C(1)	0.0743(1)	0.90493(6)	0.1917(1)
C(1a)	0.1424(1)	0.94445(6)	0.0266(1)
C(1b)	0.2670(2)	0.97986(9)	-0.0157(1)
C(2)	-0.0060(2)	0.93956(7)	0.3184(1)
C(3)	-0.1135(2)	0.90874(7)	0.3184(1)
C(3a)	-0.02811(2)	0.89794(9)	0.4389(1)
C(3b)	-0.2533(2)	0.95342(9)	0.3176(2)
C(4)	-0.1674(2)	0.84209(7)	0.2631(1)
C(4a)	-0.0355(1)	0.799909(6)	0.2459(1)
C(5)	-0.0155(2)	0.73813(7)	0.2876(1)
C(6)	0.1087(2)	0.69142(7)	0.2720(1)
C(6a)	0.1985(1)	0.71757(6)	0.1861(1)
C(7)	0.3480(1)	0.67919(6)	0.1989(1)
C(7a)	0.4702(1)	0.69850(6)	0.2964(1)
C(8)	0.5917(1)	0.65594(6)	0.3412(1)
C(8a)	0.6597(1)	0.59114(7)	0.1989(1)
C(8b)	0.6312(2)	0.52510(8)	0.1439(1)
C(9)	0.6984(1)	0.67253(7)	0.4360(1)
C(10)	0.6867(1)	0.73342(7)	0.4877(1)
C(11)	0.5787(1)	0.77689(6)	0.4447(1)
C(11a)	0.4607(1)	0.75995(6)	0.3504(1)
C(12)	0.3347(1)	0.80900(6)	0.30929(9)
C(12a)	0.2257(1)	0.79259(6)	0.19983(9)
C(12b)	0.0707(1)	0.83006(6)	0.1764(1)
Br	0.35473(2)	0.815313(7)	0.08918(1)

The standard angucyclinone numbering scheme employed is shown in Figure 2, page 37.

X-Ray crystallographic data for **(150)** is available from Professor A.H. White.

X-ray structures of **(150)** and **(153)** were by Professor A.H. White, Department of Chemistry, University of Western Australia.

X-ray structures of **(114)** and **(122)** were by Doctor E.R.T. Tiekink, Department of Chemistry, University of Adelaide.

Chapter 6. Amphibian Peptides

6.1. Introduction

The word amphibian is derived from the Greek words *'amphi'* meaning double, and *'bios'* meaning life, describing animals that generally live on land but breed in water. The young amphibians metamorphosise (change) into adult form from an early fish-like (tadpole) stage. There are three orders of amphibia[98]: (i) Anura (frogs and toads); (ii) Urodela (salamanders and newts); (iii) Apoda (worm-like burrowers). The anura order is the target of this research.

6.2. Human Interest in Anurans

The amphibians evolved from fresh water fish to inhabit the land 350 million years ago in Devonian times. This change of environment required physical and behavioural adaptations for anurans. The major development was the formation of an epidermal layer, containing multi-cellular exocrine glands, capable of secreting toxic chemicals onto the skin to protect themselves from predators including microbial pathogens, therefore increasing their chances of survival in the wild. The anuran skin is like a chemical warehouse, an extraordinary source of biologically active compounds. The contents of the anuran skin secretions have been exploited by mankind for more than 2000 years and are associated with traditional medicine.[99] The earliest recorded use is by ancient Chinese to regulate internal bodily functions and fertility.[99] More recently in some parts of South America an anuran is simply strapped onto an injury to treat bacterial infections.[100] Another example ofa well known use of the chemical activity of an anuran is the poison dart frog.[101] The native Indians from Central and South America poison the tips of their darts with the secretion of the poison dart frog by hanging the frogs by their legs over a fire inducing the secretion ofa poison over its back. The Indians then use these darts to kill animals. The poison contains toxins that dull the nerves and cause heart and respiratory failure. Toxins from the poison dart frogs are currently finding their way into medicine, where they are utilised as muscle relaxants, heart stimulants and anaesthetics.[102]

6.3. Distribution of Granular Glands

Anurans live and breed in environments where there are numerous microbial pathogens and other microscopic predators, and it is therefore not surprising that their dermal secretions contain a wide variety of host defence compounds. Some of the natural defence compounds produced by anurans include amines, steroid derivatives, peptides and toxic alkaloids.[103]

There are primarily two types of glands within the skin of most anurans; the granular and the mucosal glands.[104] Active components are liberated from the granular glands, located on the dorsal surface and legs. The glands are dispersed throughout the dermal regions of the anuran. In some species the glands are localised and enlarged in strategically placed areas that are most exposed to predatory attack. A particular example are the parotoidan and rostral glands (on the head, at the rear and front of the eye respectively) of *Litoria splendida*, shown in Figure 6.1. There are ten different glands occurring in anuran species,[105] these are classified according to their anatomical position, and are listed in Table 6.1.

Figure 6.1. The parotoidan and rostral glands of *Litoria splendida.*

Name of Gland	Anatomical Position
Rostral	Dorsal surface of the head
Supralabial	Upper lip region extending beyond the jaw
Parotoid	Shoulder region
Submandibular	Region adjacent to lower jaw
Coccygeal	Flanks each of side of the coccyx
Inguinal	Each side of the groin region
Femoral	Postural surface of each femour
Tibial	Dorsal surface of each calf
Dorsal	Distributed through the surface of the back
Submental	Underneath the chin

Table 6.1. Classification of the various glands present in anurans.

The glands are operated under the control of the central nervous system, with the release of secretion occurring in response to a variety of stimuli including stress.[106] Many of the secreted chemicals from the skin function as antibacterial agents. These agents have been shown to be bioactive peptides, killing many strains of bacteria, protozoans, and even cancer cells.[107] The extraordinary freedom from infection experienced by anurans is as a direct result of these peptides.

6.4. Production of Peptides

Active peptides are stored as inactive, processed peptides within the granular glands of the skin and are a direct product of the genetic code.[108] The granular gland (Figure 6.2) is a syncytial gland[#] and is located directly below the epidermis. The gland consists of a myoepithelial cell envelope (the outer wall), with the nuclei, endoplasmic reticulum[*] and Golgi complexes[**] located inside the cell. The lumen of the gland contains the secretory granules where the peptides are stored.[109]

[#] The syncytial gland is composed of numerous types of cells fused together, producing a giant multinucleated cell or gland.
[*] The endoplasmic reticulum is composed of a sheet of membranes, extending from the outer layer of the nuclear envelope into the cytoplasm. It is involved in the biosynthesis of lipids, proteins and carbohydrates, and is involved in sorting proteins for transportation through the cell.
[**] Golgi complexes are individual stacks of membranes near the endoplasmic reticulum. They are involved in both the modifications of peptides, and in effecting their transport to different cellular locations.

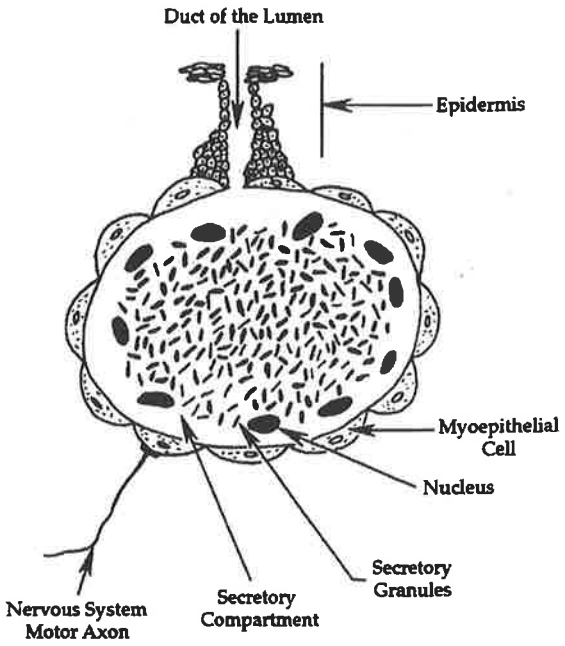

Figure 6.2.. A schematic representation of a granular gland found in anuran skin.

The production of the mature peptides occur by the same fundamental process. Transcription from DNA to mRNA transpires within the nucleus. This is followed by translation of the mRNA to produce the pre-pro-peptide. The signal peptide (pre-segment) facilitates transportation within the cell and is subsequently cleaved.[102] The storage of the mature peptide is assisted by the spacer peptide (pro-segment). The spacer peptide counteracts the activity of the mature peptide by often equalising the positive charge and assisting with the folding of the peptide to inhibit any enzymatic degradation.[110, 111] The mature peptide is dormant in the pro-peptide form. On stimulation of the granular gland by the nervous system, the pro-peptide is subject to enzyme cleavage, which ultimately produces the active mature peptide.[112] In many cases the skin peptides are post-translationally modified in order for them to be active:[113] this includes specific endoproteolytic cleavage, carboxy-terminal alpha–amidation, tyrosine sulfation and amino acid isomerisation.[114] The peptide is then released from the granule by a process known as the holocrine mechanism[#] and secreted onto the exterior surface of the skin.[115]

[#] Holocrine mechanism is a process that involves the disintegration of a cell, resulting in the release of the cellular content.

6.5. Antibacterial Action Mechanism

Mucosal areas such as the reproductive and respiratory tracts of anurans are constantly in contact with infectious microorganisms, yet the incidence of infection from these organisms is low. The mucosal surface has developed certain agents, including antibiotic peptides to combat these threats. One specific example of antibiotic peptides responsible for generating significant interest into examining the properties of antibacterial peptides are the magainins.[116] Magainin 1 was isolated from the skins of *Xenopus laevis*: demonstrating activity against bacteria, fungi and protozoa at concentrations comparable to those used for commercial antibacterial agents.[117]

Magainin 1 Gly Ile Gly Lys Phe Leu His Ser Ala Gly Lys Phe Gly Lys Ala Phe Val Gly Glu Ile Met Lys Ser (OH)

The primary structures (sequences) of antibacterial peptides together with their secondary structures are crucial for their activity.[118] Normally, most antibacterial peptides have features in common. They usually have an overall positive charge due to the presence of basic residues (for example Arg and Lys) and possess the ability to form amphiphilic#α-helices.[119] The interaction of the peptide and the cell membrane is not normally dependant upon chiral interactions, for example D- and L- magainins have all shown identical antibacterial activity.[120] The antibacterial peptides specifically target bacterial membranes due to the differences between eukaryote and prokaryote cell membranes. The bacterial (prokaryote) membrane contains: (i) greater proportion of anionic phospholipids, thereby enhancing the affinity of the anionic bacterial membrane for the basic antibacterial peptides[121] and (ii) lacks cholesterol, a steroid that has the ability to decrease the affinity of most amphiphilic antibacterial peptides for the phospholipid bilayer.[122] Some anuran peptides exhibit anticancer activity.[123] A possible mechanism for this activity may be explained by the over expression of the anionic phospholipids on the membrane surface of a cancerous cell. The basic peptides will then favour binding and lysing the overall negatively charged cancerous cell.

Amphiphilic molecules are molecules that contain both hydrophilic and hydrophobic regions.

The exact mechanism of antibacterial action by antibacterial peptides is uncertain, but is believed to involve the modification of the bacterial membrane by one of two ways. The 'Barrel-Stave' mechanism requires the peptides to be of sufficient length to form membrane channels or pores, ~~where~~ thus by disrupting the normal function of the membrane (such as the osmotic regulation and ion transport functions), which ultimately leads to lysis and destruction of the cell.[124] The "carpet-like" model of antibacterial action[125] is a "non-channel" forming mechanism not constricted by the length of the peptide and functions by disrupting the integrity of the bacterial cell membrane.

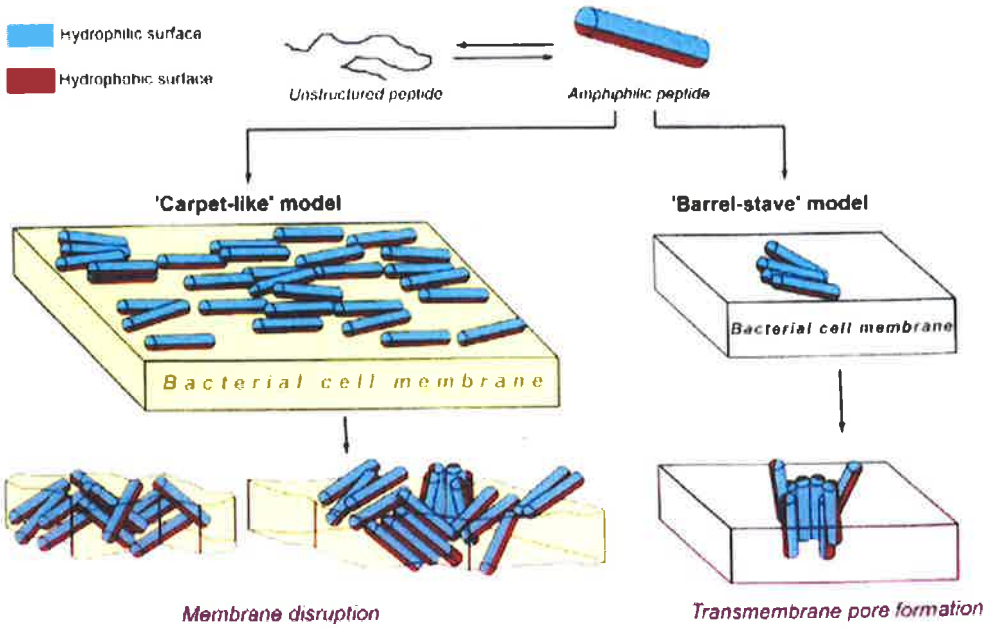

Figure 6.3.. Illustration of the 'carpet-like' model, in comparison with the 'barrel-stave'model.

The 'Barrel-Stave' mechanism

The exact mechanism for peptide antibacterial activity is not fully understood but an accepted model involves the Barrel-Stave mechanism (Figure 6.3).[126, 127] The peptides are initially unstructured in solution. The positive charge distribution causes them to be attracted to the polar head groups of the phospholipids in the bacterial cell membrane. The peptide adopts an amphiphilic α-helical structure on interaction with the membrane surface. The helical amphiphilic 'stave-like' peptides then aggregate, insert into the membrane, forming ion-sized.

pores. The pores increase in diameter by following incorporation of additional peptides. A transmembrane pore is formed when the peptides arrange themselves laterally such that the hydrophobic face of the peptide is exposed to the membrane lipid region, and the hydrophilic face lines the pore. The pore allows for the movement of ions and small solutes across the bilayer, causing a disruption of the osmotic gradient, leading to cell lysis. This mechanism requires the peptide to be of adequate length (a minimum of 20 amino acid residues) in order to span the entire bilayer. An example of an antibacterial peptide supported by this mechanism is maculatin 1.1, isolated from the skin secretions of the Australian tree frog *Litoria geminaculata*.[128] The three dimensional structure[129] of maculatin 1.1 is shown in Figure 6.4. Antibacterial peptides smaller than 20 residues cannot operate by this mechanism.

The 'Carpet-Like' mechanism

This mechanism is initially analogous to the "barrel-stave' mechanism, in that the peptides aggregate and bind in a parallel conformation to the negatively charged phospholipids of the bacterial cell membrane (Figure 6.3). The amphipathic α-helical peptides then align themselves in such a manner that the positive charges of the basic amino acids interact with the negatively charged phospholipid head groups. The peptides partially insert into the membrane by reorientating themselves so that their hydrophobic residues interact with the hydrophobic core of the membrane, while the hydrophilic residues interact with both the polar head groups of the lipid molecules and the aqueous extra cellular fluid. The lipid bi-layer expands and weakens in order to accommodate the incoming bound peptides until a threshold concentration is reached where upon the membrane is disrupted sufficiently to allow membrane penetration and ultimately cell death.[130] Short antibacterial peptides, consisting of 12-16 amino acids in length, support this non-channel forming mechanism. An example of an antibacterial peptide operating by this mechanism is citropin 1.1, isolated from the skin secretions of the Australian tree frog *Litoria citropa*.[131] The three dimensional structure[132] of citropin 1.1 is shown in Figure 6.5.

A prerequisite for both modes of action is the amphiphilic nature of the peptide with well-defined hydrophilic and hydrophobic zones. Edmunson helical wheel projections are used to predict the likelihood that a peptide may adopt an amphipathic α-helix conformation.[133] The Edmunson helical wheel projection is a two-dimensional representation of the three-dimensional structure of an α-helix where the backbone of the polypeptide chain is represented by the perimeter of the wheel. The amino acid residues are projected onto a plane perpendicular to the axis of the helix. One turn of an α-helix is 3.6 residues long, therefore each adjacent residue can be spaced 100° apart around the circumference of the circle (refer to Ch7, page 176, Figure 7.1.2. for the Edmundson helical wheel projection of the amphiphilic peptide aurein 1.2.). This corresponds to 18 residues per entire revolution of helix. The residues are numbered from the N-terminus.

Nuclear magnetic resonance (NMR) experiments are used to generate a three-dimensional structure of antibacterial peptides under study, confirming the amphipathic α-helical structure of peptides. The NMR experiments have shown the solution structures of maculatin 1.1[129] and citropin 1.1[131] to be those shown in Figures 6.4 and 6.5 respectively.

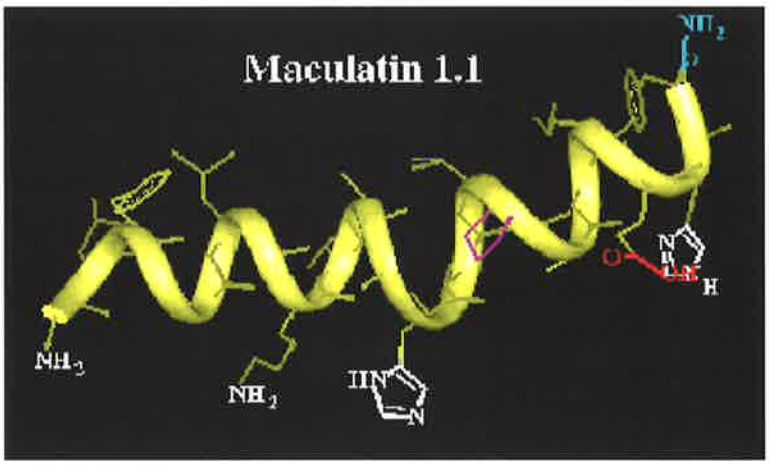

Figure 6.4. The three-dimensional structure of maculatin 1.1.
The amino acid sequence of maculatin 1.1 is: GLFGVLAKVAAHVVPAIAEHF (NH_2)

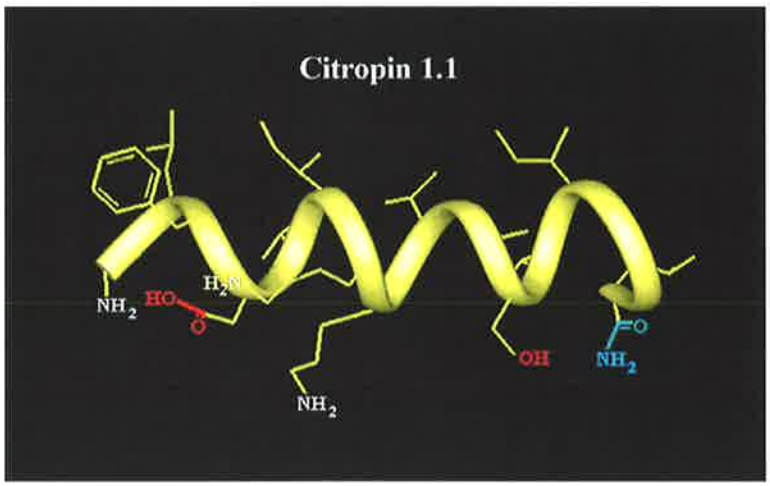

Figure 6.5. Three-dimensional structure of citropin 1.1.
The amino acid sequence of citropin 1.1 is: GLFDVIKKVASVIGGL (NH_2)

Maculatin 1.1 (Figure 6.4) is an amphiphilic, distorted α-helix with well-defined hydrophilic and hydrophobic faces. The Pro^{15} residue distorts the helix, providing flexibility in the centre of the structure the structure. This residue is essential for antibacterial activity: activity is dimished upon replacement of Pro^{15} with Ala^{15} (this synthetic modification achieves a pure α-helical structure). Citropin 1.1 (Figure 6.5) is a sixteen residue pure α-helix with well-defined hydrophilic and hydrophobic faces, thus conforming to the amphiphilic prerequisite for antibacterial activity.

6.6. Methodology

Surface Electrical Stimulation and Analysis by HPLC

Anuran researchers of the past often killed large numbers of specimens. The extraction procedures involved soaking the dried skins in aqueous methanol followed by chromatography to purify the peptides. The number of skins needed to obtain workable quantities of peptides were often in the thousands.[134] The need for a non-harmful collection was required since many anuran species are currently risking extinction. Tyler and colleagues developed a benign technique involving the use of surface electrical stimulation (SES) to induce discharge of peptide material.[135] The anuran is held by the back legs while its skin is moistened with distilled water. A platinum electrode which is attached to an electrical stimulator is massaged over the glandular region. The mild electrical stimulation induces the release of the skin secretions. The stimulus strength varies in relation to the size of the frog, and the thickness and the conductivity of the skin. The entire milking procedure is simple, quick (completed in about 30 seconds), harmless and repeatable. After stimulation the secretion is rinsed off the skin with distilled water and immediately worked up as most anurans also release a degradation enzyme. This deactivation process is believed to be a safety mechanism in order to prevent any toxic peptides from affecting the host. The content of the glands is usually replenished within several days, so successive secretions can be obtained from the same anuran.

Peptides in the crude secretion are separated and purified by reverse phase HPLC. The hydrophobic reverse phase column absorbs the hydrophobic face# of the peptide onto its surface and binds the material until a sufficient concentration of organic solvent displaces the peptide material. The ability to separate peptides by this technique is dependant on the subtle differences in the hydrophobic character of the peptide resulting from differences in the amino acid sequences. The organic component of the solvent used in this research is acetonitrile; chosen because of its high ultraviolet transparency at low wavelengths, low viscosity, and high volatility. The aqueous solvent contains an ionic modifier (trifluoroacetic acid) to adjust the pH and solubilise the peptide. The wavelength used throughout the HPLC experiments to detect the peptide bonds was 214 nm.

The amphiphilic nature of a peptide in solution ensures that one face of the peptide is hydrophobic and will interact only with the hydrophobic surface of the column while the remainder of the peptide is in contact with the mobile phase.

Mass Spectrometry (Finnigan LCQ Electrospray Mass Spectrometer)

Sequencing of peptides and proteins by mass spectrometry was a difficult undertaking prior to 1970. The development FAB (fast atom bombardment) mass spectrometry in the 1980's allowed for effective and efficient analysis of large molecular weight compounds. Further developments in mass spectrometry with electrospray and matrix assisted laser desorption ionisation have made analysis of biologically important samples more effective and available.

Mass spectrometry is a technique that allows measurement of the molecular weight of a molecule with accuracy better than 1 Da. The mass spectrometer performs three basic functions: (i) Produces ions from vaporised compounds (ionisation). (ii) Separates these ions according to their mass to charge (*m/z*) ratio (analysis). (iii) Distinguishes and records the separated ions (detection).

The structural determination of all peptides isolated in this research was by mass spectrometry experiments utilising the Finnigan LCQ electrospray mass spectrometer. This mass spectrometer is an octapole ion trap machine equipped with a liquid chromatography system. The internal schematic arrangement of the Finnigan LCQ electrospray mass spectrometer is represented in Figure 6.6.

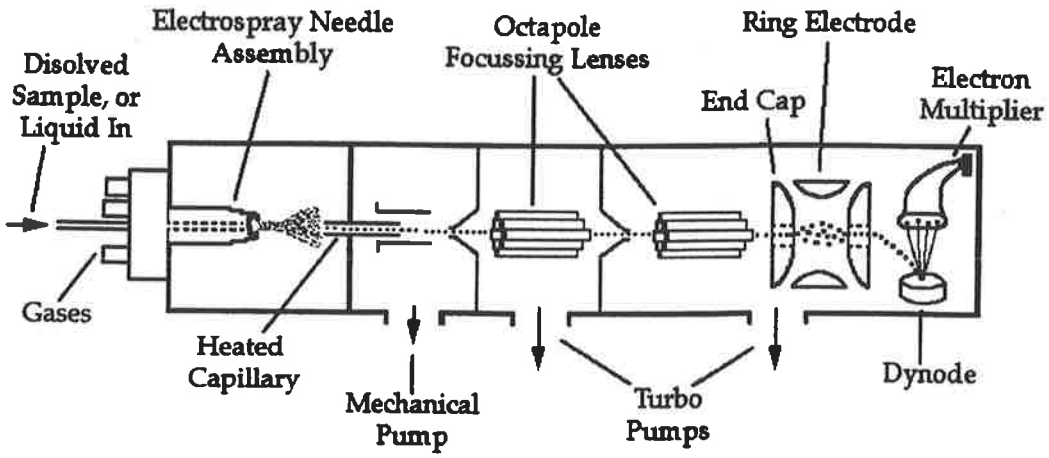

Figure 6.6. Schematic arrangement of the LCQ.

The mass range for analysis is 50-4000 Da with mass accuracy of about 0.01% and low-picomole range sensitivity. The capability of analysing large molecules is due to the fact that the elecrospary technique can impart multiply charged states. Zoom scanning, on-line liquid chromatography options and MS^n function are other capabilities of the LCQ making it the ideal tool for the analysis of large biological molecules at minimal quantities.

The soft electrospray (ES) ionisation process produces intact ions, with multiple charges, from remarkably large, complex and fragile parent species.[136] This technique involves the application of a high voltage electric field to a flow of sample liquid within the capillary (held at 4000 V), resulting in a spray of charged droplets. As the droplets evaporate, their surface density increases until the forces due to electrostatic repulsion approach equality with those due to surface tension. Extreme instability results in 'Coulomb explosion', which produces an array of daughter droplets that also evaporate until they too explode. This process continues until free ions are produced (Figure 6.7): these are passed through the octapole region (a series of lenses) of the mass spectrometer into the ion trap.

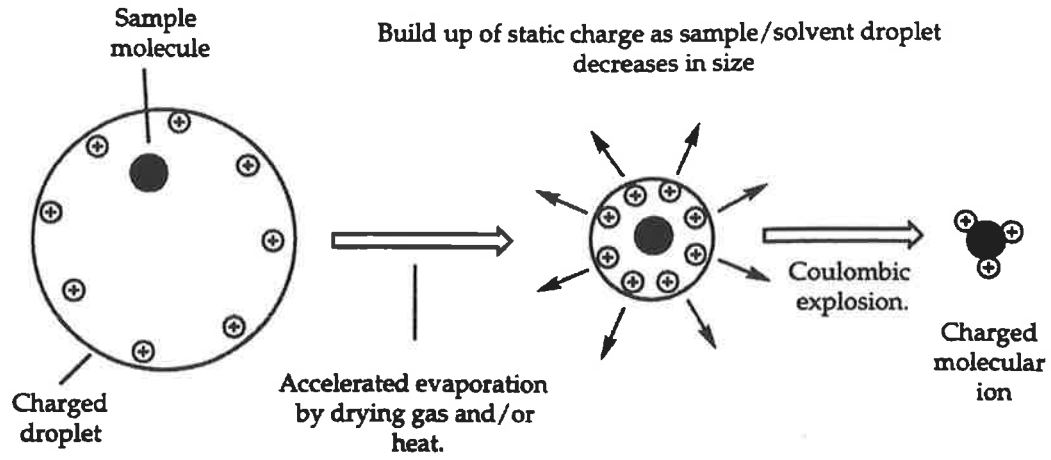

Figure 6.7. Schematic representation of the electrospray ionisation mechanism.[136]

Resolution of multiply charged ions, that often result from Electrospray ionisation of peptides, is through a process known as a ZoomScan. The ZoomScan is a high resolution scan over a narrow mass window (10 amu). For every multiple charge there exists a cluster of peaks that are produced by isotopes. The molecular difference between the isotope peaks is inversely proportional to the charge state of that particular envelope. For example, if the difference between the isotope peaks were 0.5 Da, the charge state of the cluster would be +2. For a difference of 0.25 Da the charge state would be +4.

The ion trap is the mass analyser of the LCQ, consisting of three electrodes and a central ring electrode each resembling a hyperbolic cross section, forming a chamber capable of confining the ions.[137] Application of a radio frequency (rf) voltage allows ions of appropriate *m/z* to having stable trajectories (be trapped) within the device. Increasing the amplitude of the rf voltage causes ions of increasing *m/z* to become unstable and be ejected in mass sequence from the trap into the detector to be recorded as a mass spectrum.

Fragmentation of the ion of interest is carried out by collisional activated dissociation (CAD).[138] The ion of interest is firstly isolated within the ion trap, the internal energy is increased such that it undergoes a series of rapid collisions with helium gas that is also present inside the ion trap. A succession of fragmentations result.[139] To provide the MS^2 spectra, the daughter ions produced are sequentially ejected from the ion trap and detected. MS^n experiments involve repeating the same process. This process can in principle, continue until there are no more ions to collisionally activate.

Peptide Sequencing

The sequence determination of all peptides isolated in this research was effected by analysing their characteristic mass spectral fragmentations in the positive mode. There are basically six types of peptide fragmentations, however for sequencing purposes only the most abundant fragmentations, the simple B and Y+2 cleavages are used.[140] B Cleavage ions give sequence information from the C-terminal end of the peptide, while Y+2 cleavage ions (which are formed following proton transfer) give sequence information from the N-terminal end (Figure 6.8). The masses of all the peptides and their corresponding fragments are recorded as nominal masses.[#] This sequencing technique cannot distinguish certain isomeric and isobaric amino acid residues. These residues include the isomers Ile (113 Da) and Leu (113 Da), and the isobaric residues Lys (128 Da) and Gln (128 Da). Automated Edman sequencing is used to distinguish the Ile and Leu isomers, while Lys and Gln are distinguished by Lys-C enzyme digestion experiments and/or automated Edman sequencing.

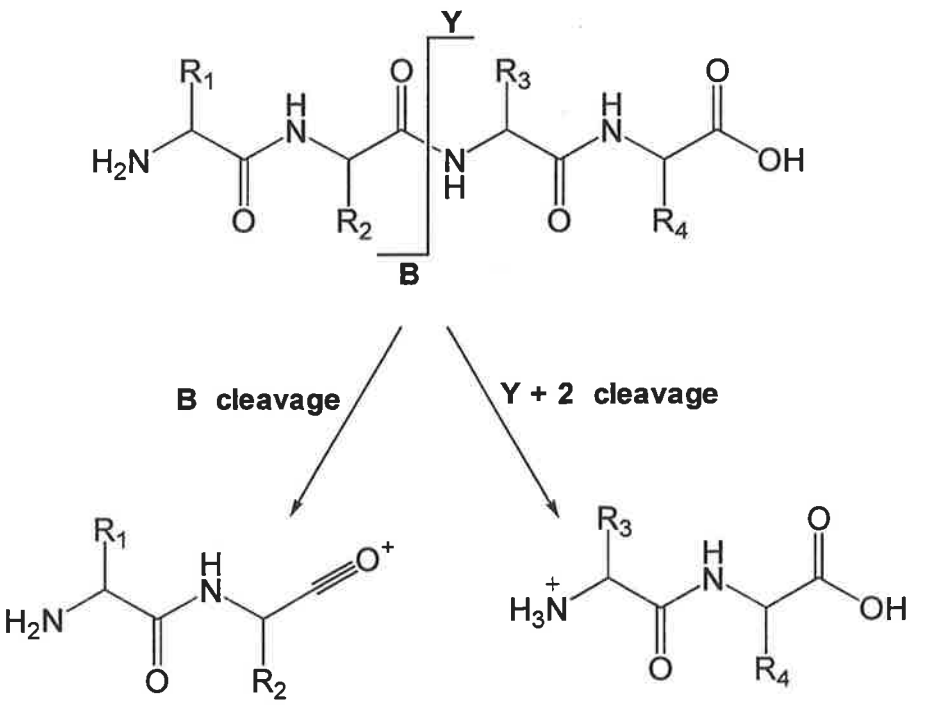

Figure 6.8. Characteristic peptide fragmentations.

[#] The nominal mass of a peptide is equal to the sum of the integral masses of the amino acid residues.

Automated Edman Sequencing

All automated Edman sequencing was performed by a standard procedure using an applied Biosystem 470A sequencer equipped with a 900A data analysis module.[141] Peptides with blocked N-terminal ends (pyroglutamate) as the first residue cannot be sequenced in this manner since the blocked group prevents coupling to the solid immobilon disk. Modified amino acids cannot be detected by the automated Edman sequencer.

Enzyme Digestion

Enzyme digestion experiments coupled with mass spectrometry are used to obtain sequence information for large peptides. Enzyme digestion of the peptides results in smaller fragments that are then sequenced by mass spectrometry. Endoprotease Lys-C is the primary digest used since the majority of the large peptides studied generally contain at least one Lys residue. Cleavage occurs at the carboxyl side of the lysine residue.

C-terminal End Group Determination

Esterification of the C-terminal end group into a methyl ester followed by analysis by mass spectrometry was used to elucidate its identity. The mass of the parent ion of the methyl ester minus that of the mass of the original peptide allows the determination of the number of CO_2H and $CONH_2$ groups in the peptide. For example (Figure 6.9), an amide group will show an increase of 15 Da on methylation, while the carboxylic acid will show an increase of 14 Da.

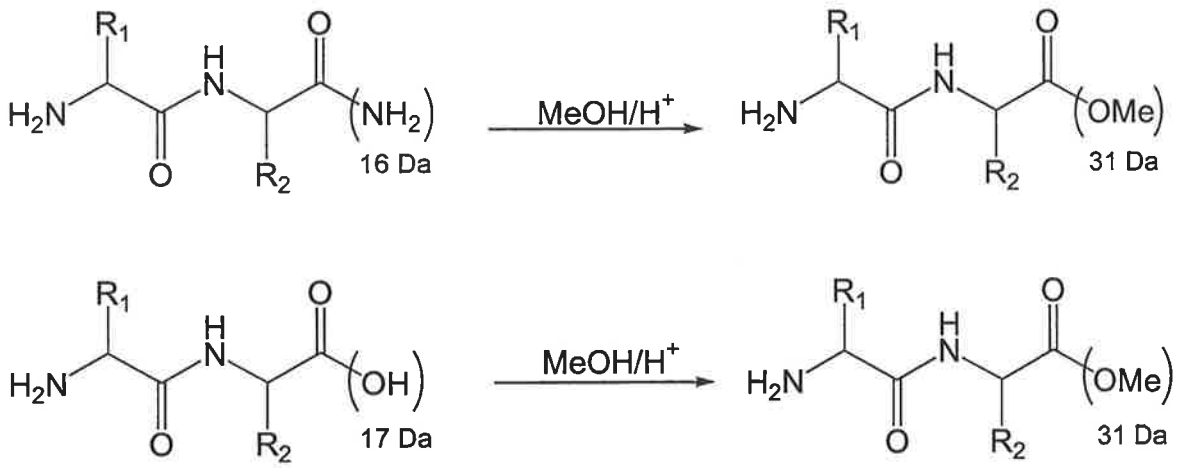

Figure 6.9. Determination of the C-terminal end groups through methylation.

Preparation of Synthetic Peptides

Peptide syntheses were carried out (commercially) by Mimotopes (Clayton, Victoria) using the standard N-α-Fmoc procedure with L-amino acids.[142] The peptides were synthesised in order that sufficient material was available for biological testing. Each synthetic peptide was checked for identity with the natural peptide by HPLC analysis and mass spectrometry.

Antibacterial Testing

Antibacterial testing was performed using the minimum inhibitory (MIC) test by the Microbiology Department of the Institute for Medical and Veterinary Science (Adelaide).[143] This assay involves measurement of inhibition of the applied test substance (peptide) against a range of microorganisms. The activities are then recorded as MIC values, which represent the minimum concentration of the test substance required to totally inhibit the growth of the particular microorganism. The lower the MIC value the more potent the antibacterial activity.

Anticancer Testing

Anticancer testing was carried out by the National Cancer Institute (Washington, DC, USA) using *in vitro* screening panel testing of the chemosensitivity of 60 human tumour cell lines towards the synthetic aurein peptides.[144]

The *Litoria* Genus

The anuran order within Australia can be divided into five families, viz. Hylidae, Myobatrachidae, Microhylidae, Ranidea, Bufonidae, which together compromise twenty nine genera. The family Hylidae contains three genera, *Litoria*, *Nyctimystes* and *Cyclorana*. The genus *Litoria* contains sixty one species which cover the majority of the Australian continent making it one of the most diverse genus of anurans.[105] Arboreal anurans (tree frogs) are characterised by their flattened disc shaped fingers and toes which secrete a sticky substance that aids climbing. Tree frogs spend the majority of their time in the high canopy trees, coming down to an aquatic environment only to breed. The Erspramer group initiated the isolation and characterisation of peptides from Australian tree frogs, with the isolation of caerulein from the tree frog *Litoria caerulea*.[145] The Adelaide group began their studies of bioactive peptides from Australian frogs in the mid 1980's. Since that time more than 25 species of Australian anurans of the genera *Litoria*, *Limnodynastes* and *Uperolia* have been studied.[146, 147] The two closely related tree frogs *Litoria aurea* and *Litoria raniformis* are the primary subjects of the research presented in this thesis.

Chapter 7. Aurein peptides

7.1. Inroduction

The two closely related species, the Green and Golden Bell Frog *Litoria aurea*, and the Southern Bell frog *Litoria raniformis* were chosen as a continuation of studies into the host defense peptides of Australian anurans of the genera *Litoria*, *Limnodynastes* and *Uperoleia*.[146, 147] The aims of the study presented in this chapter are: (i) to isolate and determine the structure of the peptides secreted from both frogs, (ii) to determine the antibacterial and anticancer activity of any new peptides discovered, and compare this spectrum of activity with those of the antibacterial peptides isolated from the previously studied tree frogs of the genus *Litoria*.

Litoria aurea occurs in coastal regions of New South Wales (Figure 7.1), with the normal habitat being large ponds containing abundant bulrushes near the bank. The dorsum of this frog is smooth, with a striking combination of green and gold colouring. The groin is a distinctive turquoise blue. The adult ranges from 57 to 108 mm in length.[148, 149] The habitat of the Southern Bell Frog *Litoria raniformis* is large pools in southern New South Wales, throughout Victoria, northern Tasmania and the south-eastern area of South Australia. It has a more warty dorsum than *L. aurea*, and it can be distinguished from that species by the presence of a pale green mid-dorsal stripe. The groin is again turquoise, and the adult is 55 to 104 mm in length.[149, 150] The two animals are shown for comparison in Figure 7.2.

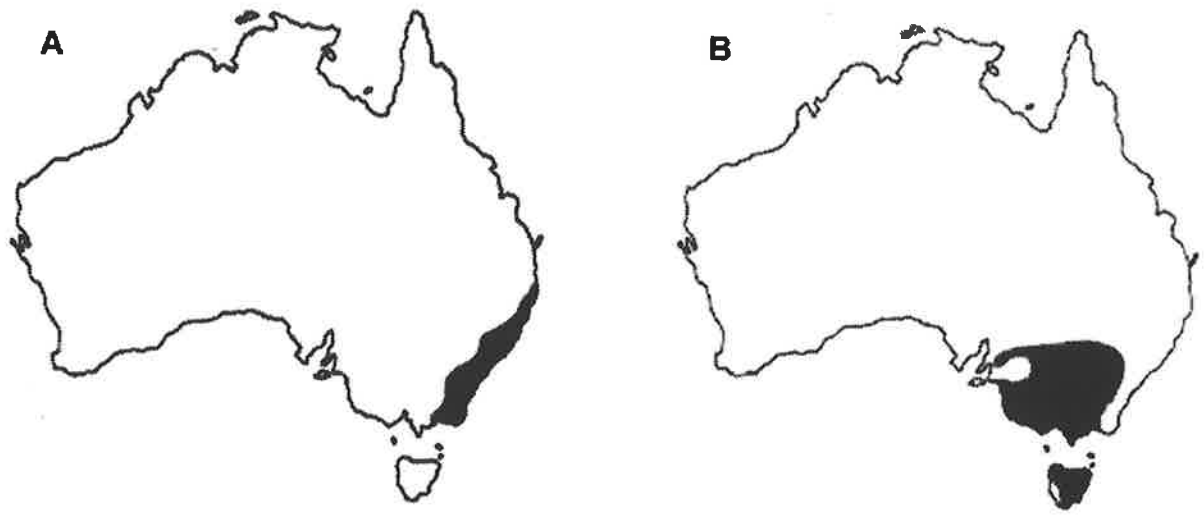

Figure 7.1. The distribution of *Litoria aurea* is indicated by the black region in map **A**, while the black region in map **B** indicates the distribution of *Litoria raniformis*.

Figure 7.2. (Top) *Litoria aurea*, **(Bottom)** *Litoria raniformis.*

7.2. Results and Discussion

General

The electrical stimulation procedure[135] was used to obtain the glandular secretions from a single specimen of *Litoria aurea* and four specimens of *Litoria raniformis* in 1998. On average, about 3 mg of solid peptide material was acquired from the single specimen of *Litoria aurea* and 10 mg from the four specimens of *Litoria raniformis* after work up. Separation of peptides was carried out using high performance liquid chromatography (HPLC). The close relations[98] between both species is evident in the HPLC chromatograms (Figures 7.3 and 7.4): a number of peptides were found to be common to both frogs.

In all, over thirty peptides were isolated following HPLC separation. Discussion on peptides falling into the neuropeptide category, having retention times lower than 17 minutes, is not included in this thesis. Twenty three peptides, which are isolated in HPLC regions 17-27 min, are discussed in this chapter. These peptides have been called aureins. There are five groups of aurein peptides isolated and characterised from *Litoria aurea* and *L. raniformis*. These are categorised as aureins 1, 2, 3, 4 and 5 and their amino acid sequences are listed in Table 7.1.

All of the aureins 1-3, together with aureins 4.2 and 5.2 have been synthesised, principally to provide sufficient material to enable biological testing of these peptides. Each pair of natural and synthetic peptides was shown to be identical using HPLC and mass spectrometry. One peptide from each group of aurein peptides will now be described including the MS structure determination of that peptide in detail. Automated Edman amino acid sequencing confirms the sequences of all the aurein peptides. The structure determinations for all of the other aurein peptides are summarised in Tables 7.2, 7.3, 7.4 and 7.5.

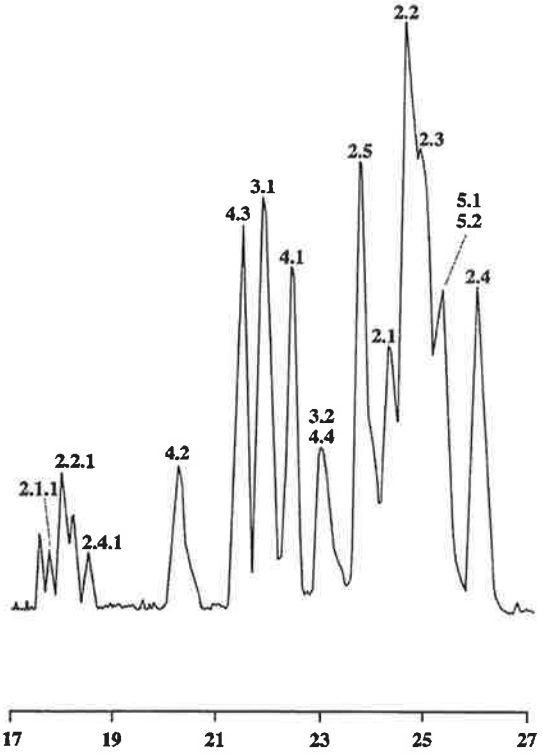

Figure 7.3. Partial region of the HPLC separation of crude skin secretions taken from the glands of *Litoria aurea*. Numbers on each peak refer to aurein numbers listed in Table 7.1.

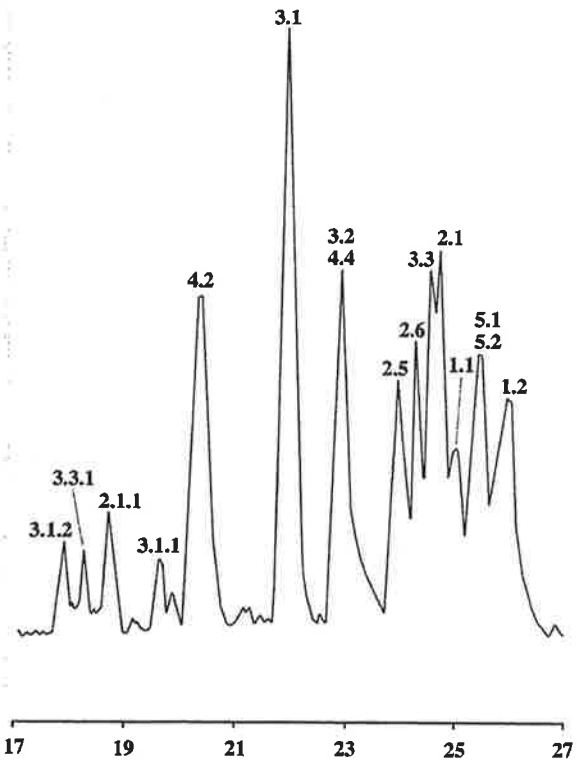

Figure 7.4. Partial region of the HPLC separation of crude skin secretions taken from the glands of *Litoria raniformis*. Numbers on each peak refer to aurein numbers listed in Table 7.1.

Aurein	Sequence	MW	L.a.	L.r.
1.1	GLFDIIKKIAESI (NH_2)	1444		*
1.2	GLFDIIKKIAESF (NH_2)	1478		*
2.1	GLLDIVKKVVGAFGSL (NH_2)	1613	*	*
2.1.1	LDIVKKVVGAFGSL (NH_2)	1443	*	*
2.2	GLFDIVKKVVGALGSL (NH_2)	1613	*	
2.3	GLFDIVKKVVGAIGSL (NH_2)	1613	*	
2.4	GLFDIVKKVVGTIAGL (NH_2)	1627	*	
2.4.1	FDIVKKVVGTIAGL (NH_2)	1457	*	
2.5	GLFDIVKKVVGAFGSL (NH_2)	1647	*	*
2.6	GLFDIAKKVIGVIGSL (NH_2)	1627		*
3.1	GLFDIVKKIAGHIAGSI (NH_2)	1736	*	*
3.1.1	GLFDIVKKIAGHIA (OH)	1480	*	*
3.1.2	FDIVKKIAGHIAGSI (NH_2)	1566		*
3.2	GLFDIVKKIAGHIASSI (NH_2)	1766	*	*
3.3	GLFDIVKKIAGHIVSSI (NH_2)	1794		*
3.3.1	FDIVKKIAGHIVSSI (NH_2)	1624		*
4.1	GLIQTIKEKLKELAGGLVTGIQS (OH)	2394	*	
4.2	GLLQTIKEKLKEFAGGVVTGVQS (OH)	2400	*	*
4.3	GLLQTIKEKLKEFAGGLVTGVQS (OH)	2414	*	
4.4	GLLQTIKEKLKELATGLVIGVQS (OH)	2424	*	*
5.1	GLLDIVTGLLGNLIVDVLKPKTPAS (OH)	2544	*	*
5.2	GLMSSIGKALGGLIVDVLKPKTPAS (OH)	2450	*	*

Table 7.1. Aurein peptides isolated from skin secretions from dorsal glands of *Litoria aurea* and *L. raniformis*. L.a. indicates peptides isolated from *Litoria aurea*. L.r. indicates peptides isolated from *Litoria raniformis*. MW refers to the nominal mass of the peptide.

Aurein 1.1

All skin peptides derived from the dorsal glands of the Australian Bell Frogs *Litoria aurea* and *Litoria raniformis* were analysed using the electrospray and MS^2 capabilities of a Finnigan LCQ ion-trap mass spectrometer. The amount of material available for the analysis of major components was of the order of 100 μg, whereas for minor components less than 10 μg of pure material was normally available. The MS techniques that were used do not allow differentiation of isomeric Leu and Ile, or of isobaric Gln and Lys. Where applicable, automated Edman sequencing was used to differentiate between Leu and Ile, and Lys-C digest / MS to distinguish Lys from Gln. The correct residue is always shown in the text. Methylation experiments together with ESMS identified all C-terminal end groups, and also indicated the number of the CO_2H and $CONH_2$ groups within the peptides.

Aurein 1.1 is one of those peptides only present in the secretion of *Litoria raniformis*. Analysis of aurein 1.1 by ESMS shows a pronounced MH^+ peak at *m/z* 1445. Methylation of aurein 1.1 yields a methyl ester, MH^+ = 1488. The difference in mass between aurein 1.1 and the methyl ester is 43 Da: this difference identifies the presence of two CO_2H groups and one $CONH_2$ group. The collision induced mass spectrum (MS/MS) of the MH^+ parent ion of aurein 1.1 is shown in Fig. 7.5.

The amino acid sequence from the C-terminal end of the peptide is given by the B cleavage ions, while that from the N-terminal end is given by the Y+2 ions.[151] The data in Figure 7.5 gives the sequence of ten of the thirteen amino acid residues, viz Asp Ile Ile Lys Lys Ile Ala Glu Ser Ile (NH_2): still to be identified are the first three residues of aurein 1.1.

Enzyme digestion using the Lys-C/ESMS procedure was used to identify the unknown first three residues of this sequence. Lys-C digestion of aurein 1.1 gives four small peptides, MH^+ at *m/z* 531, 659, 805 and 933 repectively, all formed by hydrolysis at the C-terminal end of a lysine residue. These data confirm the presence of Lys residues at positions 7 and 8. MS/MS data for one of these peptides, *m/z* 805, are shown in Figure 7.6. : this information provides the sequence of the first five residues of aurein 1.1, i.e. Gly Phe Asp Ile Ile Lys.

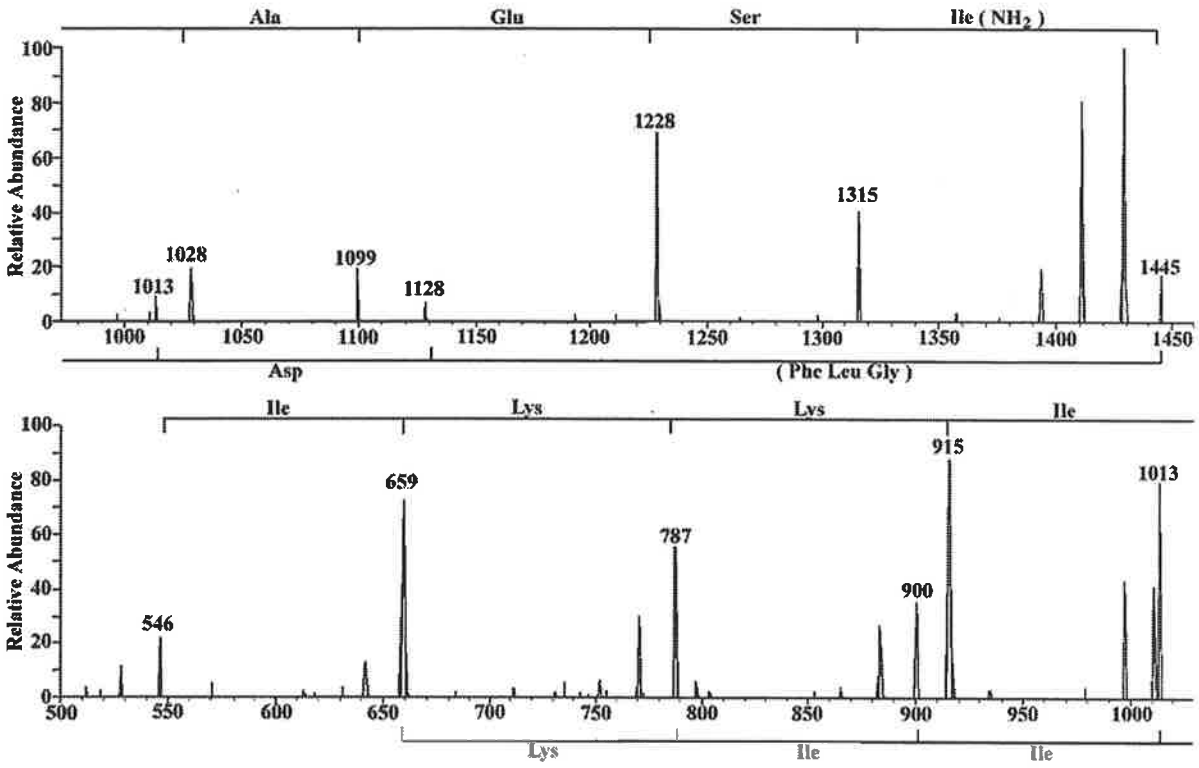

Figure 7.5. CA MS/MS of the MH^+ ion of aurein 1.1 (*m/z* 1445). The sequence derived from B cleavages is shown above the spectrum, while that from the Y+2 cleavages is indicated beneath the spectrum. (See Experimental section for full details).

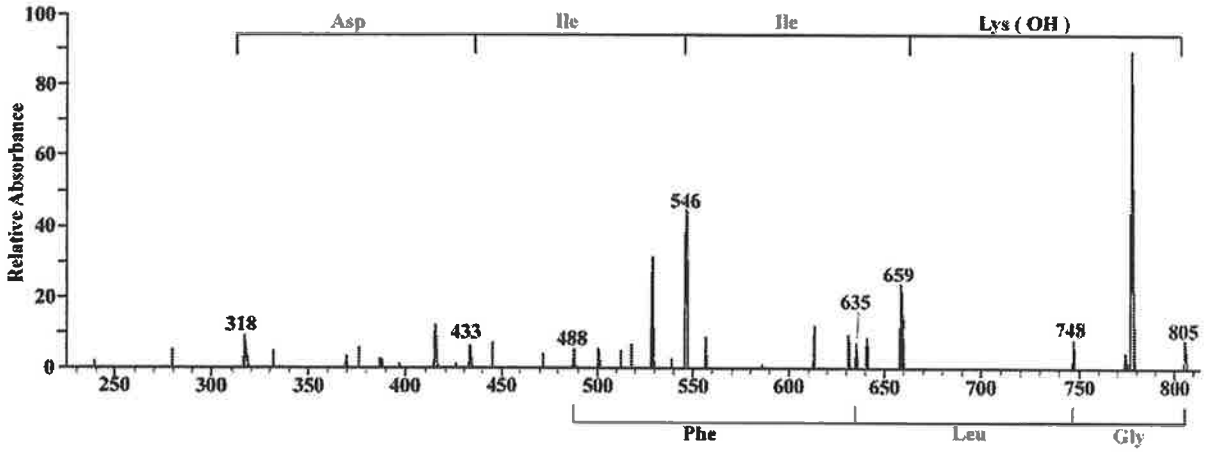

Figure 7.6. CA MS/MS of the Lys-C digest fragment ion of aurein 1.1 (*m/z* 805). (See Experimental section for full details).

Combination of the above data, together with complementary Edman sequencing gives the sequence Gly Phe Asp Ile Ile Lys Lys Ile Ala Glu Ser Ile (NH_2) for aurein 1.1. The structure determination of the related aurein 1.2 is given in Table 7.2 (see also the 3D structure of aurein 1.2 shown in Figure 7.14.).

Aurein 1.1 [MH^+ = 1445]		
Methylation gives a methyl ester, MH^+ 1488 (two CO_2H and one $CONH_2$ groups)		
MH^+ 1445	B ions	*m/z* 1428, 1315, 1228, 1099, 1028, 915, 787, 659, 546 [Ile Lys Lys Ile Ala Glu Ser Ile (NH_2)]
	Y+2 ions	*m/z* 1128, 1013, 900, 787, 659 821, 693 [(317) Asp Ile Ile Lys]
Lys-C digest		MH^+ at *m/z* 531, 659, 805, 933
MH^+ 805	B ions	*m/z* 787, 659, 546, 433,318 [Asp Ile Ile Lys (OH)]
	Y +2 ions	*m/z* 748, 635, 488 [Gly Leu Phe]
	sequence	Gly Leu Phe Asp Ile Ile Lys
Aurein 1.1 sequence		Gly Leu Phe Asp Ile Ile Lys Lys Ile Ala Glu Ser Ile (NH_2)
Aurein 1.2 [MH^+ = 1479]		
Methylation gives a methyl ester, MH^+ 1522 (two CO_2H and one $CONH_2$ groups)		
MH^+ 1479	B ions	*m/z* 1462, 1315, 1228, 1099, 1028, 915, 787, 659, 546, 433 [Ile Ile Lys Lys Ile Ala Glu Ser Phe (NH_2)]
	Y+2 ions	*m/z* 1309, 1162, 1047, 934, 821, 693 [(Gly Leu) Phe Asp Ile Ile Lys]
Aurein 1.2 sequence		(Gly Leu) Phe Asp Ile Ile Lys Lys Ile Ala Glu Ser Phe (NH_2)

Table 7.2. MS data for aurein 1 peptides isolated from *Litoria aurea* and *L. raniformis*.

Aurein 2.3

Aurein 2.3 is only produced by *Litoria aurea*. Analysis of aurein 2.3 by ESMS shows a pronounced MH^+ peak at 1614 Da. Methylation of aurein 2.3 yields a species, MH^+ = 1643, indicating that aurein 2.3 contains one CO_2H group and one $CONH_2$ group. The collision induced mass spectral (MS/MS) data for the MH^+ parent ion of aurein 2.3 are shown in Figure 8.6 and provide the partial sequence (317) Asp (222) Lys Lys Val Val Gly Ala Ile Gly Ser Leu (NH_2).

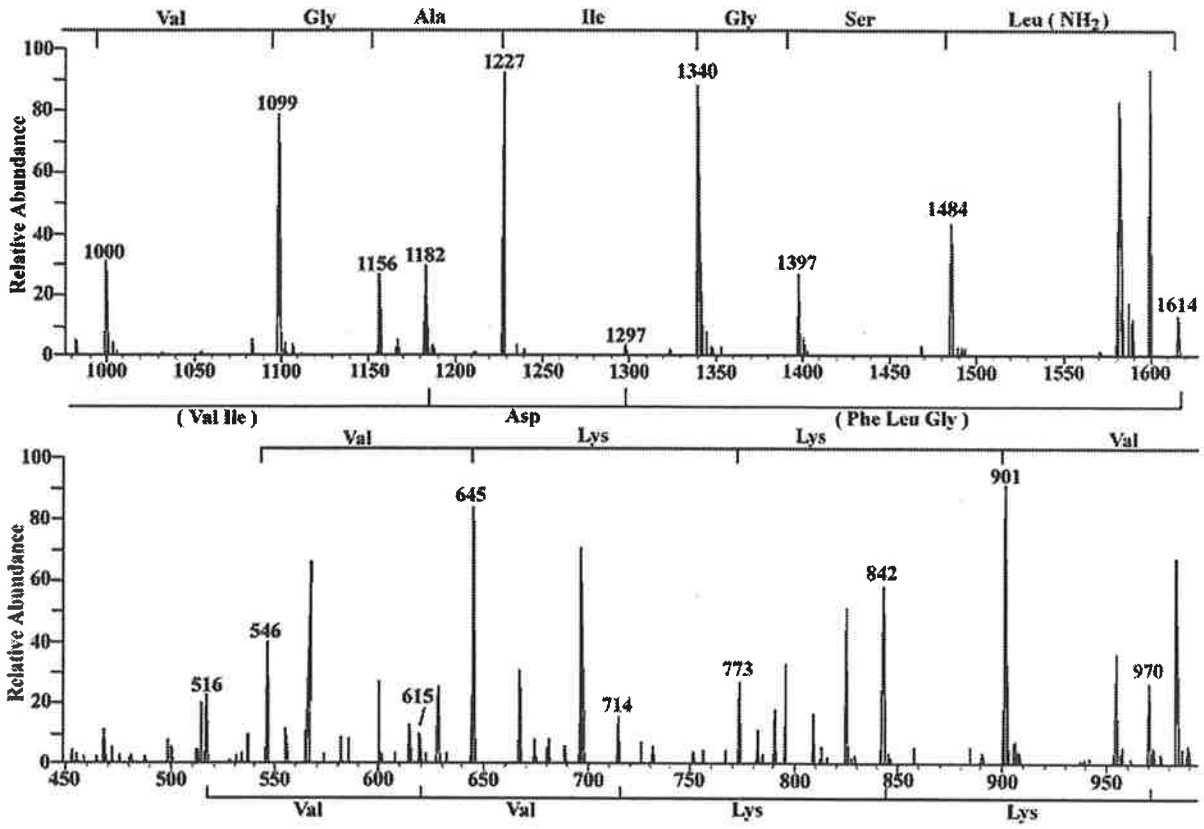

Figure 7.7. CA MS/MS of the MH^+ ion of aurein 2.3 (*m/z* 1614). (See Experimental section for full details).

A number of residues [(317) Asp (222)] at the N-terminal end of aurein 2.3 could not be identified from this spectrum. Enzyme digestion using the Lys-C / ESMS procedure was used to identify the unknown portions of the sequence. Lys-C digestion of aurein 2.3 yields four peptides, MH^+ = 714, 791, 842 and 991, indicating that there are Lys residues at positions 7 and 8. Sequence data was obtained for all four peptides, however the spectrum of *m/z* 791 was all that was required to finalise the sequence of aurein 2.3. The spectrum of *m/z* 791 is shown in Figure 7.7 and the sequence of this peptide is Gly Leu Phe Asp Ile Val Lys.

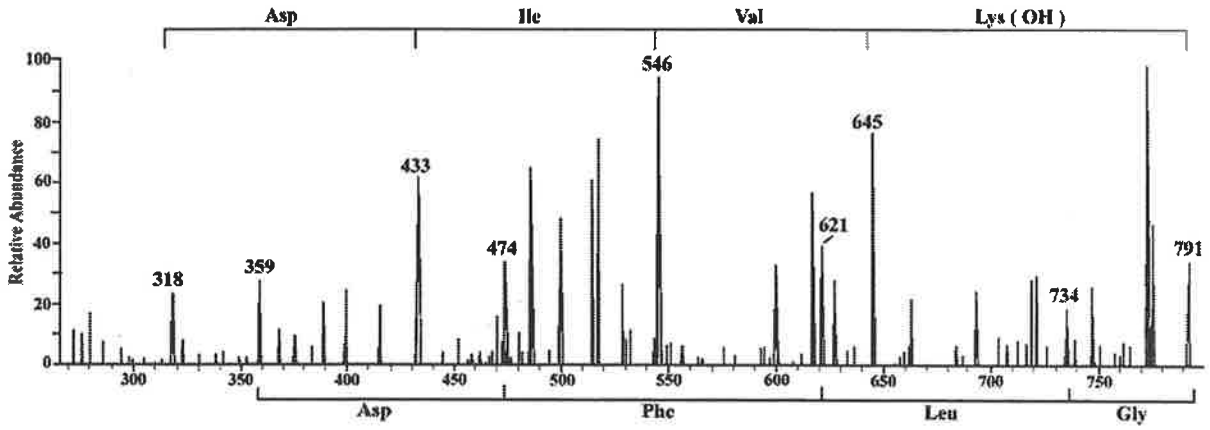

Figure 7.8. CA MS/MS of the Lys-C digest fragment ion of aurein 2.3 (*m/z* 791). (See Experimental section for full details).

Combination of these data, together with complementary Edman sequencing to identify the Leu and Ile residues, gives the primary structure of aurein 2.3 as Gly Leu Phe Asp Ile Val Lys Lys Val Val Gly Ala Ile Gly Ser Leu (NH_2). Details of the structure determination of the other six aurein 2 peptides are summarised in Table 7.3.

Aurein 2.1 [MH^+ = 1614]

Methylation gives a methyl ester, MH^+ 1643 (one CO_2H and one $CONH_2$ group)

MH^+ 1614	B ions	*m/z* 1597, 1484, 1397, 1340, 1193, 1122, 1065, 966, 867, 739, 611, 312 [(Gly Leu) Leu Asp Ile Val Lys Lys Val Val Gly Ala Phe Gly Ser Leu (NH_2)]
	Y+2 ions	*m/z* 1444, 1331, 1216, 1103, 1004, 869, 550, 493 [(Gly Leu) Leu Asp Ile Lys Lys Val Val Gly Ala]
Lys-C digest		MH^+ at *m/z* 748, 757, 876 and 885
Aurein 2.1 sequence		(Gly Leu) Leu Asp Ile Val Lys Lys Val Val Gly Ala Phe Gly Ser Leu (NH_2)

Aurein 2.1.1 [MH^+ = 1444]

Methylation gives a methyl ester MH^+ 1473 (one CO_2H and one $CONH_2$ group)

MH^+ 1444	B ions	*m/z* 1427, 1314, 1227, 1170, 1023, 952, 895, 796, 697, 569 [Lys Val Val Gly Ala Phe Gly Ser Leu (NH_2)]
	Y+2 ions	*m/z* 1216, 1103, 1004, 876, 748, 649, 550 [Ile Val Lys Lys Val Val Gly]
Sequence aurein 2.1.1.		(Leu Asp) Ile Val Lys Lys Val Val Gly Ala Phe Gly Ser Leu (NH_2)

Aurein 2.2 [MH^+ = 1614]

Methylation gives a methyl ester, MH^+ 1643 (one CO_2H and one $CONH_2$ group)

MH^+ 1614	B ions	*m/z* 1597, 1484, 1397, 1340, 1227, 1156, 1099, 1000, 901, 773, 645, 546 [Val Lys Lys Val Val Gly Ala Leu Gly Ser Leu (NH_2)]
	Y+2 ions	*m/z* 1444, 1297, 1182, 970, 842, 714, 615, 516 [(Gly Leu) Phe Asp Ile Val Lys Lys Val Val]
Lys-C digest		MH^+ at *m/z* 714, 791, 842 and 919
Aurein 2.2 sequence		(Gly Leu) Phe Asp Ile Val Lys Lys Val Val Gly Ala Leu Gly Ser Leu (NH_2)

Table 7.3. MS data for aurein 2 peptides isolated from *Litoria aurea* and *L. raniformis*

Aurein 2.3 [MH^+ = 1614]

Methylation gives a methyl ester, MH^+ 1643 (one CO_2H and one CO NH_2 group)

MH^+ 1614	B ions	*m/z* 1597, 1484, 1397, 1340, 1227, 1156, 1099, 1000, 901, 773, 645, 546 [Val Lys Lys Val Val Gly Ala Ile Gly Ser Leu (NH_2)]
	Y+2 ions	*m/z* 1297, 1182, 970, 842, 714, 615, 616 [(317) Asp (222) Lys Lys Val Val]
Lys-C digest		MH^+ at *m/z* 714, 791, 842 and 991.
m/z 791	B ions	*m/z* 773, 645, 546, 433, 318 [Asp Ile val Lys (OH)]
	Y+2 ions	*m/z* 734, 621, 474, 359 [Gly Leu Phe Asp]
	Sequence	Gly Leu Phe Asp Ile Val Lys (OH)

Aurein 2.3 sequence Gly Leu Phe Asp Ile Val Lys Lys Val Val Gly Ala Ile Gly Ser Leu (NH_2)

Aurein 2.4 [MH^+ = 1628]

Methylation gives a methyl ester MH^+ 1657 (one CO_2H and one CO NH_2 group)

MH^+ 1628	B ions	*m/z* 1611, 1498, 1441, 1370, 1257, 1156, 1099, 1000, 901, 773, 645 [Lys Lys Val Val Gly Thr Ile Ala Gly Leu (NH_2)]
	Y+2 ions	*m/z* 1571, 1458, 1311, 1196, 1083, 984, 856, 728, 629, 530 [Gly Leu Phe Asp Ile Val Lys Lys Val Val]
Lys-C digest		MH^+ at *m/z* 728, 791, 856 and 919.

Aurein 2.4 sequence Gly Leu Phe Asp Ile Val Lys Lys Val Val Gly Thr Ile Ala Gly Leu (NH_2)

Aurein 2.5 [MH^+ = 1648]

Methylation gives a methyl ester, MH^+ 1677 (one CO_2H and one CO NH_2 group)

MH^+ 1648	B ions	*m/z* 1631, 1518, 1431, 1374, 1227, 1156, 1099, 1000, 901, 773, 645, 546 [Val Lys Lys Val Val Gly Ala Phe Gly Ser Leu (NH_2)]
	Y+2 ions	*m/z* 1591, 1478, 1331, 1216, 1103, 1004, 876, 550 [Gly Leu Phe Asp Ile Val Lys]
Lys-C digest		MH^+ at *m/z* 748, 791, 876 and 919
Aurein 2.5 sequence		Gly Leu Phe Asp Ile Val Lys Lys Val Val Gly Ala Phe Gly Ser Leu (NH_2)

Table 7.3. MS data for aurein 2 peptides isolated from *Litoria aurea* and *L. raniformis* (continued).

Aurein 2.6 [MH^+ = 1628]

Methylation gives a methyl ester, MH^+ 1657 (one CO_2H and one $CO\ NH_2$ group)

MH^+ 1628	B ions	*m/z* 1611,1498, 1411, 1354, 1241, 1142, 1085, 972, 873, 745, 617, 546. [Ala Lys Lys Val Ile Gly Val Ile Gly Ser Leu (NH_2)
	Y+2 ions	*m/z* 1311, 1196, 1083, 1012, 884, 756, 657, 544. [Asp Ile Ala Lys Lys Val (Ile Gly)]
Lys-C digest		MH^+ at *m/z* 756, 763, 884 and 891.
m/z 762	B ions	*m/z* 617, 546, 433 [Ile Ala Lys]
	Y+2 ions	*m/z* 706, 593, 446, 331 [Gly Leu Phe Asp]
	sequence	Gly Leu Phe Asp Ile Ala Lys

Aurein 2.6 sequence Gly Leu Phe Asp Ile Ala Lys Lys Val Ile Gly Val Ile Gly Ser Leu (NH_2)

Table 7.3. MS data for aurein 2 peptides isolated from *Litoria aurea* and *L. raniformis* (continued).

Aurein 3.3

Aurein 3.3 is only found in the skin secretion of *Litoria raniformis*. Aurein 3.3 on electrospray ionisation gives a spectrum which shows a pronounced MH^+ species at *m/z* 1795. Methylation of aurein 3.3 yields an ester, MH^+ = 1824, indicating the presence of one CO_2H group and one $CONH_2$ in the original peptide. The collision induced spectrum (MS/MS) of the MH^+ ion of aurein 2.3 is shown in Figure 7.9 and identifies the sequence with the exception of the orientation of the first two residues, viz (Gly Leu) Phe Asp Ile Val Lys Lys Ile Ala Gly His Ile Val Ser Ser Ile (NH_2).

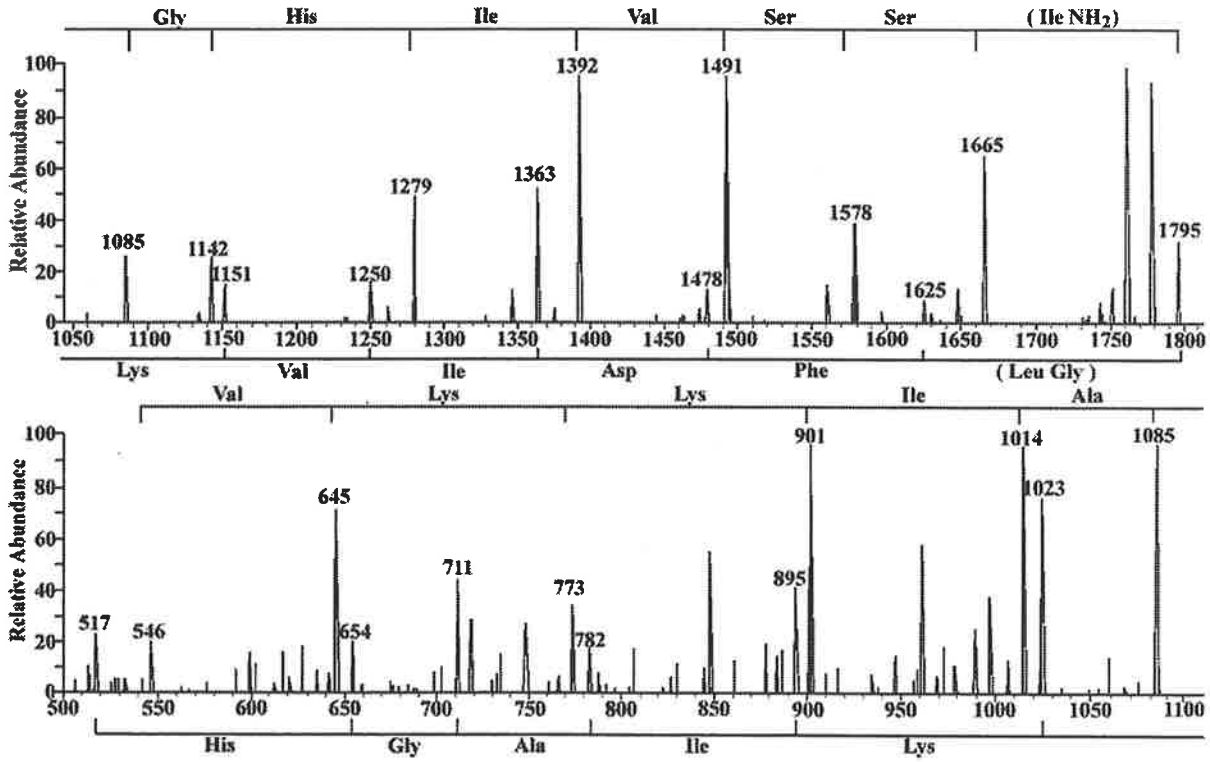

Figure 7.9. CA MS/MS of the MH^+ ion of aurein 3.3 (*m/z* 1794). (See Experimental section for full details).

Digestion of aurein 3.3 with Lys-C gave four peptides, MH^+ = 791, 895, 919, 1023. This confirms the presence of Lys residues at positions 7 and 8. The mass spectrum (Table 7.4) of the fragment *m/z* 919 gives the partial sequence of the first eight amino acids as Gly (Leu Phe) Asp Ile Val Lys Lys. These data, together with complementary Edman sequencing give the primary structure of aurein 3.3 as Gly Leu Phe Asp Ile Val Lys Lys Ile Ala Gly His Ile Val Ser Ser Ile (NH_2). Details of the structures of the other five aureins 3 are given in Table 7.4.

Aurein 3.1 [MH^+ = 1737]

Methylation gives a methyl ester, MH^+ 1766 (one CO_2H and one CO NH_2 group)

MH^+ 1737	B ions	*m/z* 1720, 1607, 1520, 1463, 1392, 1279, 1142, 1085, 1014, 901, 773, 645, 546 [Val Lys Lys Ile Ala Gly His Ile Ala Gly Ser Ile (NH_2)
	Y+2 ions	*m/z* 1680, 1567, 1420, 1305, 1192, 1093, 965, 837, 724, 653, 596 [Gly Leu Phe Asp Ile Val Lys Lys Ile Ala Gly]
Lys-C digest		MH^+ at *m/z* 791, 837, 919, and 965
Aurein 3.1 sequence		Gly Leu Phe Asp Ile Val Lys Lys Ile Ala Gly His Ile Ala Gly Ser Ile (NH_2)

Aurein 3.1.1 [MH^+ = 1481]

Methylation gives a methyl ester, MH^+ 1509 (two CO_2H groups)

MH^+ 1481	B ions	*m/z* 1463, 1392, 1279, 1142, 1085, 1014, 901, 773, 645, 546 [Val Lys Lys Ile Ala Gly His Ile Ala]
	Y+2 ions	*m/z* 1311, 1164, 1049, 936, 837, 709, 581, 468 [(Gly Leu) Phe Asp Ile Val Lys Lys Ile Ala]
Aurein 3.1.1 sequence		(Gly Leu) Phe Asp Ile Val Lys Lys Ile Ala Gly His Ile Ala (OH)

Aurein 3.1.2 [MH^+ = 1567]

Methylation gives a methyl ester, MH^+ 1596 (one CO_2H and one $CONH_2$ group)

MH^+ 1567	B ions	*m/z* 1550, 1439, 1350, 1293, 1222, 1109, 972, 915, 844, 731, 603, 475 [Lys Lys Ile Ala Gly His Ile Ala Gly Ser Ile (NH_2)
	Y+2 ions	*m/z* 1420, 1305, 1192, 1093, 965, 837, 724, 653, 596 [Phe Asp Ile Val Lys Lys Ile Ala Gly]
Aurein 3.1.2 sequence		Phe Asp Ile Val Lys Lys Ile Ala Gly His Ile Ala Gly Ser Ile (NH_2)

Aurein 3.2 [MH^+ = 1767]

Methylation gives a methyl ester MH^+ 1796 (one CO_2H and one $CONH_2$ group)

MH^+ 1767	B ions	*m/z* 1750, 1637, 1550, 1463, 1392, 1279, 1142, 1085, 1014, 901, 773, 645, 546 [Val Lys Lys Ile Ala Gly His Ile Ala Ser Ser Ile (NH_2)]

Table 7.4. MS data for aurein 3 peptides isolated from *Litoria aurea* and *L. raniformis.*

	Y+2 ions	*m/z* 1597, 1450, 1335, 1222, 1123, 995, 867, 754, 683, 626 [(Gly Leu) Phe Asp Ile Val Lys Lys (Ile Ala) Gly]
Lys-C digest		MH^+ at *m/z* 791, 867, 919 and 995.
m/z 791	B ions	*m/z* 773, 645, 546, 433, 318 [Asp Ile Val Lys]
	Y+2 ions	*m/z* 734, 621, 474, 359, 246 [Gly Leu Phe Asp Ile Val]
	sequence	Gly Leu Phe Asp Ile Val Lys
Aurein 3.2 sequence		Gly Leu Phe Asp Ile Val Lys Lys Ile Ala Gly His Ile Ala Ser Ser Ile (NH_2)

Aurein 3.3 [MH^+ = 1795]

Methylation gives a methyl ester, MH^+ 1824 (one CO_2H and one CO NH_2 group)

MH^+ 1795	B ions	*m/z* 1778, 1665, 1578, 1491, 1392, 1279, 1142, 1085, 1014, 901, 773, 645, 546 [Val Lys Lys Ile Ala Gly His Ile Val Ser Ser Ile (NH_2)]
	Y+2 ions	*m/z* 1625, 1478, 1363, 1250, 1151, 1023, 895, 782, 711, 654, 517 [Gly Leu Phe Asp Ile Val]
sequence	(Gly Leu) Phe Asp Ile Val Lys Lys Ile Ala Gly His Ile Val Ser Ser Ile (NH_2)	
Lys-C digest		MH^+ at *m/z* 791, 895, 919, 1023
m/z 919	B ions	*m/z* 901, 773, 645, 546, 433 [Ile Val Lys Lys]
	Y+2 ions	*m/z* 862, 602, 487 [Gly (Leu Phe) Asp Ile]
	sequence	Gly (Leu Phe) Asp Ile Val Lys Lys
Aurein 3.3 sequence		Gly Leu Phe Asp Ile Val Lys Lys Ile Ala Gly His Ile Val Ser Ser Ile (NH_2)

Aurein 3.3.1 [MH^+ = 1625]

Methylation gives a methyl ester, MH^+ 1654 (one CO_2H and one CO NH_2 group)

MH^+ 1625	B ions	*m/z* 1608, 1495, 1408, 1321, 1222, 1109, 972, 915, 844, 731, 603, 475 [Lys Lys Ile Ala Gly His Ile Val Ser Ser Ile (NH_2)]
	Y+2 ions	*m/z* 1478, 1363, 1250, 1151, 1023, 895, 782, 711, 654 [Phe Asp Ile Val Lys Lys Ile Ala Gly]
Aurein 3.3.1 sequence		Phe Asp Ile Val Lys Lys Ile Ala Gly His Ile Val Ser Ser Ile (NH_2)

Table 7.4. MS data for aurein 3 peptides isolated from *Litoria aurea* and *L. raniformis* (continued).

Aurein 4.4

Aurein 4.4 is a minor component of the skin secretions of both *Litoria aurea* and *raniformis*. The structure determination of aurein 4.4 is more complex than those outlined above. This peptide, using electrospray ionisation, yields pronounced peaks corresponding to MH^+ and $(M+2H)^{2+}$ ions at *m/z* 2425 and 1213 respectively. Fully methylated aurein 4.4 exhibits an MH^+ ion at *m/z* 2497, indicating that the original peptide contains three CO_2H and two $CONH_2$ groups. The collision induced spectrum of the $(M+2H)^{2+}$ ion of aurein 4.4 is shown in Figure 7.10 and gives the following partial sequence: (Gly Leu) (342) Ile Lys Glu Lys Leu Lys Glu Leu Ala Thr Gly Leu Val Thr Gly Val (Gln Ser) (NH_2).

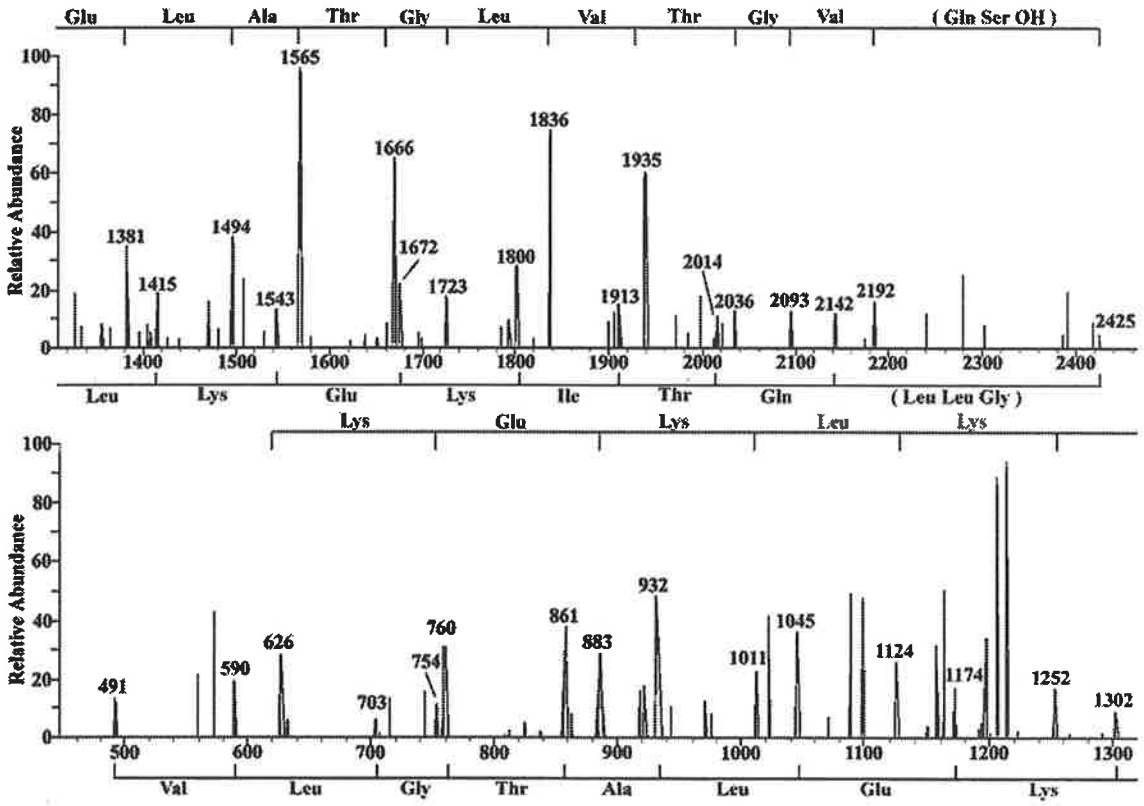

Figure 7.10. CA MS/MS of the $(M+2H)^{2+}$ ion of aurein 4.4 (*m/z* 1213). (See Experimental section for full details).

Digestion of aurein 4.4 with Lys-C gave three peptides; viz MH^+ = 772, 1174 and 1415, confirming Lys residues at positions 7, 9 and 11. The spectra of two of the Lys-C fragments, *m/z* 772 and 1415, are recorded in Table 7.5. The sequences of these two peptides are:- *m/z* 772; Gly Leu Leu Gln Thr Ile Lys, and *m/z* 1415; Leu Lys Glu (Leu Ala) Thr Gly Leu Val Thr Gly Val Gln Ser.

A combination of all these data, together with those derived from the complementary Edman results gives the overall sequence of aurein 4.4 as Gly Leu Leu Gln Thr Ile Lys Glu Lys Leu Lys Glu Leu Ala Thr Gly Leu Val Thr Gly Val Gln Ser (OH). Other aurein 4 data are contained in Table 7.5.

Aurein 4.1 [MH^+ = 2395]		
Methylation gives a methyl ester, MH^+ 2467 (three CO_2H and two $CONH_2$ groups).		
$(M+2H)^{2+}$ 1198	B ions	*m/z* 1891, 1792, 1622 1565, 1494, 1381, 1252 1011, 883, 754 [Glu Lys (Leu Lys) Glu Leu Ala Gly (Gly Leu) Val Thr (403)]
	Y+2 ions	*m/z* 1683, 1770, 1511, 1383, 829, 715 [Ile Lys Glu (611) (Ala Gly) Gly]
Lys-C digest		MH^+ at *m/z* 276, 772, 1144
m/z 772	B ions	*m/z* 754, 626, 513, 412 [Gln Thr Ile Lys]
	Y+2 ions	*m/z* 715, 602, 489, 361 [Gly Leu Ile Gln Thr]
	sequence	Gly Leu Ile Gln Thr Ile Lys
m/z 1144	B ions	*m/z* 1126, 1039, 911, 798, 741, 640, 541 [Val Thr Gly Ile Gln Ser]
	Y+2 ions	*m/z* 1015, 902, 505, 404 [Glu Leu (298) Val Thr]
	sequence	Glu Leu (298) Val Thr Gly Ile Gln Ser
Aurein 4.1 sequence		Gly Leu Ile Gln Thr Ile Lys Glu Lys Leu Lys Glu Leu Ala Gly (Gly Leu) Val Thr Gly Ile Gln Ser (OH)
Aurein 4.2 [MH^+ = 2400]		
Methylation gives a methyl ester, MH^+2472 (three CO_2H and two $CONH_2$ groups).		
$(M+2H)^{2+}$ 1200.5	B ions	*m/z* 2168, 1911, 1812, 1713, 1656, 1599, 1528, 1381, 1251, 1124, 1011, 883, 754, 626, 513 [Ile Lys Glu Lys Leu Lys Glu Phe Ala Gly Gly Val Val (257) (Gln Ser)]
	Y+2 ions	*m/z* 1888, 1775, 1647, 1518, 1390, 1277, 1149, 1020, 802, 688, 587, 490. [(512) Ile Lys Glu Lys Leu Lys Glu Phe Ala Gly Gly Val]
Lys-C digest		MH^+ at *m/z* 517, 772, 1029 and 1150 [also *m/z* 1172, the $(M+Na)^+$ ion corresponding to *m/z* 1150].

Table 7.5. MS data for aurein 4 peptides isolated from *Litoria aurea* and *L. raniformis.*

m/z 772		As for aurein 4.1 [Gly Leu Leu Gln Thr Ile Lys] (Leu^3 replaces Ile^3 in aurein 4.2).
m/z 1172	B ions	*m/z* 1154, 1067, 939, 840, 783, 682, 583, 484, 427 [Gly Val Val Thr Gly Val Gln Ser]
	Y+2 ions	*m/z* 1043, 896, 825, 768, 711, 612, 511, 412 [Glu Phe Ala Gly Gly Val Val Thr Gly]
	sequence	Glu Phe Ala Gly Gly Val Val Thr Gly Val Gln Ser
Aurein 4.2 sequence		Gly Leu Leu Gln Thr Ile Lys Glu Lys Leu Lys Glu Phe Ala Gly Gly Val Val Gln Ser (OH)

Aurein 4.3 [MH^+ = 2415]

Only sufficient additional pure material was available to make a methyl ester, M^+ 2487 (three CO_2H and two $CONH_2$ groups), and to carry out an automated Edman sequencing experiment. For the structure of aurein 4.3, see Table 7.1.

Aurein 4.4 [MH^+ = 2425]

Methylation gives a methyl ester, M^+ 2497 (three CO_2H and two $CONH_2$ groups)

$(M+2H)^{2+}$ 1213	B ions	*m/z* 2407, 2192, 2093, 2036, 1935, 1836, 1723, 1666, 1565, 1494, 1381, 1252, 1124, 1011, 883, 754, 626 [Lys Glu Lys Leu Lys Glu Leu Ala Thr Gly Leu Val Thr Gly Val (Gln Ser) (NH_2)]
	Y+2 ions	*m/z* 2142, 2014, 1923, 1800, 1672, 1543, 1425, 1302, 1174, 1045, 932, 861, 760, 703, 590, 491 [(283) Gln Thr Ile Lys Glu Lys Leu Lys Glu Leu Ala Thr Gly Leu Val
partial sequence		[(283) Gln Thr Ile Lys Glu Lys Leu Lys Glu Leu Ala Thr Gly Leu Val Thr Gly Val (Gln Ser) (NH_2)]
Lys-C digest		MH^+ at *m/z* 772, 1174 and 1415.
m/z 772		as for aurein 4.2 sequence Gly Leu Leu Gln Thr Ile Lys
m/z 1415	B ions	*m/z* 1398, 1310, 1182, 1083, 1026, 925, 826, 713, 656, 484 [(Ala Thr) Gly Leu Val Thr Gly Val Gln Ser]
	Y+2 ions	*m/z* 1302, 1174, 1045, 861, 760, 590, 491 [Leu Lys Glu (Leu Ala) (Thr Gly) Leu Val]
	Sequence	Leu Lys Glu (Leu Ala) Thr Gly Leu Val Thr Gly Val Gln Ser (OH)
Aurein 4.4 sequence		Gly Leu Leu Gln Thr Ile Lys Glu Lys Leu Lys Glu Leu Ala Thr Gly Leu Val Thr Gly Val Gln Ser (OH)

Table 7.5. MS data for aurein 4 peptides isolated from *Litoria aurea* and *L. raniformis* (continued).

Aurein 5.2

Aurein 5.2 is a minor component of the skin secretions of both *Litoria aurea* and *L. raniformis*. This is an example of a peptide of which only some 10 μg of material was available for analysis, and the available mass spectrometric data provided the sequence of 22 of the 25 residues. The 'missing' first three residues were determined using Edman sequencing. Aurein 5.2 shows pronounced peaks corresponding to MH^+ and $(M+2H)^{2+}$ (*m/z* 2451 and 1226 respectively) in its electrospray spectrum. The methyl ester of aurein 5.2 shows an MH^+ peak at *m/z* 2479 showing the natural peptide contains two CO_2H groups but no $CONH_2$ residues. The collision induced mass spectrum (MS/MS) of the $(M+2H)^{2+}$ ion from aurein 5.2 is shown in Figure 7.11, and yields sequence data for all residues except the first three. Not enough material was available for a definitive Lys-C study, and the full sequence was determined using the automated Edman technique. The primary structure of aurein 5.2 is Gly Leu Met Ser Ser Ile Gly Lys Ala Leu Gly Gly Leu Ile Val Asp Val Leu Lys Pro Lys Thr Pro Ala Ser (OH). Details of the structure determination of aurein 5.1 are summarised in Table 7.6.

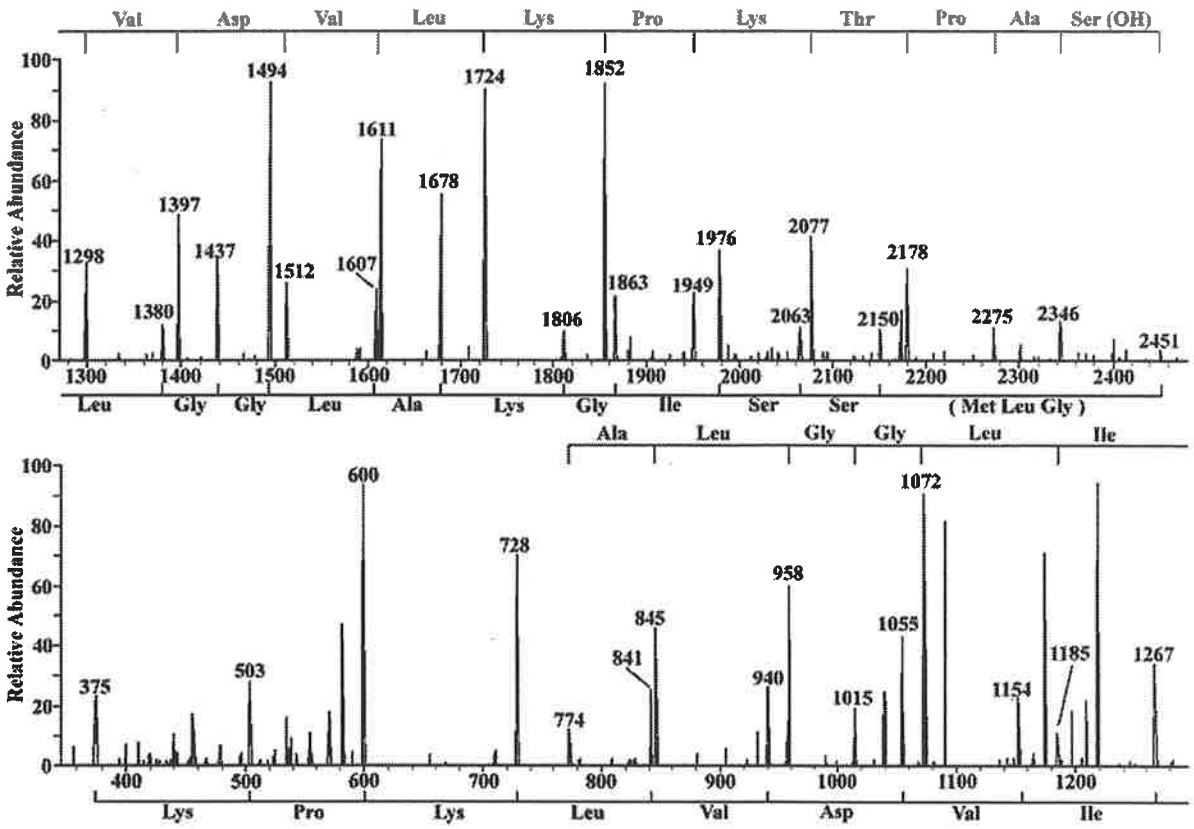

Figure 7.11. CA MS/MS of the $(M+2H)^{2+}$ ion of aurein 5.2 (*m/z* 1226). (See Experimental section for full details).

Aurein 5.1 [MH^+ = 2545]

Only sufficient additional pure material was available to determine that MH^+ = 2545, to make a methyl ester [MH^+ 2587 (three CO_2H groups)], and to carry out an automated Edman sequencing experiment. For the structure of aurein 5.1, see Table 7.1.

Aurein 5.2 [MH^+ = 2451]

Methylation gives a methyl ester, MH^+ 2479 (two CO_2H groups)

$(M+2H)^{2+}$ 1226	B ions	*m/z* 2433, 2346, 2275, 2178, 2077, 1946, 1852, 1724, 1611, 1512, 1397, 1298, 1185, 1072, 1015, 958, 845, 774 [Ala Leu Gly Gly Leu Ile Val Asp Val Leu Lys Pro Lys Thr Pro Ala Ser (OH)]
	Y+2 ions	*m/z* 2150, 2063, 1976, 1863, 1806, 1678, 1607, 1494, 1437, 1380, 1267, 1154, 1055, 940, 841, 728, 600, 503, 375 [(301) Ser Ser Ile Gly Lys Ala Leu Gly Gly Leu Ile Val Asp Val Leu Lys Pro Lys]
partial sequence		(301) Ser Ser Ile Gly Lys Ala Leu Gly Gly Leu Ile Val Asp Val Leu Lys Pro Lys Thr Pro Ala Ser (OH)
Lys-C digest		MH^+ at *m/z* 792, 1322 (very weak spectra - not sufficient for meaningful MS/MS data)
Aurein 5.2 sequence		Gly Leu Met Ser Ser Ile Gly Lys Ala Leu Gly Gly Leu Ile Val Asp Val Leu Lys Pro Lys Thr Pro Ala Ser (OH)

Table 7.6. MS data for aurein 5 peptides isolated from *Litoria aurea* and *L. raniformis*.

7.3. Anticancer Activity Determination

The selected aureins listed in Table 7.7 have been tested for anticancer activity in the NCI *in vitro* screening panel testing with 54 human tumour cell lines.[144] Results are summarised in Table 7.7. The aureins 4 and 5 show no activity but aureins 1-3 show anticancer activity against all the main groups of human cancers with IC 50 values in the 10^{-5} to 10^{-4} M concentration range. The anticancer activity is probably due to membrane activity, but the activity is only moderate, and we do not intend to investigate this activity further.

Peptide	Amino-acid sequence	Relative molecular mass
Aurein 1.1	GLFDIIKKIAESI-NH_2*	1444
Aurein 1.2	GLFDIIKKIAESF-NH_2	1478
Aurein 2.1	GLLDIVKKVVGAFGSL-NH_2*	1613
Aurein 2.2	GLFDIVKKVVGALGSL-NH_2*	1613
Aurein 2.3	GLFDIVKKVVGIAGSL-NH_2*	1613
Aurein 2.5	GLFDIVKKVVGAFGSL-NH_2	1647
Aurein 2.6	GLFDIAKKVIGVIGSL-NH_2	1627
Aurein 3.1	GLFDIVKKIAGHIAGSI-NH_2	1736
Aurein 3.2	GLFDIVKKIAGHIASSI-NH_2	1766
Aurein 3.3	GLFDIVKKIAGHIVSSI-NH_2	1794
Aurein 4.2	GLLQTIKEKLKEFAGGVVTGVQS-OH (inactive)	2400
Aurein 5.2	GLMSSIGKALGGLIVDVLKPKTPAS-OH (inactive)	2450

Cancer	Aurein 1.2	Aurein 2.5	Aurein 2.6	Aurein 3.1	Aurein 3.2	Aurein 3.3
Leukaemia	4-5	4-5	4.5	4	5	4-5
Lung	5	5	5	4	5	5
Colon	5	4-5	4-5	5	4-5	5
CNS	5	5	5	4-5	5	5
Melanoma	5	4-5	5	4-5	5	5
Ovarian	5	5	5	4-5	5	5
Renal	5	5	5	4-5	5	5
Breast	5	5	5	4-5	5	5
Total	52	41	49	34	52	53

Table 7.7. LC 50 anticancer activities of selected aurein peptides from *L.aurea* and *L.raniformis*

The data on the previous page are from the NCI testing program.[144] An asterisk indicates that this peptide, although anticancer active, was deemed not sufficiently active in the first stage (testing against three tumour lines) of the NCI testing program, to warrant second stage testing. When figures are given the table, these are a summary of the results for those peptides which were tested in the second stage of the NCI testing program against 54 human tumours. Activities are given as LC 50 values, the minimum molar concentrations required to kill 50% of the cancer cells. In the Table, these are shown as n as in 10^{-n} M. When there is no figure given, LC 50 is > 10^{-4} M. The data shown indicate only cancer groupings not the individual cancers within a particular grouping. The figure in the last line of the table indicates the total number of cancers (out of 54) that each peptide is active against within the concentration range given.

7.4. Antibacterial Activity Determination

Most tree frogs of the genus *Litoria* contain antibacterial peptides within their skin secretions (Chapter 6). Wide-spectrum antibacterial peptides so far reported within this genus have generally been caerin, maculatin or citropin type peptides, where specific examples of their activities are described elsewere.[132, 152, 128] The antibacterial activities of 16 aurein peptides from *Litoria aurea* and *L. raniformis* have been determined and compared with those of caerin 1.1 and citropin 1.1 in Table 7.8.

Aureins 1, 2 and 3 showed wide spectrum antibiotic activity against the majority of test micro organisms. The most active of the aurein peptides are aurein 1.2, aurein 2.2, aurein 2.4, and aurein 3.2. These peptides do not affect red blood cells at a concentration of 100 μg/mL (a concentration generally above that required to kill Gram positive bacteria): concentrations of 1 mg/mL of the aureins are required to destroy red blood cells.[123]

The aureins 2.1.1, 2.4.1, 3.1.2 and 3.3.1 show no bio-activity. It is a feature of anurans that they have endoproteases which degrade the antibiotic peptides after they have been on the skin surface for some period (usually between 5 - 30 mins.).[147] In this case the removal of the first two amino acid residues of the appropriate aurein peptide results in loss of bio-activity.

Aurein 1.2 only has 13 amino acid residues making it the smallest amphibian peptide yet reported to have significant antibiotic activity. Aureins 2.2, 2.4 and 3.2 have 16 and 17 amino acid residues. The majority of amphibian peptides so far reported from the genus *Litoria* that have displayed antibacterial activity contain at least 20 amino acid residues. For example, caerin 1.1 and maculatin 1.1 consist of 25 and 21 amino acids respectively. This length is important in order for the peptide to span the entire width of the phospholipid bilayer of a bacterial cell wall and comply with the "barrel-stave" model of peptide antibacterial action (described in Chapter 6.5, page 141). The recently discovered citropin 1.1 was shown to contain only 16 amino acid residues, with a length not sufficient to span the entire width of the bacterial cell wall. Aureins 1, 2 and 3 are not long enough to fully penetrate the cell wall and therefore the "barrel-stave" model cannot explain their antibacterial activity

The active aureins 1, 2, and 3 are thought to act through the "carpet-like" model of antibacterial activity (Chapter 6.5, page 141). This "non-channel" forming mechanism is not constricted by the length of the peptide, and functions by disrupting the integrity of the bacterial cell membrane. The prerequisite for this mode of action is the amphiphilic nature of the peptide with well-defined hydrophilic and hydrophobic zones.

Aurein	Amino Acid Sequence	MW	Active/Inactive
1.1	GLFDIIKKIAESI-NH_2	1444	Active
1.2	GLFDIIKKIAESF-NH_2	1478	Active
2.1	GLLDIVKKVVGAFGSL-NH_2	1613	Active
2.1.1	LDIVKKVVGAFGSL-NH_2	1443	Inactive
2.2	GLFDIVKKVVGALGSL-NH_2	1613	Active
2.3	GLFDIVKKVVGAIGSL-NH_2	1613	Active
2.4	GLFDIVKKVVGTLAGL-NH_2	1627	Active
2.5	GLFDIVKKVVGAFGSL-NH_2	1647	Active
2.6	GLFDIAKKVIGVIGSL-NH_2	1627	Active
3.1	GLFDIVKKIAGHIAGSI-NH_2	1736	Active
3.1.1	GLFDIVKKIAGHIA-OH	1480	Inactive
3.1.2	FDIVKKIAGHIAGSI-NH_2	1566	Inactive
3.2	GLFDIVKKIAGHIASSI-NH_2	1766	Active
3.3	GLFDIVKKIAGHIVSSI-NH_2	1794	Active
4.2	GLLQTIKEKLKEFAGGVVTGVQS-OH	2400	Inactive
5.2	GLMSSIGKALGGLIVDVLKPKTPAS-OH	2450	Active
caerin 1.1	GLLSVLGSVAKHVLPHVVPVIAEHL-NH_2	2582	Active
citropin 1.1	GLFDVIKKVASVIGGL-NH_2	1614	Active

Organism	**C 1.1**	**Cit 1.1**	**1.1**	**1.2**	**2.1**	**2.2**	**2.3**	
Bacillus cereus	50	25	50	100	50	100	100	
Escherichia coli								
Leuconostoc lactis	1.5	3	25	12	6	12	25	
Listeria innocua		25	100	100	100	6	12	100
Micrococcus luteus	12	25		100	100	25	100	
Pasteurella multocida	25			100				
Staphylococcus aureus	3	25		50		25	100	
Staphylococcus epidermidis	12	25		50	50	25	100	
Streptococcus uberis	12	12	100	50	100	100		

Organism	**2.4**	**2.5**	**2.6**	**3.1**	**3.2**	**3.3**	**5.2**
Bacillus cereus	25	50	100				
Escherichia coli							
Leuconostoc lactis	12	12	6	12	6	12	100
Listeria innocua		100	50	100	100	100	
Micrococcus luteus	25	100	25	100	100	100	
Pasteurella multocida						100	
Staphylococcus aureus	25	50	50	50	50	100	
Staphylococcus epidermidis	25	100	50	100	50	50	
Streptococcus uberis	25			100	50	25	50

Table 7.8. Antibacterial activities of some of the aurein peptides from *Litoria aurea* and *L. raniformis*, in comparison with the antibacterial activities of caerin 1.1 and citropin 1.1. When there is no figure indicated, the MIC value is > 100 μg ml^{-1} implying lack of activity. (See experimental for full details).

7.5. Determination of Structural Conformation

Edmunson helical wheel projections are used to predict the likelihood that a peptide may adopt an amphipathic α-helix conformation. The Edmunson helical wheel projection is a two-dimensional representation of the three-dimensional structure of an α-helix where the backbone of the polypeptide chain is represented by the perimeter of the wheel. The amino acid residues are projected onto a plane perpendicular to the axis of the helix. One turn of an α-helix is 3.6 residues long, therefore each adjacent residue can be spaced 100° apart around the circumference of the circle. This corresponds to 18 residues per entire revolution of helix. The residues are numbered from the N-terminus.[133]

The Edmunson wheel projections of the antibacterial aureins1, 2 and 3 (for example, that of aurein 1.2 is shown in Figure 7.12) show well defined hydrophobic and hydrophilic zones, suggesting that these aureins may be amphipathic α-helical peptides.

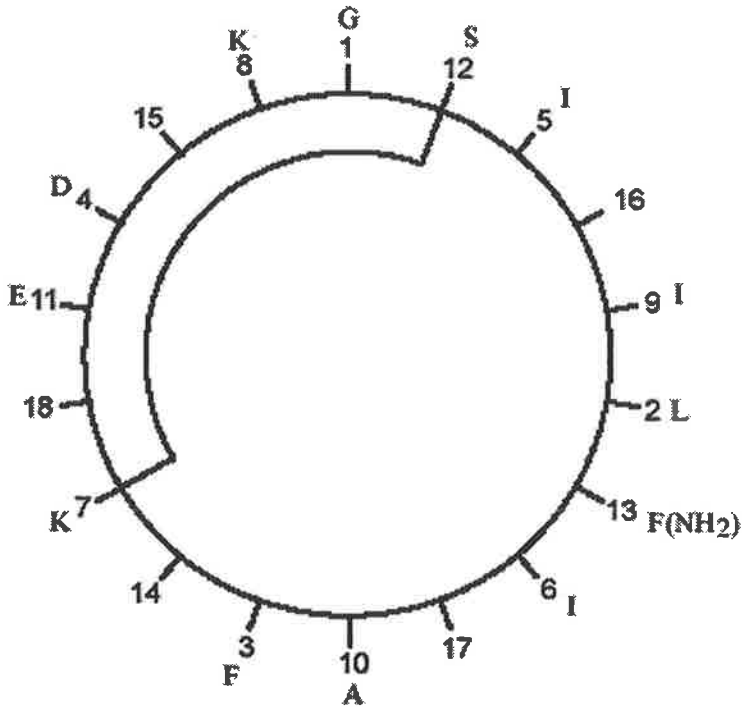

Figure 7.12. Edmunson projection of aurein 1.2 showing the well defined hydrophobic and hydrophilic zones. The left-hand side of the figure represents the hydrophilic region.

Edmunson projections of the aureins 4 suggest that they may be amphipathic peptides but the hydrophilic and hydrophobic zones are not as well defined as those of the aureins 1-3. For example, the Edmunson projection of aurein 4.2 is shown in Figure 7.13. The corresponding projections of the aureins 5 show no well defined hydrophilic and hydrophobic zones. Previous NMR studies have shown that the presence of central Gly and/ or Pro residues prevents peptides forming ideal α-helices by destabilising the overall helical formation.[152] Aureins 5 contain Pro and several central Gly residues while aureins 4 contain 'central' Gly residues. These observations may explain the lack of significant anticancer and antibacterial activities of aureins 4 and 5 when compared to those of the aureins 1-3.

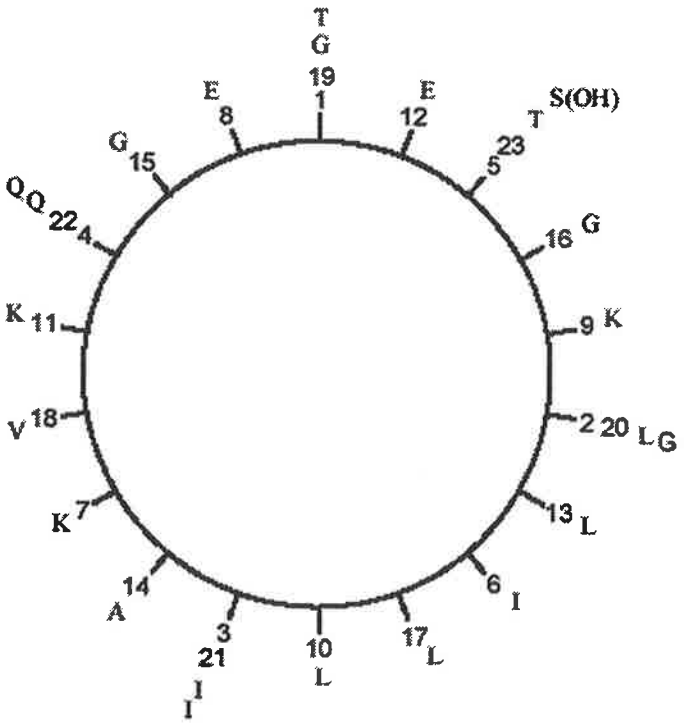

Figure 7.13. Edmunson projection of aurein 4.1.

The tertiary structure structure of aurein 1.2 (Figure 7.14) was determined by NMR (by Ms K.L. Wegener) using a deuterated trifluoroethanol/H_2O solvent system and confirms the α-helical nature of this peptide with well-defined hydrophobic and hydrophilic zones.[123]

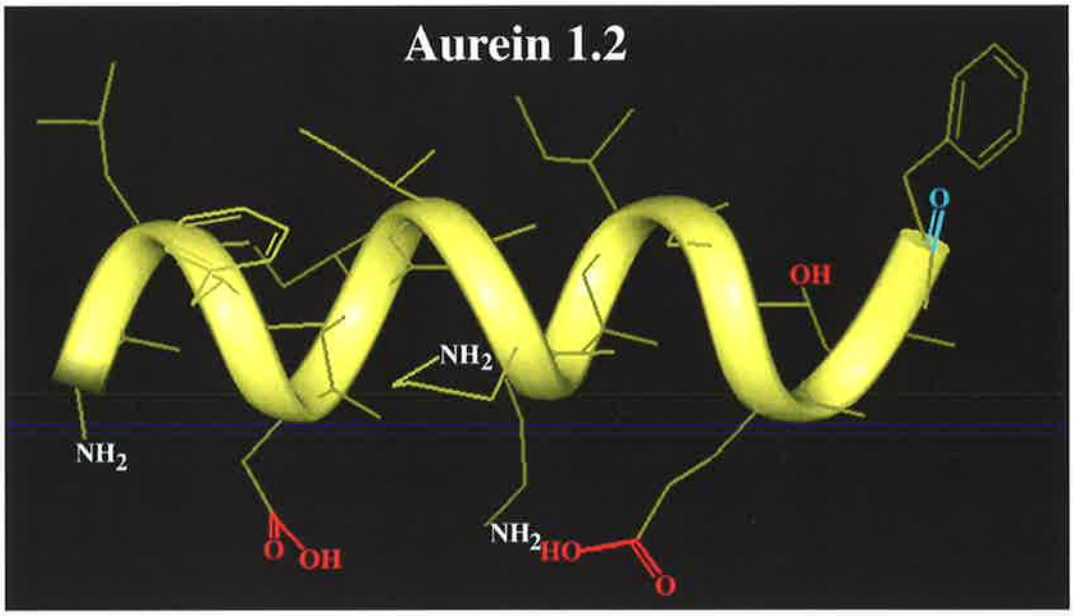

Figure 7.14. Three-dimensional structure of aurein 1.2 (from ref.[123])

7.6. Conclusions

A combination of mass spectrometric, Lys-C digest and automated Edman techniques enabled the determination of the amino acid sequences of 22 aurein peptides from skin secretions of *Litoria aurea* and *Litoria raniformis*. Five distinct groups of aurein peptides have been discovered, namely, the 13, 16, 17, 23 and 25 residue aureins 1, 2, 3, 4 and 5.

Aureins 1-3 are the major peptides produced by both *Litoria aurea* and *Litoria raniformis*. The aureins 1-3 are post-translationally modified (i.e. they have $CONH_2$ groups at the C-terminal end of the peptide) and are wide-spectrum antibiotic and anticancer peptides. One of these, aurein 1.2, is the smallest amphibian peptide yet reported to have significant antibiotic and anticancer activity. The antibacterial potency of aurein 2.2 is similar to those of caerin 1.1 and citropin 1.1. The aureins 2.1.1, 2.4.1, 3.1.2 and 3.3.1 are degradation products: they exhibit neither antibiotic nor anticancer activity.

The aurein 4 and 5 peptides have C-terminal CO_2H groups, and these peptides show no antibiotic or anticancer activity. Their role in amphibians is not known at this time. However, the 23 residue aurein 4 peptides are unusual in that they are anionic peptides (in contrast to the active aureins 1-3, all of which are basic peptides). This suggests that the aureins 4 may be spacer peptides in the inactive pro-aurein 1-3 peptides (see[153] for a review of the biosynthesis of active amphibian peptides). This has not been confirmed.

Aurein 5.2	**GLMSSIGKALGGL**I V**D**V**L**K**PK**TPAS-OH
Splendipherin	**GLVSSIGKALGGL**L**A**D**V**V**K**S**K**GQPA-OH

The aureins 5 are very similar in structure to splendipherin, the aquatic male sex pheromone of the tree frog *Litoria splendida*.[154] It is possible that the aureins 5 are also aquatic pheromones. The amino acid sequences of splendipherin and aurein 5.2 are shown for comparison above. At present we do not have sufficient numbers of males and females of *Litoria aurea* and *Litoria raniformis* in order to carry out the behavioural tests required to investigate this possibility.

Chapter 8. Experimental

8.1. Collection and Preparation of Secretions

The skin secretions from *Litoria aurea* and *Litoria raniformis* were provided through the courtesy of Associate Professor M.J. Tyler, Department of Environmental Biology, University of Adelaide. The secretions were obtained by the electrical stimulation procedure: where the frog (as appropriate) was held by the back legs, the skin moistened with deionized water, and the granular dorsal glands situated on the back were stimulated by means of a bipolar electrode of 21G platinum attached to a Palmer Student Model electrical stimulator. The electrode was rubbed gently in a circular manner on the particular gland (under study) of the animal, using 10 V and a pulse duration of 3 ms.[135] the resulting secretion was washed from the frog with deionized water (50 mL), the mixture diluted with an equal volume of methanol, centrifuged, filtered through a Milex HV filter unit (0.45 μm), and lyophilised. This procedure provided, on average, about 3 mg of solid peptide material was acquired from *Litoria aurea* and 10 mg from *Litoria raniformis*.

8.2. HPLC Separation

The HPLC system used in this research was:

Walters Millipore Lambada Max 481 LC spectrometer
Walters Millipore 510 HPLC pump
Walters Millipore 501 HPLC pump
ICI DP 800 data interface
ICI DP 800 data station

HPLC separation was achieved for each sample using a VYDAC C_{18} Protein and Peptide (218TP54) reverse phase column equilibrated with 10% acetonitrile/aqueous 0.1 % TFA. Additional purification was required for the majority of fractions in order to obtain pure components. Fractions were collected, concentrated and dried *in vacuo* for subsequent analysis. The conditions for the HPLC chromatogram represented in Figures 7.3 and 7.4 are as follows: The elution profiles increased from 10-75% acetonitrile over a period of 30 minutes using a flow rate of 1 ml/min.

8.3. Methylation of Peptides

Purified peptide (*ca* 5-10 μg) in deionised water (40 μl) was lyophilised in an Eppendorf tube. 'Acidified methanol' was added, and the resulting mixture heated at 45°C for 30 minutes. The solvent was removed in a stream of nitrogen and the solid product dissolved in methanol/water (1:1, 500 μl) and analysed by electrospray mass spectrometry.

The 'Acidified methanol' was prepared by adding methanol (858 μl) to a 10 ml screw top test tube. This was cooled in dry ice for 5 minutes, acetyl chloride (142 μl) was added under nitrogen, the test tube sealed and cooled again in dry ice for 5 minutes. The solution was allowed to warm to 20°C over a period of 1 hour, flushing with nitrogen every 15 minutes. The reagent was stored at -4°C for a maximum of 5 days.

8.4. Enzyme Digestion using Lys-C

Lyophilised peptide (ca 50 μg) was added to an Eppendorf tube and dissolved in aqueous ammonium hydrogen carbonate (0.1M, 5 μl, pH = 8) solution and endoprotease Lys-C (1 μl) was then added. The resulting solution was incubated at 45°C for 45 minutes and then analysed by electrospray mass spectrometry.

8.5. Mass Spectrometric Analysis

Electrospray mass spectra were determined using a Finnigan LCQ ion trap mass spectrometer with a mass capability to 4000 Da. The samples were dissolved in methanol/water (1:1) and infused into the electrospray source via a rheodyne injector with a 5 μl loop at 12 μl per minute. Conditions were as follows: source voltage 4.3 kV, source current 18 μA, capillary temperature 200°C, capillary voltage 3V, and sheath gas flow 30psi. MS, and MS/MS data were acquired with the automatic gain control on, a maximum time of 500 ms, and using three microscans per scan, averaging over a total of 10scans. Molecular weights of the peptides were determined from either the MH^+ or $[M + 2H]^{2+}$ ions.

8.6. Automated Edman Sequencing

Automated Edman sequencing was performed by the Department of Biochemistry (through the courtesy of Dr. J.C. Wallace), University of Adelaide, using an applied Biosystems 470A sequencer equipped with a 900A data analysis module.

8.7. Preparation of Synthetic Peptides

The syntheses of the aureins were carried out by Mimotopes (Clayton, Victoria, Aust.) using L-amino acids through the standard N-α-Fmoc method.[155] Each synthetic peptide was shown to be identical with the natural peptide by (I) electrospray mass spectrometry, (ii) co-elution of the synthetic and natural peptides on HPLC.

8.8. Antibacterial Testing

The Microbiology Department of the Institute of Medical and Veterinary Science (Adelaide, Australia) carried out the antibacterial testing. The method used involved the measurement of inhibition zones (produced by the applied peptide) on a thin agarose plate containing the microorganisms under study. The method follows a standard testing procedure.[143] Activities are recorded as MIC values, i.e. the minimum inhibitory concentration of peptide (μg) per ml required to totally inhibit the growth of the named microorganism.

8.9. Anticancer Testing

Anticancer testing was carried out by the National Cancer Institute (Washington, DC, USA) using *in vitro* screening panel testing of the chemosensitivity of 54 human tumour cell lines towards the synthetic aurein peptides.[144]

References

1. Rohr, J. and Thiericke, R., *Nat. Prod. Rep.*, 1992, 103.

2. Krohn, K. and Rohr, J., *Top. Curr. Chem.,* 1997, **188**, 127.

3. Goodfellow, M., Mordarski, M. and Williams, S.T., The Biology of the Actinomycetes, *Academic Press*, London, 1984.

4. Dann, M., Lefemine, D.V., Barbatschi, F., Shu, P., Kunstmann, M.P., Mitscher, L.A. and Bohonos, N. *Antimicrob. Agents. Chemother.*, 1965, 832.

5. Kuntsmann, M.P. and Mitscher, L.A., J. *Org. Chem.*, 1966, **31**, 2920.

6. Bowie, J. H. and Johnson, A. W., *Tetrahedron Lett.*, 1967, **16,** 1449.

7. Nagatsu, T., Ayukawa, S. and Umezawa, H., *J. Antibiot.,* 1968, **21**, 354.

8. Sezaki, M., Kondo, S., Maeda, K., Umezawa, H., Ohno, M., *Tetrahedron*, 1970, **26**, 5171

9. Nagasawa, T., Fukao, H., Irie, H., and Yamada, H., *J. Antibiot.,* 1984, **37**, 693; Irie, H., Mizuno, Y., Kouno, I., Nagasawa, T., Tani, Y., Yamada, H., Taga, T. and Osaki, K., *J. Chem. Soc., Chem. Commun.,* `1983, 174.

10. Imamura, N., Kakinuma, K., Ikekawa, N., Tanaka, H. and Omura, S., *J. Antibiot.,* 1982, **35**, 602.

11. Rohr, J., Schonewolf, M., Udvarnoki, G., Eckardt, K., Schumann, G., Wagner, C., Beale, J.M. and Sorey, S., D., *J. Org. Chem.,* 1993, **58**, 2547.

12. Rassmussen, R.R., Nuss, M.E., Scherr, M.H., Mueller, S.L. and McAlpine, J. B., *J. antibiot.* , 1986, **39**, 1515.

13 Tanaka, N., Harada, N., Kitamura, I., *Jpn. J. Cancer Research.,* 1986, **77**, 324.

14. Kawashima, A., Kishimura, Y., Tamai, M., and Hanada, K., *Pharm. Bull.*, 1989, **37**, 3429.

15. Hayakava, Y., Kim, Y.J., Furihata, K. and Seto, H., *J. Antibiot.*, 1991, **44**, 1179.

16. Oka, M., Kamei, H., Hamagishi, Y., Tomita, K., Miyaki, T., Konishi, M. and Oki, T., *J. Antibiot.*, 1990, **43**, 967.

17. Ogasavara, M., Kishi, T., Sezaki, R. and Kanamura, T., *J. Antibiot.,* 1992, **45,** 129.

18. Nagasawa, T., Fukao, H., Irea, H. and Yamada, H., *J. Antibiot.*, 1984, **41**, 693.

19. Sawada, R., Matsuda, N., Uchida, T., Ikeda, T., Sawa, T., Naganawa, H., Hamada, M. and Takeuchi, T., *J. Antibiot.,* 1991, **44**, 396.

20 Oki, T., Kakushima, M., Hirano, M., Takahashi, A., Ohta, S., Hatori, M. and Kamei, H., *J. Antibiot.*, 1992, **45**, 1512.

21. Ajukawa, S., Takeuchi, T., Sezaki, M., Hara, T., Umezawa, H. and Nagatsu, T., *J. Antibiot.*, 1968, **21**, 350.

22. Omura, S., Nakagawa, A., Fukamachi, N., Miura, S., Takahashi, Y., Komiyama, K., Kabayashi, B., *J. Antibiot.,* 1988, **41**, 812.

23. Grafe, U., Dornberg, K. and Saluz, H.P., 'Biotechnical drugs as antitumor agents', *Biotechnology: amulati volume comprehensive treatise. Vol. 7. Products of secondnary metabolism*, 1997, ed. by Kleinkauf, H. and von Dohren, H., VCH, Weinhein.

24. Fredrick, C.A., Williams, L.D., Ughetto, G., Van derMarel, G.A., Van Boom, J.H., Rich, A. and Wang, A.H.J., *Biochemistry.*, 1990, **29**, 2538.

25. Crow, R.T., Rosenbaum, B., Smith III, R., Guo, Y., Ramos, K., S. and Sulikowski, G.A., *Bioorg. Med. Chem. Lett.*, 1999, 1663.

26. Doroshaw, J.H., 'Anthracyclines and anthracenediones' *in Cancer chemotherapy and biotherapy*, 1996, 2 edn, Lippencott-Raven, Philadelphia, 1.

27. Krohn, K., Khanbabaee, K., *Liebigs. Ann. Chem.*, 1994, 1109.

28. Krohn, K., Boker, N., Florke, U. and Freud, Ch., *J. Org. Chem.,* 1997, **62,** 2350.

29. Brown, P.M. and Thompson, R.H., *J. Chem. Soc. Perkin Trans.* **1**, 1976, 997

30. Guingant, A. and Barreto, M., *Tetrahedron Lett.* 1987, **28**, 3107.

31. Larsen, D.S., O'Shea, M. and Brooker, S., *Chem. Commun.*, 1996, **2**, 203.

32. Katsuura, K. and Sniekus, V., *Tetrahedron Lett.*, 1985, **26**, 9; Katsuura, K. and Sniekus, V., *Can. J. Chem.,* 1987, **65**, 124.

33. Larsen, D.S. and O'Shea, M., *Tetrahedron Lett.*, 1993, **34**, 1373; Larsen, D.S. and O'Shea, M., *Tetrahedron Lett.*, 1993, **34**, 3769.

34. Larsen, D.S. and O'Shea, M.D., *J. Chem. Soc., Perkin Trans. 1*, 1995, 1019.

35. Carreno, C.M., Urbano, A. and Di Vitta, C., *Chem. Commun.,* 1999, 817.

36 Krohn, K., Khanbabaee, K., Florke, U. and Jones. P., *Liebigs. Ann. Chem.*, 1994, 471. Krohn, K. and Khanbabaee, K., *Angew. Chem. Int.Ed.Engl.* 1994, **33**, 99.

37 Kraus, G. and Wu, Y., *Tetrahedron Lett.,* 1991, **32**, 3803.

38 Caygill, G., Larsen, D. and McFarlane, B., *Aust. J. Chem.*, 1997, **50**, 301.

39. Krohn, K., Khanbabaee, K. and Micheel, J., *Liebigs. Ann. Chem.*, 1995, 1529.

40. Boyd, V.A. and Sulikowski, G.A., *J. Am. Chem. Soc.*, 1995 **117**, 8472.

41. Yamaguchi, M., Okuma, T., Horiguchi, A., and Minami, T., *J. Org. Chem.,* 1992, 57, 1647

42. Larsen, D.S. and O'Shea, M.D., *J. Org. Chem.*, 1996, **61**, 5681.

43. Krohn, K., Florke, U., Freud, C. and Hayat, N., *Eur. J. Org. Chem.*, 2000, 1627.

44. Kim, K. and Sulikowski, G., A., *Angew. Chem.* 1995, **107**, 2587

45. Chan, T. and Nwe, K., *J. Org. Chem.*, 1992, **57**, 6107.

46. Krohn, K. and Micheel, J., *Tetrahedron*, 1998, **54**, 4827.

47. Kim, K., Reibenspies, J. and Sulikowski, G., *J. Org. Chem.*, 1992, **57**, 5557.

48. Boyd,V., Reibenspies, J. and Sulikovski, G., *Tetrahedron Lett.,* 1995, **36**, 4001.

49. Danishevski, S. and Gordon, D., *J. Org. Chem.*, 1992, **57**, 7052.

50. Tiedemann, R. and Moore, H.W., *J. Am. Chem. Soc.*, 1998, **120**, 3801.

51. Kraus, G.A. and Wan, Z., *Tetrahedron Lett..*, 1997, **38**, 37, 6509.

52. Rozek, T., Janowski, W., Hevko, J.M., Tiekink, E.R.T, Dua, S., Stone, D.J.M. and Bowie, J.H, *Aust. J. Chem.,* 1998, **51**, 515-523.

53. Kelly, T. and Montury, M., *Tetrahedron Lett.*, 1978, **45**, 4309.

54. Kelly, T.R., Whiting, A. and Chandrakumar, N.S., *J. Am. Chem. Soc.*, 1986, **108**, 3510.

55. Luche, J, L., *J. Am. Chem. Soc.*, 1978, **100**, 226; Luche, J. L., *J. Am. Chem. Soc.*, 1981, **103**, 5454; Denmark, S. E., and Amburgey, J., *J. Am. Chem. Soc.*, 1993, **115**, 10386; Fujji, H., Oshima, K., and Ultimoto, K., *Chem. Lett.*, 1992, 967; Matsubara, S., Takahashi, H., and Ultimoto, K., *Chem. Lett.*, 1992, 3173; Leclaire, M., and Jean, P., *Bull. Soc. Chim. Fr.,* 1996, **133**, 801.

56. Datta, S., Frank, R., Quigley, G., Huang, L., Chen, S. and Sihaed, A., *J. Am. Chem. Soc.*, 1990,**113**, 3249.

57. Danishefski, S.J., Uang, B.J. and Quallich, G., *J. Am. Chem. Soc.*, 1984, **106**, 2453.

58. Brown, H.C., and Stocky, T.P., *J. Am. Chem. Soc,* 1977, **99**, 8218.

59. Marouka, K., Sakurai, M., Fujivara, J. and Yamamoto, H., *Tetrahedron Lett.,* 1986, **27**, 4895.

60. Washburn, R.M. and Levens, E., *J. Chem. Soc.*, 1950, 3125.

61. Carreno, C.M., Urbano, A. and Di Vitta, C., *J. Org. Chem.,* 1998, **63**, 8320.

62. Rozek, T., Tiekink, E.R.T, Taylor, D.K. and Bowie, J.H, *Aust. J. Chem.,* 1998, **52**, 129.

63. Krohn, K., Ballwandz, F. and Baltus, W., *Liebigs Ann Chem.*, 1993, 901; Oka, M., Konishi, M., Oki, T. and Ohashi, M., *Tetrahedron Lett.,* 1990, **31**, 7473.

64. Schroder, M., *Chem. Rev.* , 1980, **80**, 187

65. VanRheenen, V., Kelly, R.C. and Cha, D.Y., *Tetrahedron Lett.*, 1976, **23**, 1973.

66. Kolb, H.C., VanNievwenhze, M.S. and Sharpless, B.K., *Chem. Rev.*, 1994, **94**, 2483.

67. Hirschmann, R., Bailey, G.A., Walker, R. and Chemerda, J.M., *J. Am. Chem. Soc.*, 1959, **81**, 2822.

68. Kubota, T. and Hayashi, F., *Tetrahedron*, 1966, **23**, 995.

69. Rebrevic, L. and Koser, G.F., *J. Org. Chem.*, 1984, **49**, 2462.

70. Mangoni, L., Adinolfi, M., Barone, G. and Parrilli, M., *Tetrahedron Lett.*, 1973, 4485.

71. Ernst, B. and Winkler, T., *J. Am. Chem. Soc.*, 1987, **109**, 6403.

72. Reischl, W. and Zbiral, E., *Tetrahedron*, 1979, **35**, 1109.

73. Hutton, G., Jolliff, T., Mitchell, H. and Warren, S., *Tetrahedron Lett.,* 1995, 7905.

74. Barros, M.T., Alves, A.G., Godinho, L.S. and Maycock, C.D., *Tetrahedron Lett.,* 1995, 2321.

75. Hamann, L.G. and Koreeda, K., *Tetrahedron Lett.,* 1992, 6569; Agami, C., Conti, F., and Lequesne, C., *Tetrahedron*, 1995, 4043.

76 Cockerill, A.F., Davies, G.L.O., Harden, R.C. and Rackhan, D.M., *Chem. Rev*, 1973, 553

77. Wingfield, D. C., *Tetrahedron*, 1979, **35**, 443; Brown, H. C. and Krishnamurthy, S., *Tetrahedron*, 1979, **35**, 567.

78. S. Dobreff, PhD Thesis, University of Gottingen, 1989.

79. Ritzau, M., Dissertation, University of Gottingen, 1992.

80. Okawara, H., Nakai, H. and Ohno, M., *Tetrahedron Lett.*, 1982, **23**, 1087.

81. Tsunoda, T., Suzuki, M. and Noyori, R., *Tetrahedron Lett.*, 1980, **21**, 1357; Piccolo, O., Spreafico, F. and Visentin, G., *J. Org. Chem.*, 1985, **50**, 3946.

82. Rozek, T., Tiekink, E.R.T., Taylor, D.K. and Bowie, J.H, *Aust. J. Chem.,* 1998, **51**, 1057.

83. Cameron, D.W., personal communication with Bowie, J.H.

84. Ladjama, D. and Riehl, J.J., *Synthesis*, 1979, 504; Miller, R.D. and McKean, D.R., *Synthesis*, 1979, 730; Brown, C.H., *J. Org. Chem.*, 1974, **39**, 3913.

85. Adam, W., and Hadjiarapoglue, L., ~~*Top. Corr. Chem., 1993, 164, 45.*~~ Peters, K., Sauter, M. *J. Am. Chem. Soc.*, 1993, **115**, 8603

86. Cubero, I., Plaza, L.E. and Maria, T., *Carbohydr. Res.*, 1986, **154**, 71.

87. Palumbo, G., Ferreri. C. and Caputo. R., *Tetrahedron Lett.*, 1983, **24**, 1307.

88. Gould, S.J. and Cheng, X.C., *J. Org. Chem.*, 1994, **59**, 400.

89. Kern, D.L., Schaumberg, P.J., Hokanson, G.C. and French, C., *J. Antibiot.*, 1986, **39**, 469.

90. Ladjama, D. and Riehl, J.J., *Synthesis*, 1979, 504.

91. Brinkworth, C., Rozek, T., Bowie, J.H., Skelton, B.W. and White, A.H., *Aust. J. Chem.*, 2000, **53**, 403.

92. X-ray structure by A.H. White, Department of Chemistry, University of WA.

93. Rubotton, G.M., Vazques, M.A. and Pelegrina, D.R., *Tetrahedron lett.*, 1974, 4319; Rubotton, G.M. and Gruber, J.M., *J. Org. Chem.*, 1974, **43**, 1599.

94. Zhu, Y., Manske, K.J. and Shi, Y., *J. Am. Chem. Soc.*, 1999, **121**, 4080.

95. Perrin, D.D., Amarego, W.L.F. and Perrin, D.R., 'Purification of Laboratory Chemicals', 2nd eddition, *Pergamon Perrin Press*, 1980.

96. Heinzman, S.W. and Grunwell, J.R., *Tetrahedron lett.*, 1980, **21**, 4305.

97. Tochtermann, W. and Koehn, H., *Chem. Ber.*, 1980, **113**, 3249.

98. Barker, J., Grigg, G. and Tyler, M.J., 'A field guide to Australian frogs', *Surrey Beatty, Norton, NSW*, 1995.

99. Lazarus LH and Attila M. *Prog. Neurobiol.* 1993; **41**: 473.

100. Daly, J.W., Caceres, J., Moni., R.W., Gusovski, F., Moos, M., Seamon, K.B., Milton, K. and Myers, C.W., *Proc. Natl. Acad. Sci. USA*, 1992, **89**, 10960.

101. Carraway, R.E. and Cochrane, D.E., *J. Biol. Chem.*, 1987, **261**, 15886.

102. Negri, L., Lattazani, R. and Melchiorri, P., *Brit. J. Pharm.* 1995, **114**, 57.

103. Montecucchi, P.C., De Castiglone, R., Piani, S., Gozzini, L. and Erspamer, V., *Int. J. Pept. Protein. Res.*, 1981, **17**, 275.

104. Erspamer, V., 'Amphibian biology: the integument', Surrey Beaty, Norton, NSW, 1994, **1**, 178.

105. Tyler, M.J., 'Encyclopaedia of Australian animals', Harper Collins, 1992, 3.

106. Jackson, I.M. and Reichlin, S., *Science*, 1997, **198**, 414.

107. Boman, H.G., *Cell*, 1991, **65**, 205.

108. Zasloff, M., *Proc. Natl. Acad. Sci.* USA, 1987, **84**, 5449.

109. Barthalmus, G.T. and Zielinski, W.J., *Pharmacol. Biochem. Behav.*, 1988, **30**, 957.

110. Terry, A.S., Poulters, L., Williams, J.C., Hutkins, M. and Giovanni, C.H., *J. Biol. Chem.*, 1988, **263**, 5745.

111. Dockary, G.J. and Hopkins, C.R., *J. Cell. Biol.*, 1975, **64**, 724.

112. Hauser, F. and Hoffman, W., *J. Biol. Chem.*, 1992, **34**, 24620.

113. Flucher, B.E., Lenglachner, K., and Mollay, C.J., *Cell Biol.*, 1985, **64**, 724.

114. Erspamer, V., Falconeri Erspamer, G., Mazzanti, G. and Endean, R., *Comp. Biochem. Physiol.*, 1984, **77**, 99.

115. Hernandez, C., Mor, A. and Dunia, I., *Eur. J. Cell Biol.*, 1992, **59**, 414.

116. Zasloff, M., Martin, B. and Chen, H.C., *Proc. Natl. Acad. Sci. USA*, 1988, **85**, 910.

117. Giovanini, M.G., Poulter, L., Gibson, B.W. and Williams, D.H., *J. Biochem.*, 1987, **243**, 113.

118. Saberwal, G. and Nagaraj, R., *Biochem. et Biophys. Acta.,* 1994, **1197**, 109.

119. Marion, D., Zasloff, M., and Bax, A., *FEBS lett.*, 1988, **227**, 21.

120. Wade, D., Boman, A., Wahlin, B., Drain, C.M., Andreau, D., Boman, H.G. and Merrifield, R.B., Proc. *Natl. Acad. Sci. USA*, 1990, **87**, 4761.

121. Jacob, L. and Zasloff, M., 'Antimicrobial peptides: Ciba Foundation Symposium 186', *Wiley and Sons, New York, NY*, 1994, 197.

122. Nakajima, Y., Qu, X.M. and Natori, S., *J. Biol. Chem.*, 1987, **262**, 1665.

123. Rozek, T., Wegener, K.L., Bowie, J.H., Olver, I.N., Carver, J.A., Wallace, J.C. and Tyler, M.J., *Eur. J. Biochem.* 2000, **267**, 1.

124. Waal, A., Gomez, A.V., Mensick, A. and Grootegoed, J.A., *FEBS Lett.*, 1991, **293**, 219.

125. Shai, Y., *Trends. Biochem. Sci.*, 1995, **20**, 460.

126. Ehrenstein, G. and Lecar, H., *Rev. Biophys.*, 1977, **10**, 1.

127. Ojcius, D.M. and Young, J.D., *Trends Biochem. Sci.*, 1991, **16**, 225.

128. Rozek, T., Waugh, R.J., Steinborner, S.T., Bowie, J.H., Tyler, M.J. and Wallace, J.C., *J. Peptide Sci.*, 1998, **4**, 111.

129. Chia, B.C.S., Carver, J., Mulhern, T.D. and Bowie, J.H., *Eur. J. Biochem.,* 2000, **267**, 1894.

130. Feurle, G.E., Hamscher, G., Meyer, H.E. and Metzger, J.W., *J. Biol. Chem.*, 1992, **276**, 22305.

131. Wabnitz, P.A., Bowie, J.H., Wallace, J.C. and Tyler, M.J., *Raid Commun. Mass Spectrom.* 1999, **13**, 1724.

132. Wegener, K.L., Wabnitz, P.A., Carver, J., Bowie, J.H., Chia, B.C.S., Wallace, J.C. and Tyler, M.J., *Eur. J. Biochem.,* 1999, **265**, 627.

133. Schiffer, M. and Edmundson, A.B., *J. Biophys.,* 1967, **7**, 121.

134. Roseghini, M., Erspamer, W. and Endean, R., *Comp. Biochem. Physiol.,* 1976, **54**, 31.

135. Tyler, M.J., Stone, D.J.M. and Bowie, J.H., *J. Pharmacol. Toxicol. Methods* 1992, **28**: 199.

136. Fenn, J.B., Mann, M., Meng, C.K., and Wong, S.F., *Mass Spectrom. Rev.,* 1990, **9**, 37.

137. Cooks, R.G. and Kaiser, R.E., *Acc. Chem. Res.*, 1990, **23**, 213.

138. March, R.E., *Int. J. Mass Spectrom. Ion Processes*, 1992, **118**, 71.

139. Ionscher, K.R. and Yates, J.R., *Anal. Biochem.*, 1997, **144**, 1.

140. Roepstroff, P. and Fohlman, *J., Biomed. Mass Spectrom.*, 1984, **11**, 601.

141. Hunkapiller, M.W., Hewick, R.M., Drever, W.J. and Hood, L.E., *Methods Enzymol.,* 1983, **91**, 399.

142. Maeji, N.J., Bray, R.M., Valerio, R.M. and Wang, W., *Peptide Res.*, 1995, **8**, 33.

143. Jorgensen, J.H., Cleeland, W.A., Craig, G., Doerm, M., Ferraro, J., Finegold, C.M., Hansen, S.L., Jenkins, S.G., Novick, W.J., Pfaller, M.A., Preston, D.A., Reller, L.B., and Swenson, J.M., *Natl. Committee Clin. Lab. Stand.,* 1993, **13**, 1. Document M7-A3.

144. see the NCI web site - http://dtp.nci.nih.gov

145. Anastasi, A., Erspamer, V. and Endean, R., *Arch. Biochem. Biophys.*, 1968, **125**, 57.

146. Bowie, J.H., Chia, B.C.S.. and Tyler, M.J., *Pharm. News*, 1998, **5**(6), 16.

147. Bowie, J.H., Wegener, K.L., Chia, B.C.S., Wabnitz, P.A., Carver, J.A., Tyler, M.J. and Wallace, J.C., *Protein and Peptide Lett.*, 1999, **6**, 259.

148. Lesson, R.P., *Zoologie,* 1829, **2** (1), 34, Paris, Arthus Bertrand.

149. Barker, J., Grigg, G.C. and Tyler, M.J., *A Field Guide to Australian Frogs*, Surrey, Beatty and Sons, Chipping Norton, New South Wales, Aust., 1995, 40.

150. Kerferstein, W., *Nachr.Ges.Wiss.Göttingen*, 1867, 341.

151. Biemann, K. and Martin, S., *Mass Spectrom Rev.*, 1987, **6**, 1.

152. Wong, H., Bowie, J.H. and Carver, J.A., *Eur. J. Biochem.,* 1997, **247**, 545.

153. Ganz, T., *Antimicrobial Peptides. Ciba Symposium 186,* Boman, H.G., Marsh, J. and Goode, J.A., Eds., Wiley, Chichester, 1994; 62.

154. Wabnitz, P.A., Bowie, J.H., Tyler, M.J., Wallace, J.C. and Smith, B.P., *Nature* (London), 1999, **401**, 444; *Eur. J. Biochem.*, 2000, **267**, 269.

155. Maeji, N.J., Bray, R.M., Valerio, R.M. and Wang, W., *Peptide Res.,* 1995; **8**, 33.

Publications

Rozek, T., Janowski, W., Hevko, J.M., Tiekink, E.R.T., Dua, S., Stone, D.J.M. and Bowie, J.H. (1998). Syntheses of angucyclinones related to ochromycinone. *Australian Journal of Chemistry*, 51(6), 515-523.

Rozek, T., Tiekink, E.R.T., Taylor, D.K. and Bowie, J.H. (1998). Syntheses of angucyclinones related to ochromycinone. II. Regio- and stereo-selective reduction of a tetrahydroangucyclinone. *Australian Journal of Chemistry*, 51(11), 1057-1060.

Rozek, T., Taylor, D.K., Tiekink, E.R.T. and Bowie, J.H. (1999). Syntheses of angucyclinones related to ochromycinone. III - An 11-hydroxy isomer and some reduced analogues. *Australian Journal of Chemistry*, 52(2), 129-135.

Rozek, T., Waugh, R.J., Steinborner, S.T., Bowie, J.H., Tyler, M.J. and Wallace, J.C. (1998). The maculatin peptides from the skin glands of the tree frog Litoria genimaculata: A comparison of the structures and antibacterial activities of maculatin 1.1 and caerin 1.1. *Journal of Peptide Science,* 4(2), 111-115.

Rozek, T., Wegener, K.L., Bowie, J.H., Olver, I.N., Carver, J.A., Wallace, J.C. and Tyler, M.J. (2000). The antibiotic and anticancer active aurein peptides from the Australian Bell Frogs Litoria aurea and Litoria raniformis - The solution structure of aurein 1.2. *European Journal of Biochemistry,* 267(17), 5330-5341.